AD-A014 957

RESPONSE OF ARCHING WALLS AND DEBRIS FROM INTERIOR WALLS CAUSED BY BLAST LOADING

Bernard Gabrielsen, et al

URS Research Company

Prepared for:

Defense Civil Preparedness Agency

February 1975

DCPA Work Unit 1123G
Contract No. DAHC20-71-C-0223

February 1975
URS 7030-23

Final Report

RESPONSE OF ARCHING WALLS and DEBRIS FROM INTERIOR WALLS CAUSED BY BLAST LOADING

Approved for public release;
distribution unlimited.

URS RESEARCH COMPANY

Final Report

RESPONSE OF ARCHING WALLS
and
DEBRIS FROM INTERIOR WALLS CAUSED BY BLAST LOADING

by

B. Gabrielsen, Ph.D.
C. Wilton
K. Kaplan
SCIENTIFIC SERVICE, INC.
830 Charter Street
Redwood City, California 94063

February 1975

for the

DEFENSE CIVIL PREPAREDNE'S AGENCY
Washington, D.C. 20301

Contract No. DAHC20-71-C-0223
Work Unit 1123G

Approveu for public release;
distribution unlimited.

This report has been reviewed in the Defense Civil Preparedness Agency and approved for publication. Approval does not signify that the contents necessarily reflect the views and policies of the Defense Civil Preparedness Agency.

URS 7030-23

URS
A URS Company
RESEARCH COMPANY
155 BOVET ROAD · SAN MATEO, CA 94402 · (415) 574-5000

Unclassified

SECURITY CLASSIFICATION OF THIS PAGE (When Data Entered)

REPORT DOCUMENTATION PAGE		READ INSTRUCTIONS BEFORE COMPLETING FORM
1 REPORT NUMBER	2 GOVT ACCESSION NO	3 RECIPIENT'S CATALOG NUMBER
4 TITLE (and Subtitle) RESPONSE OF ARCHING WALLS AND DEBRIS FROM INTERIOR WALLS CAUSED BY BLAST LOADING		5 TYPE OF REPORT & PERIOD COVERED Final Report Nov 1973 - Oct 1974
		6 PERFORMING ORG REPORT NUMBER URS 7030-23
7 AUTHOR(s) Bernard Gabrielsen, C. Wilton, K. Kaplan Scientific Service, Inc.		8 CONTRACT OR GRANT NUMBER(s) DAHC20-71-C-0223
9 PERFORMING ORGANIZATION NAME AND ADDRESS URS Research Company 155 Bovet Road San Mateo, California 94402		10 PROGRAM ELEMENT PROJECT TASK AREA & WORK UNIT NUMBERS Work Unit 1123G
11 CONTROLLING OFFICE NAME AND ADDRESS Defense Civil Preparedness Agency Washington, D.C. 20301		12 REPORT DATE February 1975
		13 NUMBER OF PAGES 252
14 MONITORING AGENCY NAME & ADDRESS(if different from Controlling Office)		15 SECURITY CLASS (of this report) Unclassified
		15a DECLASSIFICATION DOWNGRADING SCHEDULE

16 DISTRIBUTION STATEMENT (of this Report)

Approved for public release; distribution unlimited.

17 DISTRIBUTION STATEMENT (of the abstract entered in Block 20 if different from Report)

18 SUPPLEMENTARY NOTES

19 KEY WORDS (Continue on reverse side if necessary and identify by block number)

Shock Tests, Nuclear Weapons, Nuclear Effects, Walls, Structural Properties, Performance (Engineering), Civil Defense

20 ABSTRACT (Continue on reverse side if necessary and identify by block number)

The objectives of the study were to derive information on the response of building walls to blast loading from large nuclear weapons that can be used to improve estimates of building damage and casualties. To this end, simulated tests were conducted in the URS Shock Tunnel at Fort Cronkhite, California, under the sponsorship of the Defense Civil Preparedness Agency.

DD FORM 1 JAN 73 1473 EDITION OF 1 NOV 65 IS OBSOLETE

Unclassified

SECURITY CLASSIFICATION OF THIS PAGE (When Data Entered)

In this facility, full-scale walls (8-1/2 ft x 12 ft) were exposed to short duration air blast waves. Full instrumentation and photographic coverage were obtained which allowed detailed analysis of results to be made. During this reporting period, walls made of unreinforced masonry were tested to assess the differences between gapped and rigid arching. In addition, interior walls of various materials of construction were tested to determine the characteristics of the debris produced when they failed.

It was found that differences in blast pressures required to cause failure of rigid and of gapped arched walls are substantial; in the case of an 8-in. thick brick wall undergoing "one way" arching, a rigid arching wall would require about 16 psi loading pressure to fail, whereas a gapped arching wall would require only about 2.5 psi The results of the tests of arching walls tended to confirm the predicted differences in strength between gapped and rigid arching walls.

Velocities and displacement observed during tests on interior walls were of the same order as predicted values. The debris that formed on the initial failure of the walls tended to be in fairly large pieces, and it acquired some impressive velocities within a short travel distance (e.g., 70 mph at 3 ft for a sheetrock wall exposed to 1.7 psi incident pressure pulse). Clay tile and concrete block walls moved much slower than sheetrock walls, but they still acquired high velocities after relatively short travel distances (e.g., 40 mph at 6 ft for a concrete block wall exposed to 4 psi incident pressure pulse).

Summary Report

RESPONSE OF ARCHING WALLS
and
DEBRIS FROM INTERIOR WALLS CAUSED BY BLAST LOADING

by

B. Gabrielsen, Ph.D.
C. Wilton
K. Kaplan
SCIENTIFIC SERVICE, INC.
830 Charter Street
Redwood City, California 94063

February 1975

for the

DEFENSE CIVIL PREPAREDNESS AGENCY
Washington, D.C. 20301

Contract No. DAHC20-71-C-0223
Work Unit 1123G

Approved for public release;
distribution unlimited.

This report has been reviewed in the Defense Civil Preparedness Agency and approved for publication. Approval does not signify that the contents necessarily reflect the views and policies of the Defense Civil Preparedness Agency.

URS 7030-23

URS RESEARCH COMPANY
A URS Company
155 BOVET ROAD · SAN MATEO, CA 94402 · (415) 574-5000

Summary Report

RESPONSE OF ARCHING WALLS AND DEBRIS FROM INTERIOR WALLS CAUSED BY BLAST LOADING

TYPE AND OBJECTIVES OF STUDY

In this study, analysis and experiment are combined to provide information on the response of building walls to blast loading from nuclear weapons. The objectives of the study are to derive information that can be used to improve estimates of building damage and casualties.

The two major subjects studied during this reporting period were: 1) arching walls made of unreinforced masonry, with emphasis on gapped as opposed to rigid arching *; and 2) the characterictics of the debris produced by interior walls after their failure. A few tests were made on reinforced brick walls.

ARCHING WALLS

Arching theory shows that the blast pressures required to cause failure for gapped arching walls are smaller than those required for rigid arching walls. In both cases, failure occurs through internal forces applied along "hinges" of an arch, but the failure mechanisms of gapped

---

* Arching is the phenomenon through which a wall attains increased resistance to forces normal to its face because it is prevented from moving in a direction parallel to its face. Rigid arching occurs when a wall is in intimate contact with the element -- part of the building frame, for example -- that prevents this motion. Gapped arching occurs when there is a small gap between the wall and the restraining element.

arching walls involves the tensile strength of the wall materials, while that of rigid arching walls involves the larger compressive strength of the materials.

The differences in blast pressures required to cause failure are substantial; in the case of an 8-in. thick brick wall undergoing "one way" arching (in which in-plane motions are prevented on just two wall edges) a rigid arching wall would require about 16 psi loading pressure to fail, a gapped arching wall would require only about 2.5 psi loading pressure. (Here, "loading pressure" refers to what the wall experiences, generally peak-reflected blast overpressure for an exterior wall, rather than to the incident blast overpressure.)

Because of the lower failure pressure of a gapped arching wall, and because such a wall must move only about half the distance that a rigid arching wall must move in order to fail, the differences in energy absorbed by the walls in the failure process are also large. The energy absorbed by an 8-in. thick wall undergoing gapped arching is only about one-thirteenth that absorbed by a similar wall undergoing rigid arching. Note, however, that even a gapped arching wall is far stronger than one which is not undergoing arching at all.

Shock Tunnel tests of arching walls, which during this period were concentrated on gapped arching walls, tended to confirm the predicted differences in strength between gapped and rigid arching walls. For example, with 8-in. thick walls, loading overpressures that caused failure of gapped arched walls (about 4 psi) were only 1/3 to 1/5 of those that

caused failure of rigid arched walls (about 13 to 19 psi). The manner in which the walls failed suggested that the threshold failure loading pressure was probably close to the 2.5 psi predicted value.

In some analytical work on arching and related phenomena, it is shown that a wall that contains a crack but would otherwise undergo rigid arching, is likely to fail in a manner similar to that of an uncracked, gapped arching wall. If it does not fail first in this manner, ordinary rigid arching would then occur.

Prior to this reporting period, information on the ability of masonry to resist the kinds of forces involved in rigid arching, (called compressive line-load strengths) had been acquired through specially devised static tests in which forces were actually applied along a corner, that is, along a line, of a test specimen. This should not be necessary in the future because a method of predicting compressive line-load strengths from ordinary compression tests (in which forces are applied over the entire face of a test specimen) has been devised.

DEBRIS FROM INTERIOR WALLS

The analytic work on the debris problem was divided into two parts. One part was directed toward locating the point of failure of masonry interior walls that are cantilevered from the floor. (This is a common support condition for interior walls in large buildings where false ceilings are used to cover utility ducts and the like). The second part of the analytical work was directed toward predicting velocities and displacements of the

debris from interior walls of sheetrock, concrete block, and clay tile that fail under blast loading.

Shock Tunnel tests were run to acquire experimental information on these three types of walls. Velocities and displacements observed during the tests were of the same order as predicted values. The debris that formed on the initial failure of the walls tended to be in fairly large pieces, and it acquired some impressive velocities within a short travel distance. Within about three feet of travel, for example, sheetrock walls were moving at about 70 mph from a 1.7 psi incident pressure pulse, and at about 100 mph from a 4 psi incident pulse. Clay tile and concrete block walls moved much slower than sheetrock walls, of course, but they still acquired high velocities after moving only a short distance. Under the 4 psi incident loading, within a travel distance of six feet, the velocity of the debris from concrete block walls was about 40 mph, and that from clay tile walls about 30 mph.

REINFORCED BRICK WALLS

Finally a small amount of test data on reinforced brick walls was acquired. Two such walls, 8-in. thick and mounted as simple beams, were placed in the Shock Tunnel. One did not fail at an incident pressure of about 1 psi, but did at 2 psi; the other failed on the first loading at an incident pressure of about 2 psi. These near threshold failure pressures were larger than those of similarly mounted (but pre loaded) 8-in. thick unreinforced brick walls.

ABSTRACT

The objectives of the study were to derive information on the response of building walls to blast loading from large nuclear weapons that can be used to improve estimates of building damage and casualties. To this end, simulated tests were conducted in the URS Shock Tunnel at Fort Cronkhite, California, under the sponsorship of the Defense Civil Preparedness Agency.

In this facility, full-scale walls (8-1/2 ft x 12 ft) were exposed to short duration air blast waves. Full instrumentation and photographic coverage were obtained which allowed detailed analysis of results to be made. During this reporting period, walls made of unreinforced masonry were tested to assess the differences between gapped and rigid arching. In addition, interior walls of various materials of construction were tested to determine the characteristics of the debris produced when they failed.

It was found for gapped walls that differences in blast pressures required to cause failure are substantial; in the case of an 8-in. thick brick wall undergoing "one way" arching, a rigid arching wall would require about 16 psi loading pressure to fail, whereas a gapped arching wall would require only about 2.5 psi. The results of the tests of

arching walls tended to confirm the predicted differences in strength between gapped and rigid arching walls.

Velocities and displacement observed during tests on interior walls were of the same order as predicted values. The debris that formed on the initial failure of the walls tended to be in fairly large pieces, and it acquired some impressive velocities within a short travel distance (e.g., 70 mph at 3 ft for a sheetrock wall exposed to 1.7 psi incident pressure pulse). Clay tile and concrete block walls moved much slower than sheetrock walls, but they still acquired high velocities after relatively short travel distances (e.g., 40 mph at 6 ft for a concrete block wall exposed to 4 psi incident pressure pulse).

ACKNOWLEDGEMENTS

This volume reports work accomplished by URS Research Company and Scientific Service, Inc. (subcontract 7030-74-100) at the Fort Cronkhite Shock Tunnel under the sponsorship of the Defense Civil Preparedness Agency. This report was prepared by Dr. Bernard Gabrielsen, K. Kaplan, and C. Wilton of Scientific Service, Inc. W.H. Van Horn of URS Research Company acted as project coordinator, and all experimental work was carried out by Joseph Boyes and M. Paul Kennedy, also of URS. Typing and report layout was done by Mrs. L. Wilton.

The helpful comments and suggestions of the Contract Officers Technical Representative, Dr. M.A. Pachuta, are hereby gratefully acknowledged.

CONTENTS

TABLES

FIGURES

FIGURES

Section 1

INTRODUCTION

Section 1

INTRODUCTION

The structural integrity of a building, and the size, shape, and velocity of casualty producing debris produced by blast loading from a nuclear weapon depend on the mounting conditions, material properties, and failure mechanism of the exterior and interior walls of the structure.

Because of the importance of wall panels, DCPA has sponsored a research program to develop a methodology for predicting wall panel failure. To minimize the number of experiments required, and maximize the number of different panel and mounting conditions for which failure predictions can be made, a combined analytic and experimental approach has been used. Methods for predicting conditions under which walls fail are developed analytically; experiments provide needed input information (material properties, strengths, etc.) and are also used to assess the validity of the prediction methods developed.

The analytical part of the overall program has led to the development of important new theories of wall behavior (see, for example, Ref. 1, 5, and 7) and material response (for example, as in Ref. 1 and 8) and has included use of a number of computer programs such as SAMIS and MACE.* The experimental

---

* SAMIS - Structural Analysis Matrix Interpretive System
MACE - Mechanical Analysis of Continuous Elastic System

part of the program has included both static and dynamic tests: the static tests dealing generally with material properties and being conducted with a variety of loading devices; the dynamic tests dealing generally with wall behavior and employing full scale walls mounted in a shock tunnel.

Early emphasis has been on walls composed of brittle materials such as unreinforced brick, concrete block, and tile because of the large number of structures containing shelter spaces that employed such materials. Walls mounted as both simple beams (supported on two edges) and as plates (supported on four edges) have been studied, and the importance of wall "preload"* and arching** have been investigated, along with the characteristics of debris from interior walls. A few tests of reinforced brick walls were made.

This report concentrates on arching, reinforced brick walls, and interior walls. There are four sections following this introduction.

Section 2 deals with both arching walls and the limited data on reinforced brick walls. It begins with a summary of the current state of knowledge of arching phenomena. Both rigid and gapped arching*** are discussed. The section also contains new analytical material on the influence of a ran-

* Preload is defined as the load imposed on a wall of interest by the structure above it.

** Arching is the phenomenon through which a wall attains increased resistance to forces normal to its face because it is prevented from moving in a direction parallel to its face.

***Rigid arching occurs when a wall is in intimate contact with the element -- part of a building frame, for example -- that prevents wall motion parallel to its face. Gapped arching occurs when there is a small gap between the wall and the restraining element.

dom crack in a wall on arching phenomena; and on a technique for predicting total "line-load resistance"*. The section ends with a brief description of the results of the two tests carried out on reinforced brick walls.

Section 3 deals with the characteristics of debris from interior walls subject to blast loading. It begins with a summary of the results of the most recent tests, then describes analytical approaches to determining debris velocities, and compares analytical with test results. The objective of this part of the program was to determine the type, size, and early time velocity of debris fragments. The emphasis during this reporting period was on interior wall panels constructed of sheetrock, clay tile, and concrete block; and on developing information suitable for casualty predictions.

Section 4 presents a series of charts indicating the progress on the wall panel program to date.

Appendix A contains detailed test reports of the tests conducted in the shock tunnel during the current reporting period on both exterior walls (including two gapped arching walls) and interior walls of sheetrock, concrete block and clay tile.

Appendix B contains data on static tests conducted in support of the full scale shock tunnel wall test program (and includes corrections to data tables presented in Ref. 1.)

** As will be seen, in both rigid and gapped arching, in-plane forces on wall elements tend to be applied along a line, as at one edge of a crack, rather than over the entire cross section of a wall.

Appendix C presents a discussion on the influence of limited cyclic loading on wall strength (low level fatigue).

The work described in this report was monitored by the Hazard Evaluation and Vulnerability Reduction Division of DCPA and carried out under contract No. DAHC-20-71-C-0223 with URS Research Company. The report itself was prepared by Scientific Service Inc. under URS subcontract number 7030-74-100. The responsibilities of Scientific Service Inc. under this subcontract were: design of the test programs; data analysis and correlation; failure theory development; preparation of technical reports, and other consulting services as necessary.

Section 2

ARCHING AND REINFORCED BRICK WALLS

Section 2

ARCHING AND REINFORCED BRICK WALLS

BACKGROUND ON ARCHING

Prior analytical and experimental effort initially concentrated on walls of brittle materials (brick, clay tile, and concrete block) that acted as simple beams (the walls were supported on two edges, with the other two edges free), or as simple plates (the walls were supported on all four edges). It was found that where this type of support did not include resistance to forces parallel to the faces of the walls, or where this resistance was limited to preload values of the order of the weight of a few stories of walls, resistance to blast loadings was quite small. All such walls with openings (windows or doors) would fail at incident blast overpressures of four psi or less; all such solid walls (with no openings) would fail at overpressures of two psi or less.

The reason for this was simple: blast wave pressures applied normal to the upstream face of a wall supported at its edges would cause the wall to flex and induce tension in the downstream face of the wall. Tensile strengths of brick and mortar composites (or of similar brittle materials) are quite low; thus tensile cracks would form in the downstream face of the wall. Since there would be essentially no resistance -- other than the wall's inertia -- to the out-of-plane forces still being imposed by the blast wave, the wall would fail.

More recently, attention has been paid to conditions under which resistance to blast forces, even after a wall has cracked, can be very large. This can occur where the edges of a wall are enclosed within a rigid frame that does not permit in-plane movement, that is, movement of the wall parallel to its face. When such a wall is loaded normal to its face, it resists downstream motion because the elimination of in-plane motions does not allow individual wall elements to rotate freely about the wall's edges. In other words, the wall forms an arch between its rigid supports.

The potential importance of arching was recognized many years ago during the era of above-ground weapons testing in Nevada. Arching theory developed at that time -- supported by experiment both in Nevada and more recently in the shock tunnel -- indicated that resistance to out-of-plane wall motions could increase by factors of 10 or more if in-plane motions were totally prohibited.

During the course of the current program, however, a question arose about the strengh of walls which, though located within members that would prohibit in-plane motions, were separated from these members by a gap. The question had pertinence for two reasons: because some manuals of construction practice indicate that the inclusion of such a gap (or equivalent, a low-strength, flexible seal) between an infill wall and a frame is good building practice (it permits design frame action to occur); and because even where infill walls are carefully grouted into framing elements, mortar shrinkage is likely to cause the small gaps to form between wall and frame.

Analysis of this problem, subsequently supported by experiment, indicated that a form of arching could still occur where there was a small gap between wall and frame (gapped arching). However, it was of a different kind than the arching that occurred where there was no gap ("rigid arching"). Most importantly, the increase in resistance to blast pressures caused by gapped arching was found to be substantially less than that caused by rigid arching.

SUMMARY OF BASIC RIGID AND GAPPED ARCHING THEORY *

Fig. 2-1 and 2-2 illustrate the important difference between rigid and gapped arching. (Only "one-way" arching in which the wall is restrained on only two edges, is discussed**). Fig. 2-1 contains sketches showing how walls behave in the two cases (exaggerated for clarity). In rigid arching on the left, blast induced forces (or actually any force normal to the face of the wall) push the wall to the left. However, the wall is prevented from rotating about its top and bottom supports. Tensile (flexural) cracks form at the top, bottom, and center (where tensile stress is highest), but the wall elements cannot move downstream. A three-hinged arch forms with loadings along lines at the downstream edges of the top and bottom of the wall, and at the upstream edge of the crack.

---

* Summarized from Ref. 1 and Ref. 5

** Only limited work was done on "two-way"arching (where a wall is restrained on all four edges), preliminary calculations indicated that such walls should be about 1.5 times as strong as one-way arched walls.

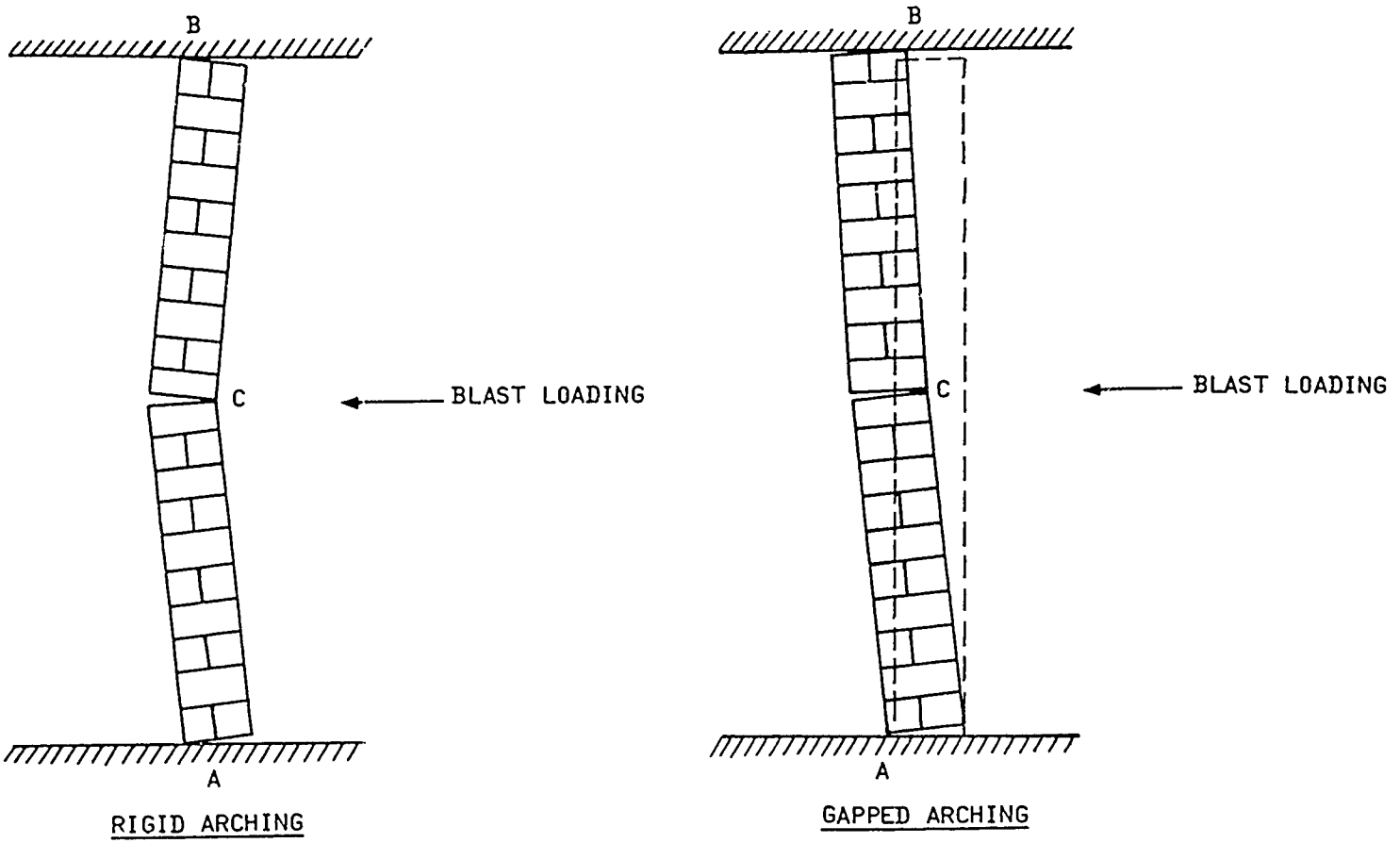

Fig. 2-1. Sketch Illustrating the Differences in Motion Between Rigid and Gapped Arching.

In gapped arching on the right, in Fig. 2-1, the gap permits the wall to move, either by bending or because of a crack at its base until the upstream edge at the top of the wall contacts the upper restraint. The original position of the wall is shown by the dashed line. A tensile crack forms at the wall center where maximum tensile stresses still occur. Again a three-hinged arch forms, but one which is not as symmetrical as in the rigid case. Loadings are at the downstream edge of the wall bottom, at the upstream edges of the tensile crack and the top of the wall. Note that the gap can be very small; (as shown in Ref. 1, it can be as little as about 0.01 in. - one hundreth of an inch - for an 8-in. thick, 96-in. high wall) the only requirement is that the upstream edge at the top of the wall contact the restraint.

Fig. 2-2 shows the directions of forces on the two parts of each wall. The general formulas for these forces per unit length of wall and the initial magnitudes of these forces for a wall with a height (ℓ) of 96 in. and a thickness, (t) of 8 in. are given in Table 2-1 for a uniform pressure (p) Fig. 2-2 shows that in rigid arching, the resultant forces are either directed into the wall (R_A and R_B) or are parallel to the wall face (at C). In the gapped arching case, however, there are forces (R_B and R_C) directed away from the upper part of the wall, and both the force directed into the wall (R_A) and the in-plane force (H) are about twice as large as they are in the rigid arching case. Forces directed into the wall would tend to cause compressive (crushing) failures; those directed away from the wall would tend to cause tensile (spalling) failures which occur at much lower stress values. Thus, the upper part of the wall in gapped arching should fail essentially in ten-

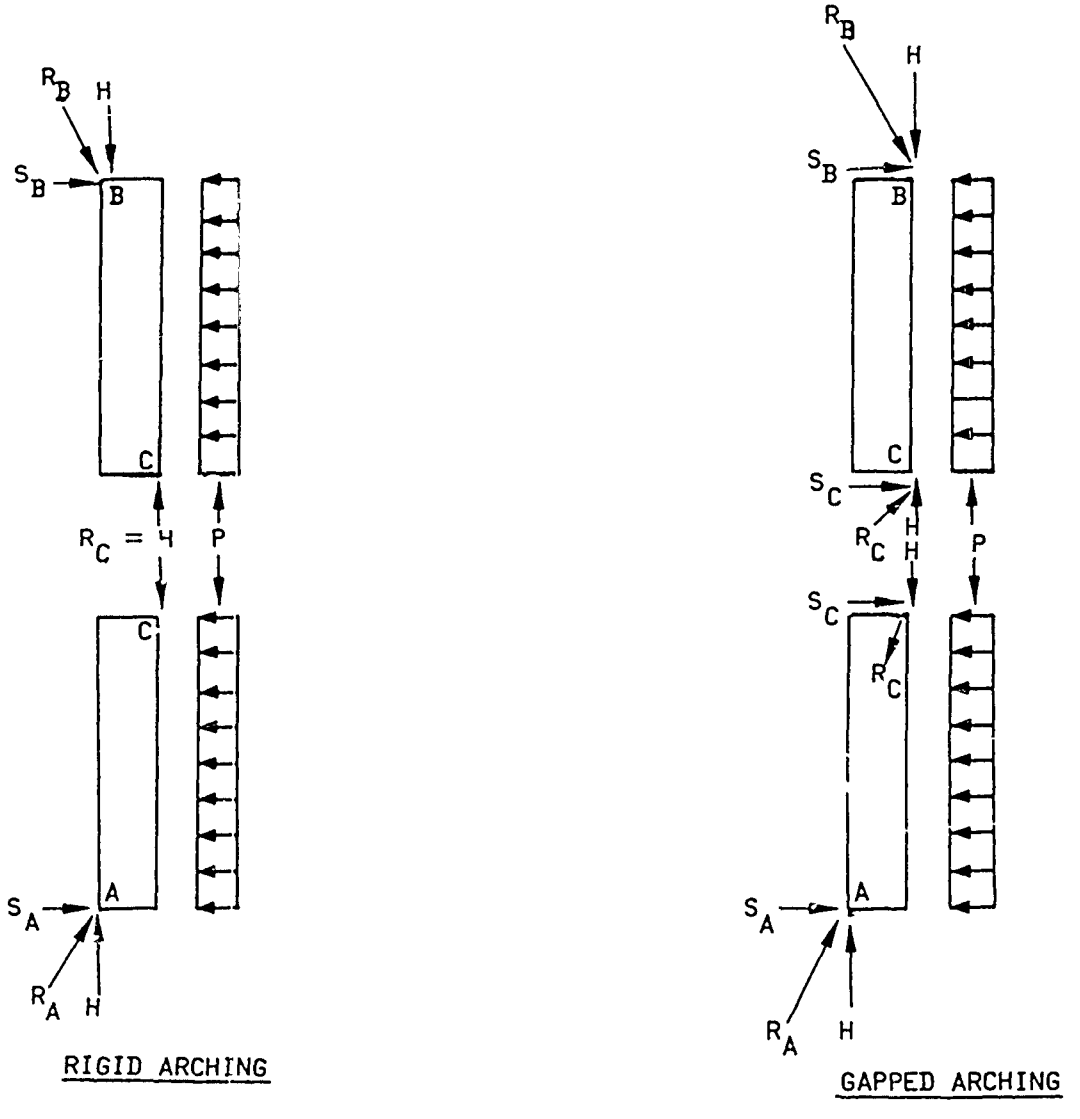

Fig. 2-2. Free Body Diagrams Showing Forces in Rigid and Gapped Arching. (See Table 2-1 for force values.)

sion at far lower incident pressures than those that would cause failure in rigid arching, since tensile strengths of masonry composites are lower than compressive strengths. Furthermore, since R_B and R_C are equal, the upper part of the wall should tend to move downstream without rotation. In other words, there is no tendency for a gapped arching mode of failure to convert to a rigid arching mode of failure, even when the gapped arching mode is instituted by a very small gap.

TABLE 2-1 FORCES IN RIGID AND GAPPED ARCHING

(See Fig. 2-2)

Force	Rigid Arching		Gapped Arching	
	General Formula	Value for ℓ = 96 in. t = 8 in. (lb/in)	General Formula	Value for ℓ = 96 in. t = 8 in. (lb/in)
H	$p\ell^2/8t$	144p	$p\ell^2/4t$	288p
S_B	$p\ell/2$	48p	$p\ell/4$	24p
R_B	$(H/\ell)\sqrt{\ell^2 + (4t)^2}$	152p	$(H/\ell)\sqrt{\ell^2 + t^2}$	289p
S_C	-	0	$p\ell/4$	24p
R_C	H	144p	$(H/\ell)\sqrt{\ell^2 + t^2}$	289p
S_A	$p\ell/2$	48p	$3p\ell/4$	72p
R_A	$(H/\ell)\sqrt{\ell^2 + (4t)^2}$	152p	$(H/\ell)\sqrt{\ell^2 + (3t)^2}$	297p

STRENGTH CONSIDERATIONS

In order to determine the resistance of both rigid and gapped arching walls, information is needed on the strength of wall materials subjected to the kind of forces that would cause either crushing or spalling failures along a line (that is, at the "hinges' of the arches). A variety of special static tests have been used to determine such "line load" strengths, and during this reporting period, techniques have been developed for predicting compressive line-load strength from standard compression tests.

Summary of Static Tests

One series of tests were made using tilted brick-mortar composite specimens to determine the strength of wall composites under compressive (crushing) line loads. The basic test geometry for these static tests is sketched below.

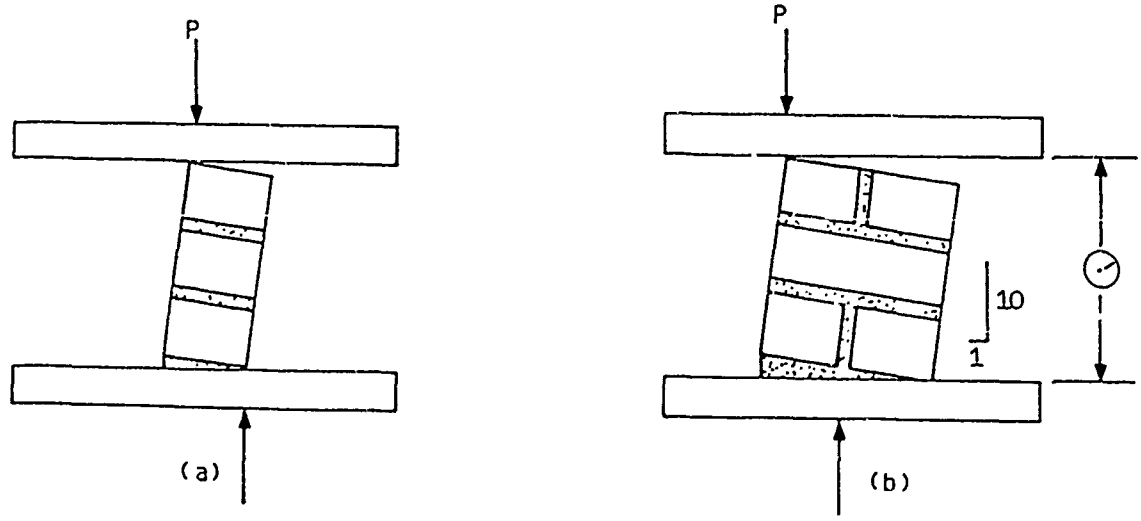

Results from 11 tests with test setup (a) showed that failure occurred at an average total load (p) of 28,100 lbs. (Values ranged from 18,000 to 35,000 lbs. as shown in Table B-5 in Appendix B). The average line load at failure f_ℓ for the approximately 8 in. long specimens used was 3300 lb/in. (range 2100 to 4000 lb/in.). In the test setup (b) results from 11 tests gave an average p value of 43,100 lbs. (range: 35,000 to 52,000 lb) and an average f_ℓ value of 5100 lb/in. (range 4100 to 6000 lb/in.) again using approximately 8-in. long specimens.

Fewer line loading tests were made with concrete block, and brick-concrete block mortar composites. Test set ups are sketched below:

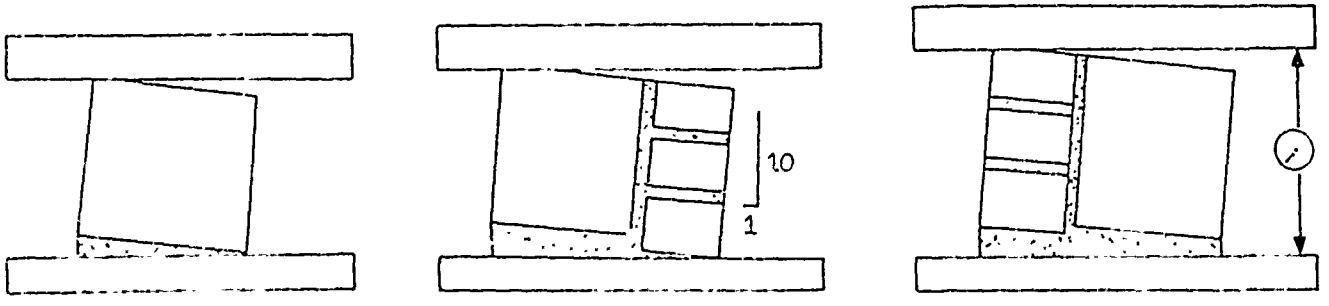

(c) (d) (e)

Average results were as follows:

Specimen	Number of tests	average p (lb)	average f_ℓ lb/in.
(c)	4	30,200	4,000
(d)	3	39,000	4,600
(e)	4	23,200	3,000

Additional tests were conducted to develop an approximation of strength under the tensile (spalling type) of line loading that could occur in the gapped arching case at points B or C in Fig. 2-1 and 2-2. That test set up is shown in the sketch below.

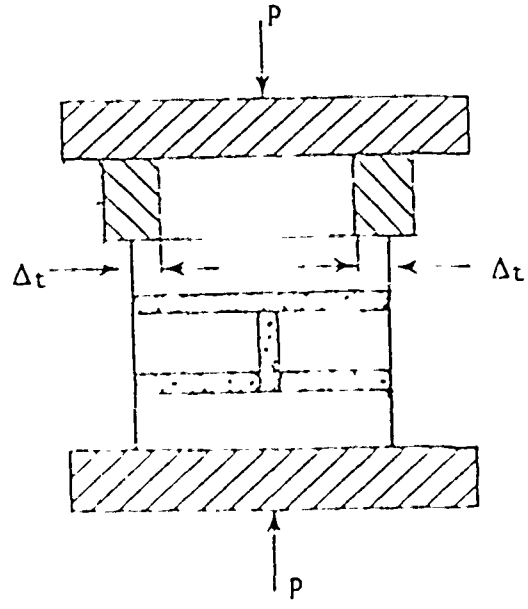

Two values of Δt were tested, ½ in. and ¼ in. For the latter, spalling was clearly occuring, and on four tests, the average P was 13,390 lb. and the average f_ℓ was 824 lb/in. As expected, these tensile line loading strengths are far below those for compressive line loading.

For more details on all these static tests described above, see Ref. 1.

Development of Line Load Strength Prediction Techniques

During this reporting period consideration was given to the development of a prediction technique for line load resistance of walls based on compressive strength test data. Both brick and concrete block walls have been considered.

For brick test specimens consider the test set-up shown below.

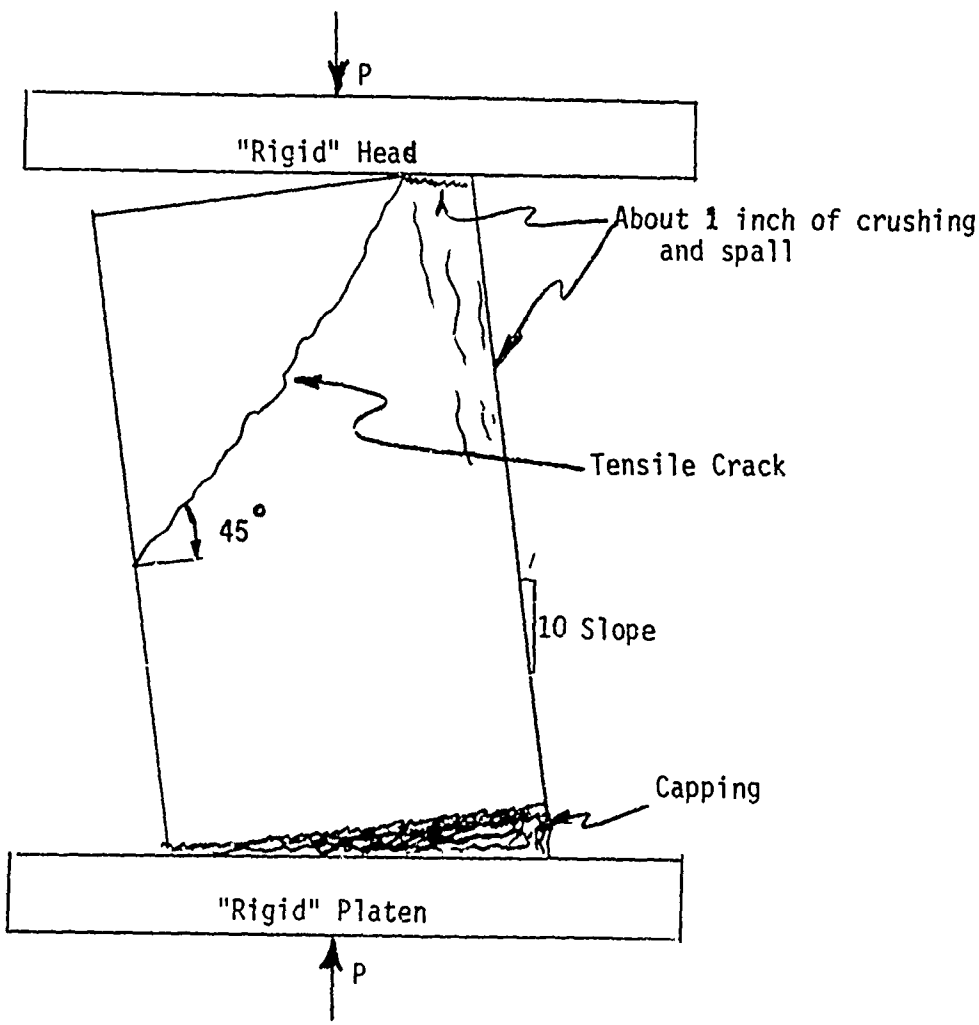

Assume the tensile crack is caused by pure shear as shown below.

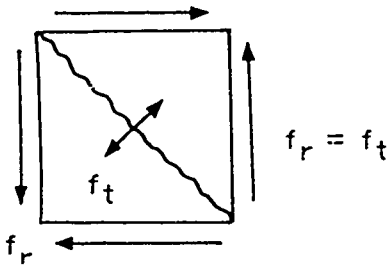

There are a number of sources relating tensile strength f_t to compressive strength f_c':

From Ref. 2

for brick $f_t = 12\sqrt{f_c'}$

for mortar $f_t = 10\sqrt{f_c'}$

From Ref. 3

$f_t = 12\sqrt{f_c'}$

From Ref. 4

$f_t = 7.5\sqrt{f_c'}$

Therefore, as a rough average, let $f_t = 10\sqrt{f_c'}$

In the force diagram sketched below, if a unit width is assumed:

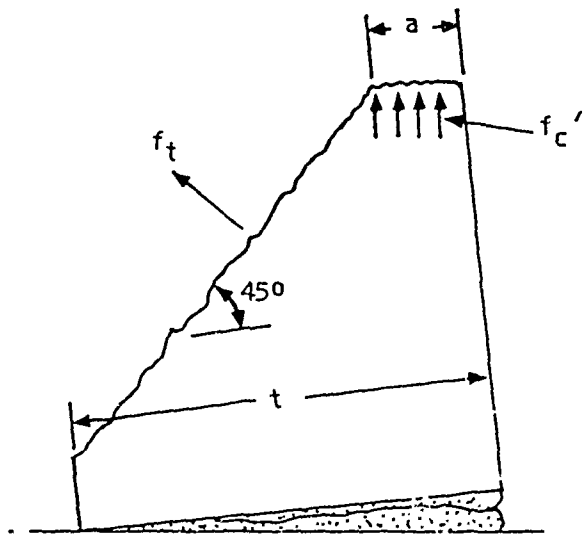

Total resistance, f_ℓ, is predicted to be

$$f_\ell = f_c'a + f_t (t-a) \cos 45^\circ$$

From Table 3, Appendix B, for the 15 tests with an ASTM, 3 brick and mortar composite, $f_c' = 2400$ psi.

Line load tests were also made on test specimens that were three bricks high, in a geometry like sketches (a) and (b) shown at the beginning of the static test portion of this section. The following results were observed.

f_ℓ = 3100 lb/in. (4 in. thick line load specimen, 14 tests)

f_ℓ - 4500 lb/in. (8½ in. thick line load specimen, 14 tests)

For this test series, using the observed f_c' of 2400 psi, an "a" of 1 in., and the 4 and 8½ in. thicknesses for "t", the total resistance equation gives f_ℓ values of 3439-lb/in. and 4998-lb/in. respectively.

Thus, we have the following:

Wall Thickness	f_ℓ (predicted) lb/in	f_ℓ (test) lb/in
4	3439	3300
8½	4998	5100
12	6557	-

A second type of static test series, in which conditions more nearly simulate those of an arching wall, was conducted at the shock tunnel site and are reported in Appendix B. In this series, beams were built horizontally into a 4 ft. wide, heavy-walled passageway and mortared in so that they performed as a rigid arch. They were loaded in a direction normal to their faces at the 1/3 points. (See Fig. B-3-B and the upper part of

Fig. B-4). A free-body diagram of one-half the beam is sketched below.

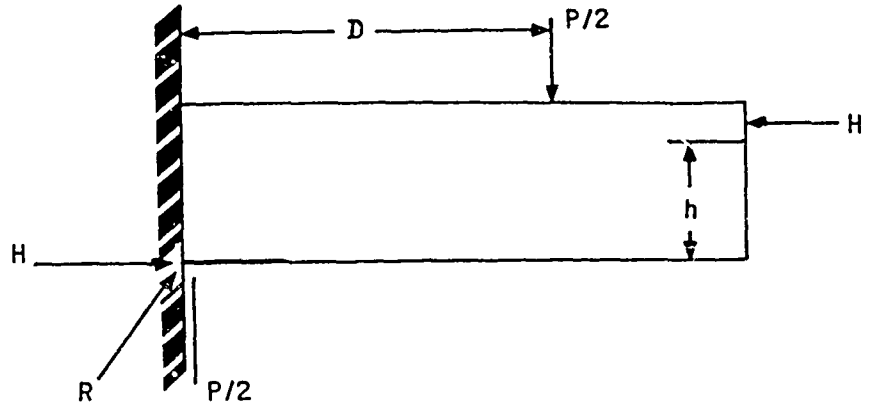

Taking moments about the left lower corner we have

$$H_h = (P/2)d, \text{ or } H = Pd/2h$$

in which h, the uncrushed portion of the beam is about 3 in., d = 16 in., and P = 10,479 lb. Therefore, H = 27,944 lb., the resultant force $R = \sqrt{H^2 + (P/2)^2}$ = 28,431 lb., and the line load at failure, calculated by dividing R by the brick width of 8.625 in., is 3296 lb/in. This compares quite favorably with either the calculated value of 3439 lb/in. or the static test value of 3300 lb/in.

From the work on solid brick just described and from test observations on hollow clay tile and concrete block composites, several statements can be made with some confidence.

1) Hollow units, like concrete block and clay tile, have lower line load capacity than solid units.
2) From static test observations, the width of crushed material with hollow units is less than with solid units.
3) The shear/tension type of failure that goes along with the line-load phenomenon is apparently a reduced value with hollow walls because of the lack of shear/tension material.

From these observations we can make the following hypothesis: The ultimate line load capacity is proportional to the shear/tension capability of the unit. Further, the width of the crushed zone is reduced or controlled by the shear/tension capacity of the unit. Therefore, referring to the force diagram given earlier for the brick, the total line load resistance should be

$$f_\ell = k\left[f_c a + f_t\,(t-ak)\cos 45^\circ\right]$$

Where $k = b_s/b$

and b_s is the width of sheared material (Webs)

and b is the width of the block

This expression is identical with that for brick, except for the addition of the factor "k".

As with brick, two types of static tests have been made with which this expression can be evaluated. In the first, a beam made of concrete blocks was constructed between walls of a passageway and loaded in a direction normal to its face at the 1/3 points. (See Fig. B-3-A and lower part of Fig. B-4). This is identical with the brick beam test geometry which led to the following equation for H, the horizontal force at the beam edge.

$$H = Pd/2h$$

Using P from the static tests (11,600 lb.), d = 16 in., and h $\simeq$ 6.625* we have: H = 14,010 lb. The resultant force R = 15,160, and the line load at failure (R divided by the block width of 15.625 in.) is f_ℓ = 970 lb/in.

Let us compare this result with that from the line load predictor equation for a 16.in. block. For a nominal 16 in. block, the total block width is about 15-5/8 in. and the material through the center of the block where shearing takes place consists of three webs each about 1.27 in. thick. Therefore:

$$k = 3(1.27)/15.625 = 0.244$$

Compressive strength tests reported in Appendix B give f_c' = 2560 psi, $f_t = 10\sqrt{2560}$ (see derivation for brick mortar composite; this is a value for mortar), and a = 1 in. Thus:

$$f_\ell = 0.244\ (2560 + 10\sqrt{2560}\ \ (7.625-0.244)\ 0.707) = 1268 \text{ lb/in.}$$

which is reasonably close to the value from the beam tests (970 lb/in).

In a second static test series, a single nominal 8 x 8 x 8 in. block was loaded as shown at the beginning of this portion of the section. Corrected measurements of f_ℓ reported in Appendix B are f_ℓ = 4000 lb/in. The corrected value was derived by using a value of 7.625 which is the width of a standard concrete block in place of 8.8 in., the nominal width of a standard brick, which had inadvertently been used.

*The blocks were nominally 7.625 in. thick; an h of 6.625 in. allows for a crushing zone with a total width of one inch.

In the prediction equation used earlier k = 2 (1.27)/7.625 = 0.3331, so that f_ℓ = 1722 lb/in. The measured value does not compare favorably with the predicted value (3961 lb/in. vs. 1722 lb/in.), for reasons unknown. Results of other static and dynamic shock tunnel tests suggest that the experimental value may be questionable.

COMPARISON OF TEST RESULTS WITH THEORY

Test information given in Table 2-2 tends to confirm the results of the analytical work described earlier. Among walls with no window or door openings that underwent rigid arching, 8-in. thick brick, one-way arched walls failed on initial reflected pressure loadings of between about 13 and 19 psi (5.5 to 8 psi incident). As shown in the Table, some other walls were first loaded at lower levels and cracked, but they did not fail until loaded again, sometimes even a third time, at either the same low overpressure level or at higher levels. A single 8-in. thick, concrete block, one-way arched wall was tested to failure on initial loading, of about 10 psi loading pressure, (4.5 psi incident). Two similar walls subjected to two way arching failed at 9 and 11 psi loading pressures (4-5 psi incident), i.e. at about the same overpressure loading as for one-way arching, instead of at expected higher values. However, expected higher strength in two way arching was found for 4-in. thick brick walls, which were about 30 percent stronger than similar one-way arched walls.

Brick concrete block composite, one-way arched walls appeared to have strengths like those of similarly mounted brick walls, failing at over 11 psi loading pressure (about 5 psi incident).

TABLE 2-2

Summary of Arched Wall Tests

Solid Walls

Test Number	Incident (and Reflected) Overpressure (psi)	Remarks
		4-in. Brick (one-way)*
68a	.75 (1.5)	Wall cracked
68b	1.7 (3.5)	Wall failed
		4-in. Brick Arched Wall (two-way)**
83a	2.2 (4.7)	Wall cracked
83b	2.1 (4.4)	Wall failed
		8-in. Brick (one-way)*
71a	1.9 (4.1)	Test for natural period
71b	2.9 (6.4)	Wall cracked
71c	4.3 (9.2)	Cracks enlarged
74	5.5 (12.9)	Wall failed
75	5.9 (13.8)	Wall failed
76	5.6 (13.1)	Wall failed
87a	5.7 (13.4)	Wall cracked
87b	6.3 (14.2)	Cracks enlarged
88a	7.8 (19.0)	Wall cracked
88b	3.6 (8.0)	Cracks enlarged
94	7.8 (19.0)	Wall failed
9C	6.7 (15.5)	Wall failed (pre-split)

*Geometrically restrained on top and bottom.
**Geometrically restrained on all four sides.

TABLE 2-2 (cont.)

Summary of Arched Wall Tests

Solid Walls

Test Number	Incident (and Reflected) Overpressure (psi)	Remarks
		8-in. Brick (one-way) with a gap
97	2.3 (4.9)	Wall failed
98	1.9 (4.9)	Wall failed
		8-in. Concrete block (one-way)*
77	3.3 (8.2)	Wall cracked
77	2.0 (4.3)	No additional damage
77	3.4 (8.5)	Wall failed
78	4.5 (10.2)	Wall failed
		8-in. Concrete block (one-way)* with a gap
115	4.1 (9.1)	Wall failed
116	1.7 (3.5)	Wall failed
		8-in. Concrete block arch wall (two-way)**
89	5.0 (11.4)	Wall failed
90	4.0 (4.3)	Wall failed
(Arched)		10-in. Composite brick and Concrete block Arched wall (one-way)*
79	5.6 (13.1)	Wall failed
92a	3.5 (7.8)	Wall cracked

*Geometrically restrained on top and bottom.
**Geometrically restrained on all four sides.

TABLE 2-2 (cont.)

Summary of Arched Wall Tests

Solid Walls

Test Number	Incident (and Reflected) Overpressure (psi)	Remarks
		10-in. Composite brick and concrete block Arched Wall (one-way) (cont)
92b	3.5 (7.8)	No additional damage
92c	5.0 (11.4)	Cracks enlarged
Walls with an opening		8-in. Brick wall with window (38" x 62") (one-way)*
80a	5.7 (13.4)	Wall cracked
80b	6.3 (14.2)	Wall failed
84a	6.4 (14.5)	Wall cracked
84b	7.8 (19.0)	Wall failed
85a	6.2 (14.0)	Wall cracked
85b	5.8 (13.5)	Cracks enlarged
85c	7.5 (18.0)	Slight additional cracking
85d	9.5 (23.8)	Wall failed
		8-in. brick with doorway (one-way)
86a	6.1 (14.3)	Wall cracked
86b	8.4 (20.5)	Cracks enlarged
		8-in. Brick with doorway (with gap)
95	8.6 (21.2)	Wall failed

*Geometrically restrained on top and bottom.

A few tests were made of walls with window and doorway openings, mounted so as to undergo rigid arching. As expected, these were stronger than solid walls (or rather they required higher incident overpressures to cause failure). Indeed, the single 8-in. thick, one-way arching wall with a doorway only cracked when subjected to a 6.1 psi incident pressure, and the cracks only enlarged when struck by a second shock with an incident overpressure of 8.4 psi.

(All similar walls without any openings failed at or below 8 psi incident overpressure.) Similarly, one of the two 8-in. thick brick walls with a window opening only failed when subjected to an incident overpressure of 7.8 psi (after three earlier loadings from 5.7, 6.3, and 6.4 psi incident overpressures). The second such wall only failed at 9.5 psi incident, after being struck and cracked by 6.2, 5.8, and 7.5 incident overpressure shocks.

Most of the tests involving gapped arching were undertaken during this reporting period. The single previous test was made before the decrease in strength due to the presence of a small gap was appreciated. It was an 8-in. thick wall with a doorway and was subjected to an incident overpressure of 8.6 psi. It failed catastrophically. The more recent tests used shock waves with overpressures much closer to expected failure overpressures. Two 8-in. thick brick walls failed at 1.9 and 2.3 psi incident overpressure, and one concrete block interior wall failed at 2.0 psi incident overpressure. (One additional test was conducted for debris data on a concrete block interior wall at an incident overpressure of 4.1 psi with expected catastrophic results.)

ENERGY CONSIDERATIONS

There are very large differences between the shock wave energy required to cause failure of a gapped arching wall and a rigid arching wall. ("Failure" as used here means the point at which the wall becomes unstable, i.e. it will fall without the aid of any outside forces.) This comes about for two reasons. First, in rigid arching, the mode of failure (crushing) requires much higher loading pressures than the mode of failure (spalling) in gapped arching. With an 8-in. thick, brick and mortar, one-way arching wall, for example, a loading pressure of over 16 psi is required to cause crushing in rigid arching, while only about 2.5 psi is required to cause spalling in gapped arching.

The second reason is that the center of a rigid arching wall must move twice as far (t vs t/2) as a gapped arching wall before actual failure occurs. After crushing in the one case and spalling in the other begins to occur, the walls still offer resistance to motion in the areas in which material failure is taking place. With a rigid arching wall, this resistance continues until the central crushing zone is in line with the crushing zones at the walls edges, both of which are near the front face of the wall. With a gapped arching wall, however, one of the material failure zones is at the back face of the wall. The line between these zones passes through the middle of the wall and an unstable geometry occurs when the center material failure zone (the back edge of the central

crack) moves only one half the thickness of the wall. Thus, an 8 in. thick wall fails after its center has displaced 6 to 8 in. if it is undergoing rigid arching, but only 3 to 4 in. if it is undergoing gapped arching.

It should be appreciated though, that if <u>any</u> arching occurs, energy required to cause failure is very much greater than if no arching occurs at all. An 8-in. thick brick wall mounted as a beam requires only about 0.7 psi for a tensile crack to appear at which time the wall's centerline will have moved only about 0.04 in. After the wall cracks, only inertial forces (the weight of the wall elements) resist the pressure forces normal to the wall, but, the wall will not be unstable until its centerline has moved about 8 in. At that point it will have absorbed only about 1/9 the energy that a gapped arching wall will absorb.

THE INFLUENCE OF A RANDOM CRACK ON RIGID ARCHING

Consider the system sketched below which represents a wall of unit width whose length is "ℓ" and whose thickness is "t". The wall is being loaded normal to its face by a uniform load "p", but is prevented from moving parallel to its face. In other words, it is undergoing arching with the forces at points A and C composed of forces "H" applied parallel to its face; and forces "R_{VL}" normal to its face. ("R_L" and "R_R" are the resultant forces.) The wall is cracked a distance "x" from one end at point B. Points D and E mark the wall centerline.

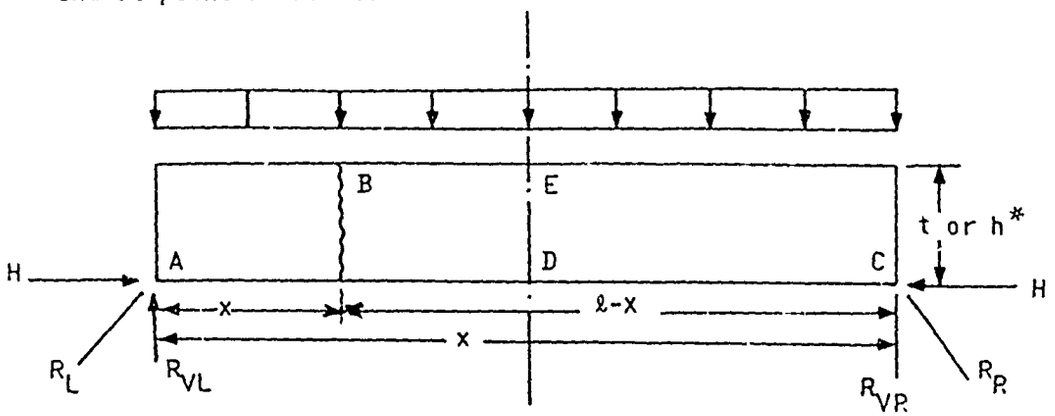

Forces on the two parts of the wall are as shown below.

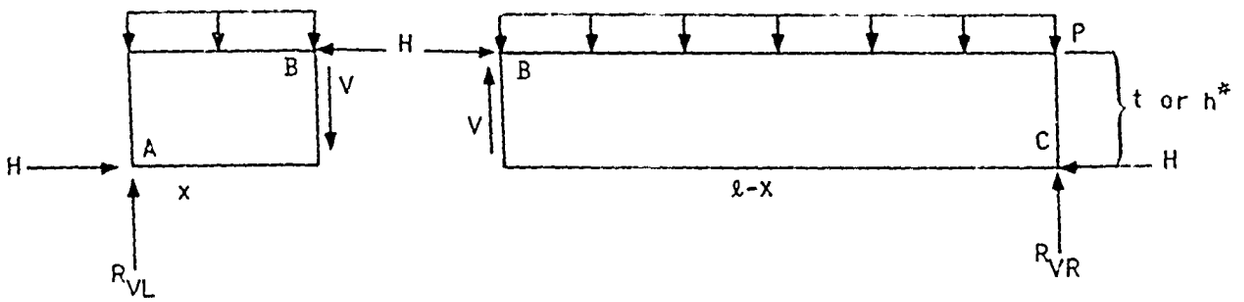

* If crushing occurs at A, B, or C as a result of application of these forces, the distance, "h" between lines of application of force H at A and B on the left free body, or at points B and C on the right free body will be less than the wall thickness "t".

The relationships between these forces are

$$H = (px/2h)\ (\ell - x)$$

$$R_{VL} = R_{VR} = p\ell/2$$

$$V = (p/2)\ (\ell - 2x)$$

$$R_L = R_R = \frac{p}{2}\sqrt{\left[x^2\ (\ell-x)^2/h^2\right]\ell^2}$$

The third equation above shows that if $x = \ell/2$, that is, if the crack is located in the center of the wall, V=0. There are no shear forces along the crack, and all phenomena are those of rigid arching discussed earlier. If, however, $x \neq \ell/2$, $V \neq 0$. The free body diagram of the portion of the wall with length $>\ell/2$ is shown below.

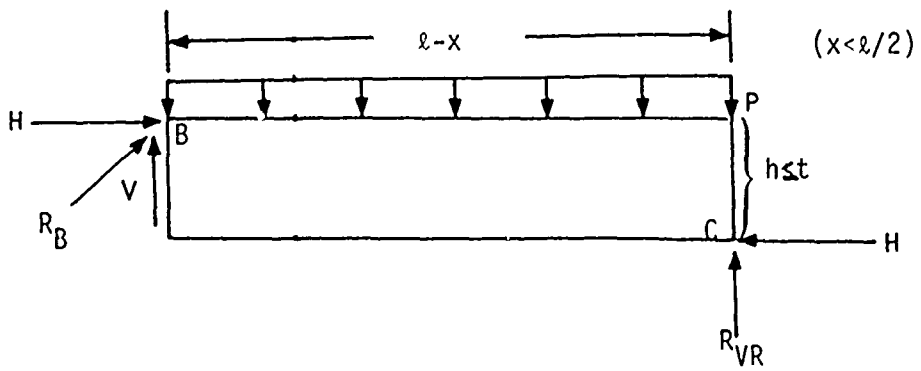

Note that $R_B = \sqrt{(H^2 + V^2)}$ is directed away from the body in a manner that would tend to encourage spalling similar to that for gapped arching. This means that this portion of the wall has thrust lines outside the body as sketched below.

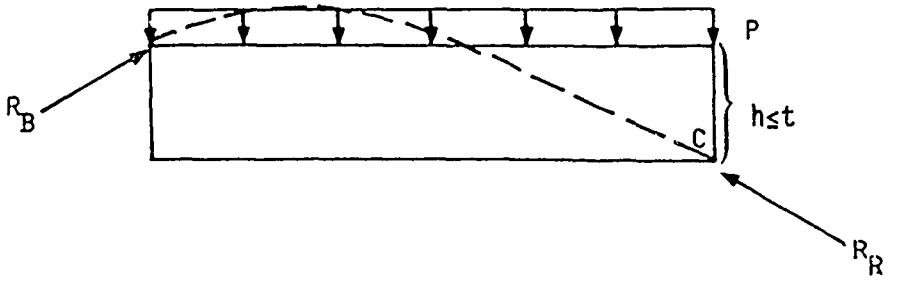

This body can fail in one of two ways: in bending at the point of maximum moment; or in spalling at the point of application of R_B, that is, spalling due to application of a line load. Previous work suggests that the line load spalling will occur, because the line load capacity for this outward directed force is likely to be less than the tensile strength of the material. To determine how much less, we must first consider the bending problem and determine what the maximum tensile force is.

Consider the following sketch with z being an arbitrary distance from the crack.

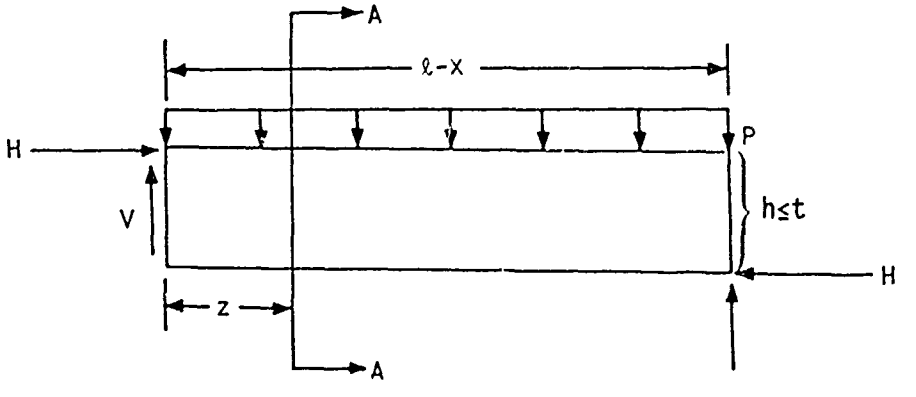

$$H = \frac{px}{2h}(\ell - x)$$

$$V = \frac{p}{2}(\ell - 2x)$$

$$\ell - x > \ell/2$$

At section AA, the bending moment, M, is:

$$M = +H\frac{h}{2} + Vz - \frac{pz^2}{2}$$

$$M = \frac{p}{2}\left[(\ell - 2x)z + \frac{x}{2}(\ell - x) - z^2\right]$$

The maximum fiber stress at section AA, f_t, is given by

$$f_t = \frac{6M}{t^2} - \frac{H}{t}$$

$$f_t = \frac{p}{t^2}\left[3(\ell - 2x)z + x(\ell - x) - 3z^2\right]$$

where 'h' is assumed to be equal to 't' (a conservative assumption for tension).

In order to locate the maximum stress, take the derivative of f_t with respect to z and set it equal to zero.

$$\frac{\partial f_t}{\partial z} = \left[p/t^2\right]\left[3(\ell - 2x) - 6z\right] = 0$$

or

$$z = \tfrac{1}{2}(\ell - 2x)$$

This value of z is the center line of the wall, which can most easily be seen by finding the distance of z from the right end of the wall, i.e. $(\ell - x) - z$.

Thus, wherever the crack, the maximum stress occurs at the wall center line. A sketch of the wall, with the thrust line (shown by the dashed line) in keeping with the preceding discussion, is shown below. Note that the line is parallel to the wall face at the center line.

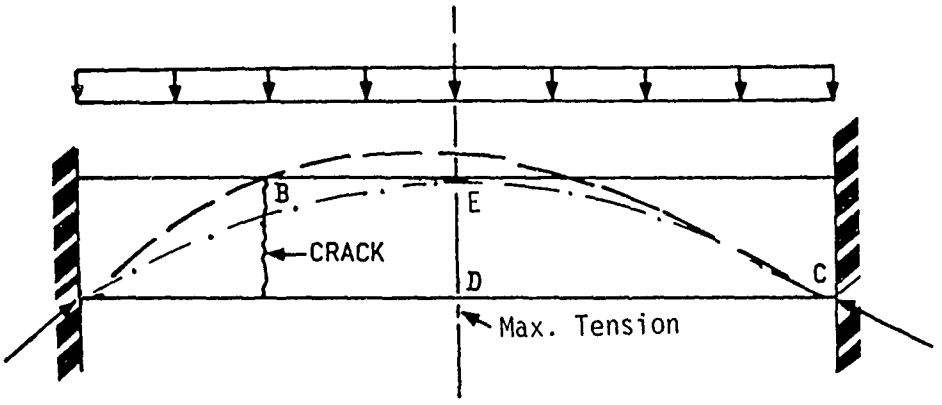

The actual stress at the wall center line is dependent on the location of the crack; it is least if the crack is at the center line, in which case f_t max. = $(1/4)p(\ell/t)^2$, and increases to a maximum when the crack is at the edge of the wall where $(3/4)p(\ell/t)^2$. However, the preceding diagram suggests that as soon as the tensile strength at D is exceeded, conditions will revert to those of rigid arching in which a tensile crack occurs at the center line, and a hinge forms at E. That is, although the initial hinges are at A, B, and D, high tensile forces at the center line could cause a flexural crack to occur at D. If this happens the crack at B must close.

In rigid arching, the line of action of the force at the central hinge point (point E in the preceding diagram) is parallel to the face of the wall. (See the dotted thrust line.) At that point there are no outward directed forces that would encourage spalling as there are in gapped arching, and as there

would be at point B before tensile failure at the wall center line resulted in rigid arching. This suggests more strongly that the lower bound strength for a cracked arch would be dictated by a line load type of failure at hinge B.

TESTS ON REINFORCED BRICK WALLS

During the period covered by this report, the shock tunnel tests were conducted on an important class of walls -- reinforced brick -- not hitherto tested. Only two such walls were tested. Both were 8 in. thick and mounted as simple beams (supported at the top and bottom). They were exterior walls; that is, they were not located behind a window or door opening in the shock tunnel.

The overpressure levels used for the tests were clearly very near the threshold values for wall failure. One wall was subjected to an overpressure (about 1 psi incident) below failure level -- the wall cracked, but did not fail -- and then to a second overpressure (about 2 psi incident) that resulted in failure though in very little debris translation. The second wall was tested only at 2 psi incident level, and it too failed, though again with little debris translation.

These walls were considerably stronger than unreinforced walls, a conclusion that must be inferred from tests on preloaded unreinforced walls mounted as beams. (Non preloaded walls were not tested at incident pressures below 1.5 psi, and at about this incident pressure the failure threshold was

clearly exceeded.) However, three 8-in. thick walls were mounted as beams and preloaded to 16,500 lb (the equivalent of a two-story curtain wall atop the test wall) and 23,500 lb (the equivalent of a three-story curtain wall). These walls were subjected to incident pressure pulses of 0.75 psi, which was evidently quite close to the threshold value of pressure for wall failure. One wall, preloaded 16,500 lb, cracked but did not come out of the frame when first struck with the 0.75 incident pulse, then collapsed when struck again. A second wall with the same preload collapsed when first struck with the 0.75 psi pulse. The third wall, preloaded to 23,500 lb, cracked its full width but did not collapse. (It was not loaded a second time.)

The analysis of preloading of walls given in Ref. 5 indicates that its effect is to increase wall resistance some 10 to 20%. However, even without this added effect, the threshold failure pressure for the reinforced brick walls (below 2 psi, but above 1 psi) is larger than the apparent threshold value (0.75 psi) for the unreinforced walls. In neither test did any of the reinforcing rods fail, through they were very severely strained, and the individual pieces of debris, still connected to each other, were quite large (see Fig. 2-3). Additional test details are given in Appendix A.

Fig. 2-3. Debris from Wall Number 99.

Section 3

DEBRIS FROM INTERIOR WALLS

Section 3

DEBRIS FROM INTERIOR WALLS

In this section the tests conducted in the Shock Tunnel on full scale interior partition walls are first described and summarized. Following this, an analytical technique for predicting debris characteristics is presented, and predicted and measured results are compared. The section ends with a brief discussion of the problem of predicting debris velocities caused by nuclear weapons.

TEST PROGRAM

Tests were conducted on sheetrock, concrete block, and clay tile interior walls. The primary data gathered was initial fragment size and early time velocity of these fragments. A summary of these tests is presented in Table 3-1

These walls were tested at two locations in the Shock Tunnel shown in Fig. 3-1. The first was at a point within the tunnel, Location A (approximately 100 ft from the mouth of the compression chamber), and the second, at the end of the tunnel, Location B (approximately 138 ft from the mouth of the compression chamber). A few of the sheetrock wall panels were tested at Location A to allow comparison of results with some previous debris tests conducted at this location in the tunnel. However, at this location it is difficult to obtain good movies of the failing wall as it translates down the tunnel and as shown in Fig. 3-1 there is a bend in the tunnel,

TABLE 3-1

Summary of Tests

Sheet Rock Wall Tests

4-in. Sheetrock; timber stud; interior; solid (with no opening).

Test Number	Mounting Location	Peak Incident Overpressure (psi) (3)
101	A	3.5 (4.9)
102	B	1.7 (2.0)
106	B	3.8 (6.0)
110	B	3.8 (6.0)

4-in. Sheetrock; timber stud; interior; with doorway opening.

111 (1)	B	3.9 (6.0)
112 (2)	B	3.8 (6.0)

4-in. Sheetrock; metal stud; interior; solid walls (with no opening).

103	B	1.8 (2.0)
104	A	1.8 (2.0)
105	A	3.5 (6.0)
107	B	3.9 (6.0)

4-in. Sheetrock; metal stud; interior; with doorway opening.

113 (1)	B	1.7 (2.0)
114 (1)	B	3.8 (6.0)

Note: 1 Door closed
2 Door open
3 Quoted values measured in room. Value in parenthesis is estimated value in front of a nonfailing wall with a 27% open window.

TABLE 3-1 (cont.)

Concrete Block Wall Tests

8-in. Concrete block; interior; solid (with no openings).

Test Number	Mounting Location	Peak Incident Overpressure (psi) (3)
108	B	3.6 (6.0)
109	B	4.0 (6.0)
115 (4)	A	4.1 (6.0)
116 (4)	A	1.7 (2.0)
117	B	3.8 (6.0)

8-in. Concrete block; interior; with doorway opening.

118	B	3.6 (6.0)

Clay Tile Wall Tests

6-in. Clay tile; interior; solid (with no opening).

119	B	1.6 (2.0)
120	B	3.9 (6.0)

Note: 3 See previous page.
4 Gapped arched mounting condition.

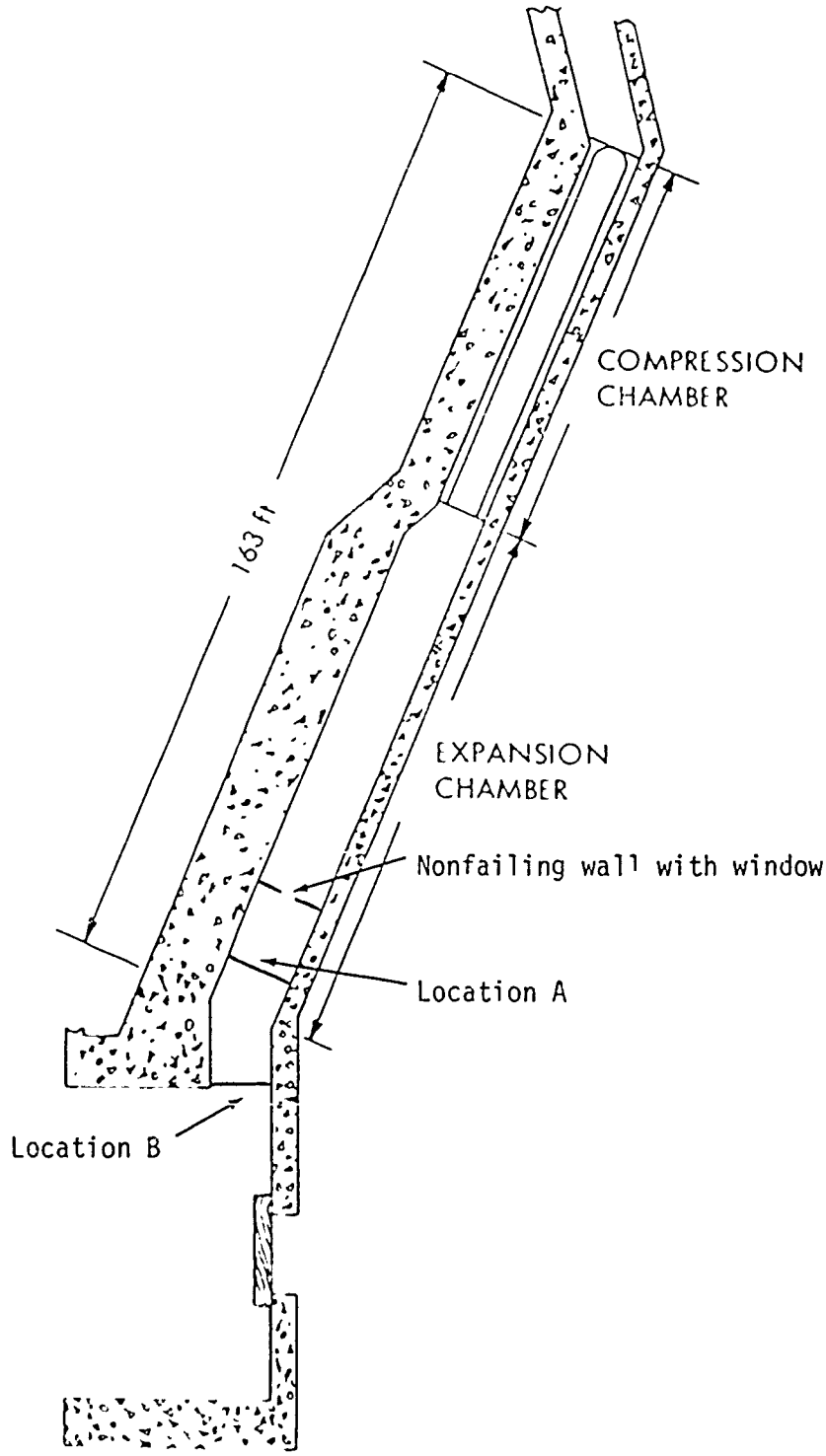

Fig. 3-1 . Plan of Shock Tunnel

approximately nine ft behind the wall. Impact with this obstacle changes the character of the translating debris and prevents further gathering of useful data. For these reasons the majority of the wall panels were tested at Location B at the end of the Shock Tunnel. Here the failing walls can travel approximately 50 ft before impact with the far wall of the casemate; in addition it is relatively easy to obtain good movies of wall motion. The general behavior of the walls at Locations A and B appeared to be the same, suggesting that the blast loadings at the two locations were not far different.

The wall panels were tested behind a nonfailing wall panel with a 27% window opening. A photograph of this wall in place in the Shock Tunnel is shown in Appendix A (Fig. A-2). Also presented in this appendix are the detailed test reports and pre and posttest photographs of each test. The remainder of this section will be concerned with a summary of results from each type of wall investigated.

Sheetrock Walls

A total of twelve sheetrock walls were investigated during this program, one half constructed using wood studs and one half using metal studs. These walls were supported in the Shock Tunnel as plates, i.e. with the perimeter members nailed to the rigid concrete walls of the tunnel.

There were some significant differences between the mode of break-up between the timber stud and metal stud walls, although both types seemed to

"punch out" of the support frame as a single unit.

In the case of the timber stud walls at the lower incident overpressure values (< 2 psi) the walls remained essentially intact as they translated. There was some separation of the sheetrock from the studs and sizable cracks were noted at the joints in the sheetrock. The debris from these walls remained in relatively large pieces as noted in Fig. 3-2, posttest photographs of wall 102 (peak incident overpressure 1.7 psi).

In the tests at higher overpressures (> 3.5 psi) the sheetrock separated from the wood studs early in the translation process and in most cases the wall was partially or wholly disintegrated soon after leaving the support frame. Typical debris from these tests is shown in Fig. 3-3, posttest photographs of wall 106 (peak incident overpressure 3.8 psi).

In the case of the sheetrock walls with metal studs, the walls tended to remain almost entirely intact as they translated across the casemate and the resulting debris for all pressure levels tended to be in one, large, approximately wall-size piece. Any break-up was caused by impact with the wall of the casemate. This can be noted in Fig. 3-4, posttest photographs of wall 113 (peak incident overpressure 1.7 psi) and Fig. 3-5, posttest photographs of wall 107 (peak incident overpressure 3.9 psi).

Data on displacement as a function of time for each of the sheetrock walls was obtained from the motion picture films and is presented in Appen-

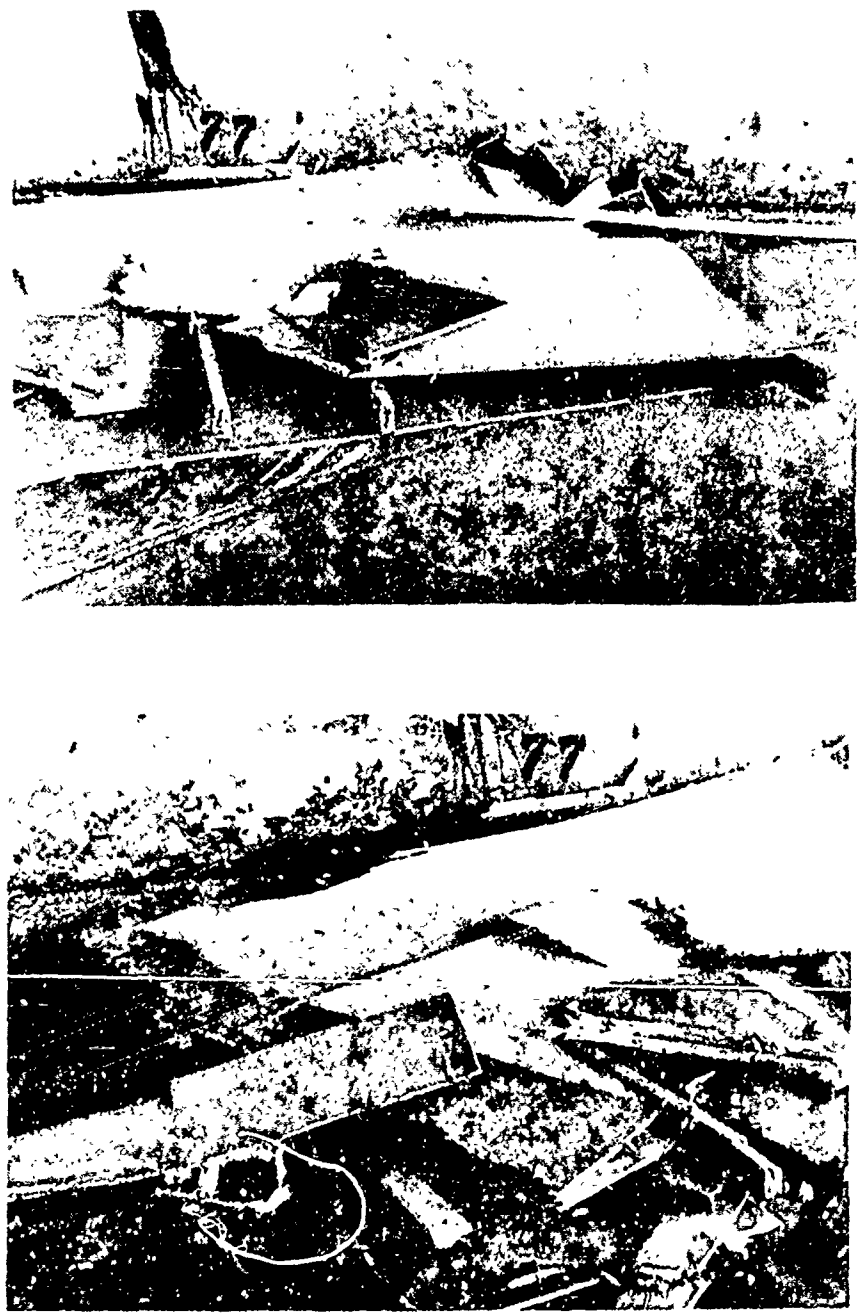

Fig. 3-2. Posttest Photographs, Wall 102.

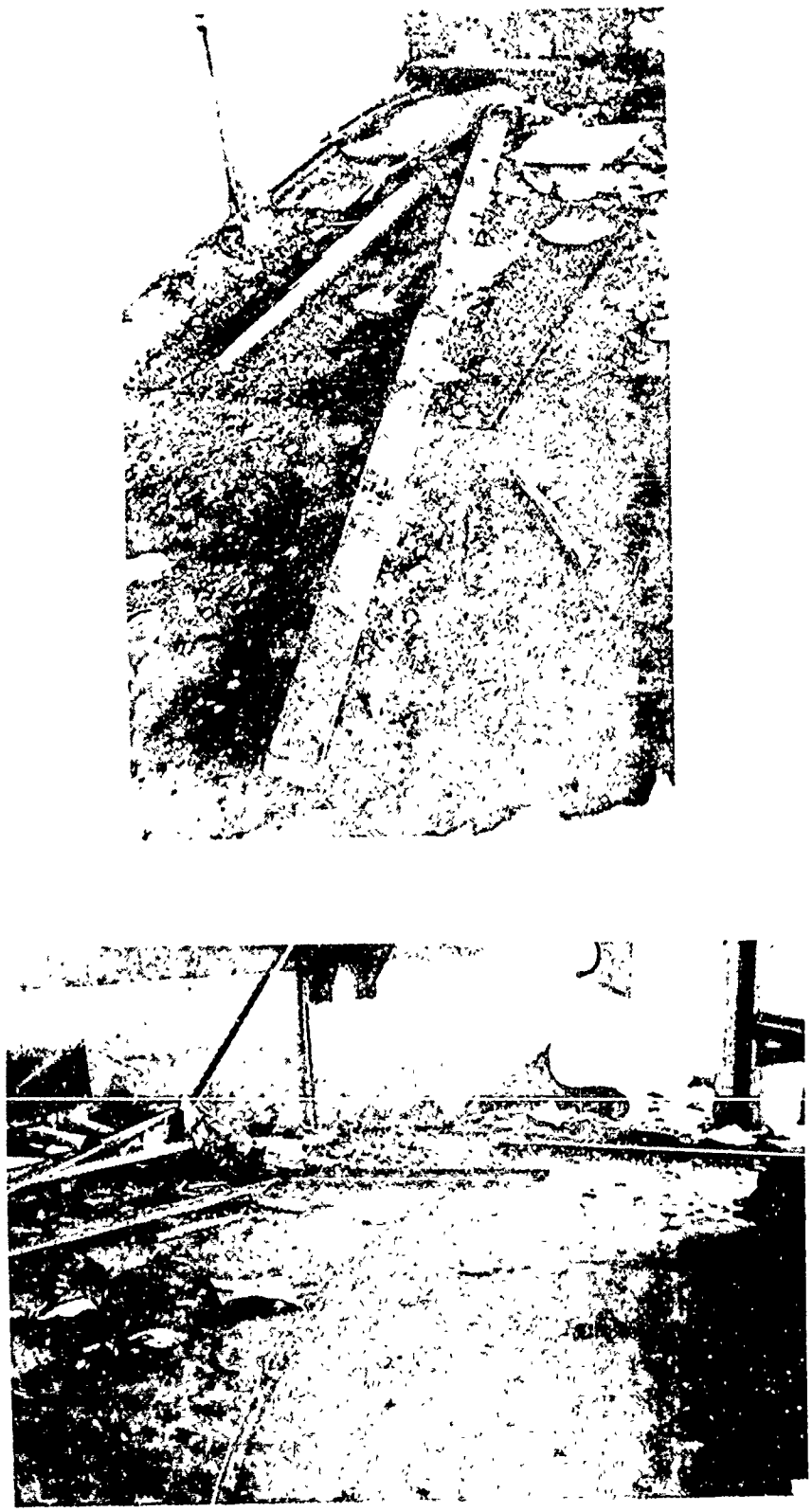

Fig. 3-3. Posttest Photographs, [illegible]

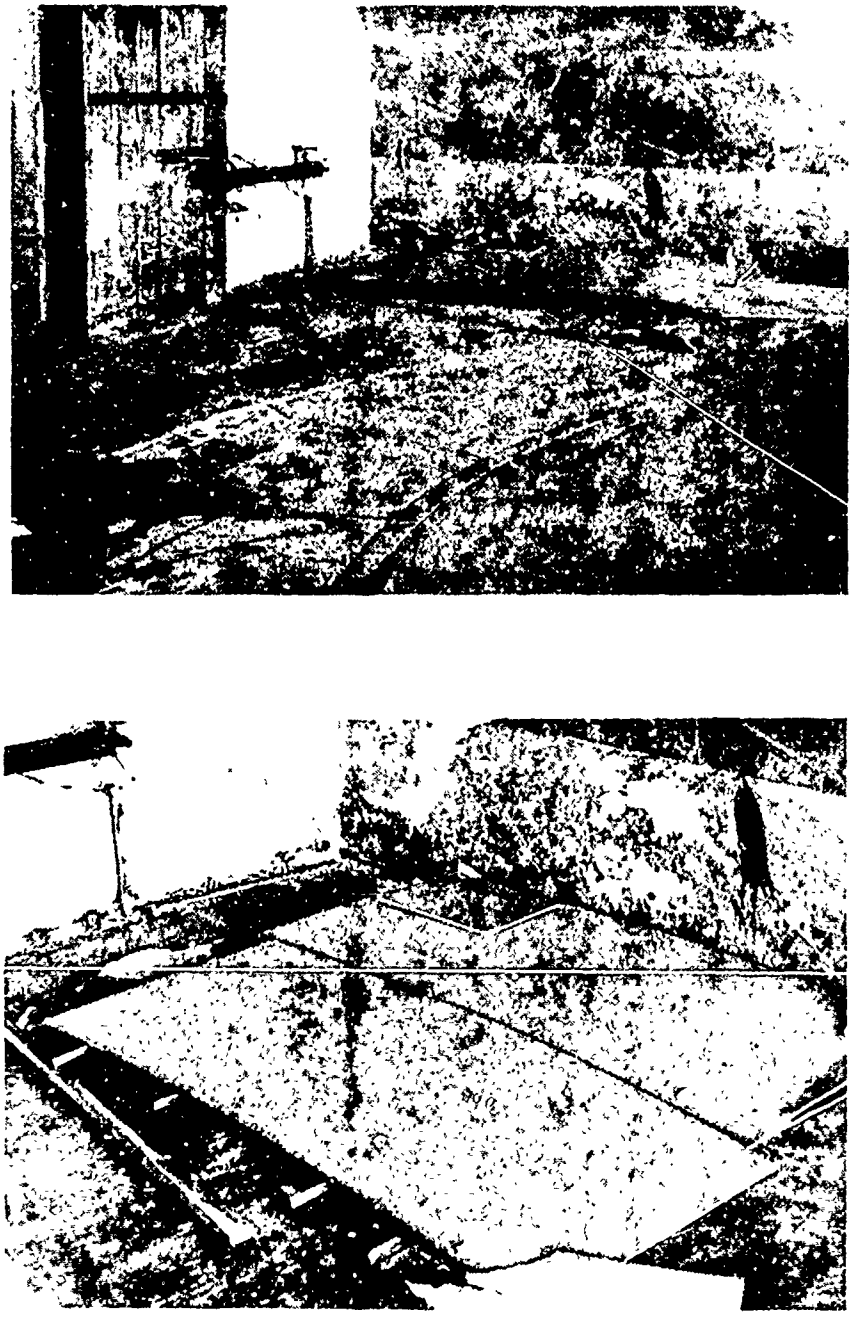

Fig. 3-4. Posttest Photographs, Wall Number 113.

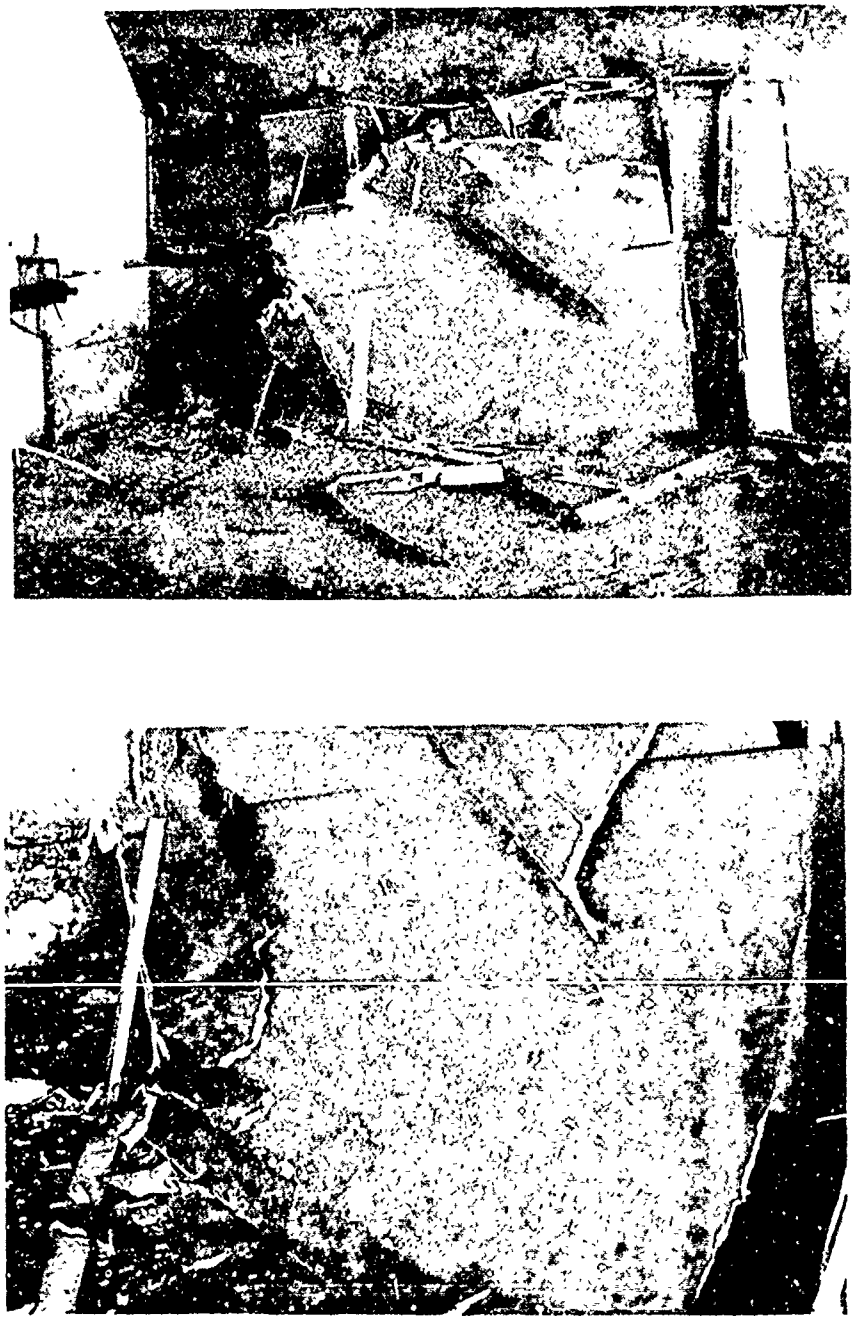

Fig. 3-5. Posttest Photographs, Wall Number 107

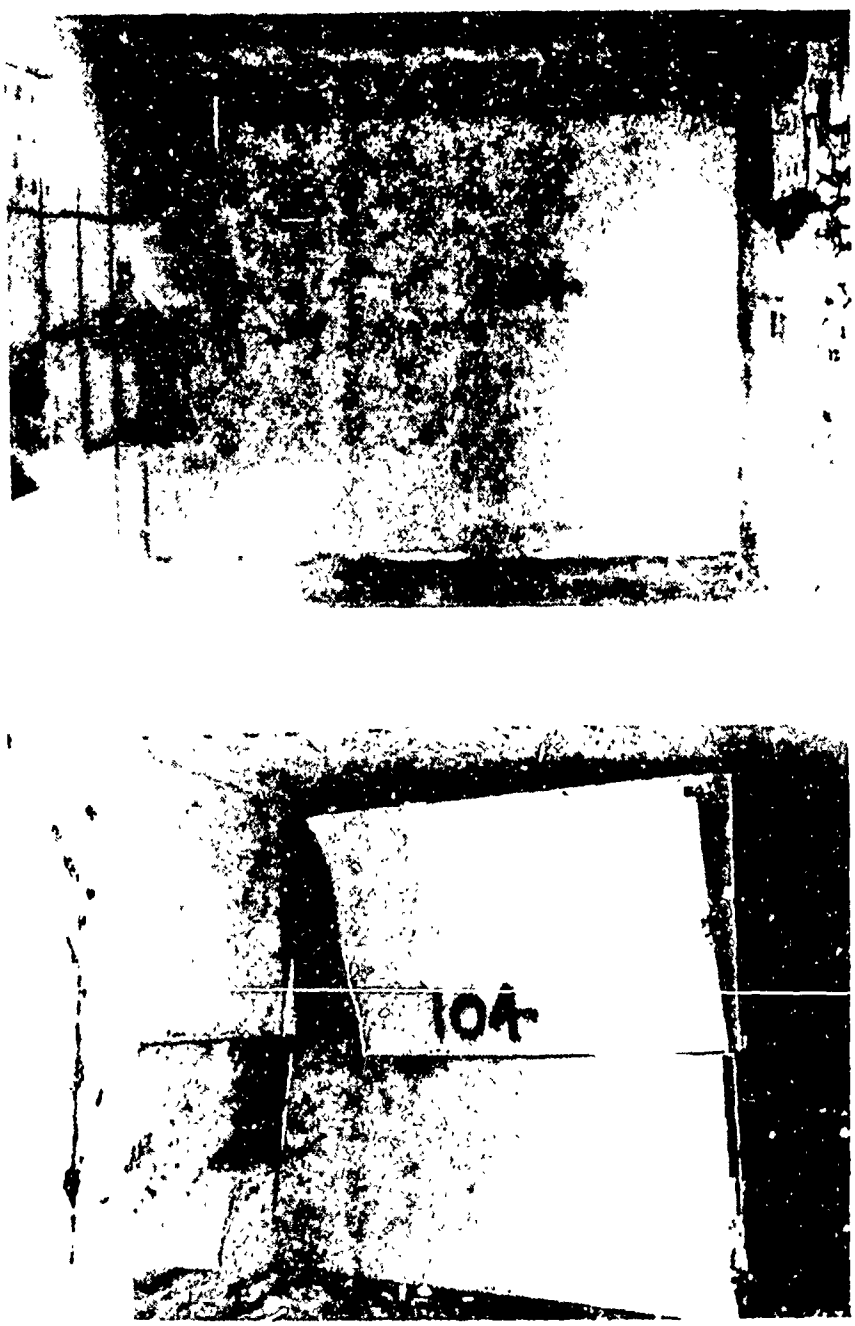

Fig. 3-6. Pre and Posttest Photographs, Wall Number 104.

dix A. This data was measured from time of first visible motion of the wall. Times for wall displacements were determined at 6-in. intervals for a distance of six feet when possible. (In some tests, particularly at Location A, the wall was obscured by dust after moving a distance of only 3 to 3.5 ft.)

This data from the tests conducted at Location B is summarized in Fig. 3-7 (tests 102, 103, and 113 conducted at overpressure loads of 1.7 and 1.8 psi) and in Fig. 3-8 (tests 110, 107, 111,112, and 114 conducted at overpressure levels of 3.5 to 3.9 psi). The calculated average velocity after a travel distance of approximately two feet is presented in Table 3-2. It will be noted that the data for the lower overpressure tests is quite consistant with values of 100 to 105 ft/sec for solid walls with both timber and metal studs and for a metal stud wall with a closed doorway opening.

The data for the higher overpressure tests is also quite consistent with the exception of test 110 (140 ft/sec) which is about 15% lower than tests 107 (166 ft/sec), 114 (156 ft/sec), and test 112 (155 ft/sec).

Concrete Block Walls

Six concrete block walls were investigated during this program, see Summary Table 3-2. Two of these (wall numbers 115 and 116) were gapped arched, a support condition which is discussed in detail in Section 2. The remaining four were supported as cantilever beams, fixed to the floor with the top and sides free to move. This is a typical support condition for interior walls in large buildings that have false ceilings for heating, lighting, and other

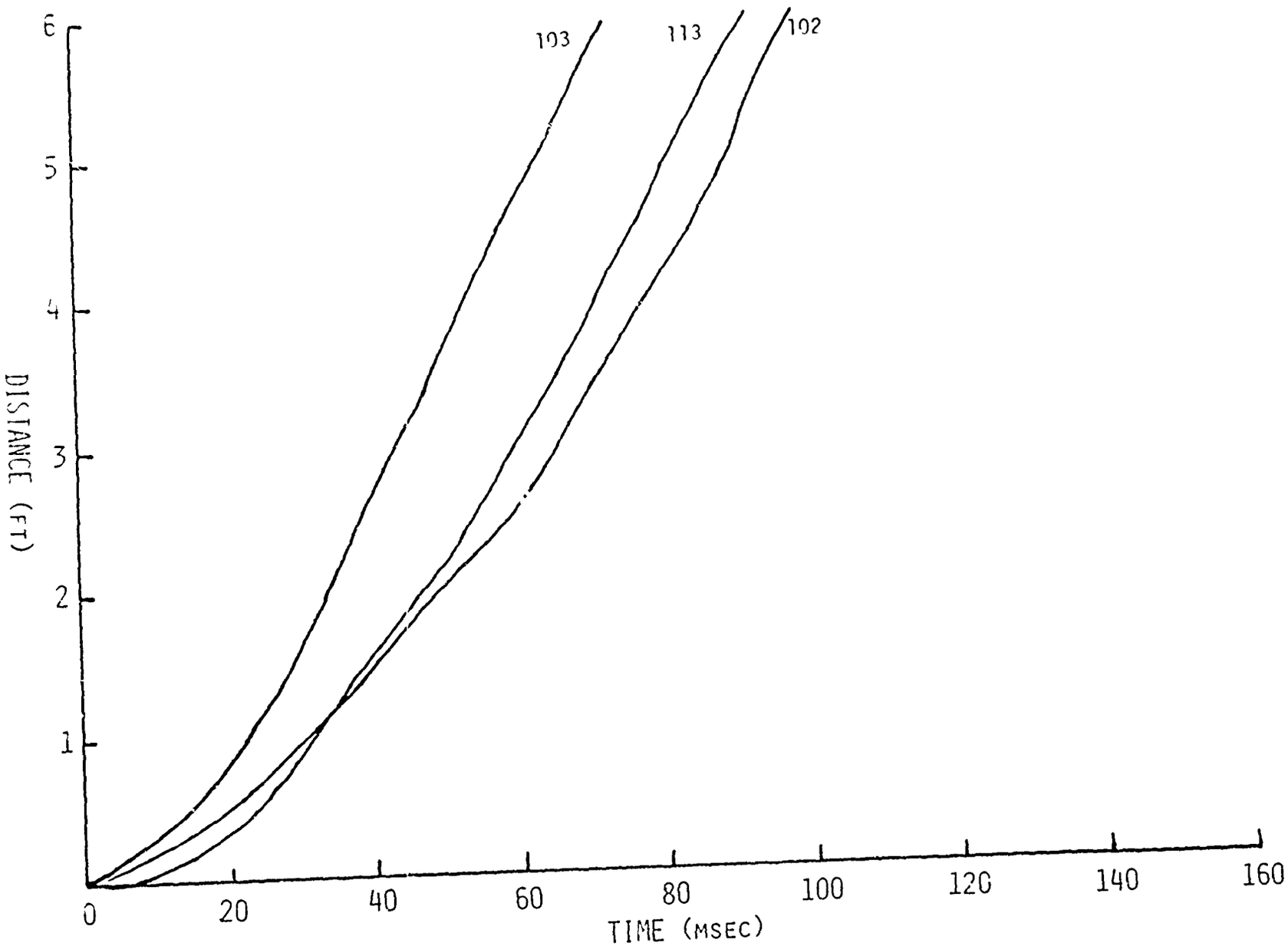

Fig.3-7 Displacement as a function of time, Wall numbers 102, 103, and 113.

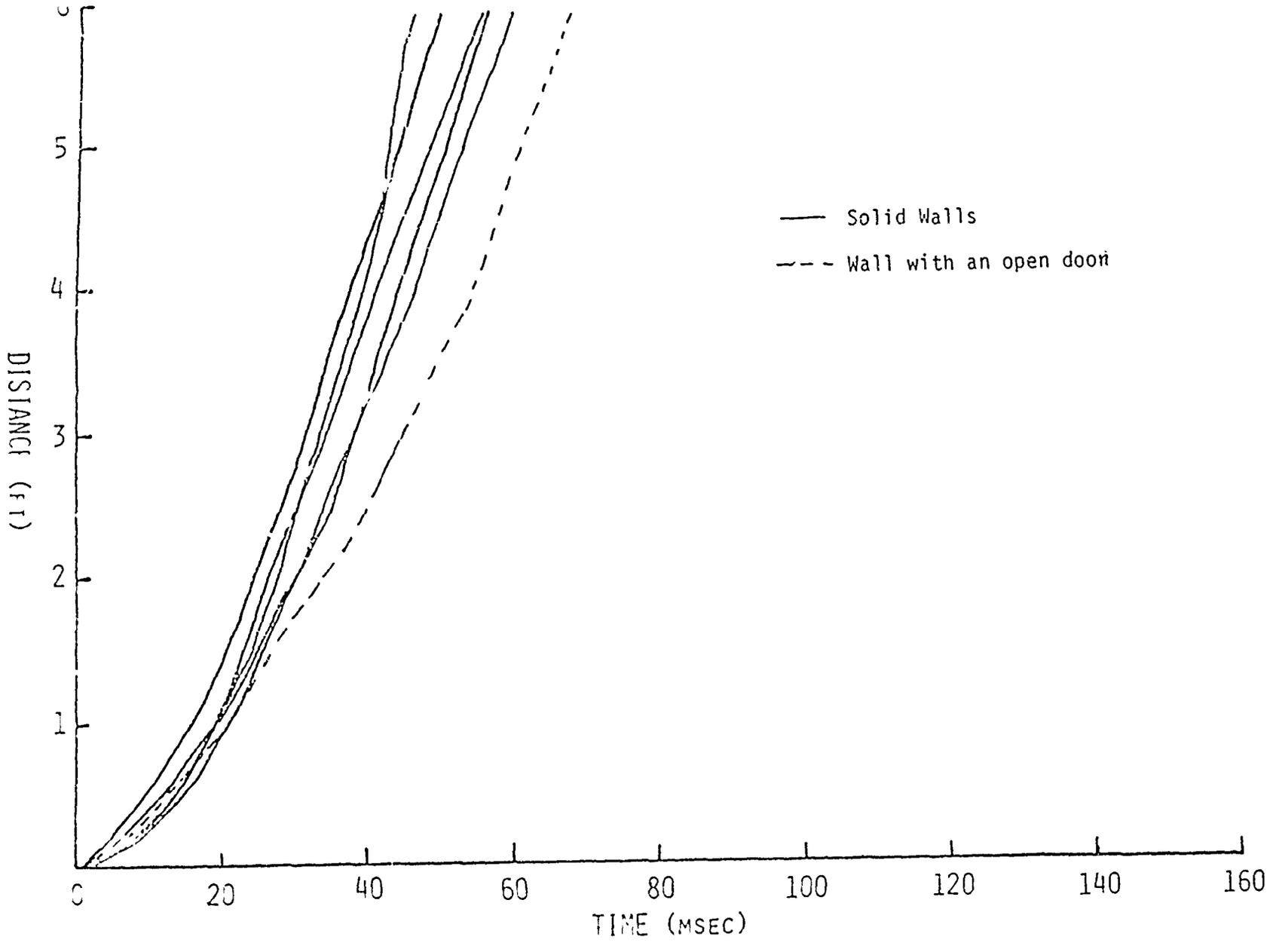

Fig. 3-8 Displacement as a function of time, Wall numbers 106, 107, 110, 112 and 114.

TABLE 3-2

Summary of Velocity Data

Sheetrock Walls

Type	Wall Number	Peak Incident Overpressure (psi)	Velocity ft/sec
Timber stud (solid)	102	1.7	90
" " "	106	3.8	167
" " "	110	3.8	140
Timber stud (door open)	112	3.8	155
Metal stud (solid)	103	1.8	100
" " "	107	3.9	166
Metal stud (door closed)	113	1.7	100
Metal stud (door closed)	114	3.8	156

services. Three of these (wall numbers 108, 109, and 117) were solid walls with no openings) and were enclosed in a light-weight steel "picture frame" support for construction and handling purposes. A four-inch gap was left at the top of these walls and a two-inch gap was left at each side. The fourth wall (number 118) contained a doorway opening, was not enclosed in the picture frame, and had a six inch gap at the top and two-inch gaps at the sides. Pre and posttest photographs of each of these two types of cantilever walls are shown in Fig. 3-9.

Of the gapped arched walls, wall number 115 (tested at a peak incident overpressure of 4.1 psi) had several large pieces of debris (each containing 8-10 blocks) which translated between 40 and 50 ft before impacting the ground. Wall number 116 (tested at a peak incident overpressure of 1.7 psi) completely disintegrated and struck the tunnel floor within the first 20 to 25 ft. A minimum amount of debris scattered as far as 90 ft but almost all (approximately 90%) remained within 25 ft of the mounting location. Posttest photographs of the debris from this test are noted in Fig. 3-10.

The cantilever walls, 108, 109, and 117 were all tested at about the same overpressure level (3.6 to 4 psi). The failure patterns, however, were quite different between wall 108 and walls 109 and 117. Wall 108 had initial cracks between the third, fourth, and fifth rows (the wall is eleven rows high) and completely disintegrated early in the failure process. Wall 109

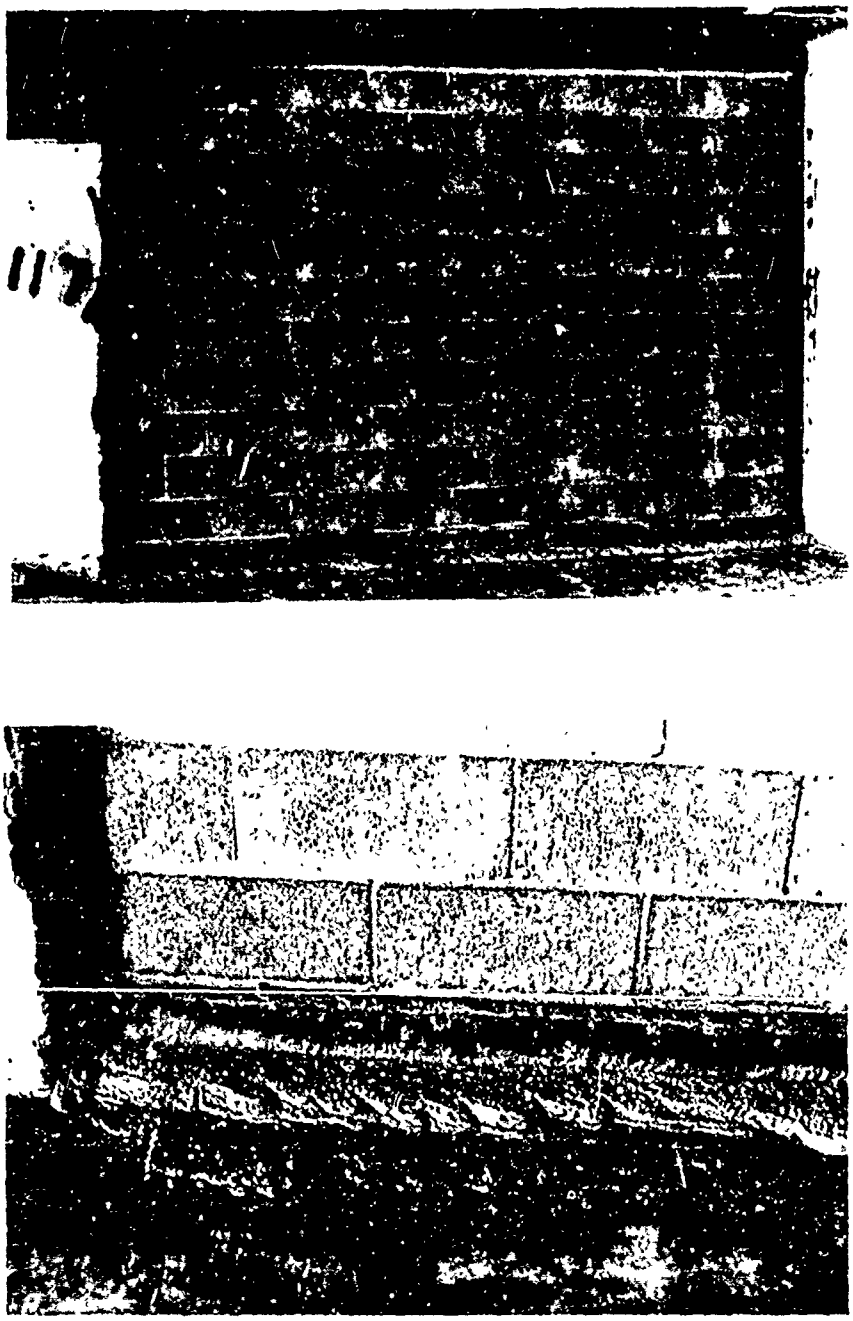

Fig. 3-9. Pretest Photographs, Walls Number 117 and 118.

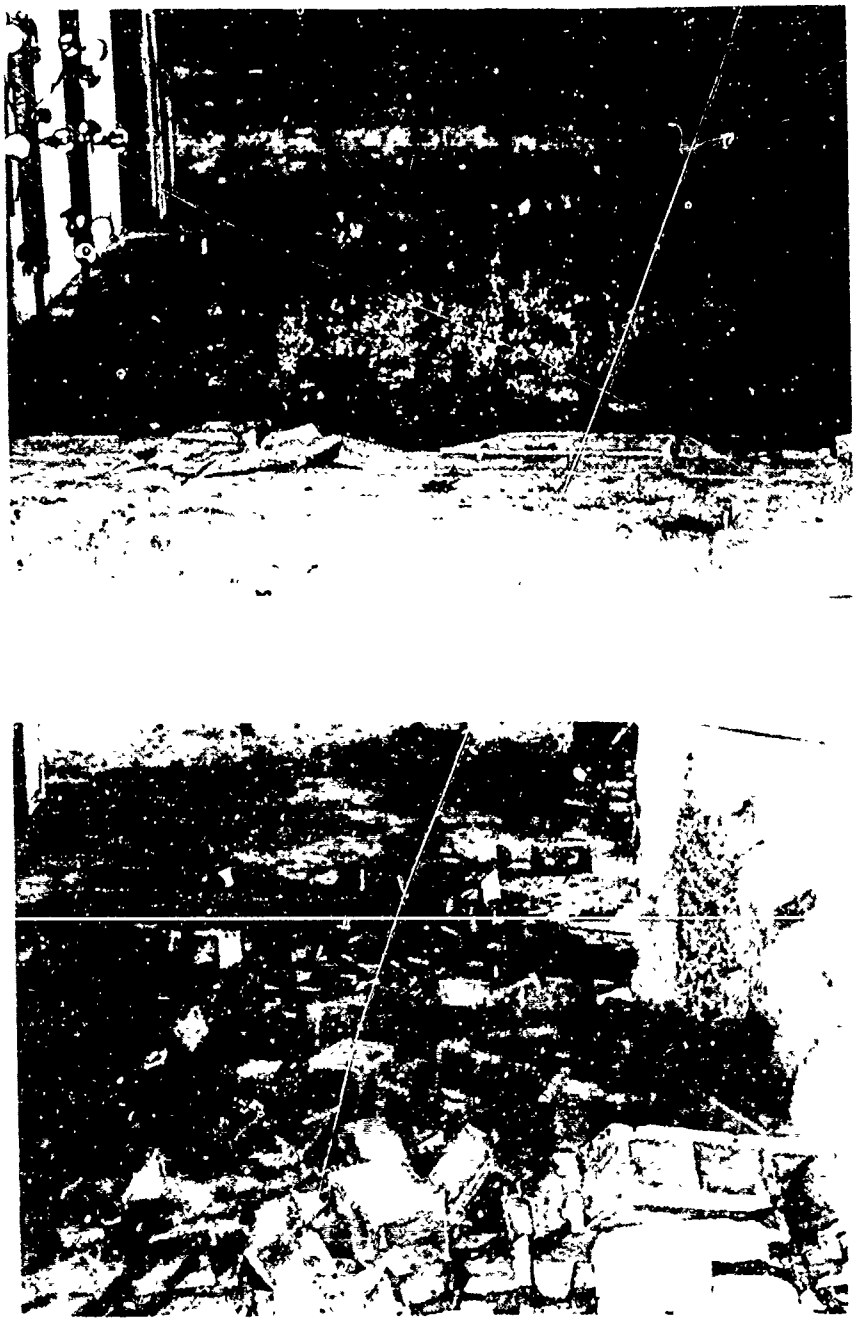

Fig. 3-10. Posttest Photographs, Wall Number 116.

had initial cracks between the third and fourth and the sixth and seventh rows. The lower section, three blocks high, fell over and impacted the floor. The top section (five blocks high and almost the width of the wall) did not appear to break up until impact approximately 40 ft across the casemate. The middle section, three blocks high and about two thirds the width of the wall, remained intact until impact with the floor some distance form the wall. Similarly, wall 117 broke up into a few very large pieces and impact of two thirds of the wall was at distances of 25 to 35 ft from the mounting location. Post-test photographs of the debris from these walls is presented in Figs. 3-11 and 3 12.

The cantilever wall with a doorway (118) was tested at 3.6 psi and failed very similarly to walls 109 and 117, with the top two thirds of the wall impacting at a distance of 25 to 30 ft. Photographs of the debris from this test are presented in Fig. 3-13. Displacement as a function of time data for the tests conducted at Location B are summarized in Fig. 3-14. The velocity data for these tests is presented in Table 3-3. This data tends to confirm the quite different break up mechanism as noted between walls 108, 109, and 117. Wall 108 which indicated more break-up and smaller fragments had a measured velocity of 80 ft/sec. Walls 109 and 117, on the other hand, remained in large pieces and exhibited velocities of 50 and 52 ft/sec. As expected wall 118, which had a doorway opening, which allows for rapid loading relief, indicated a much lower velocity of 38 ft/sec.

Clay Tile Walls

Two clay tile walls (wall number 119 and 120) were tested during this

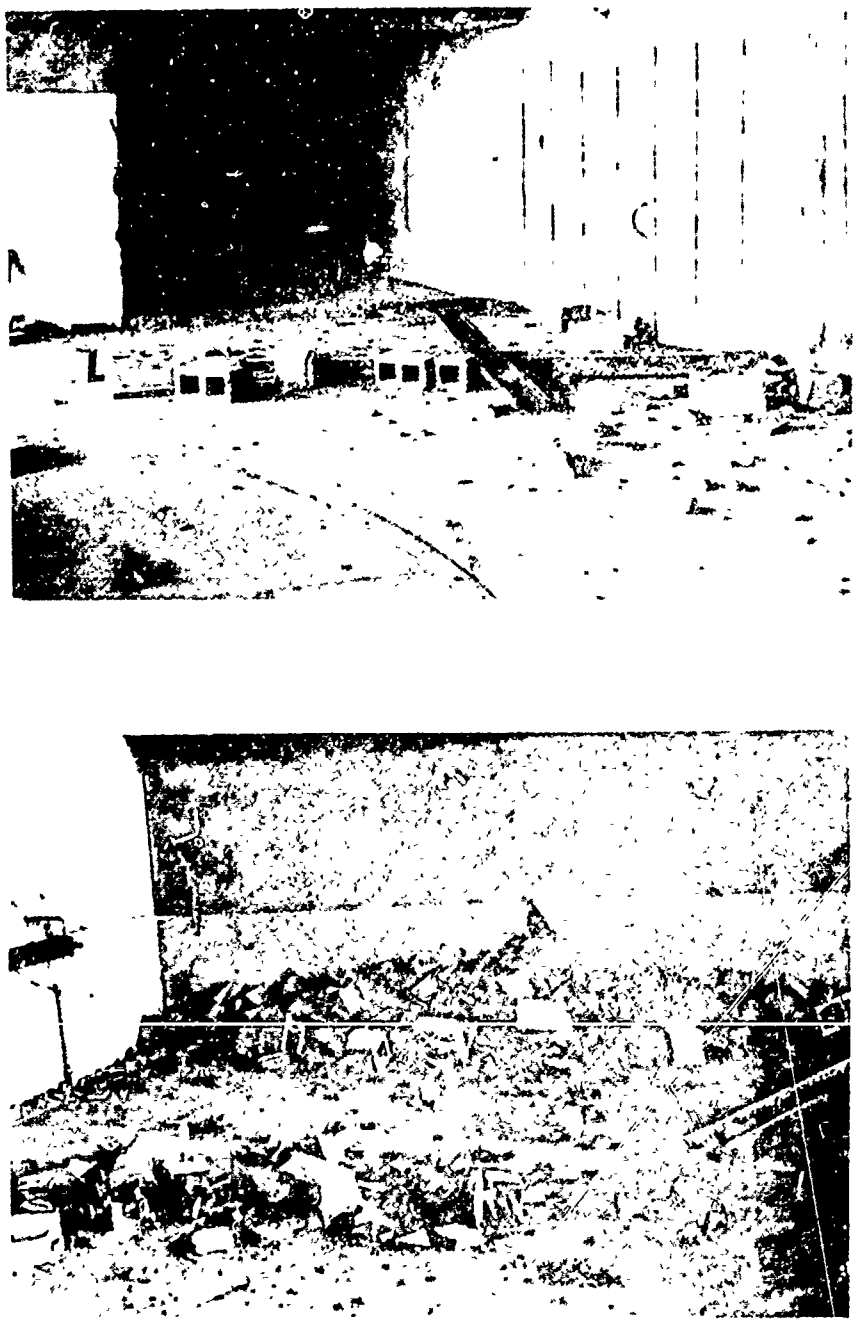

Fig. 3-11. Posttest Photographs, Wall Number [illegible]

Fig. 3-12. Posttest Photographs, Wall Number 117.

Fig. 3-13. Posttest Photographs, Wall Number 118.

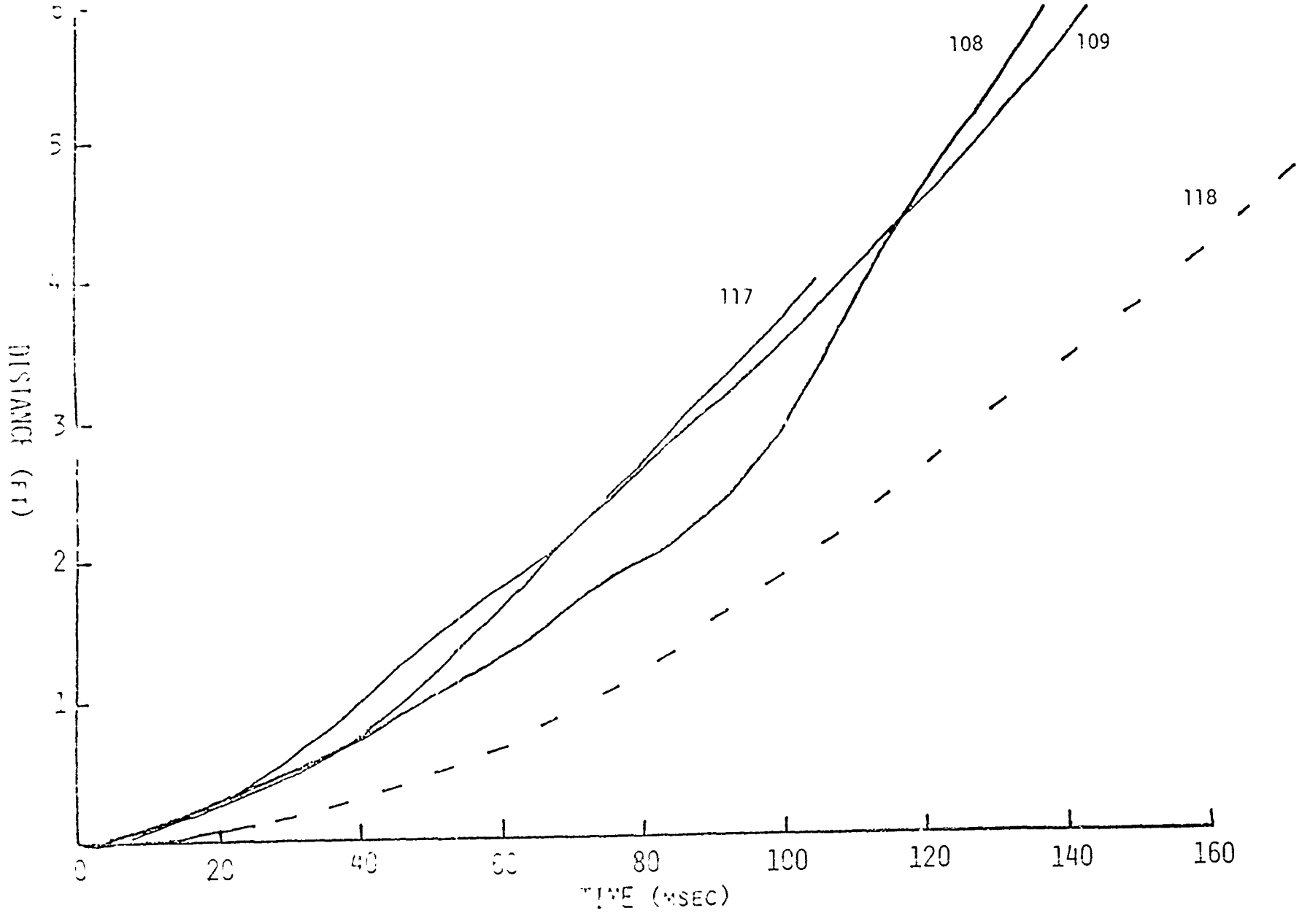

Fig. 3-14. Displacement as a function of time, Wall numbers 108, 109, 117 and 118.

TABLE 3-3

Summary of Velocity Data

Concrete Block Walls

Type	Wall Number	Peak Incident Overpressure (psi)	Velocity ft/sec
Solid Wall	108	3.6	80
" "	109	4.0	50
" "	117	3.8	52
Doorway opening	118	3.6	38

program. They were supported as a cantilever beam, i.e. with the bottom grouted to the floor of the tunnel and with a four inch gap at the top and two inch gaps at the sides. A pretest photograph of one of these walls is presented in Fig. 3-15

Wall number 119 (tested at a peak incident overpressure of 1.6 psi) cracked below center with the bottom piece falling over and striking the floor and with the top section traveling approximately 16 ft before striking the floor and breaking up. It attained a peak velocity of about 16 ft/sec.

Wall 120 (tested at a peak incident overpressure of 3.9 psi) also cracked below center and would probably have failed the same as 119. As this crack opened up, however, the upper part of the wall was forced up more than four inches and struck the top of the tunnel which caused a diagonal crack in the top section. Very little further break-up occured as the top section traveled airborne most of the way across the casemate. It attained a final velocity of about 44 ft/sec. Posttest photographs of the debris of these walls is presented in Fig. 3-16 and Fig. 3-17 and the displacement as a function of time data obtained from the motion picture film is presented in Fig. 3-18.

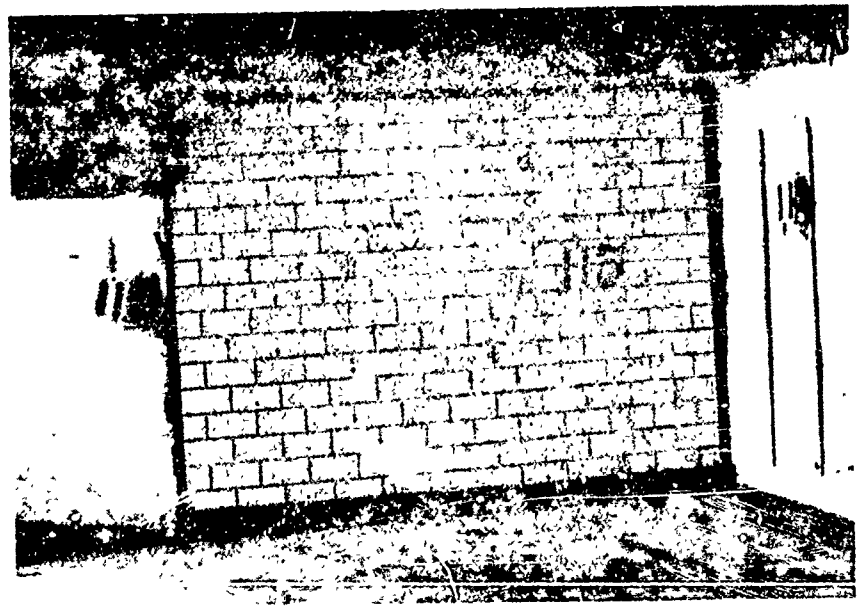

Fig. 3-15. Pretest Photograph, Wall Number 119.

Fig. 3-1h Posttest Photographs, Wall Number 119.

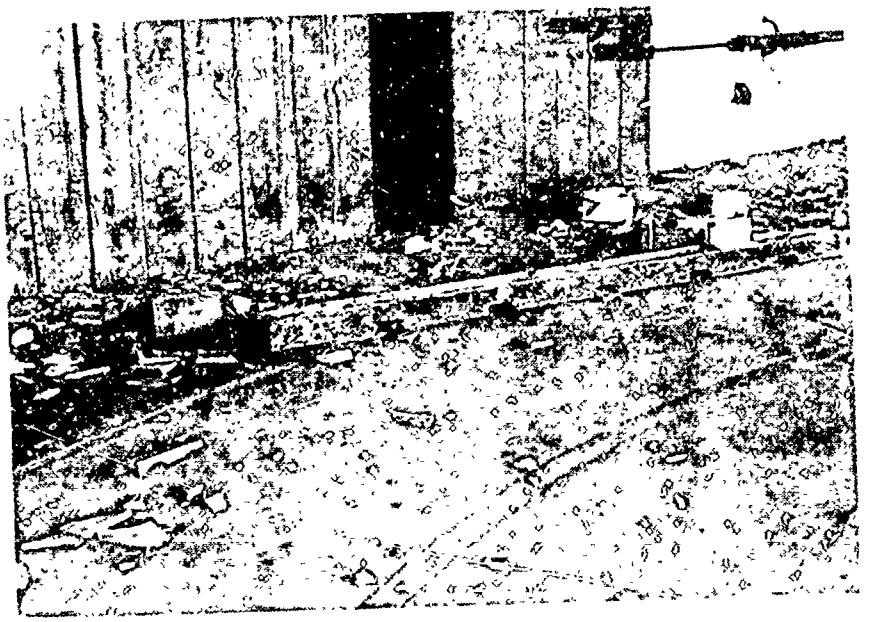

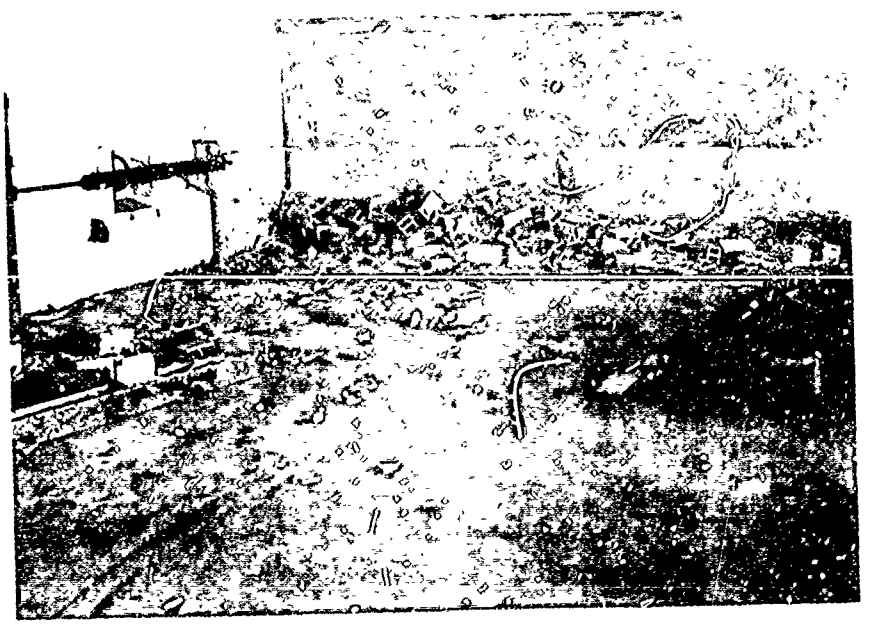

Fig. 3-17. Posttest Photographs, Wall Number 120

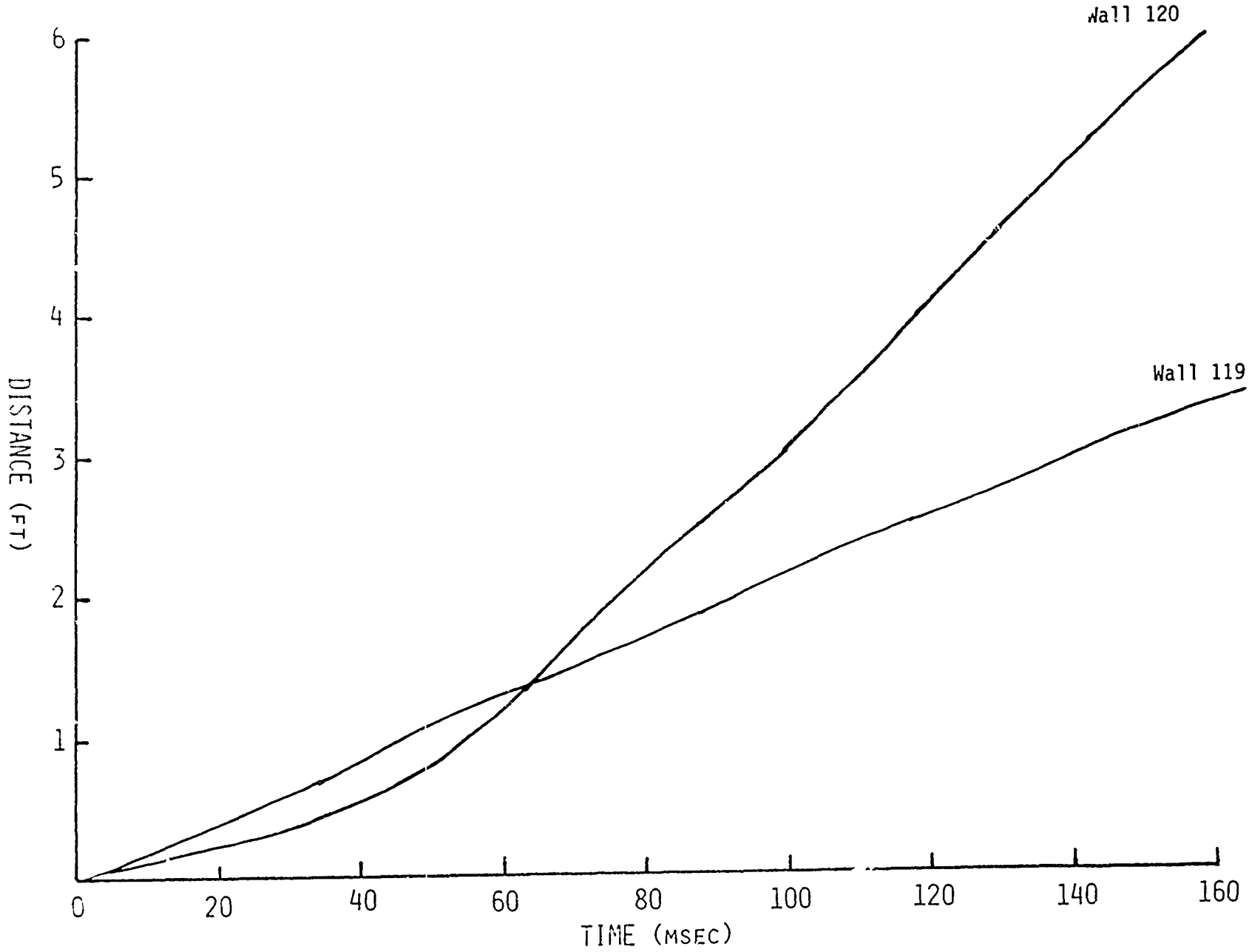

Fig. 3-18 Displacement as a Function of Time, Clay Tile Walls Number 119 and 120.

DEBRIS VELOCITY

General Analytical Considerations

Predictions of the velocities achieved by elements of interior walls accelerated by a blast wave can only be carried out by means of a chronological dynamic analysis of wall response to blast loading, leading from the arrival of the shock front to failure of the wall, its subsequent fragmentation, and finally to the kinematics of the debris.

In order to render such an analysis suitable for practical purposes, fairly simple mathematical models must be generated which, however, have to be sufficiently factual to yield consistently reliable results. In developing pertinent processes and procedures, actual experimental observations must serve as modeling guides, and theoretical results must be carefully tested against field data.

Two types of interior walls were considered: sheetrock-stud walls (both timber and metal studs were used) mounted essentially as plates, that is, supported on all four edges; and concrete block or clay tile walls fixed at the base with a substantial ($\sim$ 4 in.) gap at the top (this being simulant of interior masonry walls that extend from the floor to a false, very light weight ceiling).

Previous tests had indicated that the sheetrock walls tend

to fail as a unit at the supports and move for some distance without excessive fragmentation. When break-up began to occur, the initial pieces were all quite large. (Once such a wall struck the floor, or actually any obstacle, far greater fragmentation took place.)

For the masonry walls, no previous experimental data were available, so an estimate was made of how break-up might occur. The assumptions made are shown in the following sketch.

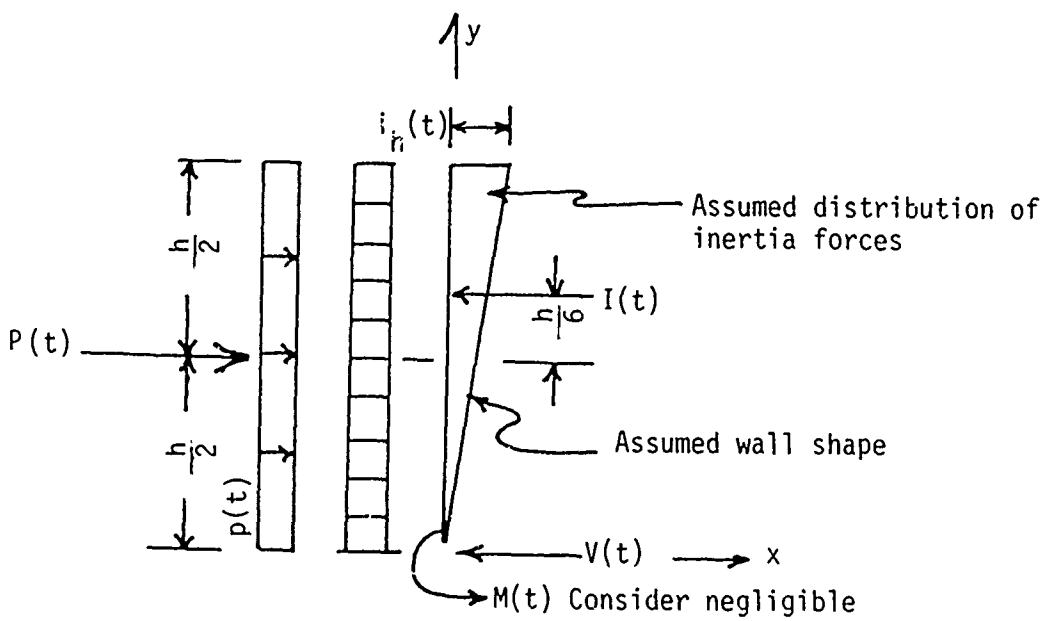

Summing moments about I(t) we have

$$h \cdot p(t) \cdot (h/6) - V(t) \cdot (2h/3) = 0$$

or

$$V(t) = h \cdot p(t)/4$$

Summing forces for static equilibrium we find

$$I = ph\text{-}V = 3ph/4$$

from which,

$$i_h = 3p/2, \text{ or } i_y = 3py/2h$$

Using these values, moments on the wall as a function of y are:

$$M(y) = (hpy/4) - (py^2/2) + (py^3/4h)$$

from which the location and value of the maximum moment can be derived. The location is at

$$y = h/3 = 32 \text{ in.} *$$

and the maximum moment is

$$M \text{ max.} = (p\ h^2)/27 (= 341.3p \text{ for } h = 96 \text{ in.})$$

With a modulus of rupture of 50 psi (approximately the bond strength of the mortar) and a section modulus per unit length, Z , taken as if the wall were solid ($Z = w^2/6$, where w is the width of a block, approximately 5.75 in.), the failure moment of the wall is

$$M_f = 50 \times 12 \times (5.75)^2/6 = 3306 \text{ in. lb/ft}$$

At an incident pressure of about 1.5 psi (lower than the lowest incident pressure used in the Shock Tunnel), the maximum moment upon arrival of the shock front (at which time pressure on the wall would be the peak reflected pressure of about 3 psi) would be

$$M \text{ max} = 341 \times 3 \times 12 = 12{,}276 \text{ in. lb/ft}$$

This is much greater than the failure moment so it is justified to assume that the wall fails instantly with arrival of the shock front.

After wall failure, forces F(t) applied by the blast wave to the failed systems -- i.e. to dynamic systems with zero resistivity -- are used to

* Note that both clay tile and concrete block walls cracked near this distance from the floor of the tunnel.

determine wall element accelerations,

$$a = F(t)/M$$

from which velocities can be calculated.

It should be emphasized that the wall failures discussed above are of a fairly simple type, which facilitates behavior predictions. In more complicated cases, a more complex analysis, based on energy concepts, will be required. Briefly, the energy quantum absorbed by the wall up to fragmentation or failure of the supports must be compared to the work done by the shock front on the wall. If the latter is greater than the former, fragmentation or support failure results. If there is fragmentation, debris of predictable size moves with an initial velocity established by analysis of the wall as a resistive distributed mass system subject to a suddenly applied load. Following failure, the fragments may or may not be subject to further accelerating depending on whether the failure time is less or greater than the decay time for the overpressure. In any case, fragmentation renders the wall non-resistive and acceleration becomes proportional to force. If, on the other hand, there is support failure, the wall immediately becomes non-resistive and accelerates in accordance with the unbalanced pressure on it. In this case, too, there will be fragmentation if the energy quantum absorbed by the wall, vibrating freely after support failure, exceeds a critical value which can be determined.

Debris Velocity Calculation

Calculations of the velocity attained by wall debris at the end of the

loading pulse (i.e. approximately 100 msec) were made using the loading pattern sketched below to accelerate wall elements. The load is applied only to the upstream face of the wall.

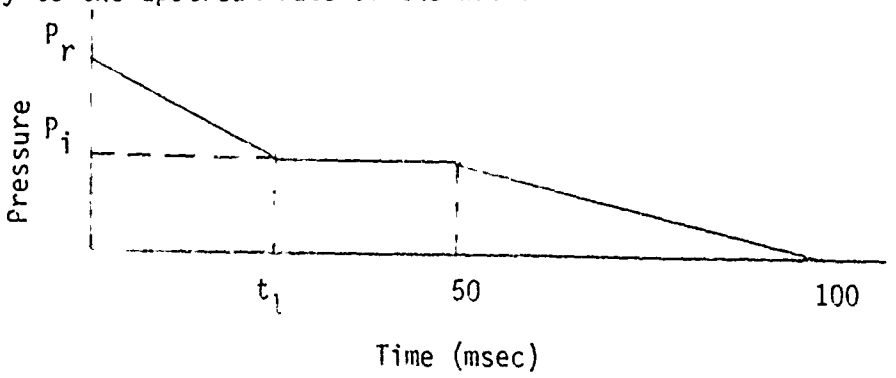

The wall first experiences peak reflected pressure (P_r) taken as twice incident pressure (P_i). This loading decreases linearly with time until, at the end of the clearing time (t_1) -- taken as approximately $3S/C_o$ where S is ½ the wall height, and C_o is sound velocity -- it equals P_i. It remains at that value until 50 msec after first loading (an average of the length of the flat top for the incident pressure pulses) and then decreases linearly with time to zero at a time of 100 msec.

For walls with an open doorway, the presence of the doorway was assumed to allow pressure to build up on the back face of the wall, to a value of P_i. The time over which this build up occurs was taken as $8S/C_o$ at which time the accelerating pressure becomes zero.

This model employs many simplifications, some of which are listed below.

- Actual reflected pressure is greater than twice incident pressure. (For incident pressures up to about 4 psi, however, the error is less than 12%.)

- While gaps around the concrete block and clay tile walls allow the process of clearing to start as soon as the shock strikes the wall, the clearing time formula given is approximately that for the front face of a block remote from any flow restriction, such as the tunnel walls and ceiling. (The common formula is actually 3S/U where U is shock velocity.) Thus the true clearing process might well take more time than given by the formula. For the sheetrock walls, no gaps were left around the walls. For these, clearing could not begin at time zero.
- At the end of the clearing time, the loading pressure should drop to its stagnation value $P_i + C_d q$, where C_d is a drag coefficient and q is the dynamic pressure behind the shock. (For incident pressures up to about 4 psi, however, the error is less than about 10%, because C_d is frequently taken as unity, and the dynamic pressure is less than 10% of the incident pressure.)
- The tail of the pulse (between 50 and 100 msec) decreases with time more as a modified exponential rather than linearly.
- No loading on the downstream face was assumed, for solid walls or walls with closed doors, although the process of clearing on the upstream face implies that pressure will build up on the downstream face.
- For walls with open doorways the pressure build up time used is approximately twice that normally taken for the back face of a solid block remote from any flow restrictions except the surface on which the block rests. A slower time for pressure build-

up than that for a block appears justified because the build-up would occur largely through the doorway, that is, around one edge of the wall and not around all edges as occurs with a block. However, use of a factor of two times the block build-up time can only be considered an approximation.

- o The effect of decelerations caused by the movement of the wall through the air was ignored. Calculations indicated the effect on wall velocities would only be two to three percent for even the fastest moving wall (sheetrock, with an incident pressure of about 4 psi).
- o Finally there was assumed to be no decrease in velocity due to energy absorbed in causing the wall to fail.

In the case of solid walls, velocity (v) and total movement or displacement (s) at various times are:

$$v_{0-t_1} = (A/M)\ P_i\ [2t-t^2/(2t_1)]$$

$$s_{0-t_1} = (A/M)\ P_i\ [t^2-t^3/(6t_1)]$$

$$v_{t_1-50} = v_{t_1} + (A/M)\ P_i[t-t_1]$$

$$s_{t_1-50} = s_{t_1} + v_{t_1}(t-t_1) + (A/M)\ P_i\ [(t^2/2) + (t_1 t) + (t_1^2/2)]$$

$$v_{50-100} = v_{50} + (A/M)\ P_i[2t-t^2/100-75]$$

$$s_{50-100} = s_{50} + v_{50}(t-50) + (A/M)\ P_i[t^2-(t^3/300)-75t+1666.7]$$

Where A/M is the inverse of the wall's mass (not weight) per unit area, and P_i is the initial shock overpressure incident on the back wall.

Comparison Of Predicted And Experimental Results

With all the simplifications discussed on the preceding pages, the acceleration model gives results that compare quite well with experimental information. This is shown on Figs. 3-19 through 3-22. Fig. 3-19 shows the combined experimental values of displacement vs time for all sheetrock walls with or without a door subjected to shockwaves with incident pressures of 3.8 to 3.9 psi. The curve labelled "calculated" was derived from the acceleration model using an average wall density of 4.75 lb/ft^2, and an average incident pressure of 3.85 psi. Fig. 4-20 is a similar plot for sheetrock walls subjected to incident overpressures of 1.7 to 1.8 psi. As with Fig. 3-19, the calculated curve is contained within the envelope of the experimental curves.

Results with clay tile walls were mixed. The calculated curve, shown in Fig. 3-21, for high incident overpressures lies very close to the experimental curve, but that for low incident overpressures lies well below the experimental curve. The calculated and experimental velocities for this condition, however, are very close at 100 msec. (The slopes of the curves are almost identical.) The early part of the experimental curve for p_1=1.6 psi might be suspect. The entire curve appears to have a constant slope, which means that the velocity -- starting at time zero -- became constant, whereas the wall should accelerate under the influence of the blast wave. (A finite velocity at zero time implies infinite acceleration.) A possible cause for the difference between calculated and measured displacements is the difficulty in identifying zero time from the motion picture records. If

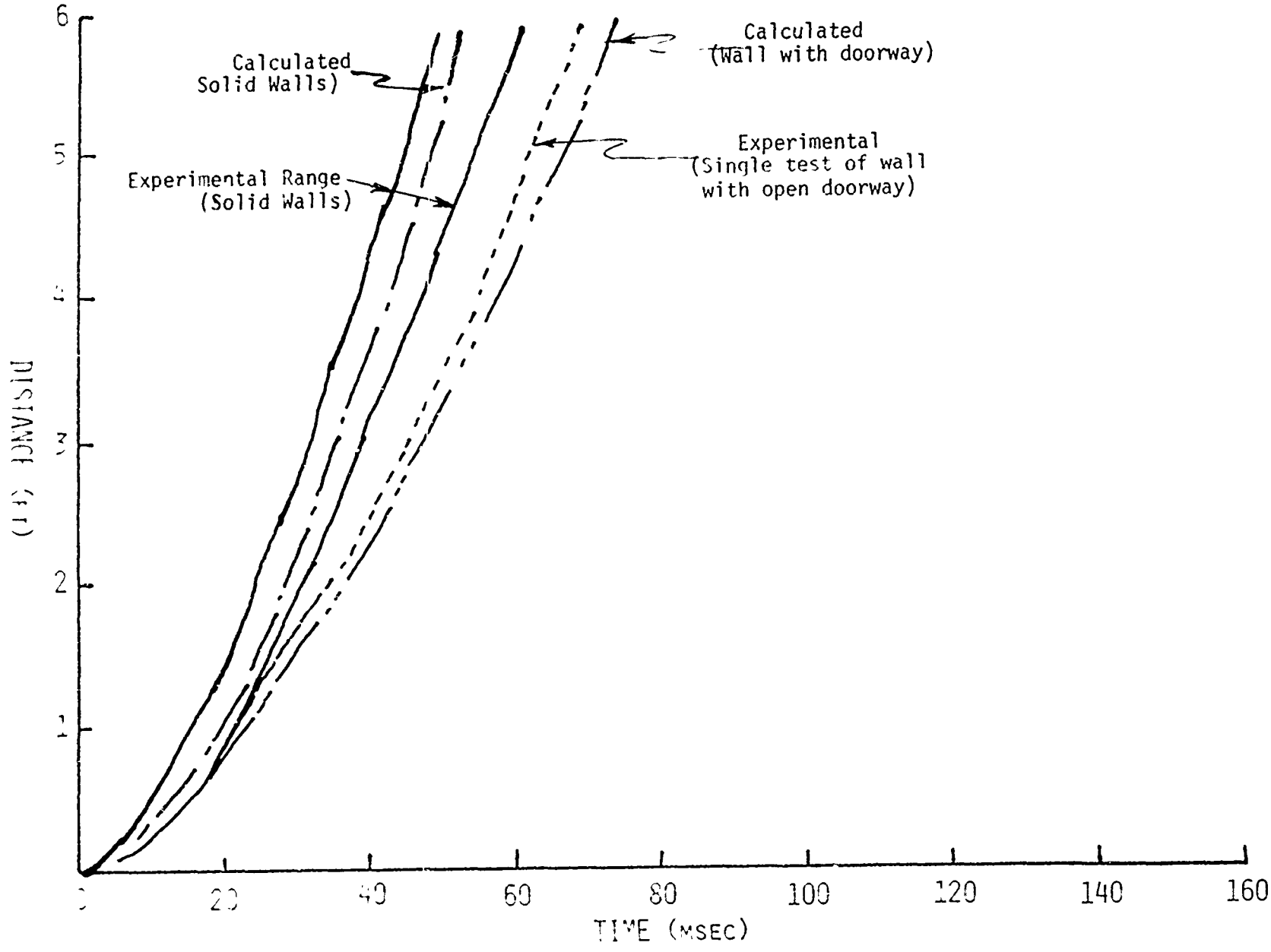

Fig. 5-19 Experimental and Calculated Displacement vs Time for Sheetrock Walls. Incident overpressure ≈ 3.85 psi.

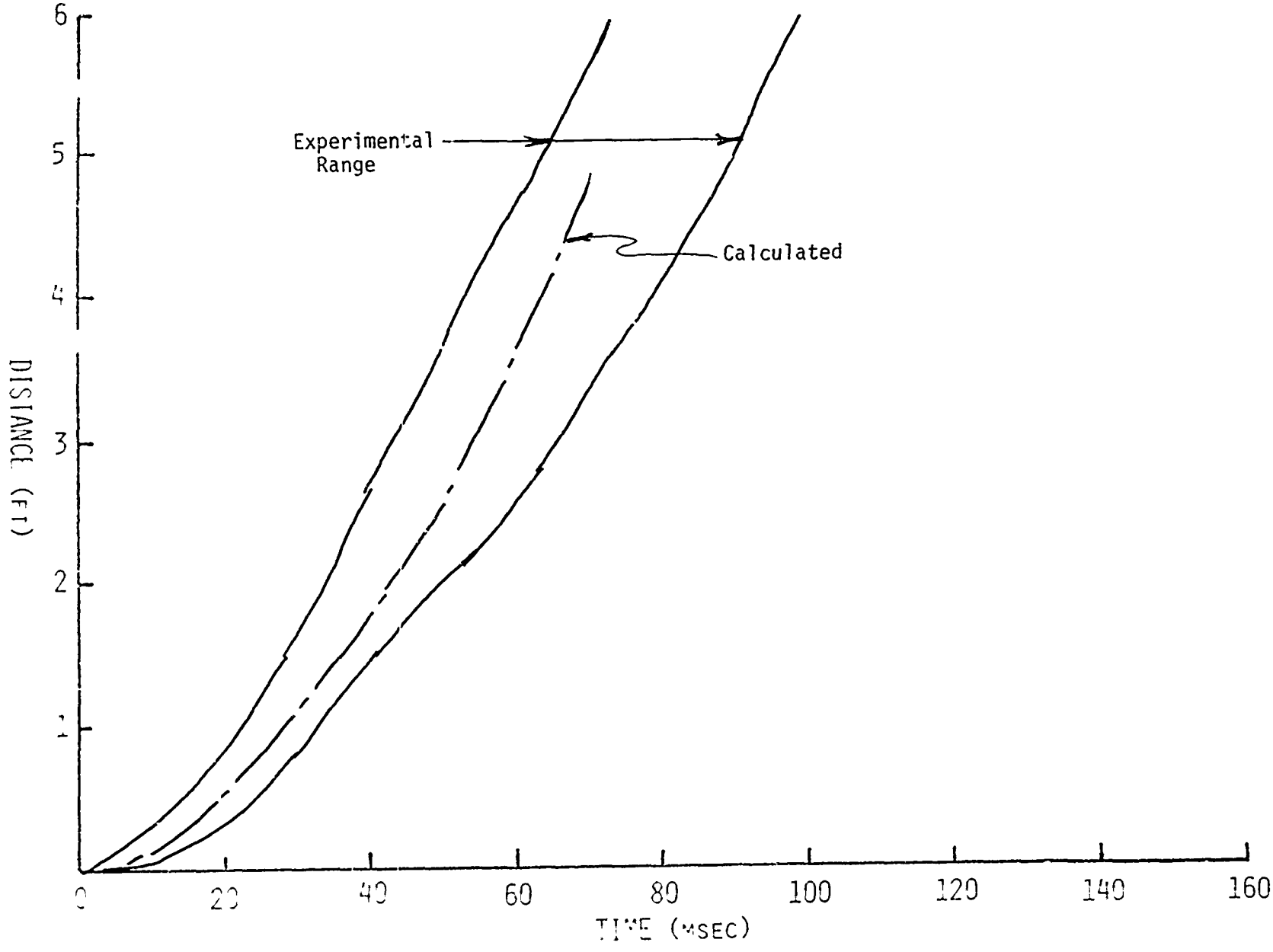

Fig. 3-20 Experimental and Calculated Displacement vs Time for Solid Sheetrock Walls. Incident overpressure ≈ 1.75 psi.

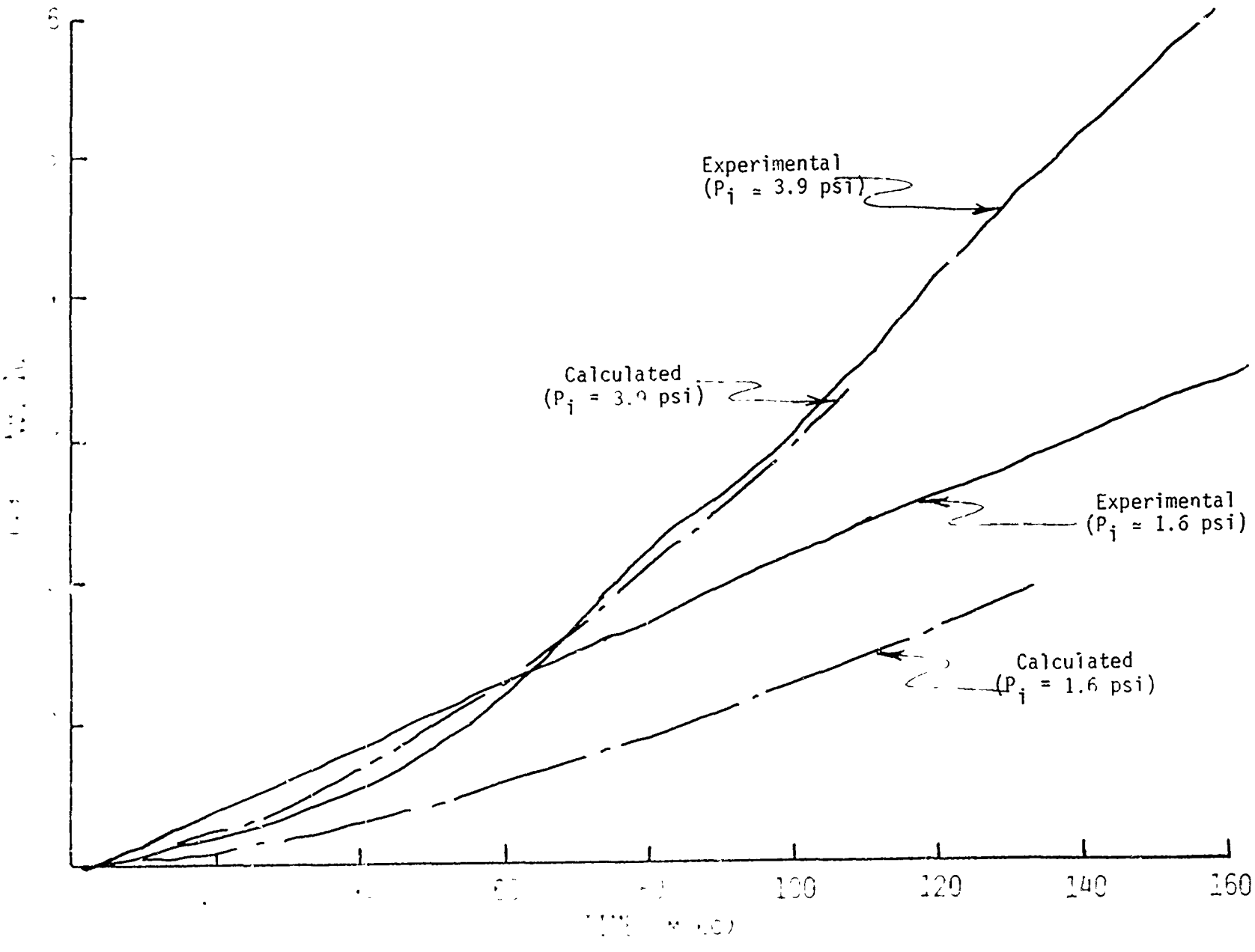

Experimental and Calculated Displacement vs Time for Solid Clay Tile Walls.
Support pressure 1.6 and 3.9 psi.

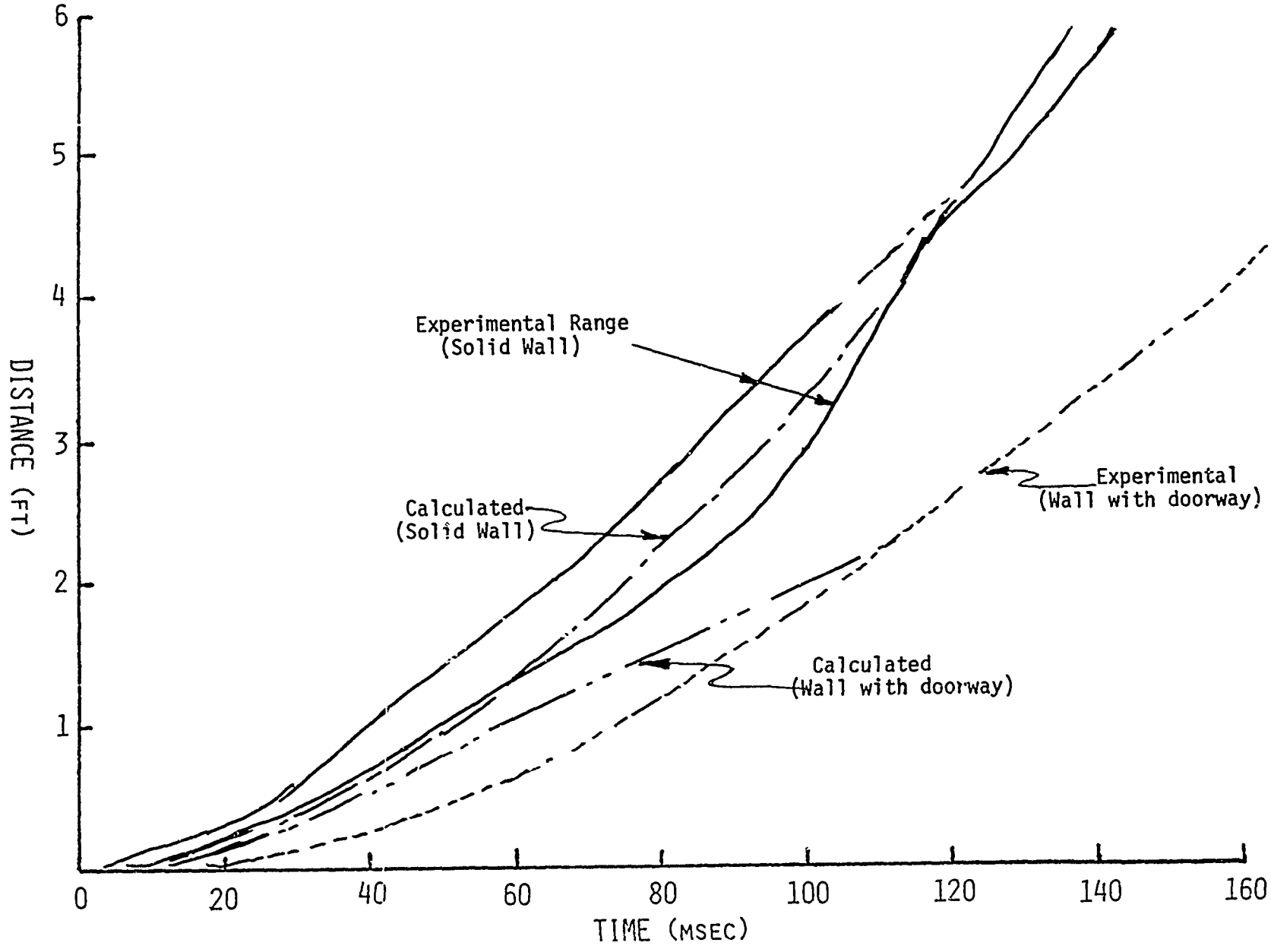

Fig. 3-22 Experimental and Calculated Displacement vs Time for Concrete Block Walls. Incident overpressure ≈ 3.8 psi.

actual zero time were somewhat earlier than that recorded, the measured curve would tend to lie closer to the calculated curve.

The results for the solid concrete block walls, shown in Fig. 3-22, are very good; the calculated curve lies within the envelope of the experimental curve. The results for the wall with a doorway are less satisfactory. The experimental evidence suggests that acceleration continues for at least 50 msec after the $8S/C_o$ time used in the calculations.

Calculated displacements and velocities for the various classes of walls are shown in Table 3-4. As can be seen from the table, calculated "final" velocities (either at t = 100 msec, the approximate end of the loading pulse, or at about the time of the last acquisition of experimental information) of solid walls tend to be somewhat higher than measured velocities, except in the case of the concrete block walls. However, the concrete block wall with the highest velocity, wall 109, appeared to attain that velocity after the loading pulse ceased. It is thus suspect, because acceleration should cease after the loading ceases, and velocity should become constant (or even decrease if drag is significant.)

The largest percentage difference occurs with the sheetrock wall subjected to the high overpressure loading, where calculated velocity is about 40% greater than experimental velocity. Reference to Fig. 3-19, however, indicates that calculated displacements are consistent with experimental displacements, but roughly constant experimental velocities were achieved at times between 45 and 50 msec. These sheetrock walls were moving very fast (about 100 mph),

TABLE 3-4

Calculated Debris Movement Velocity

Wall Type	Incident Overpressure (psi)	Time, t* (msec)	Debris Movement at Time, t		Debris Velocity at Time, t	
			Calculated (ft)	Experimental** (ft)	Calculated (ft/sec)	Experimental*** (ft/sec)
Sheetrock (solid)	1.75	50	2.6	2-3.5	95	102
	"	70	4.8	3.5-6	123	
Sheetrock (solid)	3.85	50	5.7	4.5-6	210	150
Sheetrock (open doorway)	3.85	60	5.8	5	135	155
Clay tile (solid)	1.6	50	0.4	1	13.8	16
	"	100	1.3	2	20.0	
Clay tile (solid)	3.9	50	0.9	1	33.6	44
	"	100	3.1	3	48.7	
Concrete block (solid)	3.6	50	1.0	1-1.5	36.7	61
	"	100	3.3	3-4	53.2	
Concrete Block (with open doorway)	3.6	60	1.0	0.5	23.7	38

* Zero time is taken as the time of shock wave arrival at the wall.

** Experimental displacements are given to the nearest 0.5 ft.

*** Experimental velocities are final averages.

and were in the process of breaking up under the strong loading, so that differences between calculated and experimental information could be expected. Note, however, that the casemate area into which these walls were projected could well allow venting around the wall at a faster rate than would occur in an actual structure, so that velocities within a structure might be closer to the calculated values. Calculated final velocities achieved by walls with doorways are somewhat lower than experimental velocities.

Preliminary Work on Debris Velocities From Nuclear Weapons

The general success of the techniques used to predict velocities of wall elements under loadings generated in the shock tunnel, suggest that similar approaches can be used to predict velocities at early times of elements from walls loaded by blast waves from nuclear weapons. To this end preliminary work has been done to develop the loading pulses which might be used for such predictions. The techniques should not be used for times longer than about 100 msec because later phenomena -- wall element rotation, for example -- lead to completely different mechanisms for wall element acceleration. (The elements are accelerated by drag from flow around them.)

A loading pulse that appears to be suitable can be developed from the following considerations.

- Ref. 6 indicates that the initial pressure on the back wall (for a room with a window opening of about 30%) is about equal to the incident pressure outside the room.

- In the derivation given earlier in this section, within a time of $3S/C_o$, where S is one half the height of the interior partitions and C_o is the sound velocity in ambient conditions, the loading pressure was assumed to drop linearly to about one half the initial loading pressure. (Recall that the shock tube pulse was assumed to have a constant pressure to a time of 50 msec and then to drop linearly to zero at a time of 100 msec.)
- Incident pressure in a blast wave from a nuclear weapon (without taking into account reflections from nearby structures) is related to time by

  $$\Delta p(t) = \Delta p(0)(1-t/t^+)e^{-t/t^+}$$

  where $\Delta p(t)$ = incident overpressure as a function of time t and t^+ = the duration of the positive overpressure phase.

These considerations lead to a loading pulse with the following characteristics:

1. At time zero (when the shock wave first strikes the interior wall) the loading pressure p_ℓ is the peak overpressure of the incident shock wave, $\Delta p(0)$.

2. Between time zero, and a time t_a = 2.7 S msec, where S is one half the height of an interior wall measured in feet, the loading pulse drops linearly to a value of

$$p_\ell = (\Delta p(0)/2)(1-t_a/t^+)e^{-t_a/t^+}$$

For the average 8 ft high wall, $t_a \approx 10$ msec.

3. At later times -- up to about 100 msec -- the loading pulse is

$$p_\ell = \Delta p(t)/2$$

For megaton range weapons, with durations on the order of seconds, a constant incident pressure up to a time of 100 msec can be assumed with little loss in accuracy. For example, with a blast wave whose duration is about 4 sec (e.g., a pulse with a peak overpressure of about 3 psi from a near-surface burst of a 1 MT weapon) pressure would have fallen only about 5% from its peak value at a time of 100 msec.

In Fig. 3-23 approximate loading pulses on interior walls for blast waves from weapons with yields of 1 MT, 1 kt, and 0.01 kt have been plotted. Also shown on that figure is the loading pulse used to make predictions of wall element velocities for shock tunnel conditions, starting with the same incident loading.

Note that the 1 MT pulse is identical with the shock tunnel pulse up to 50 msec, but then it remains at a value of $\Delta p(0)/2$ while the shock tunnel pulse decreases to zero. This suggests that early time wall element velocities from a 1 MT blast are likely to be larger than those calculated for the shock tunnel. In contrast, the 1 kt pulse is first lower than the shock tunnel pulse, but after about 60 msec it becomes higher. This suggests that wall element velocities from 1 kt weapons will be similar to shock tunnel velocities. Finally, the 0.01 kt loading pulse lies entirely below the shock tunnel pulse, thus 0.01 kt wall element velocities should be considerably below shock tunnel velocities.

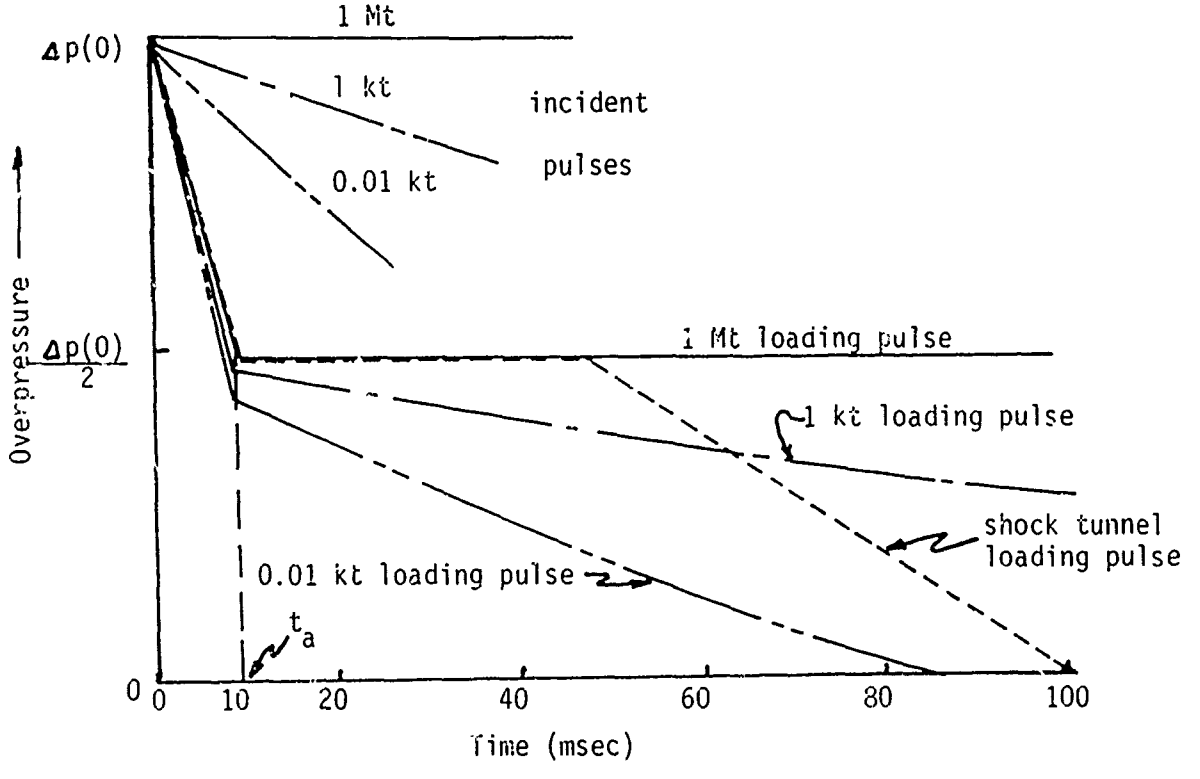

Fig. 3-23. Loading Pulses for Debris Velocity Predictions

Section 4

PROGRAM STATUS REPORT

UPDATE OF FAILURE STRENGTH MATRIXES

In Ref. 1, the results of the entire wall strength program to date were summarized in very brief form by preparing what was termed a "Failure Strength Matrix" for solid walls, walls with window openings, and walls with doorway openings. The matrixes were entered on the side with types of wall mounting, and at the top with wall material and location (exterior or interior). Each intersection of the matrix showed the incident blast overpressure that would result in failure and in addition, showed whether the values were from tests or predictions.

For predicted values, the chart also showed whether confidence in the predictions was high or low. Thus, it was possible to display the usable results and status of the program in just three pages. In this section, the matrixes are brought up-to-date.

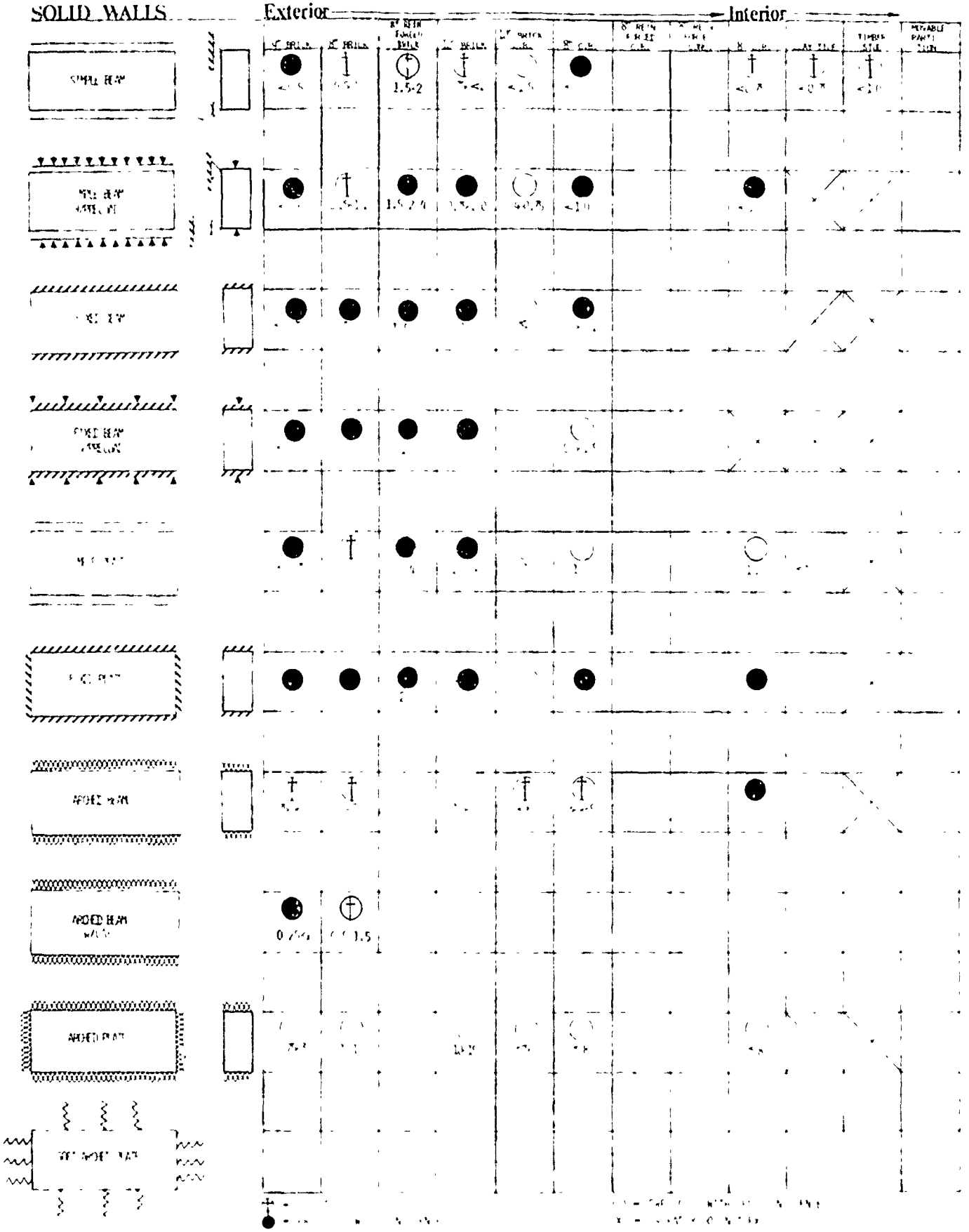

Fig. 4-1. Failure Strength Matrix - Solid Walls. (The numbers in the matrix are incident overpressures.)

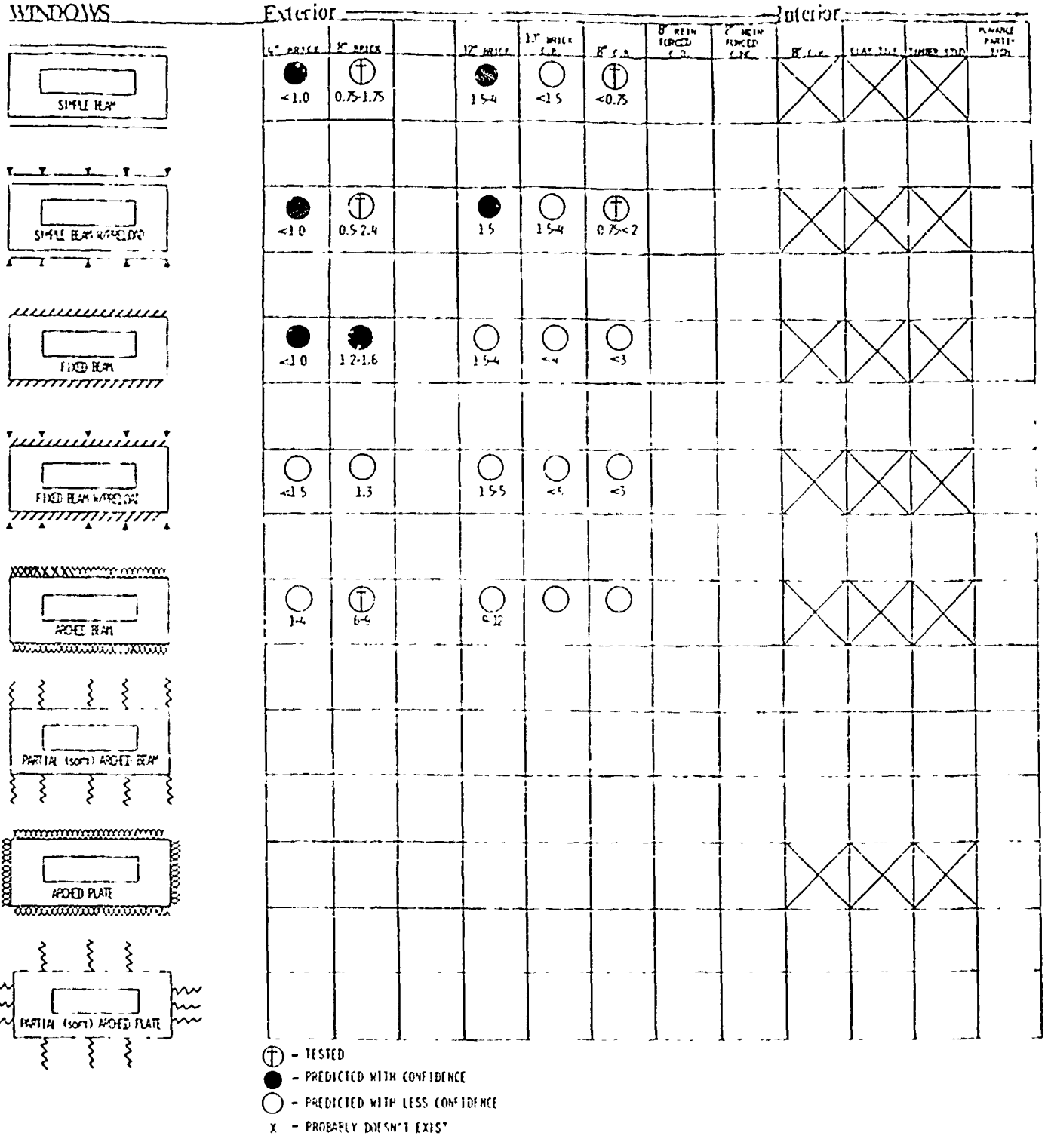

Fig. 4-2. Failure Strength Matrix - Windows. (The numbers in the matrix are incident overpressures.)

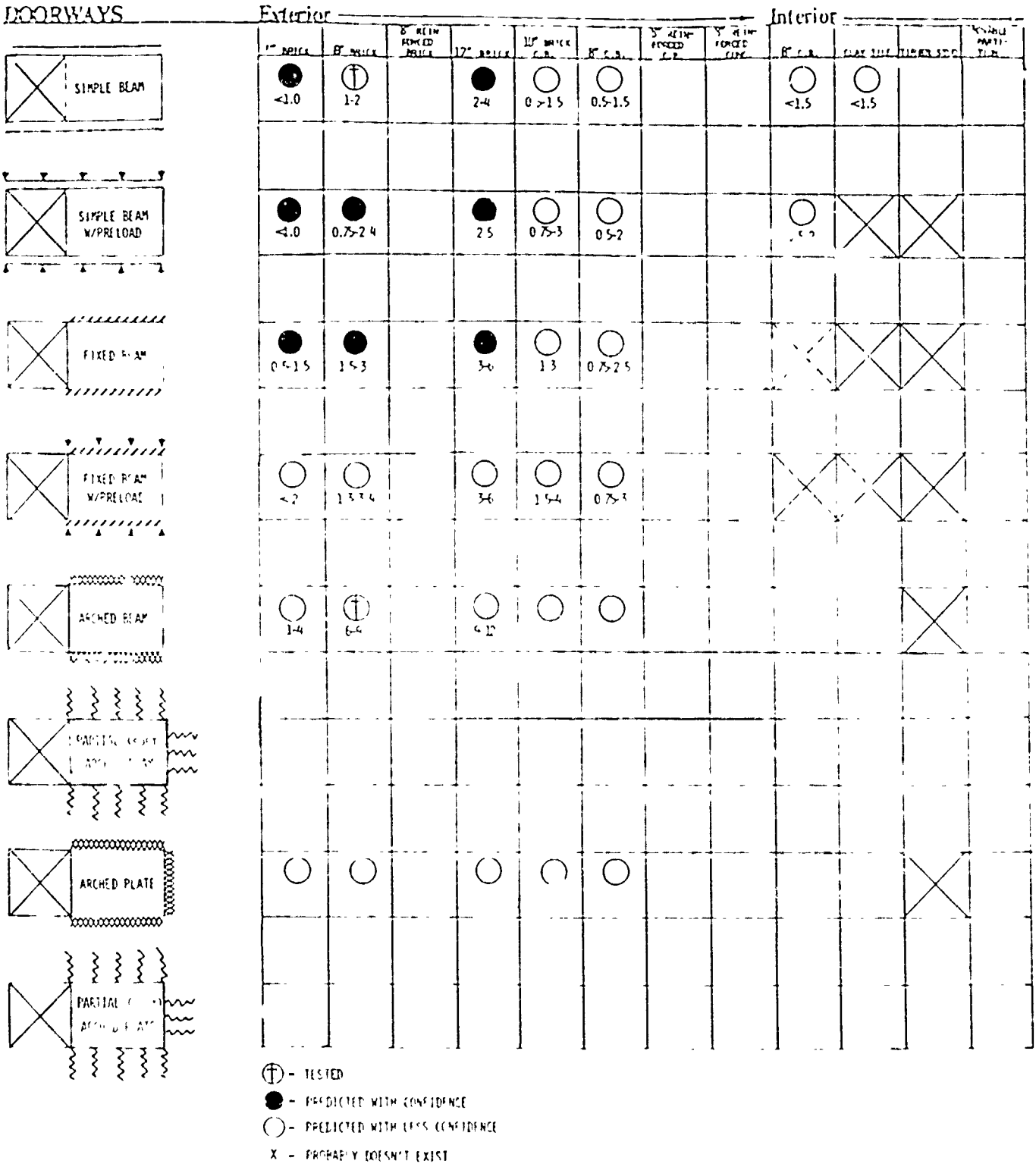

Fig. 4-3 Failure Strength Matrix - Doorways. (The numbers in the matrix are incident overpressures.)

Section 5

REFERENCES

Section 5

REFERENCES

1. Gabrielsen, B.L., and C. Wilton, Shock Tunnel Tests of Arched Wall Panels, URS 7030-19, Final Report, December 1974, URS Research Company, San Mateo, California.

2. Willoughby, A.B., C. Wilton, B.L. Gabrielsen, J.V. Zaccor, A Study of Loading, Structural Response, and Debris Characteristics of Wall Panels, URS 680-5, Final Report, URS Research Company, San Mateo, California, July 1969.

3. Plummer, Harry C., Brick and Tile Engineering, Structural Clay Products Institute, Washington, D.C., 1967.

4. ACI 318-71, American Concrete Institute Building Code Requirements for Reinforced Concrete.

5. Wilton, C., and B.L. Gabrielsen, Shock Tunnel Tests of Preloaded and Arched Wall Panels, URS 7030-10, Final Report, June 1973, URS Research Company, San Mateo, California.

6. Glasstone, S. (Ed.), The Effects of Nuclear Weapons, revised ed., Superintendent of Documents, U.S. Government Printing Office, Washington, D.C., 1964.

7. Wilton, C., B.L. Gabrielsen, P. Morris, Structural Response and Loading of Wall Panels, URS 709-11, Final Report, July 1971, URS Research Company, San Mateo, California.

8. Wilton, C., B. Gabrielsen, J. Edmunds, S. Bechtel, Loading and Structural Response of Wall Panels, URS 709-4, November 1969, URS Research Company, San Mateo, California.

Appendix A

SHOCK TUNNEL (DYNAMIC) TEST DATA

TEST REPORTS

Appendix A

SHOCK TUNNEL (DYNAMIC) TEST DATA

Presented in this appendix are the test data for the wall panel tests conducted in the Shock Tunnel during this reporting period. Wall panel types tested included exterior walls constructed of reinforced and non-reinforced brick, and interior walls constructed of non-reinforced concrete block, of non-reinforced clay tile, and of sheetrock with both metal and wood studs.

A summary of these tests is presented in Table A-1. Descriptions of the mounting conditions, mounting locations and construction details of the various walls is presented below. This is followed by the test reports of each test presented in numerical order.

Exterior Wall Panels

Four exterior panels were investigated; two gapped arch, non-reinforced brick walls, and two reinforced brick walls supported as simple beams. The gapped walls were mounted in the Shock Tunnel as shown in Fig. A-1. The bottom was rigidly supported by concrete which was poured after the wall was installed in the tunnel. A gap of approximately 0.2 in. for wall 97 and 0.1 in. for wall 98 was left between the mortar cap and the roof of the Shock Tunnel. To assure freedom of motion of the sides of the wall, gaps approximately 0.5 in. wide were left between the test wall and the walls of the tunnel.

TABLE A-1

Summary of Tests

Test Number	Description	Mounting Location	Number of Strands	Incident Overpressure *	
Exterior Walls					
97	Non-reinforced brick (Gapped arched)	A	2	2.3	
98	Non-reinforced brick (Gapped arched)	A	2	1.9	
99	Reinforced brick-beam	A	1	1.0	
99A	Reinforced brick-beam	A	2	2.0	
100	Reinforced brick-beam	A	2	2.0	
Interior Walls					
101	Sheetrock-timber stud	A	4	3.5	(4.9)
102	Sheetrock-timber stud	B	2	1.7	(2.0)
103	Sheetrock-metal stud	B	2	1.8	(2.0)
104	Sheetrock-metal stud	A	2	1.8	(2.0)
105	Sheetrock-metal stud	A	4	3.5	(4.9)
106	Sheetrock-timber stud	B	5	3.8	(6.0)
107	Sheetrock-metal stud	B	5	3.9	(6.0)
108	Concrete block	B	5	3.6	(6.0)
109	Concrete block	B	5	4.0	(6.0)
110	Sheetrock-timber stud	B	5	3.8	(6.0)
111	Sheetrock-timber stud (door closed)	B	5	3.9	(6.0)

TABLE A-1 (cont.)

Summary of Tests

Test Number	Description	Mounting Location	Number of Strands	Incident Overpressure *	
Interior Walls (cont.)					
112	Sheetrock-timber stud (door open)	B	5	3.8	(6.0)
113	Sheetrock-metal stud (door closed)	B	2	1.7	(2.0)
114	Sheetrock-metal stud (door closed)	B	5	3.8	(6.0)
115	Concrete block (gapped arched)	A	5	4.1	(6.0)
116	Concrete block (gapped arched)	A	2	1.7	(2.0)
117	Concrete block (gapped 4 in.)	B	5	3.8	(6.0)
118	Concrete block (doorway)	B	5	3.6	(6.0)
119	Clay tile	B	2	1.6	(2.0)
120	Clay tile	B	5	3.9	(6.0)

* Tabulated values without parentheses are peak incident overpressures measured just upstream from the test wall. For walls 101 through 120, these measurements were made in the room. Values in parentheses estimate values in front of a nonfailing wall with 27% open window.

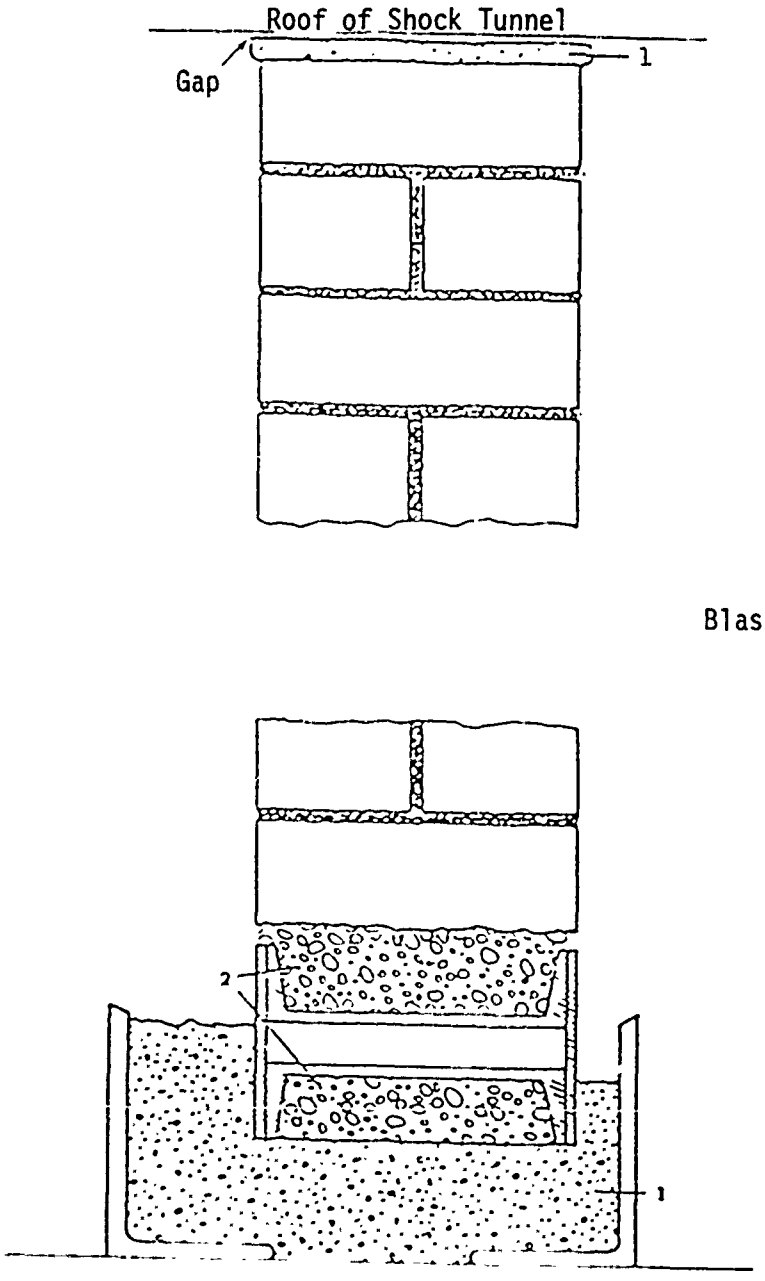

Fig. A-1 Top and Bottom Support System for Walls 97 and 98

(Note: 1. Mortar installed when wall placed in Shock Tunnel.

2. Mortar installed when wall was constructed.)

The reinforced brick walls were supported as simple beams (attached but free to rotate at the top and bottom and with the sides free to move). The reinforcement consisted of #4 bars placed vertically on 24 in. centers and #3 bars placed horizontally on 16 in. centers (steel percentages: 0.1% vertical, 0.086% horizontal).

Interior Wall Panels

The interior panels tested in this series included concrete block, clay tile, and sheetrock* with both wood and metal studs. All of these were placed behind a nonfailing wall panel with a 27% window opening. A photograph of this nonfailing wall in place in the Shock Tunnel is shown in Fig. A-2. The photograph was taken looking upstream (toward the Shock Tunnel compression chamber) and also shows one of the plate girders on which some of the interior wall panels were mounted.

One of the basic requirements of this test program on interior walls was to obtain data on debris velocity and particle size. In previous test programs in the Shock Tunnel the wall panels were installed in the tunnel some 45 ft from the open end, (location A in Fig. A-3). At this location, the breakup of the wall can be followed for approximately 15 ft to the point where the tunnel bends as shown in Fig. A-3. It is, however, difficult to obtain good photographs at this location because of lighting and camera placement problems. To obtain better velocity and debris size information a number of the wall panels were placed near the mouth of the tunnel at the entrance to the casemate

* Sheetrock was affixed to both sides of these walls.

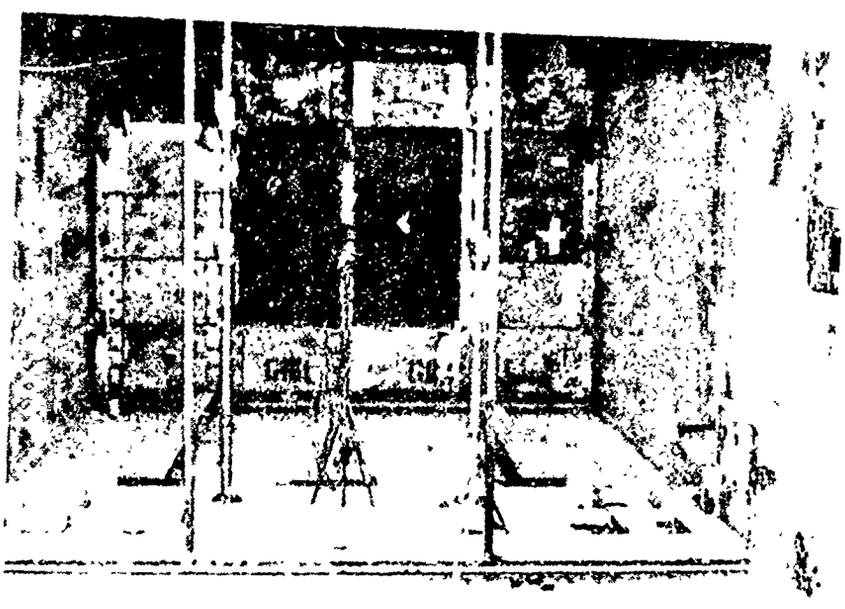

Fig. A-2. Photograph of Nonfailing Wall With Window Opening.

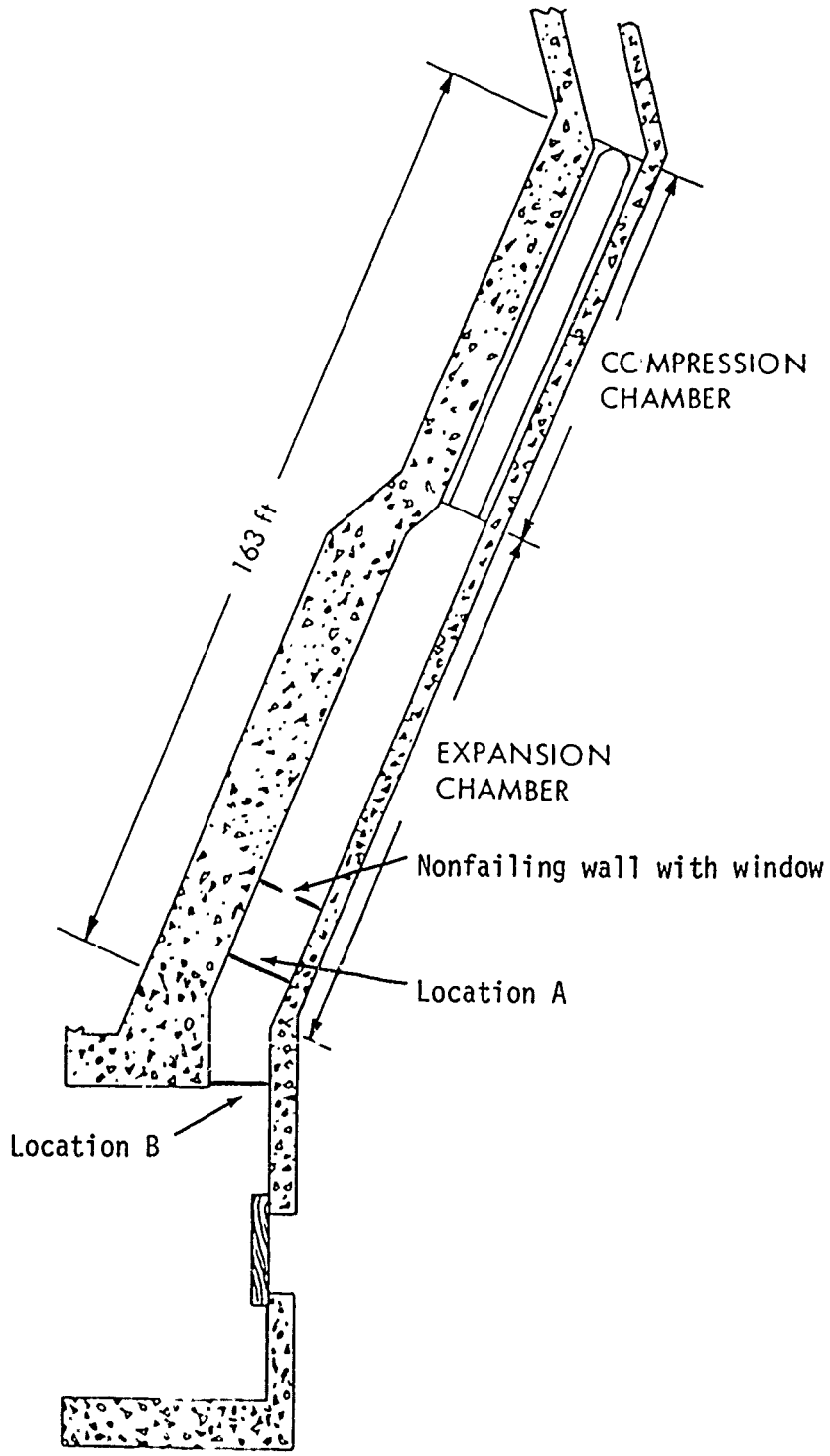

Fig. A-3. Plan of Shock Tunnel

area, (Location B Fig. A-3). Some preliminary tests indicated that motions of walls placed at Location B were similar to those of walls at Location A. In addition, at Location B the lighting was much better and a camera could be placed to the side of the wall. The locations of all the walls are included in the reports for each test given later in this appendix.

Construction Details

Construction of the concrete block and hollow clay tile walls was relatively straightforward. They were built on steel H beams outside the Shock Tunnel area and allowed to cure for at least 28 days. Construction materials and techniques used were those commonly employed, including type 'S' mortar and a mortar thickness of approximately ½ in.

To install sheetrock walls with wood studs, a perimeter 2 x 4 in. wood frame was affixed to the concrete tunnel using explosively driven nails spaced 24 in. apart. Vertical 2 x 4 in. wood studs were spaced 16 in. on center and were fastened to this frame at the ends with four No. 8 nails. The sheetrock panels were 48 in. wide, 144 in. long, and ½ in. thick. They were attached to the studs with their long axes horizontal, which resulted in horizontal joints 6 in. and 54 in. from the floor. The sheetrock was fastened to both sides of the wall with 1-½ in. long No. 4 sheetrock nails spaced 6 in. on center. A standard wood door frame was used on the wall panels with the doorway opening, and the door was installed to open upstream.

For the sheetrock walls with metal studs, sheet metal channels were fastened to the ceiling and floor of the tunnel with explosively driven nails. Sheet metal studs were installed vertically in these channels on 16 in. centers and the studs at the edges were nailed to the concrete tunnel walls by explosively driven nails. The sheetrock panels were installed with their long axes horizontal and held in place by 1 in. long self-tapping screws 6 in. on centers. Sheetrock was placed on both sides of the wall.

Test Report Wall No. 97

Type: 8-in. Non-reinforced; exterior; solid (with no openings).

Support Conditions: Gapped arched.

The bottom of this wall was mortared to the shock tunnel floor and a gap approximately 0.2 in. wide was left along the top of the wall. To insure one way arching a gap about 0.5 in. wide was left along both sides of the wall.

Test Results

One test was conducted on this wall using two 60-ft strands of Primacord which gave an average peak incident overpressure of 2.3 psi. The wall failed, with the three crack gauges indicating crack times of 28.6, 35.2, and 26.5 msec. The longest crack time, 35.2 msec, was from a crack at the center of the wall. Analysis of the motion picture films indicated that a horizontal crack about 2/3 of the way up the wall appeared first, with additional cracks appearing much later 1/3 of the way up the wall. The major part of the debris from this test landed within the first thirty feet with only a few pieces landing beyond that distance. The location and size of the debris fragments can be seen in the photographs in Fig. 97-1 and Fig. 97-2.

Fig. 97-1. Pre and Posttest Photographs, Wall Number 97.

Fig. 97-2. Posttest Photographs, Wall Number 97.

Test Report Wall No. 98

Type: 8-in. Non-reinforced brick; exterior; solid (with no opening).

Support Conditions: Gapped arched.

The bottom of this wall was mortared to the shock tunnel floor and a gap approximately 0.1 in. wide was left along the top of the wall. To insure one way arching an gap about 0.5 in. wide was left along both sides of the wall.

Test Results

One test was conducted using two strands of Primacord. The average peak incident overpressure was 1.9 psi. The three crack gauges indicated crack times of 35.5, 32, and 39.9 msec, but they are all from a single stepped crack extending from the 19th row of bricks on one side of the wall, to the 17th row on the other. As in the previous test, essentially all the debris landed within the first 30 feet. The amount and location of the debris can be seen in the posttest photographs presented in Fig. 98-1 and Fig. 98-2. Posttest inspection also indicated numerous pieces of brick upstream from the wall's initial location which had apparently been spalled off the top edge of the wall. A number of these fragments can be seen in the photographs in Fig. 98-3.

Fig. 98-1. Posttest Photographs, Wall Number 98.

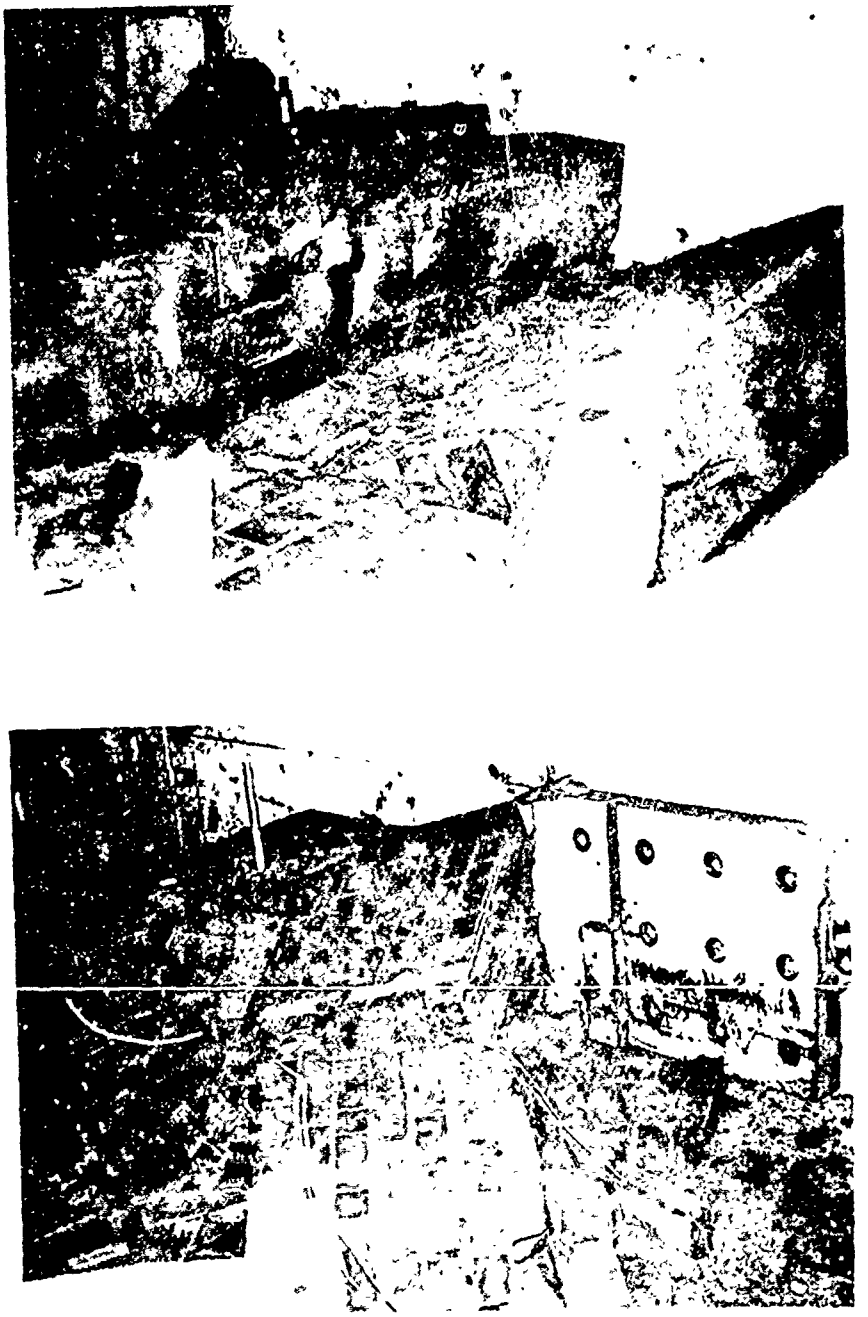

Fig. 98-2. Posttest Photographs, Wall Number 98

Fig. 98-3. Posttest Photographs, Wall Number 98

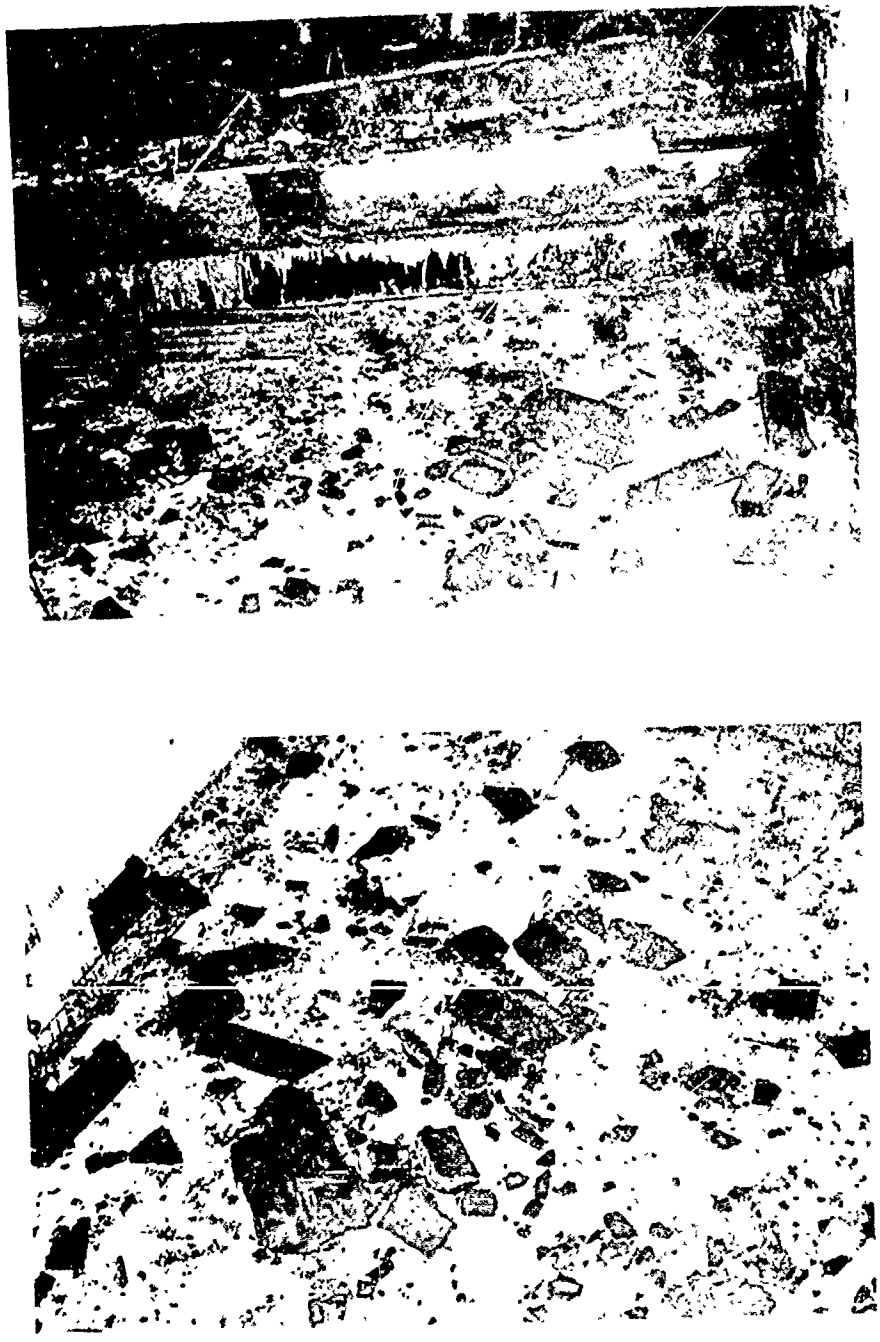

Fig. 98-4. Upstream Wall Fragments, Wall Number 98.

Test Report Wall No. 99

Type: 8-in. Reinforced* brick; exterior; solid (with no opening).

Support Conditions: Simple beam.

The top and bottom of this wall were attached but free to rotate and the sides gapped and free to move.

Test Results

Two tests were conducted. In the first test using one strand of Primacord (average peak incident overpressure about 1 psi) the wall cracked horizontally at several locations at and below the center line. The crack gauges recorded crack times of 16, 17.2, and 23.6 msec. The initial crack was located about 1/3 of the way up the wall. In the second test using two strands of Primacord (average peak incident overpressure about 2 psi) the wall failed. There was, however, very little translation and the majority of the debris landed within the first ten feet as shown in the posttest photographs presented in Figs. 99-1 through 99-3.

* Steel percentages: 0.1% vertical, 0.086% horizontal.

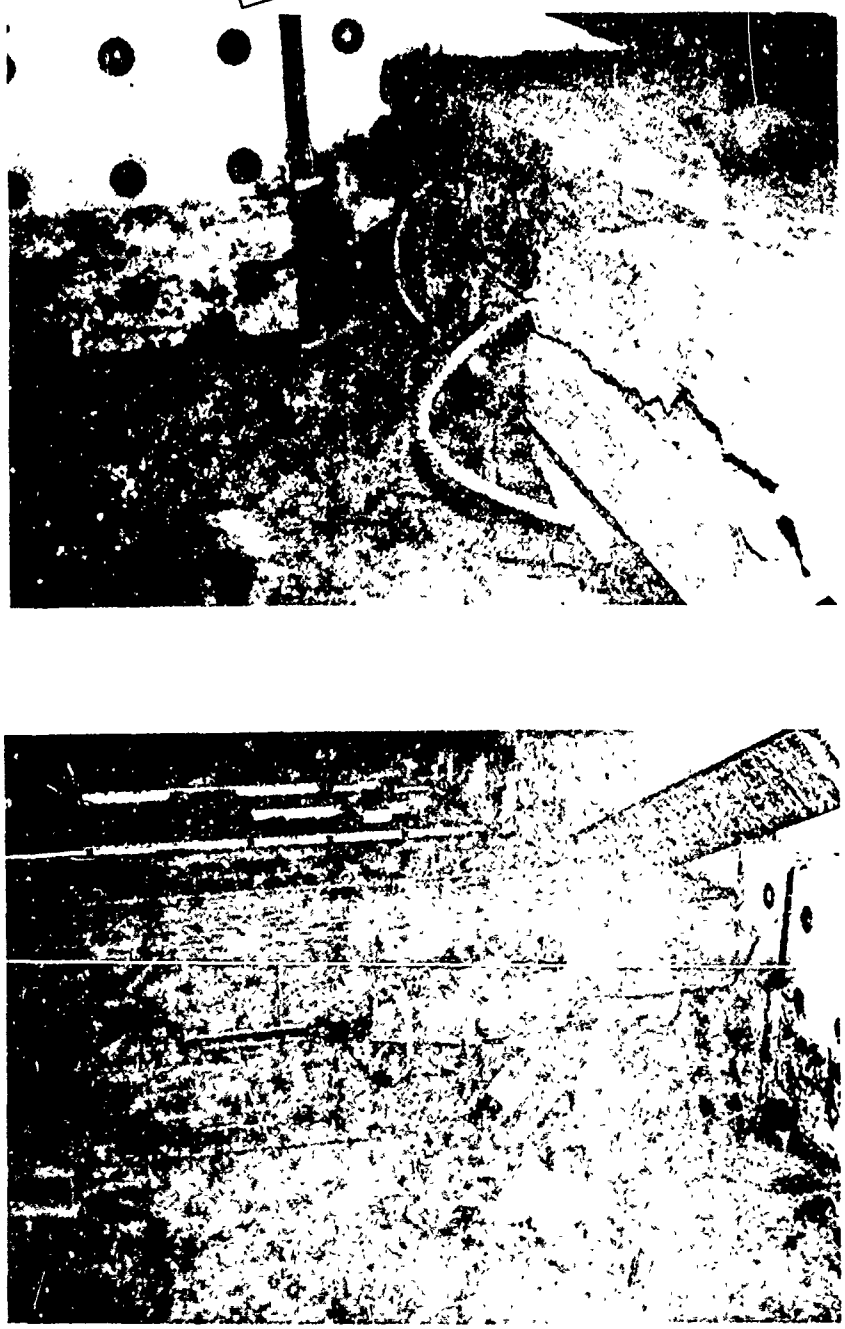

Fig. 99-1. Posttest Photographs, Wall Number 99

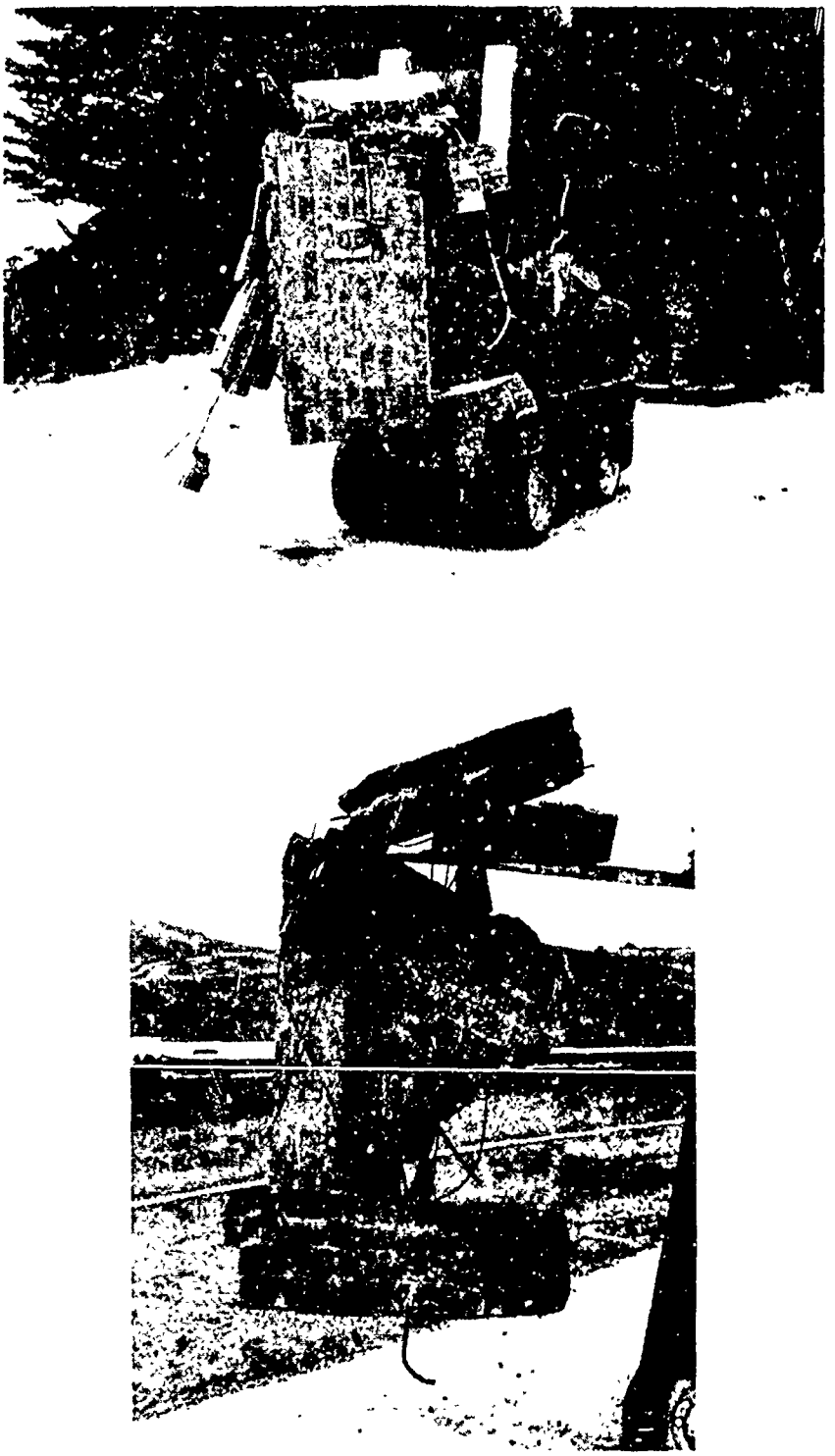

Fig. 99-2. Debris From Wall Number 99.

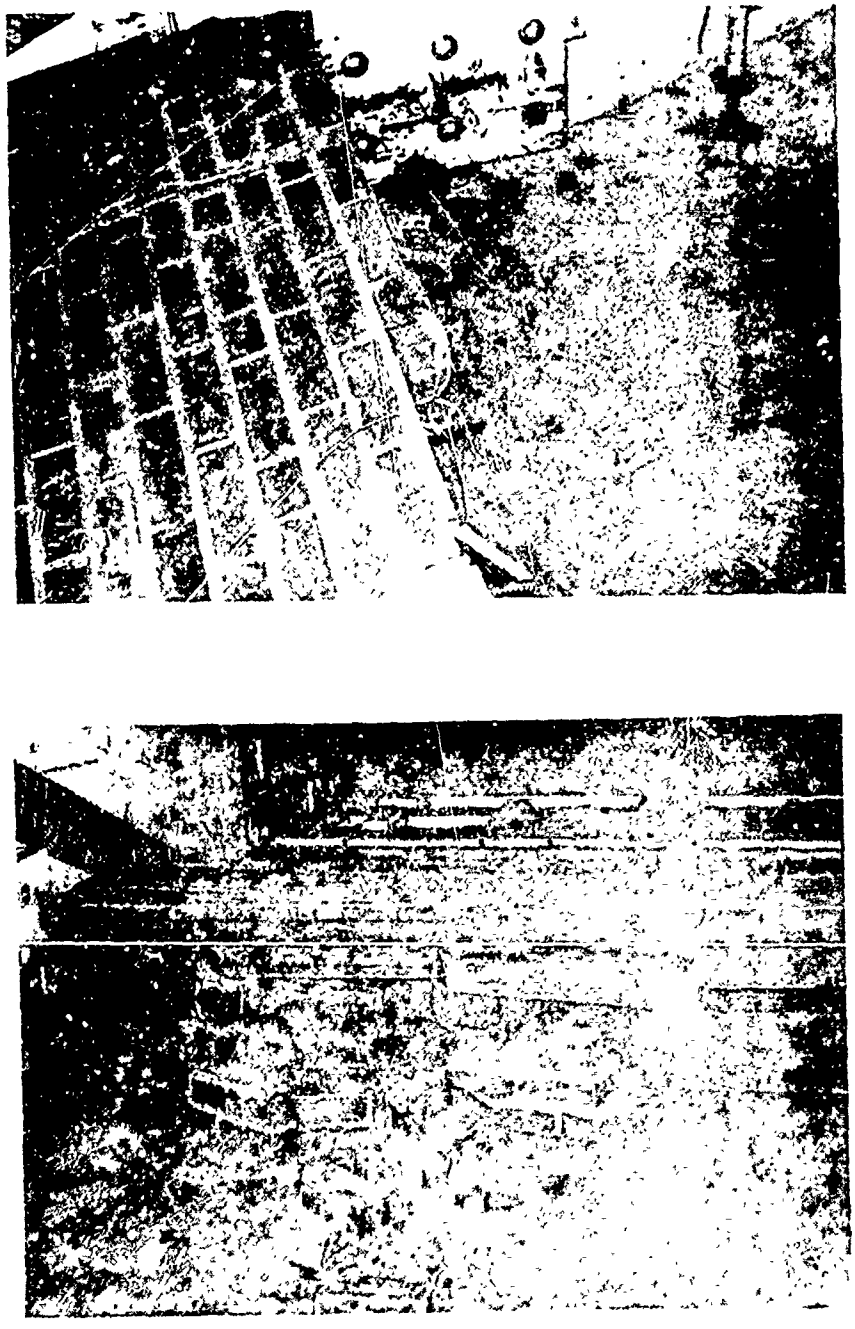

Fig. 99-3. Posttest Photographs, Wall Number 99

Test Report Wall No. 100

Type: 8-in. Reinforced* brick; exterior; solid (with no openings).

Support Conditions: Simple beam.

The top and bottom of this wall were fixed but free to rotate and the sides gapped and free to move.

Test Results

One test was conducted using two strands of Primacord (average peak incident overpressure about 2 psi). The initial crack appeared horizontally between the 12th and 13th rows of brick. The crack started at the right side and continued for six brick lengths before jumping down one row and continuing on the left edge. A second crack appeared horizontally two brick rows below the initial crack. The second crack opened up into a large gap before the upper portion of the wall collapsed on the lower portion. Recorded crack times for this test were 1.7, 1.8, and 18 msec. The majority of the debris landed within the first 7½ ft. The reinforcing bars were severly strained but none of them were broken. Pre and posttest photographs of this wall are provided in Figs. 100-1 through 100-3.

* Steel percentages: 0.1% vertical, 0.086% horizontal.

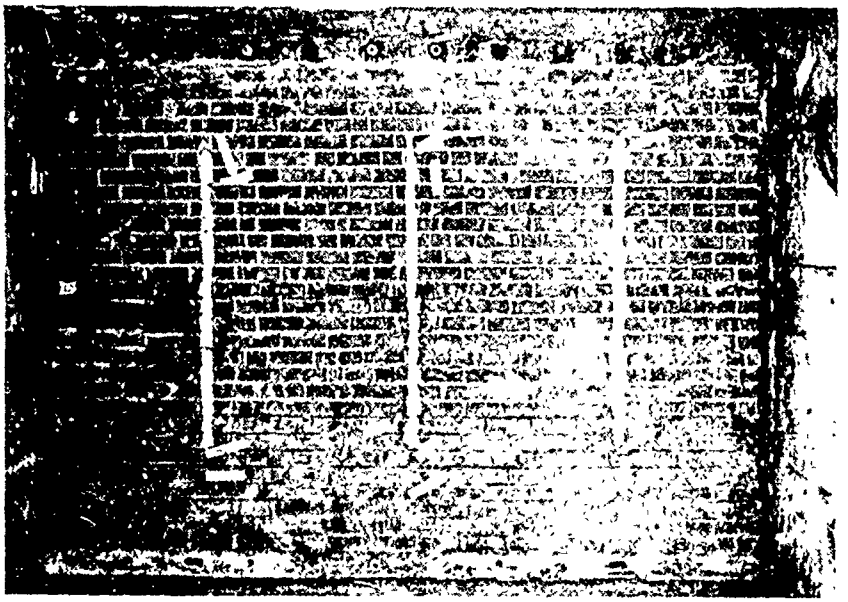

Fig. 100-1. Posttest Photographs, Wall Number 100

Fig. 100-2. Posttest Photographs, Wall Number 100

Fig. 100-3. Posttest Photographs, Wall Number 100.

Test Report Wall No. 101

Type: 4-in. Sheetrock with timber studs; interior; solid (with no openings).

Support Conditions: Simple plate.

All four edges of this wall were attached to the tunnel.

Special Conditions

Tested 14.5 ft behind a nonfailing wall with a 27% window opening; mounting location A (Fig. A-3).

Test Results

This wall was tested once using four 60-ft strands of Primacord (average peak incident overpressure 3.5 psi.) Initally numerous minute cracks appeared on the downstream face of the sheetrock. The wall translated relatively intact until it hit the bend in the tunnel. The wall broke up, with the majority of the debris continuing on to the far side of the casemate., a distance of 87 ft from the original location of the wall. Pre and posttest photographs of this wall are shown in Figs. 101-1 and 101-2. A plot of displacement vs. time obtained from analysis of the motion picture records is presented in Fig. 101-3.

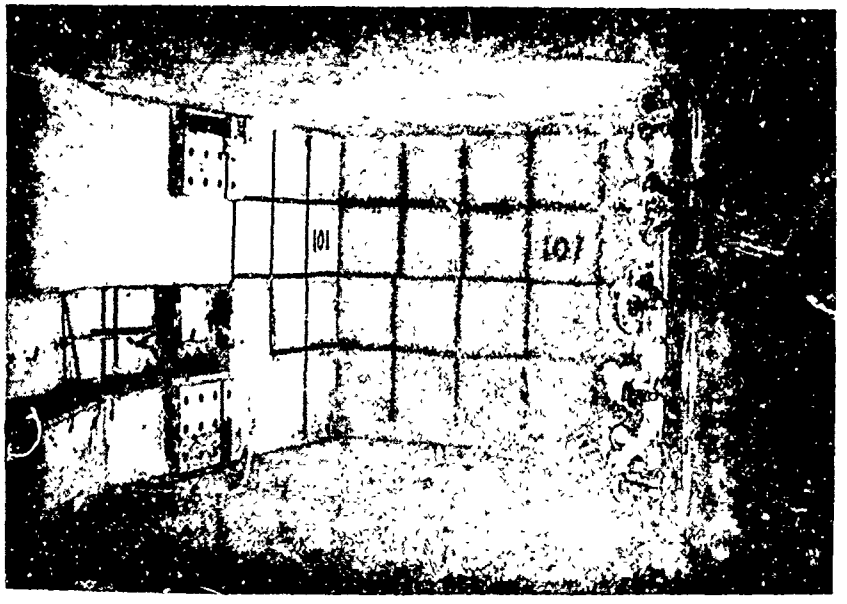

Fig. 101-1. Pre and Posttest Photographs, Wall Number 101.

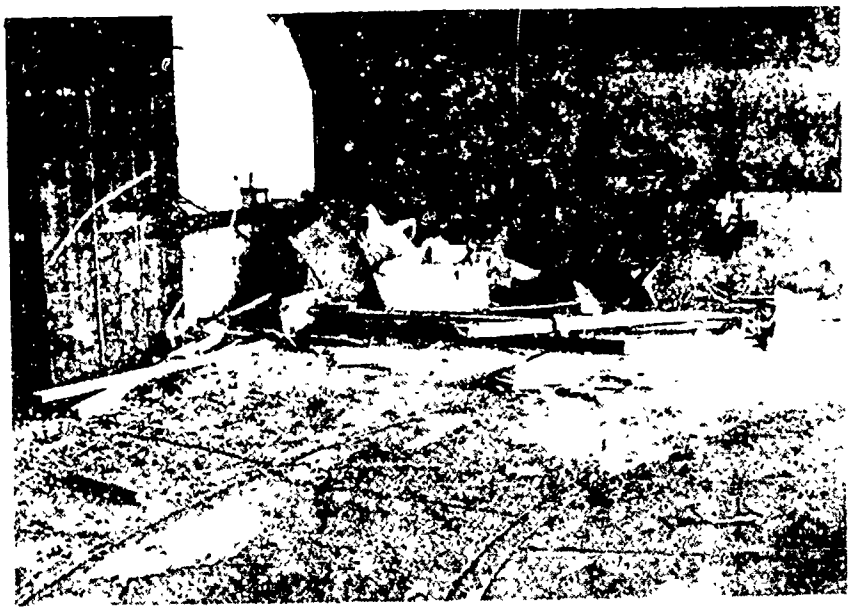

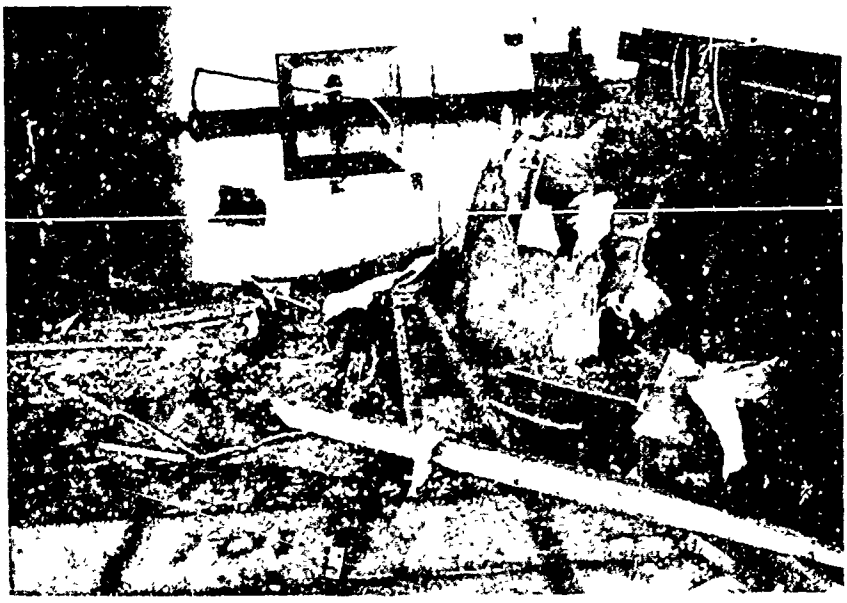

Fig. 101-2. Posttest Photographs, Wall Number 101.

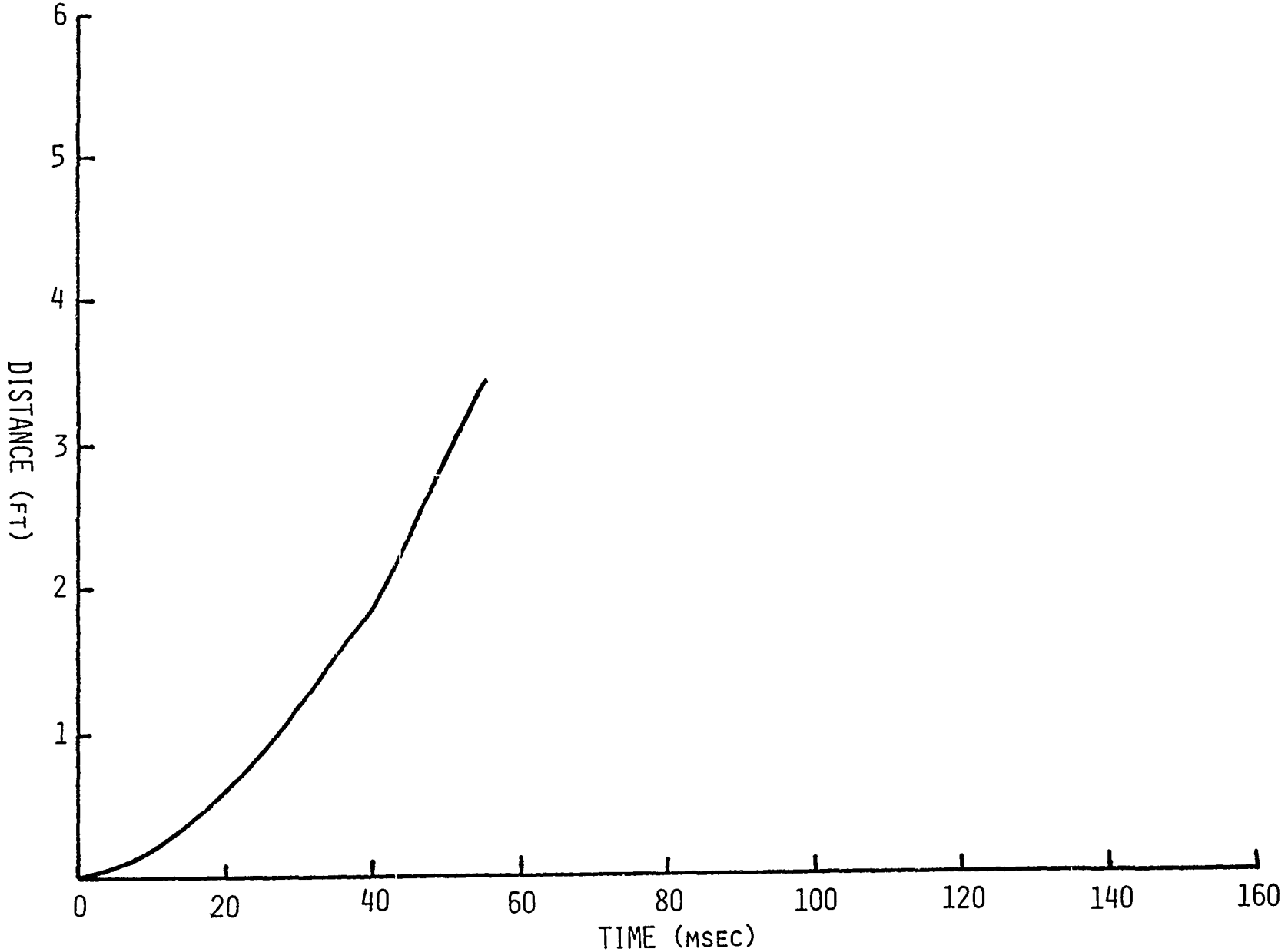

Fig. 101-3. Displacement as a Function of Time, Wall Number 101.

Test Report Wall No. 102

Type: 4-in. Sheetrock with timber studs; interior; solid (with no openings).

Support Conditions: Simple plate.

All four edges of this wall were attached to the tunnel.

Special Conditions

Tested 37.5 ft behind a nonfailing wall with a 27% window opening; mounting location B (Fig. A-3).

Test Results

This wall was tested once using two 60-ft strands of Primacord (average peak incident overpressure ~ 1.7 psi). The wall was removed from the edge supports apparently in one piece, and remained intact until impact with the far wall of the casemate, a distance of 50 ft. The resulting debris was in large pieces as shown in the photographs in Figs. 102-1 and 102-2. A plot of displacement as a function of time is presented in Fig. 102-3.

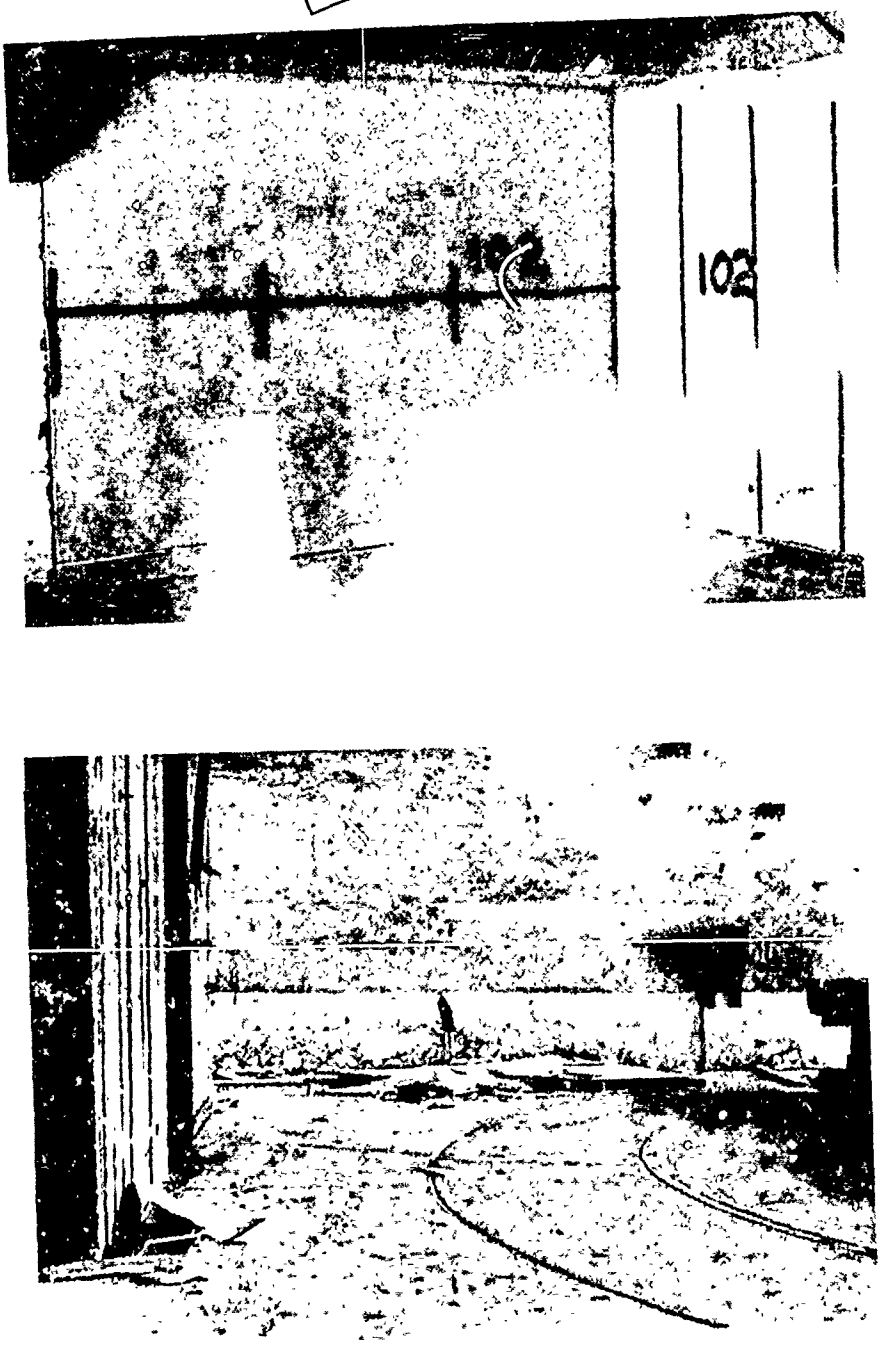

Fig. 102-1. Pre and Posttest Photographs, Wall Number 102.

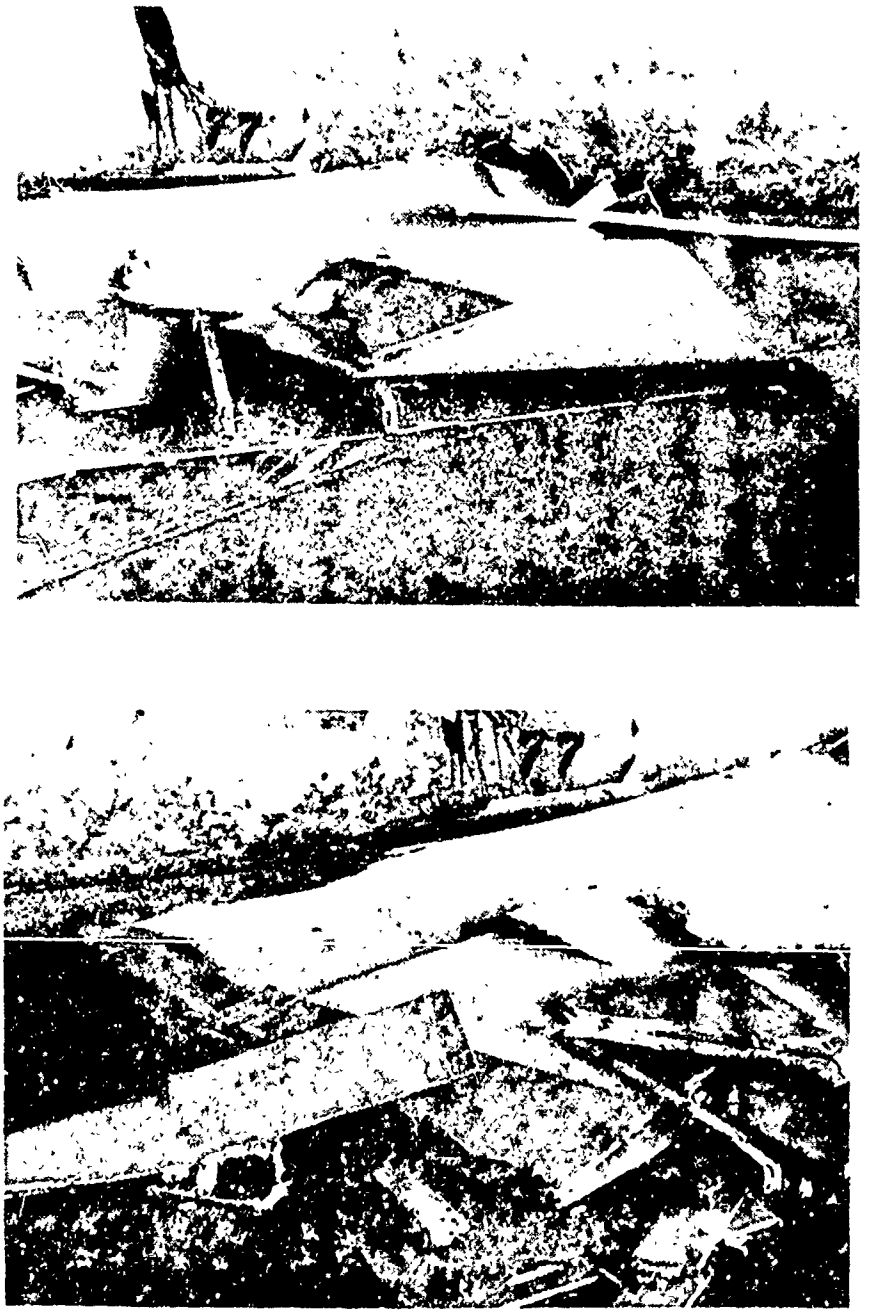

Fig. 102-2. Posttest Photographs, Wall Number 102.

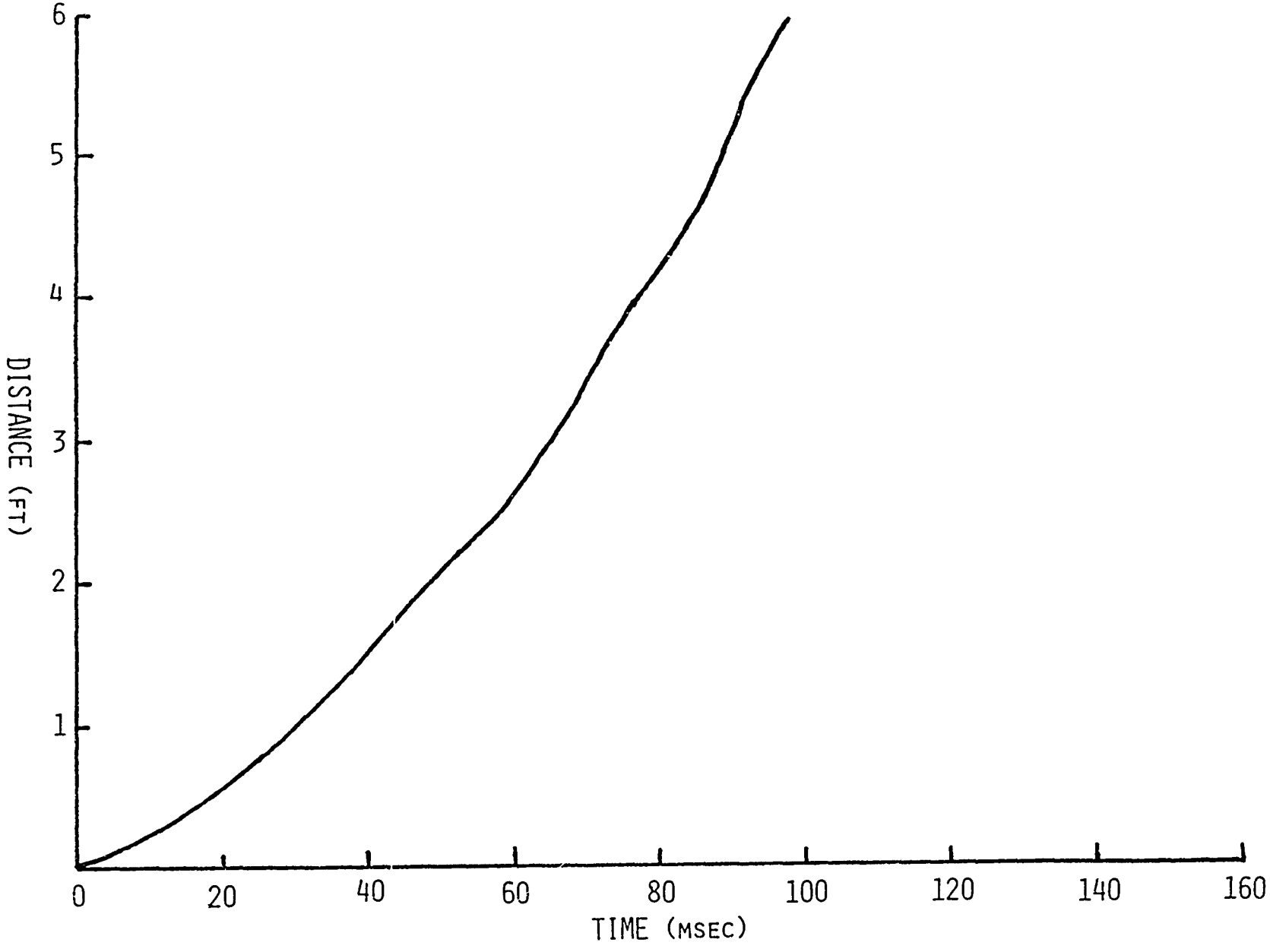

Fig. 102-3. Displacement as a Function of Time, Wall Number 102.

Test Report Wall No. 103

Type: 4-in. Sheetrock with metal studs; interior; solid (with no openings).

Support Conditions: Simple Plate

All four edges of the wall were attached to the tunnel.

Special Conditions

Tested 37.5 behind a nonfailing wall with a 27% window opening mounting location B (Fig. A-3).

Test Results

This wall was subjected to one test using two 6 ft strands of Primacord (average peak incident overpressure 1.8 psi). No cracks or separation of the sheetrock from the metal studs was evident as the wall separated from the edge supports and was translated across the casemate. The edge stud from one side was pulled loose from the concrete and translated separately. The debris was essentially in one large piece as can be seen in the photographs in Figs. 103-1 and 103-2. A plot of displacement vs time is presented in Fig. 103-3.

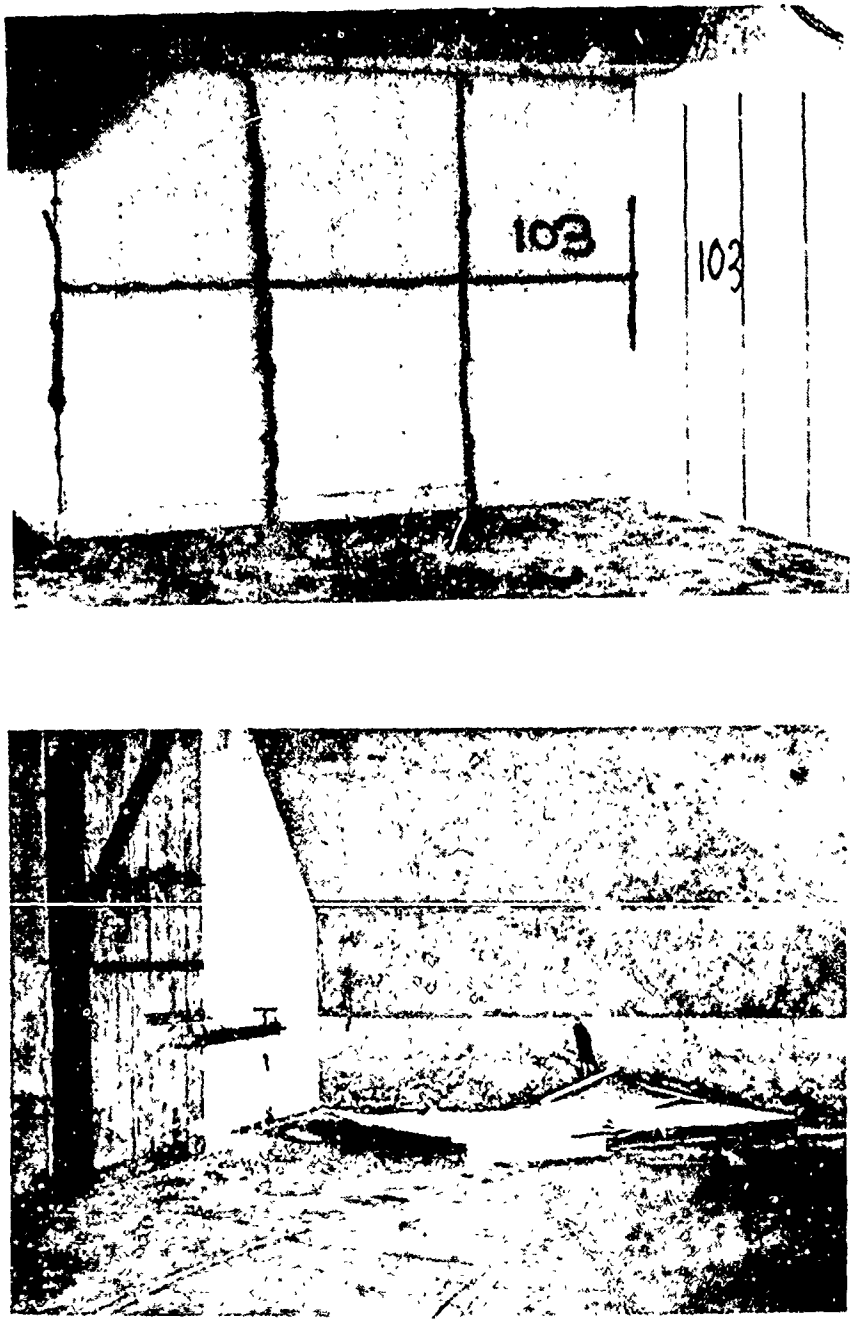

Fig. 103-1. Pre and Posttest Photographs, Wall Number 103.

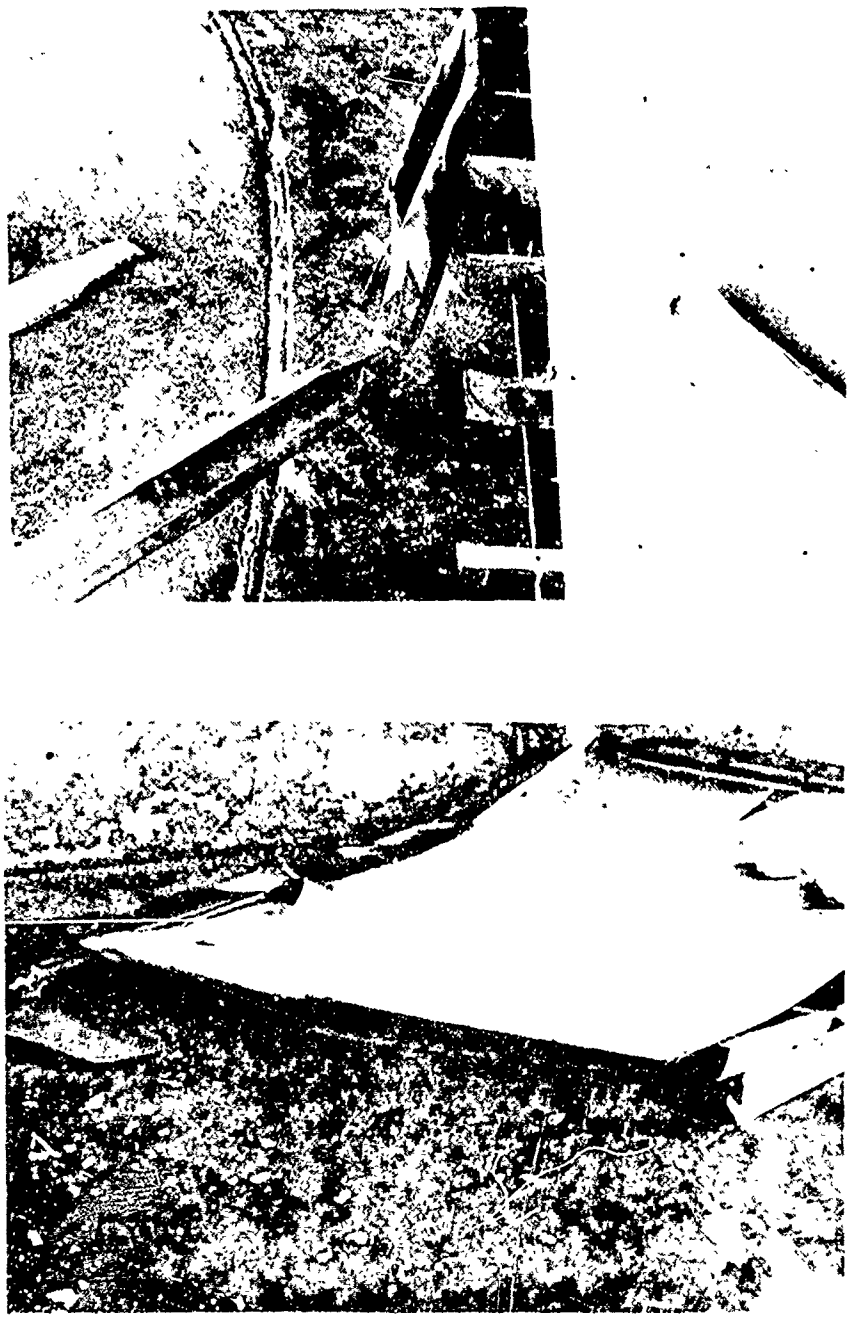

Fig. 103-2. Posttest Photographs, Wall Number 103.

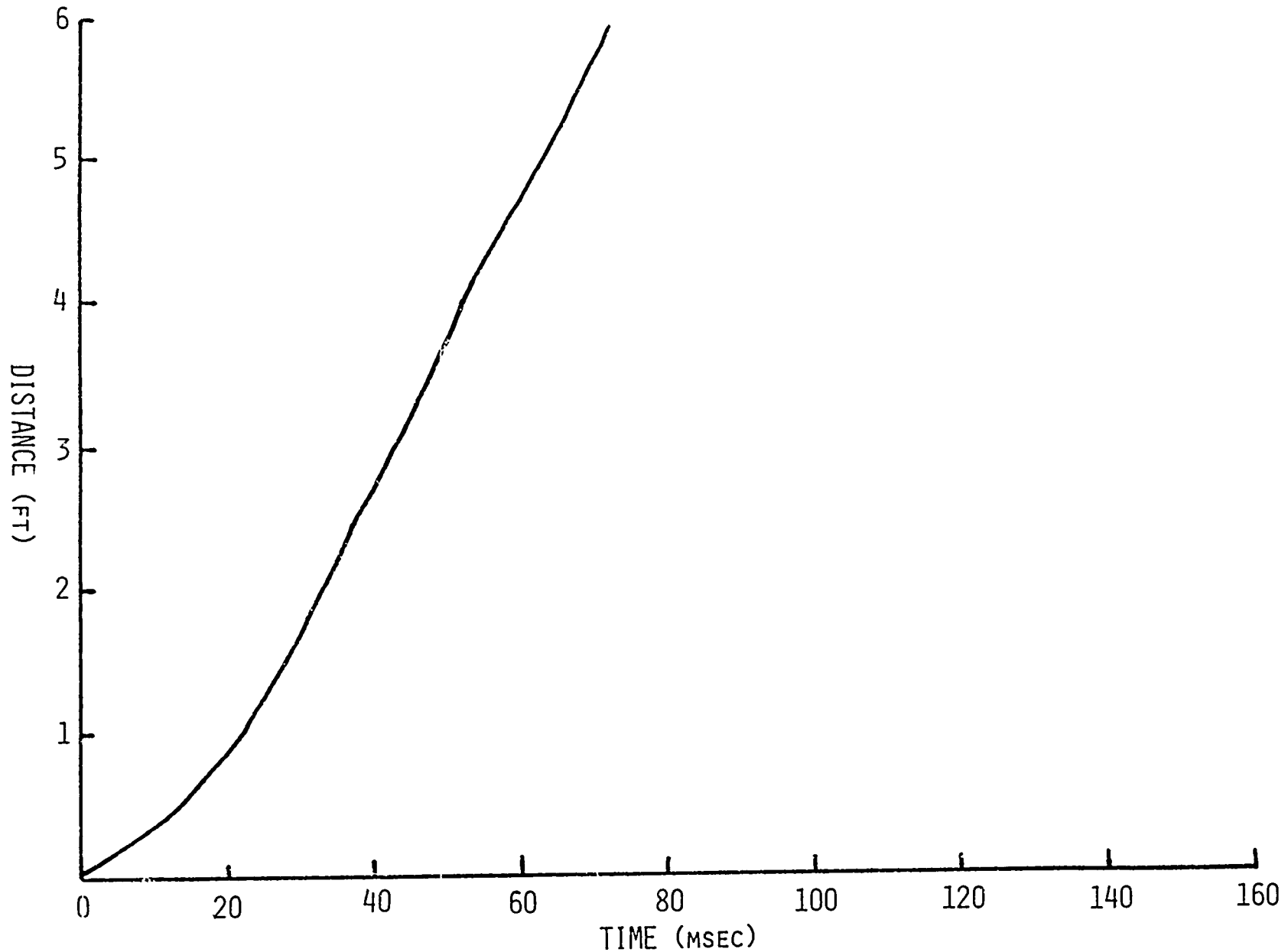

Fig. 103-3. Displacement as a Function of Time, Test Number 103.

Test Report Wall No. 104

Type: 4-in. Sheetrock with metal studs; interior; solid (with no openings).

Support Conditions: Simple Plate

All four edges of the wall were attached to the tunnel.

Special Conditions

Tested 14.5 ft behind a nonfailing wall with a 27″ window opening-mounting location A (Fig. A-3).

Test Results

One test was conducted using two strands of Primacord (average peak incident overpressure 1.8 psi). The wall remained essentially intact as it was removed from the support frame and was translated down the shock tunnel. The wall remained vertical and stopped after moving approximately 16 ft as shown in the photographs in Figs. 104-1 and 104-2. The initial blast did cause several cracks in the sheetrock panels and opened gaps between panels, as is evidenced by smoke and dust coming out of the gaps and cracks. There was only a slight amount of debris from small pieces of sheetrock torn off along the panel edges. A plot of displacement as a function of time is presented in Fig. 104-3.

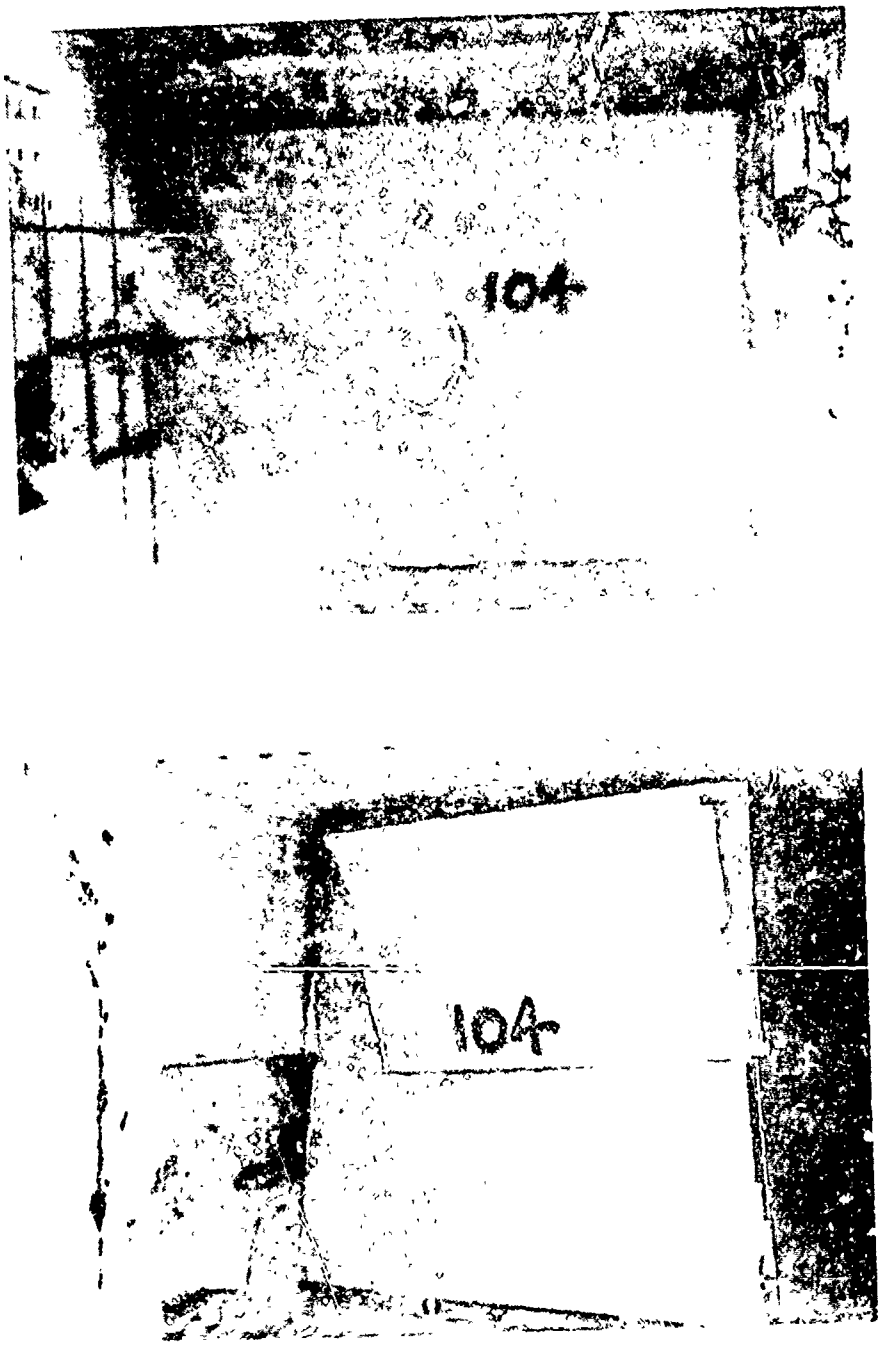

Fig. 104-1. Pre and Posttest Photographs, Wall Number 104.

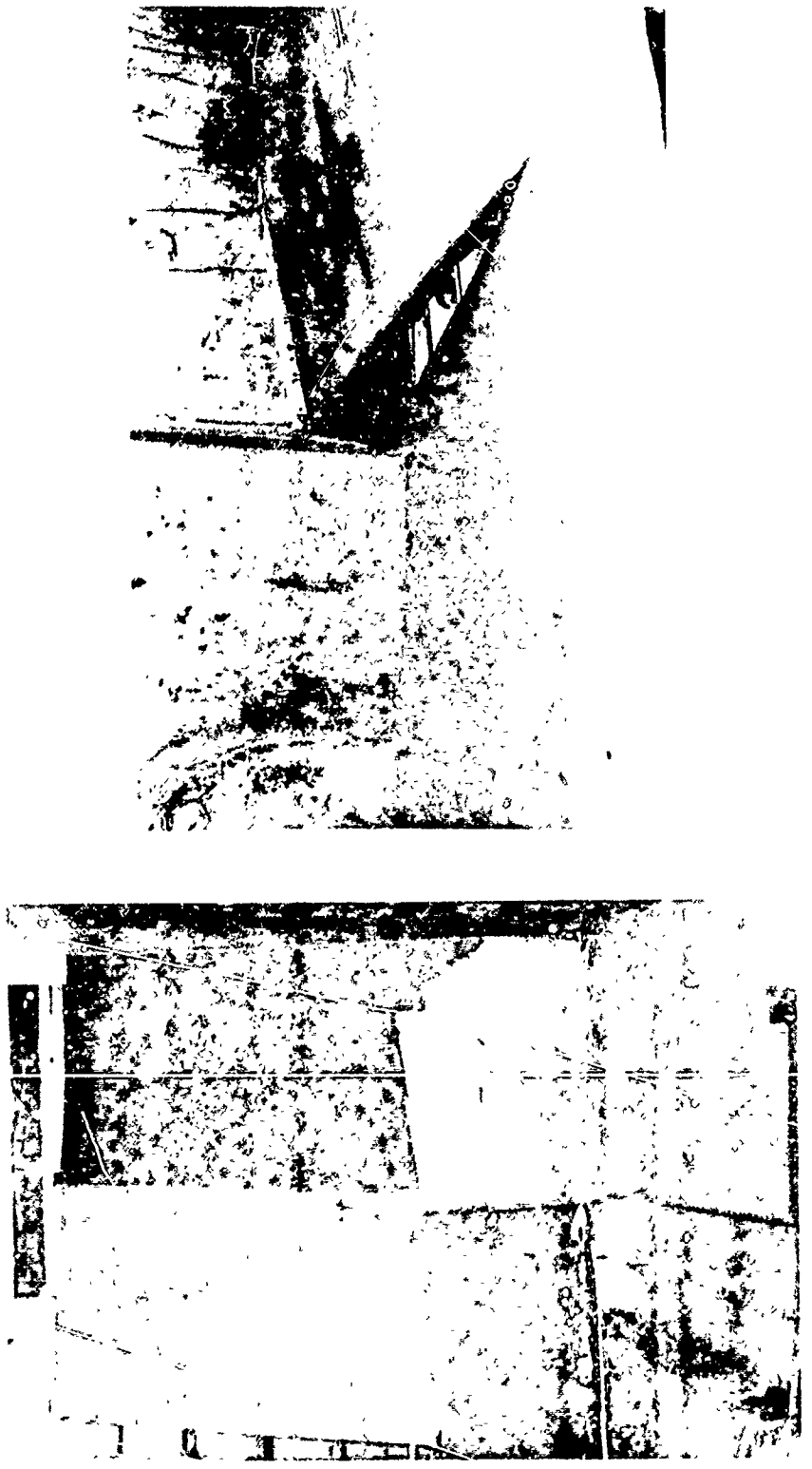

Fig. 104-2. Posttest Photographs, Wall Number 104.

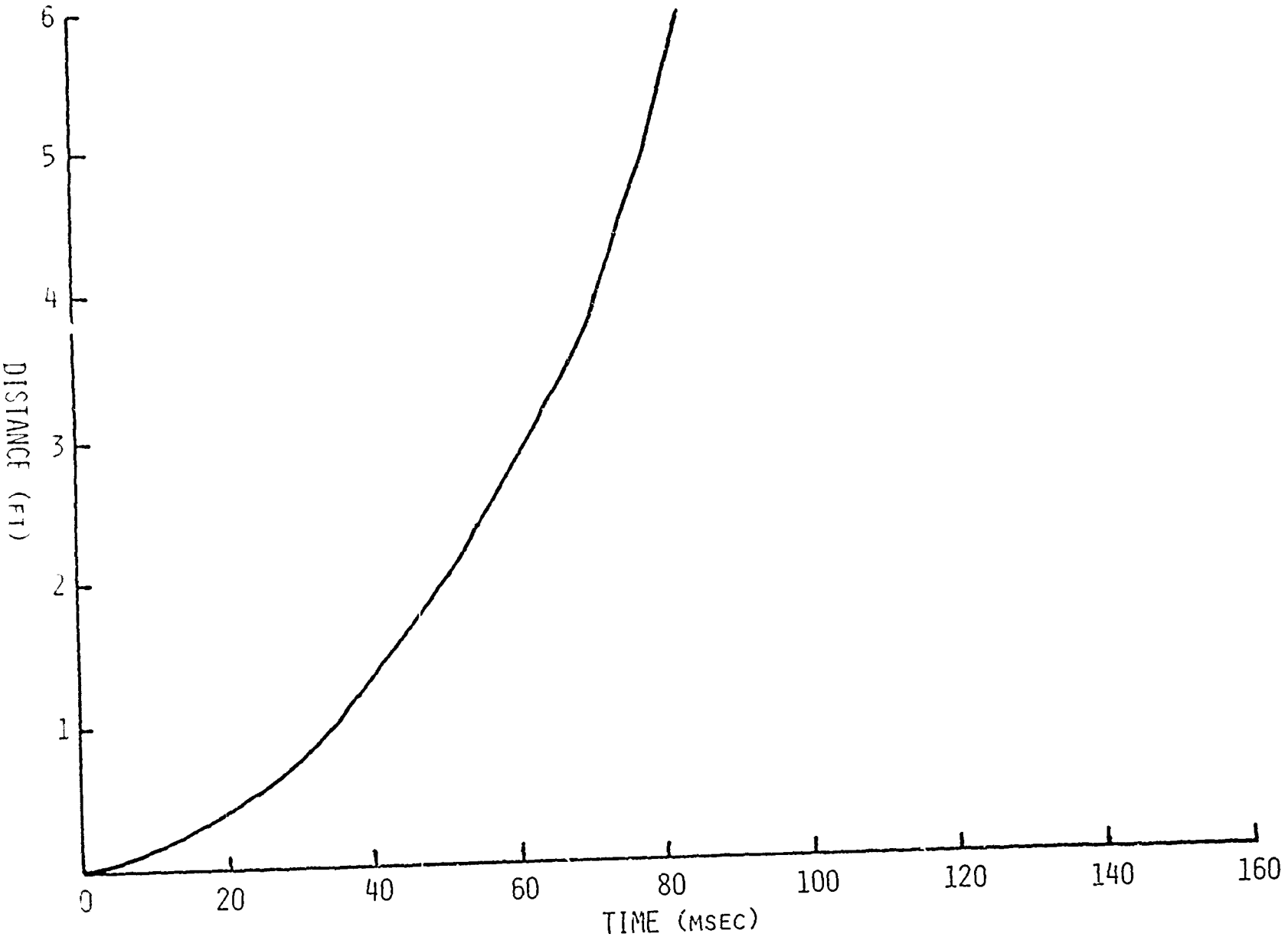

Fig. 104-3. Displacement as a Function of Time, Wall Number 104.

Test Report Wall No. 105

Type: 4-in. Sheetrock with metal studs; interior; solid (with no openings).

Support Conditions: Simple Plate

All four edges of the wall were attached to the tunnel.

Special Conditions

Tested 14.5 ft behind a nonfailing wall with a 27% window opening-mounting location A (Fig. A-3).

Test Results

One test was conducted using four 60-ft strands of Primacord (average peak incident overpressure 3.5 psi). The wall translated down the tunnel, remaining intact until it struck the bend of the tunnel; with the exception of two vertical cracks at the first and second metal studs on one side. Then, with the exception of a few pieces of sheetrock and two perimeter metal studs, the wall debris continued until impact with the far casemate wall, a distance of approximately 87 ft from the original wall location. The type, sizes, and location of the debris can be seen in the photographs in Fig. 105-1 and 105-2. A plot of displacement as a function of time is presented in Fig. 105-3.

Fig. 105-1. Posttest Photographs, Wall Number 105.

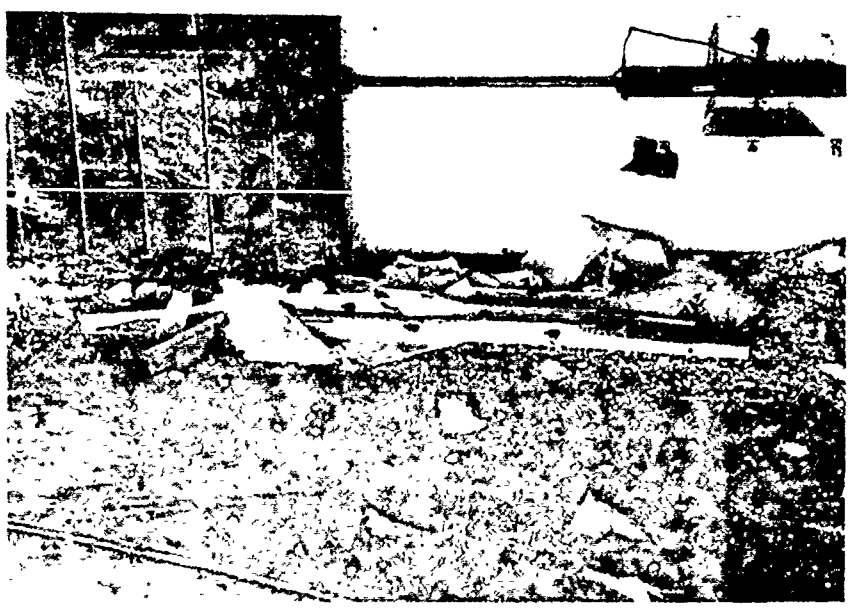

Fig. 105-2. Posttest Photographs, Wall Number 105.

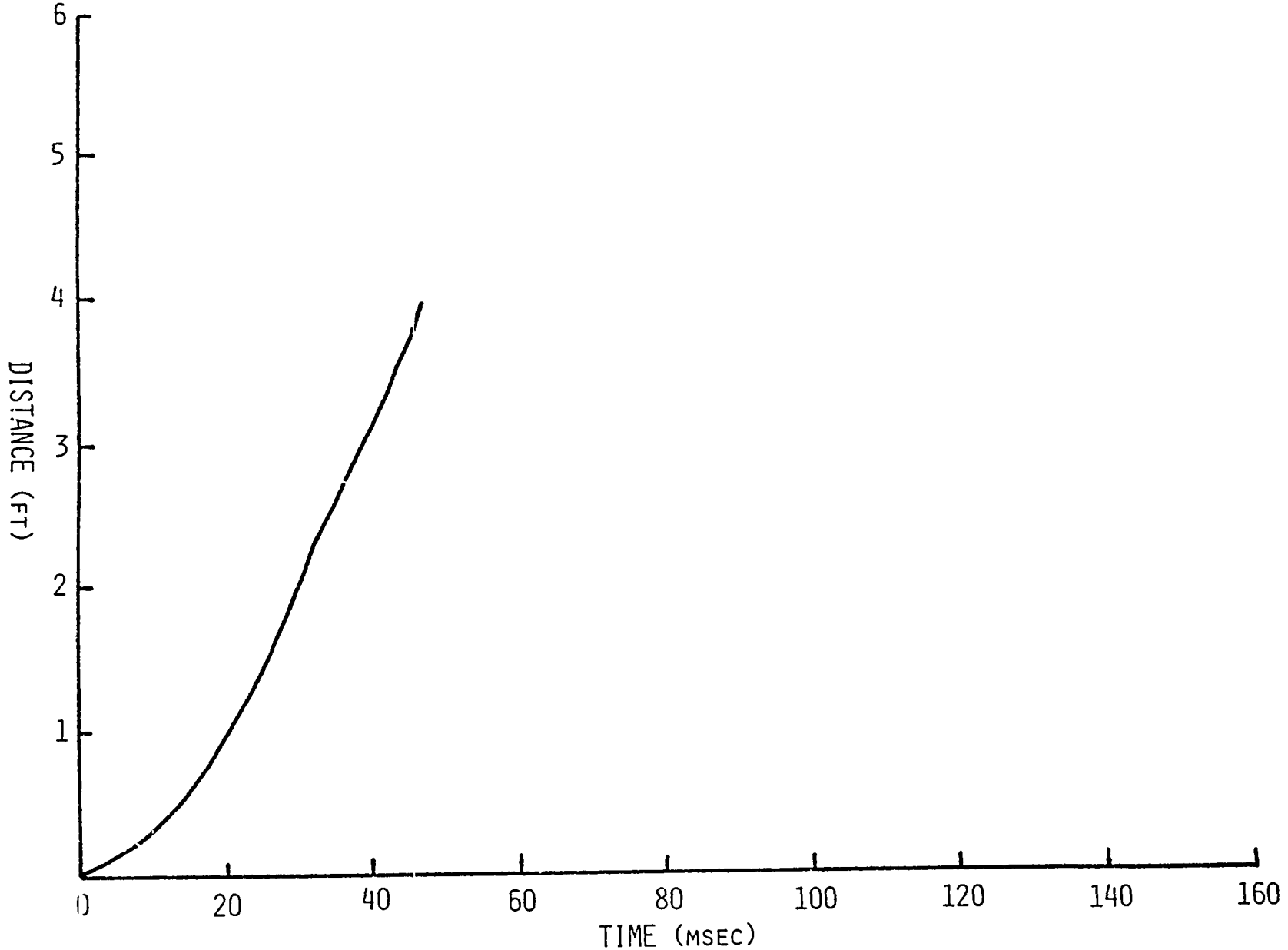

Fig. 105-3. Displacement as a Function of Time, Wall Number 105.

Test Report Wall No. 106

Type: 4-in. Sheetrock with timber studs; interior; solid (with no openings).

Support Conditions: Simple plate.

All four edges of the wall were attached to the tunnel.

Special Conditions

Tested 37.5 ft behind a nonfailing wall with a 27% open window.

Test Results

This test used 5-60 ft strands of Primacord (average peak incident overpressure 3.8 psi). This loading separated the wall from the edge support and opened gaps between all the sheetrock panels. As the wall traversed the casemate, these gaps opened up, the panels separated from the wood studs, and the wall quickly disintegrated. Other similar walls did not disintegrate in this manner, but the test crew noted that the test was conducted during a period of very high humidity and the wall had remained installed in the tunnel several days before testing and probably absorbed considerable moisture. Photographs of the test are presented in Figs. 106-1 and 106-2. A plot of displacement as a function of time for this test is presented in Fig. 106-3.

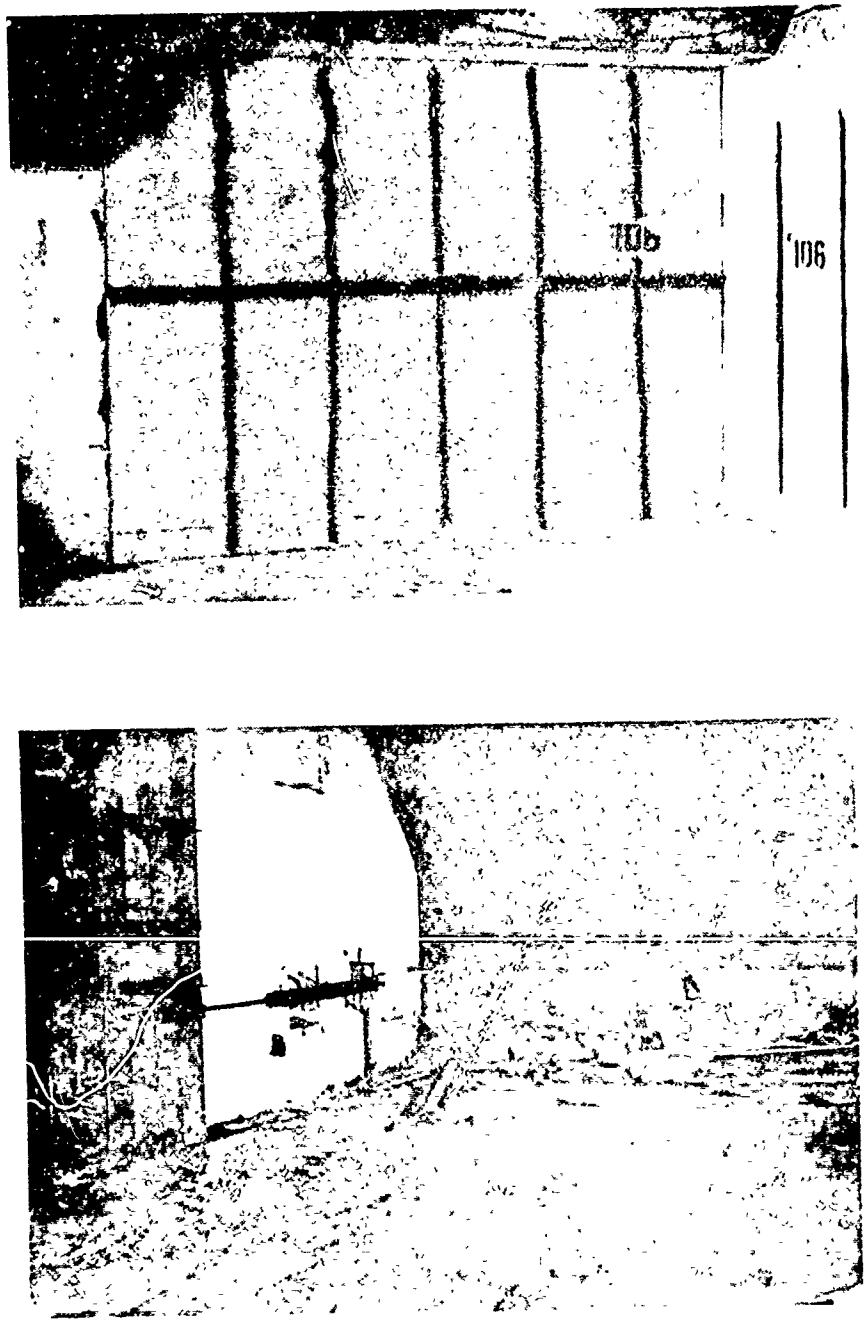

Fig. 106-1. Pre and Posttest Photographs, Wall Number 106.

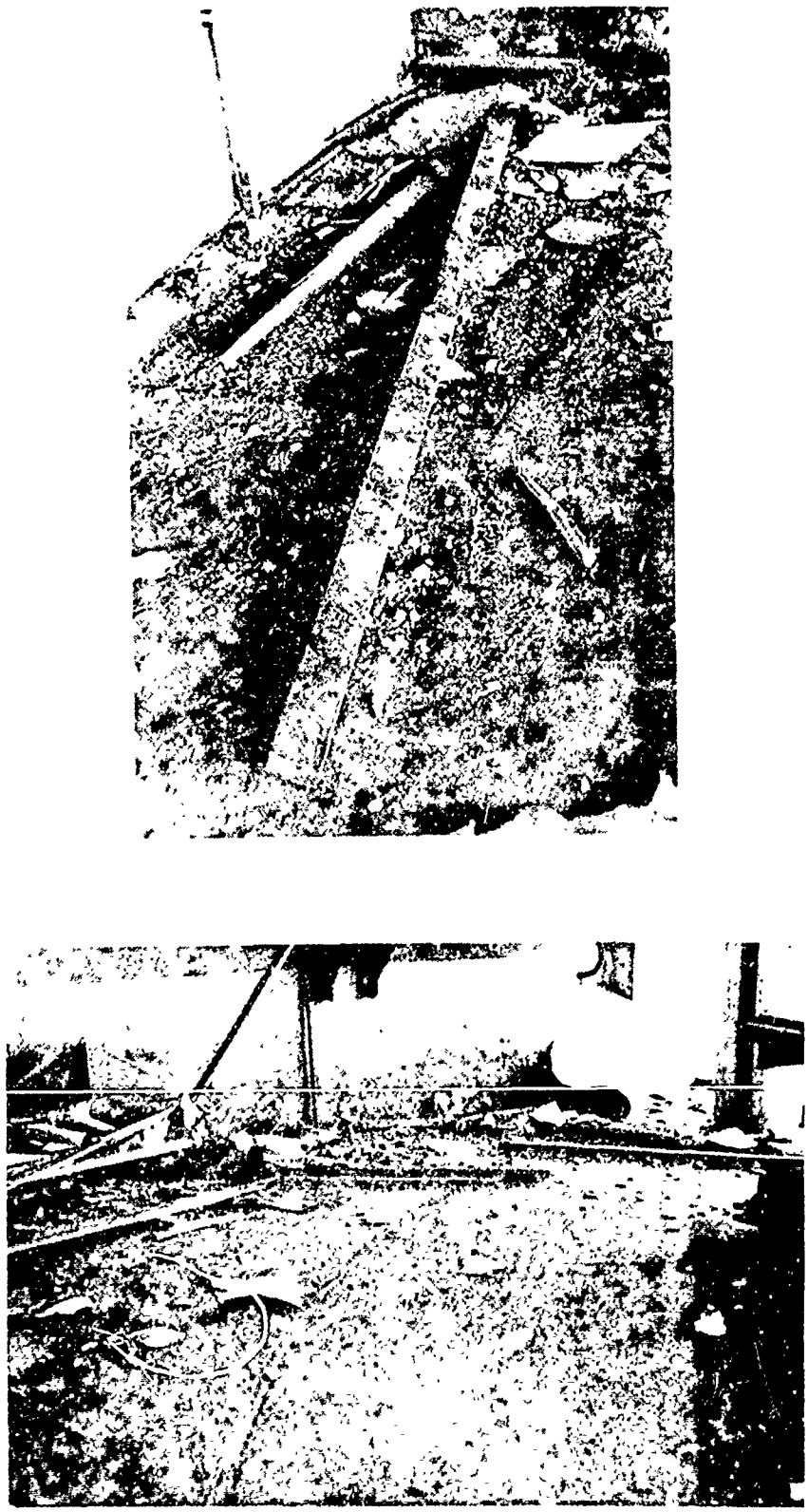

Fig. 106-2. Posttest Photographs, Wall Number 106.

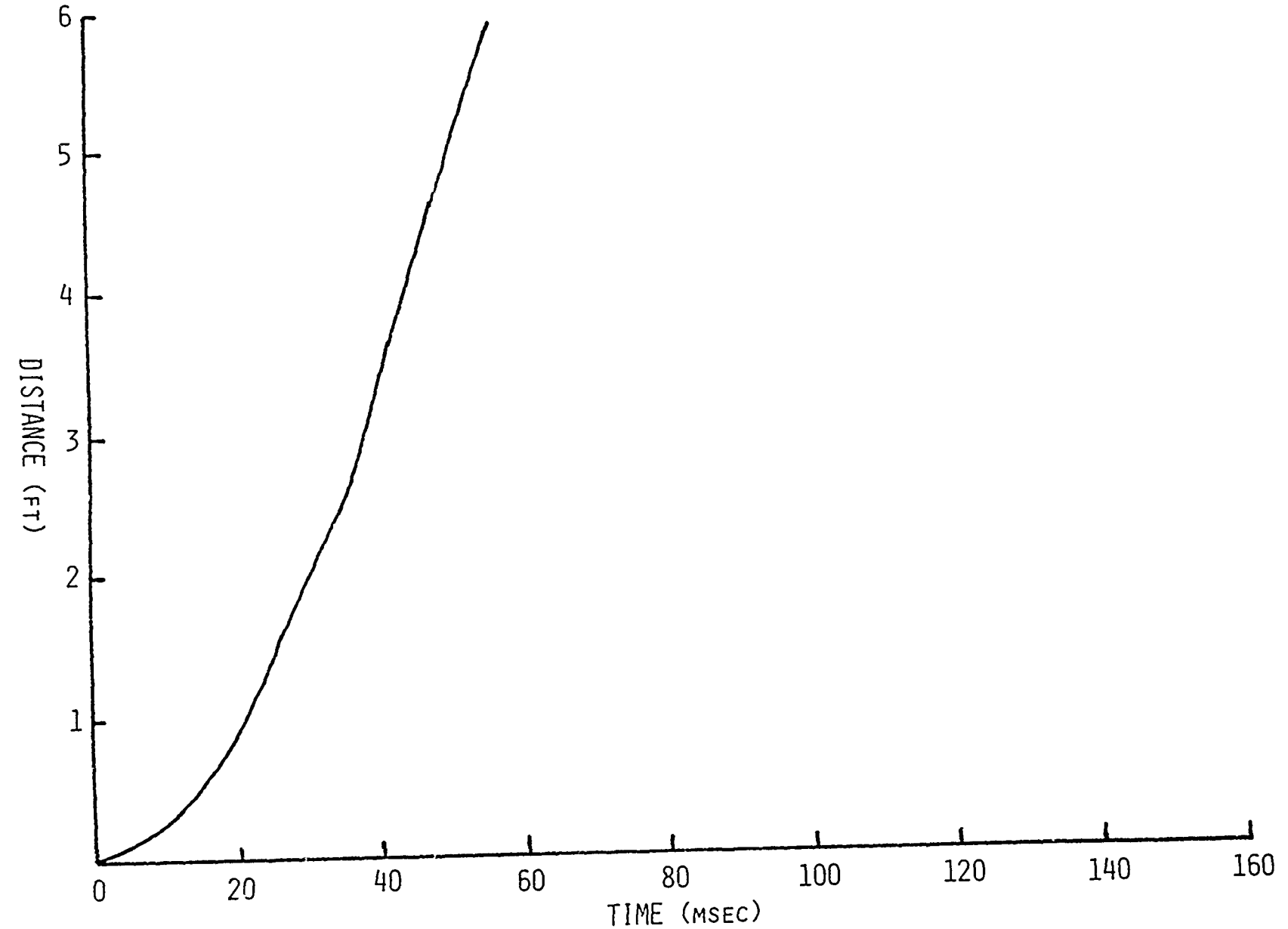

Fig. 106-3. Displacement as a Function of Time, Wall Number 106.

Test Report Wall No. 107

Type: 4-in. Sheetrock with metal studs; interior; solid (with no openings.)

Support Conditions: Simple plate.

All four edges of the wall were attached to the tunnel.

Special Conditions: Tested 37.5 ft behind a nonfailing wall with a 27% window opening.

Test Results

This wall was exposed to the air blast from five 60 ft strands of Primacord (average peak incident overpressure 3.9 psi). The wall panel separated from its parimeter edge support, and with the exception of a metal stud and some small pieces of sheetrock on one side, remained intact as it traversed the casemate area. In fact the wall remained vertical after impact with the far casemate wall as shown in the photograph in Fig. 107-1. A plot of displacement as a function of time is shown in Fig. 107-2.

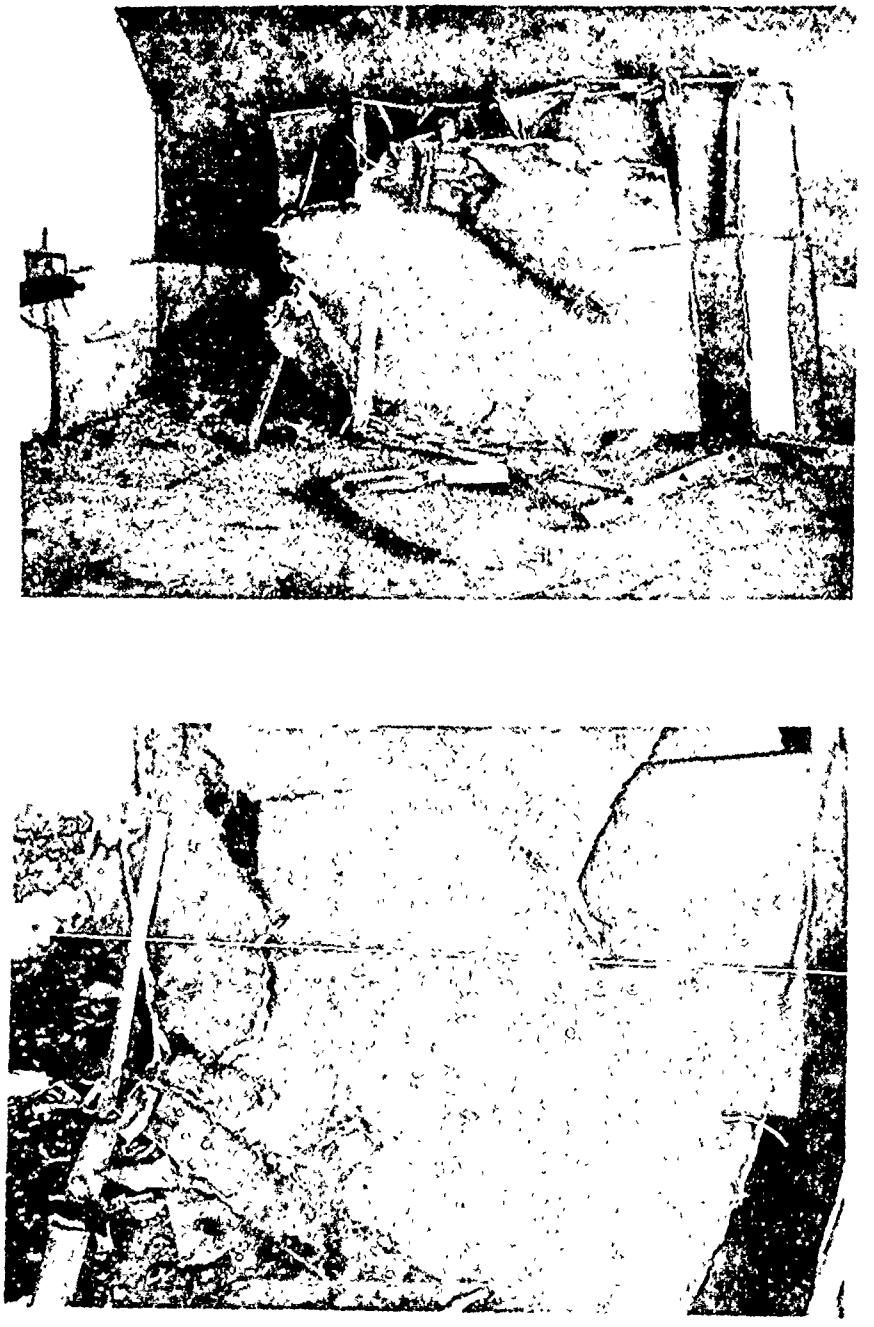

Fig. 107-1. Posttest Photographs, Wall Number 107.

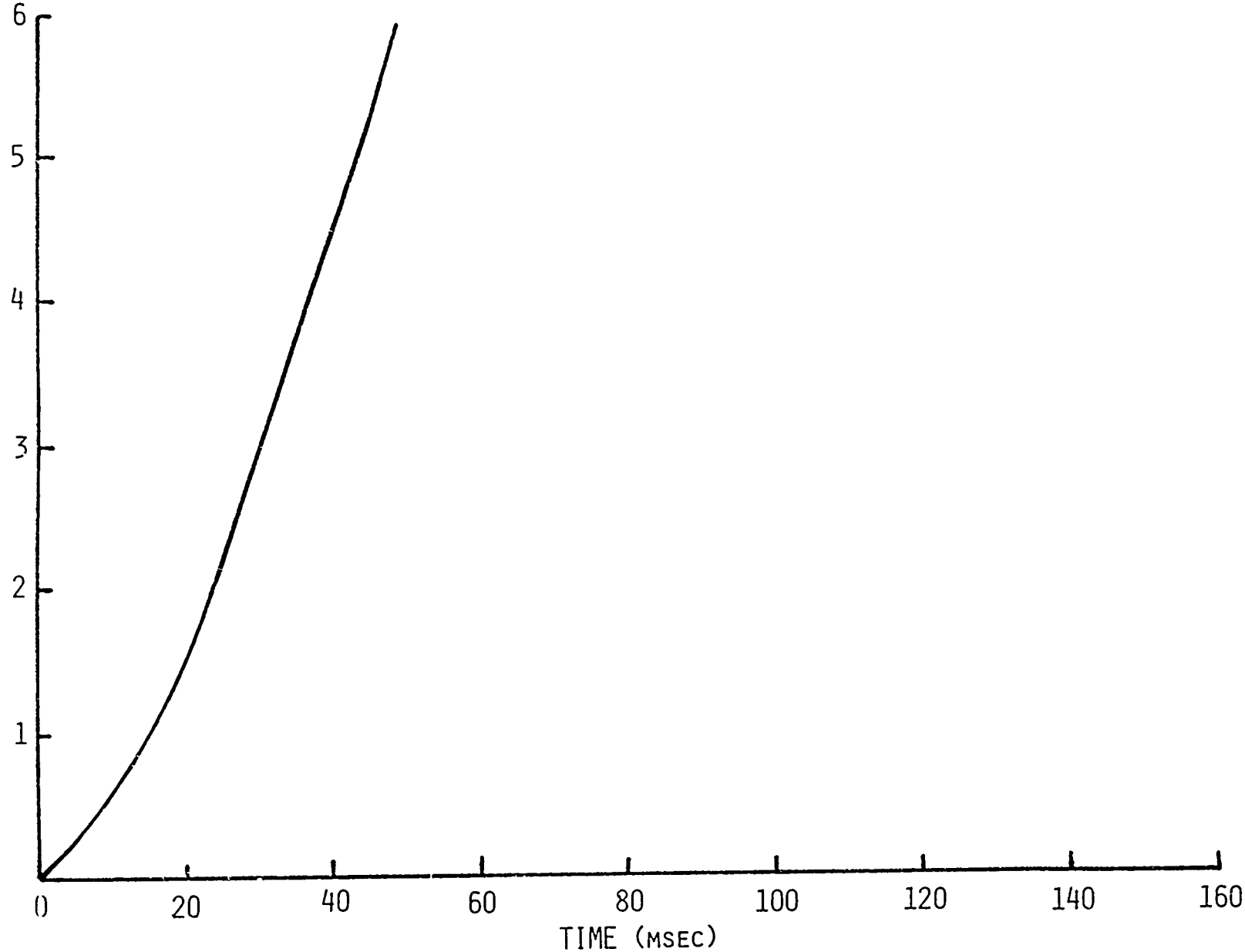

Fig. 107-2. Displacement as a Function of Time, Wall Number 107.

Test Report Wall No. 108

Type: 8-in. Concrete block; interior; solid (with no openings).

Support Conditions: Cantilever beam fixed at the bottom by mortar and enclosed in a light weight steel "picture" frame for construction and handling purposes. A four in. gap was left at the top and a two in. gap was left at each side.

Special Conditions: Tested 37.5 ft behind a nonfailing wall with a 27% window opening.

Test Results

This wall was tested using five 60 ft strands of Primacord (average peak incident overpressure 3.6 psi). The initial crack was horizontal at the mortar joint between the third and fourth rows of block (the wall is eleven rows high). A second crack appeared between the fifth and sixth rows. Immediately after this, numerous cracks appeared across almost every row and the wall disintegrated. Pre and posttest photographs of the test are presented in Figs. 108-1 and 108-2. A plot of displacement as a function of time is presented in Fig. 108-3.

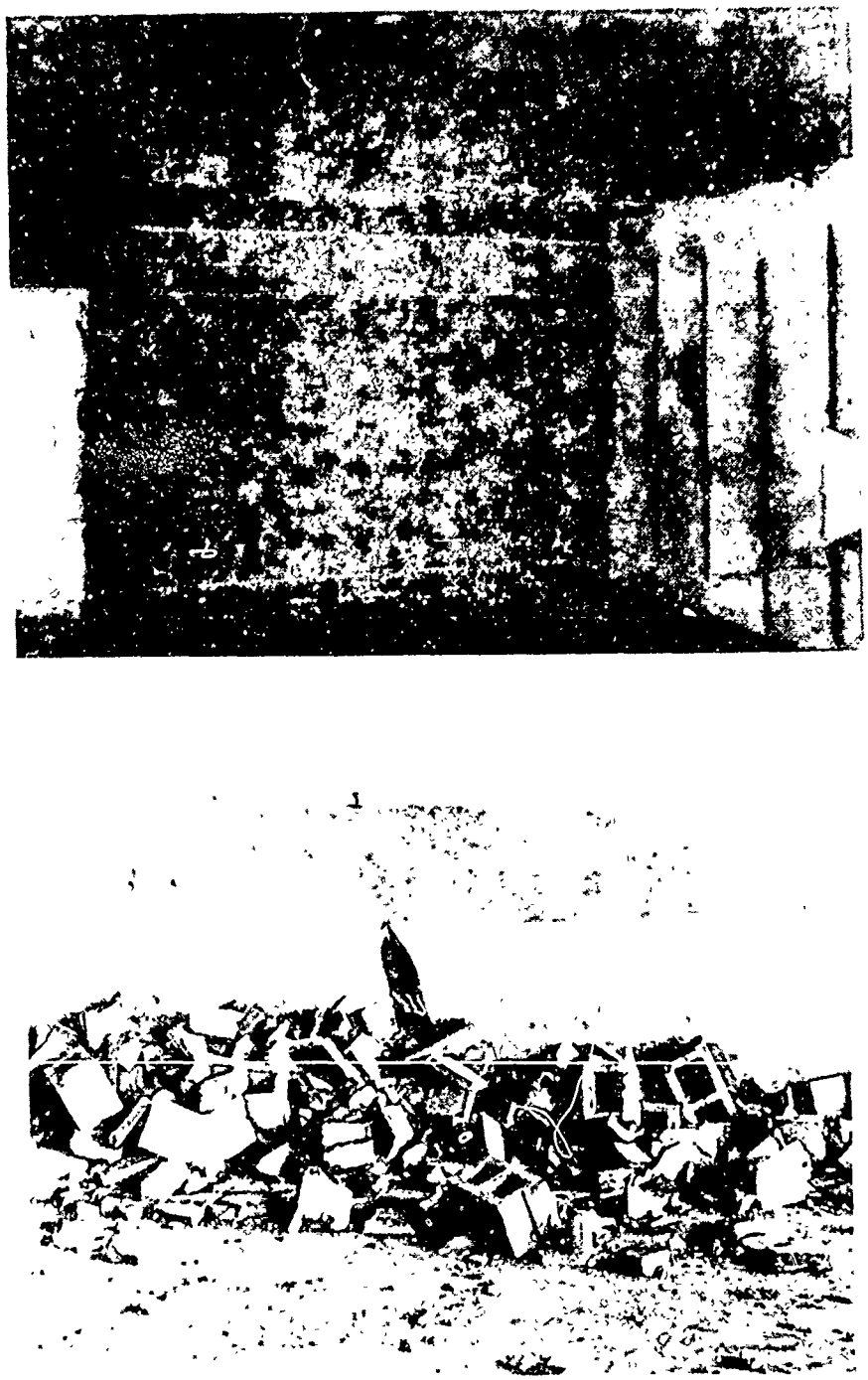

Fig. 104-1. Pre and Posttest Photographs, Wall Number 103.

Fig. 108-2. Posttest Photographs, Wall Number 108.

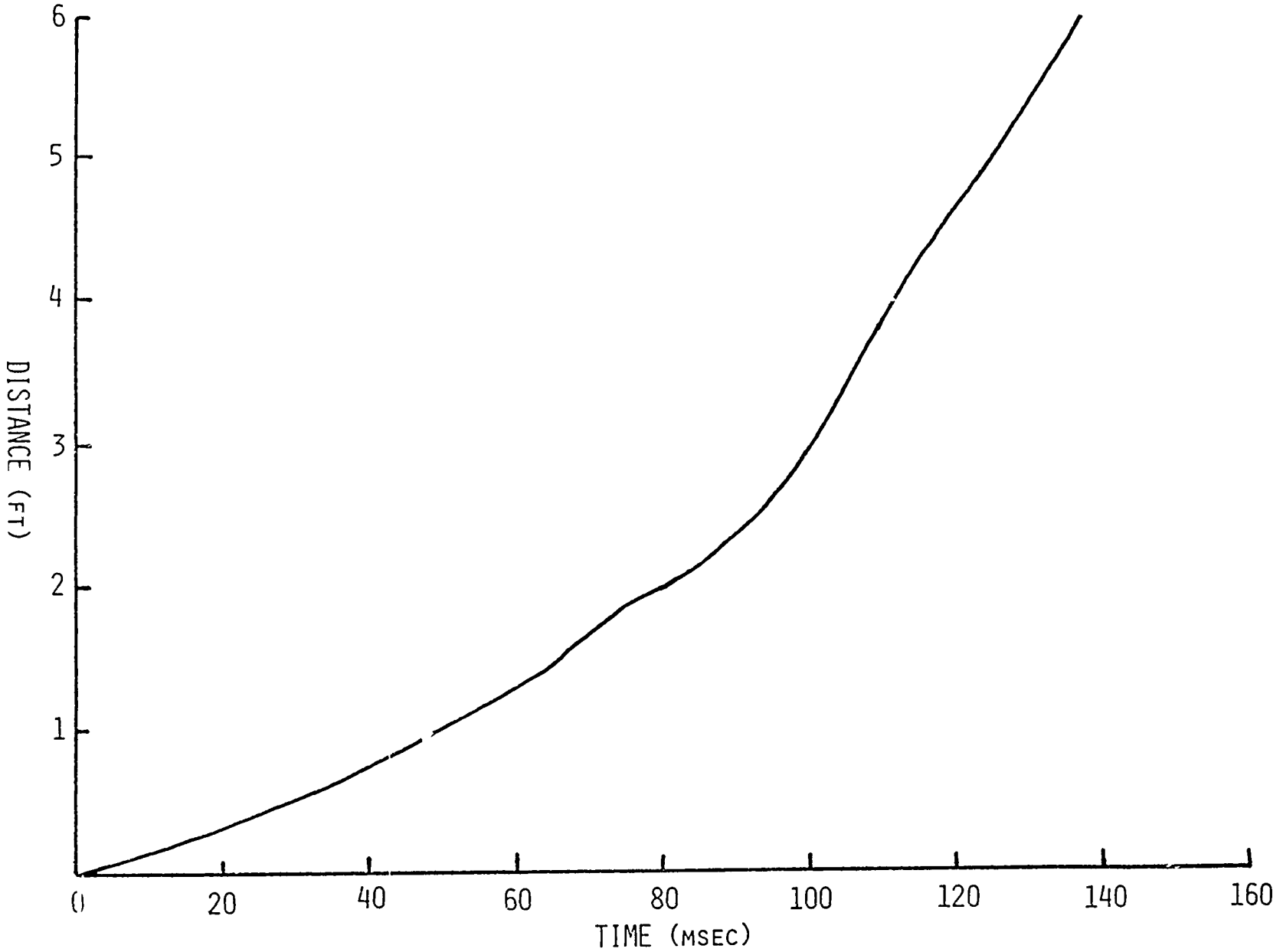

Fig. 108-3. Displacement as a Function of Time, Wall Number 108.

Test Report Wall No. 109

Type: 8-in. Concrete block; interior; solid (with no openings).

Support Conditions: Cantilever beam fixed at the bottom by mortar, and enclosed in a light weight steel "picture" frame for construction and handling purposes. A four in. gap was left at the top and a two in. gap was left at each side.

Special Conditions: Tested 37.5 ft behind a nonfailing wall with a 27% window opening.

Test Results

One test was conducted on this wall using five 60-ft strands of Primacord (average peak incident overpressure 4.0 psi). The initial crack appeared between the fifth and sixth rows and between the seventh and eighth rows of blocks. The failure of this wall was quite different from that of wall 108. Though test conditions were very similar, the pieces from the upper two thirds of the wall remained intact for a much longer time. The top piece (5 blocks high and almost the width of the wall) did not appear to break up until impact with the floor approximately 40 feet away. The next lower piece, 3 blocks high and about 2/3 the width of the wall, also remained intact until impact with the floor. Posttest photographs of this wall can be seen in Figs. 109-1 and 109-2. A plot of displacement as a function of time is presented in Fig. 109-3.

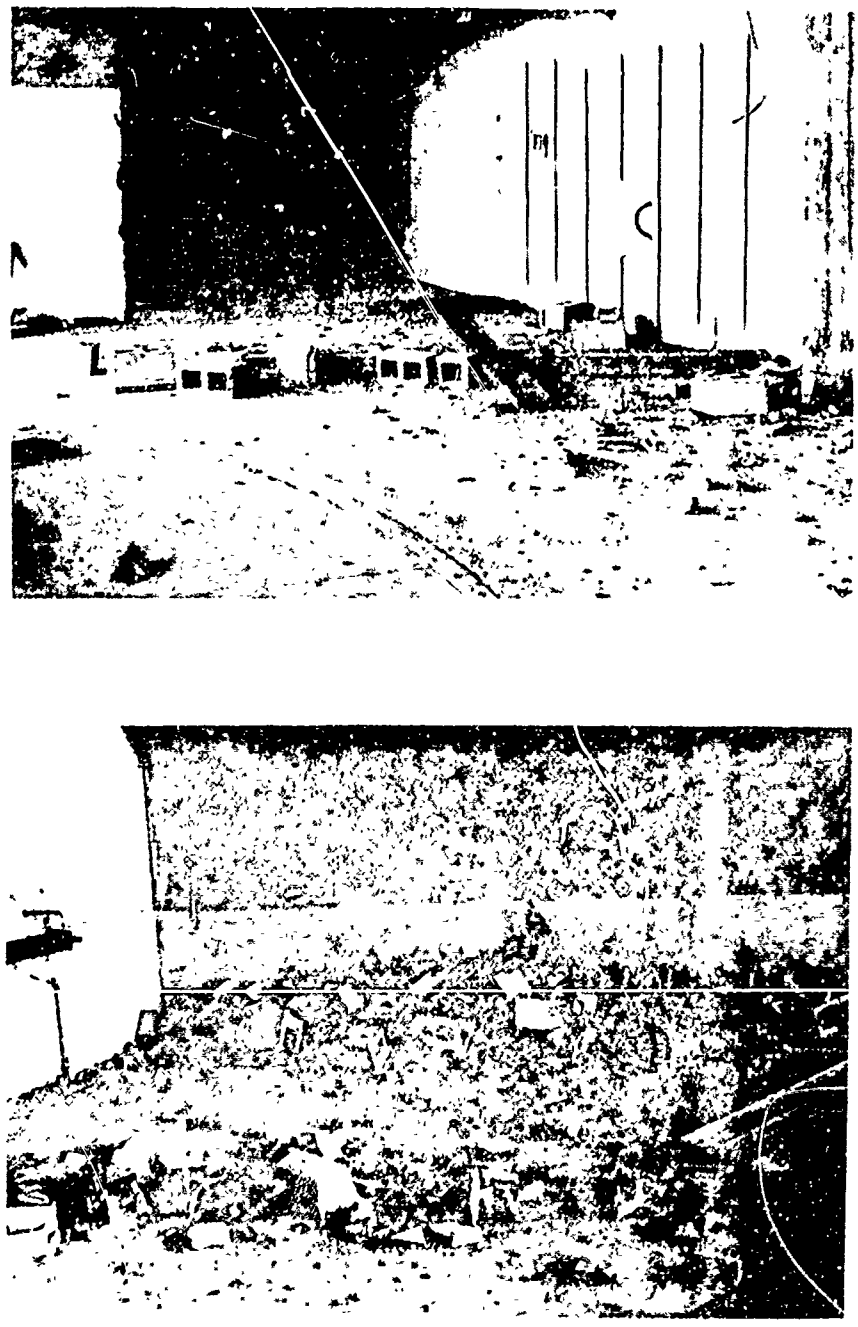

Fig. 109-1 Posttest Photographs, Wall Number 109.

Fig. 109-2. Posttest Photographs, Wall Number 109.

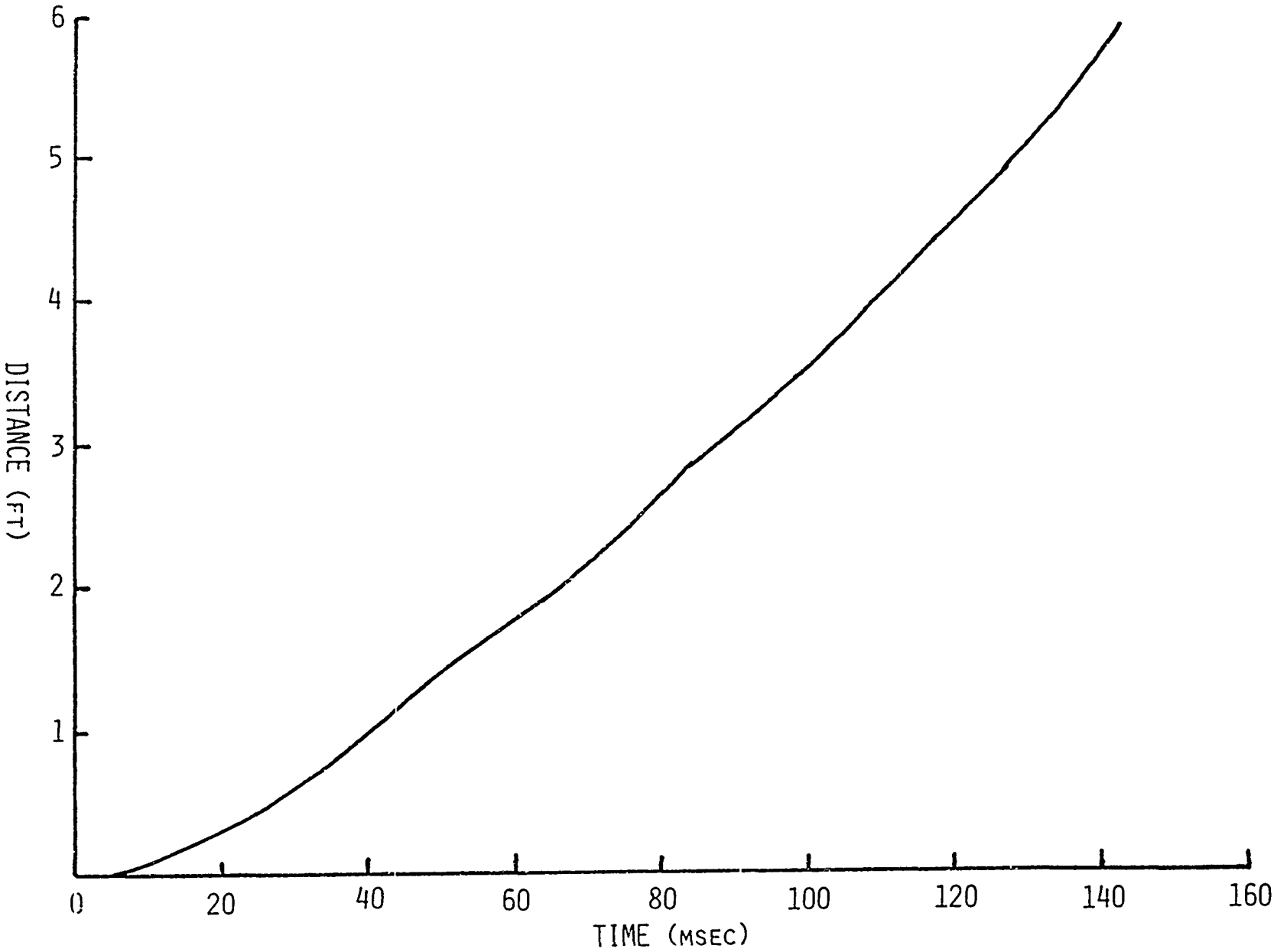

Fig. 109-3. Displacement as a Function of Time, Wall Number 109.

Test Report Wall No. 110

Type: 4-in. Sheetrock; timber stud; interior; solid (with no openings).

Support Conditions: Simple plate.

All four edges of the wall were attached to the tunnel.

Special Conditions: Tested 37.5 ft behind a nonfailing wall with a 27% window opening. A manikin seated in a chair and a table were placed approximately eleven feet from the wall.

Test Results

One test was conducted using five 60-ft strands of Primacord (average peak incident overpressure 3.8 psi). The initial shock separated the wall from its edge supports and a gap opened between the top and bottom row of sheetrock panels. The panels remained together, but the wood structural members were separated from the sheetrock before the panels collided with the table and manikin, immediately after which, the sheetrock developed a manikin-sized hole. The table was completely destroyed and was buried in the debris against the far wall. The manikin was moved approximately 35 ft but still remained in the chair. Pre- and posttest photographs of this test are presented in Figs. 110-1 through 110-3. A plot of displacement as a function of time is presented in Fig. 110-4.

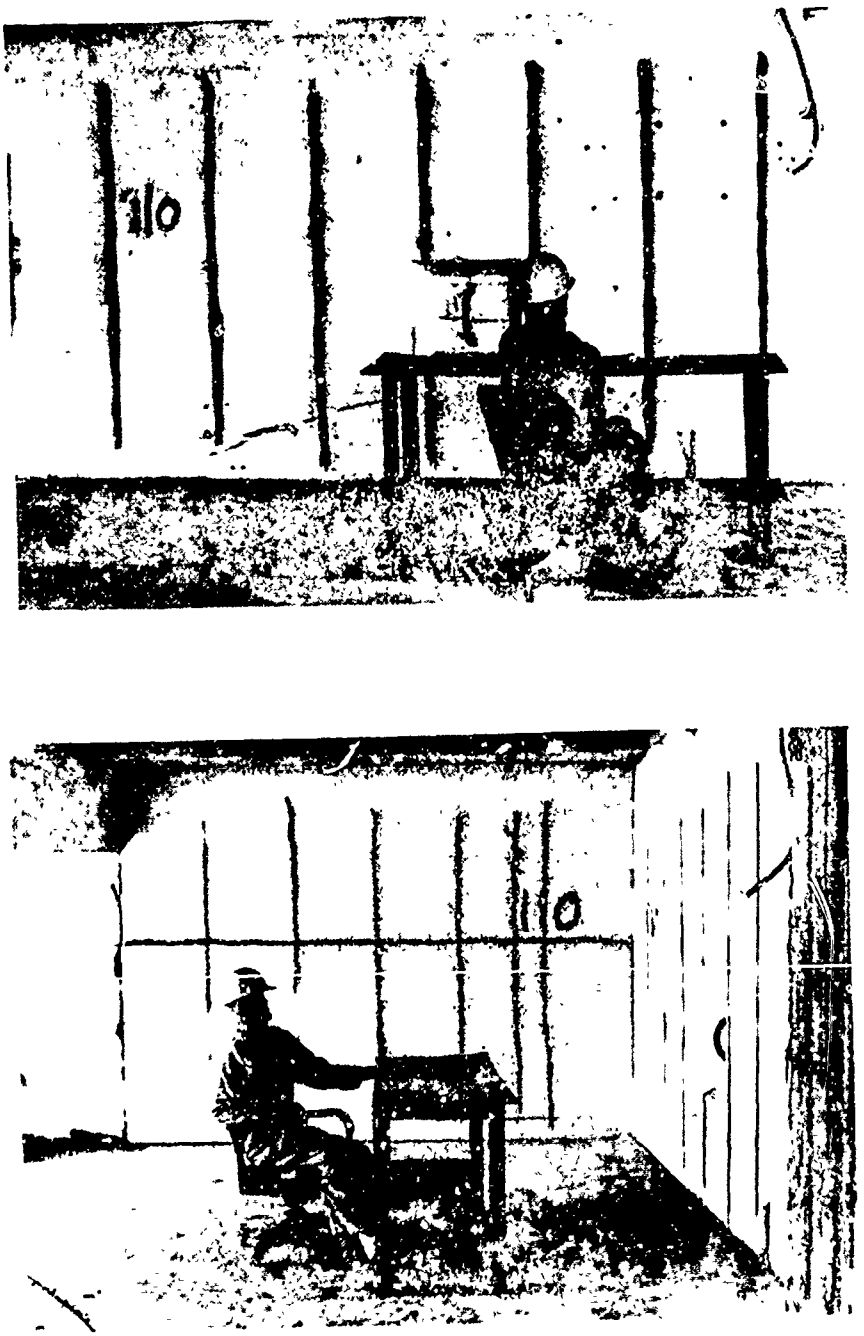

Fig. 110-1. Pretest Photographs, Wall Number 110.

Fig. 110-2. Posttest Photographs, Wall Number 110.

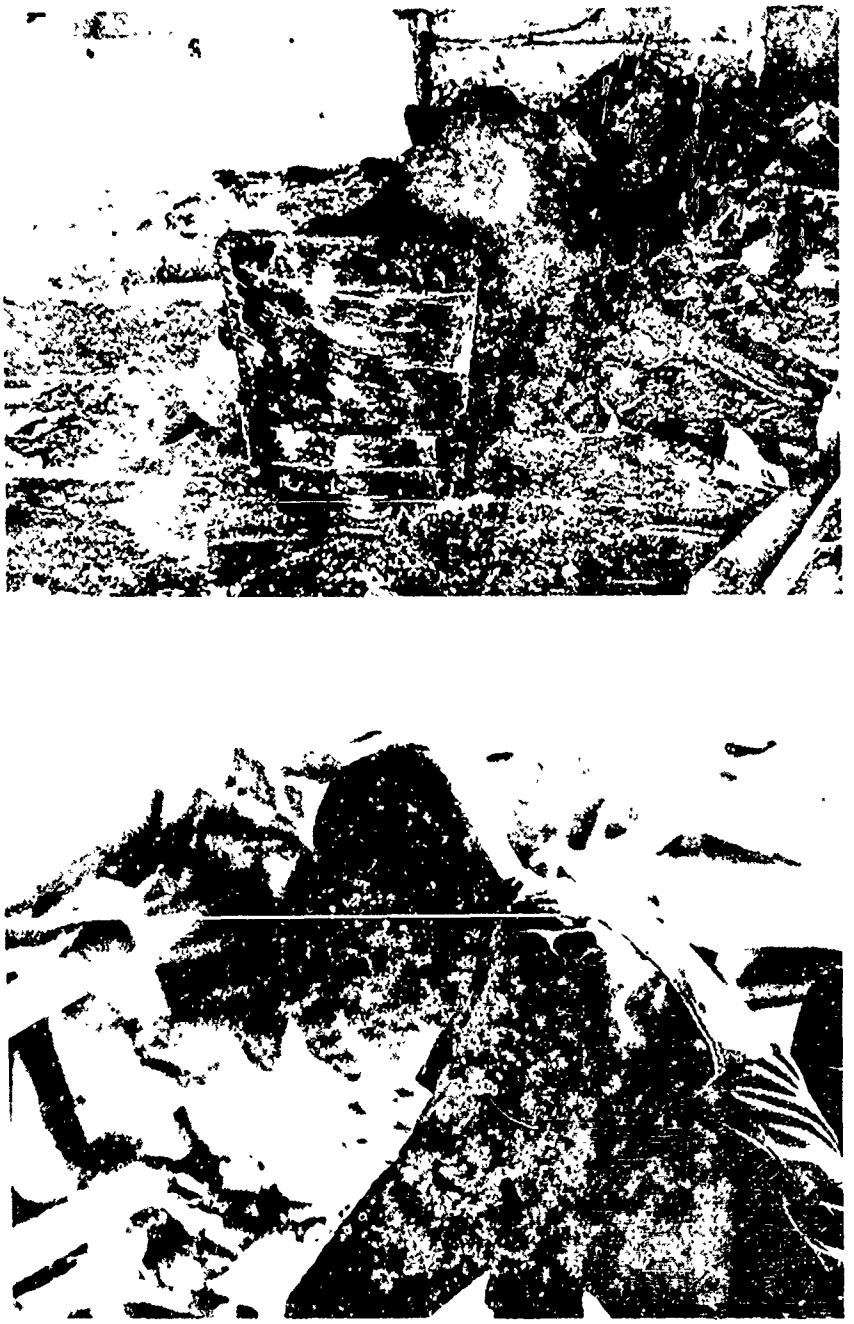

Fig. 110-3. Posttest Photographs, Wall Number 110.

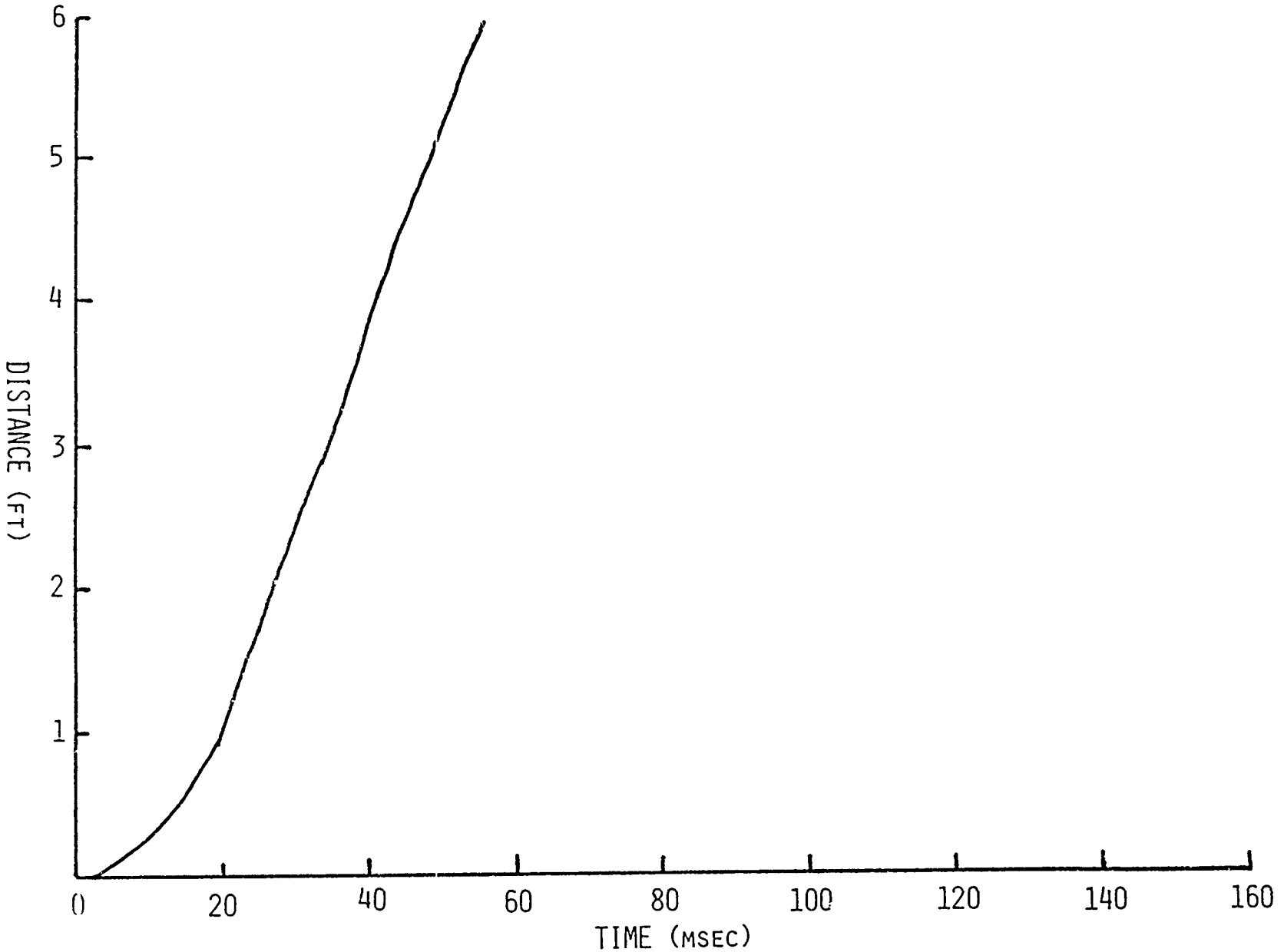

Fig. 110-4. Displacement as a Function of Time, Wall Number 110.

Test Report Wall No. 111

Type: 4-in. Sheetrock; timber stud; interior; with door (door closed for test).

Support Conditions: Simple plate.

All four edges of the wall were attached to the tunnel.

Special Conditions: Tested 37.5 ft behind a nonfailing wall with a 27% window opening.

Test Results

One test was conducted using five 60-ft strands of Primacord (average peak incident overpressure 3.9 psi). The door was broken loose first and continued ahead of the wall across the casemate. The wall started disintegrating as soon as it was removed from the support frame and was completely broken up by the time it had traveled 15 ft. Pre- and pre and posttest photographs are presented in Figs. 111-1 and 111-2. A plot of displacement as a function of time is presented in Fig. 111-3.

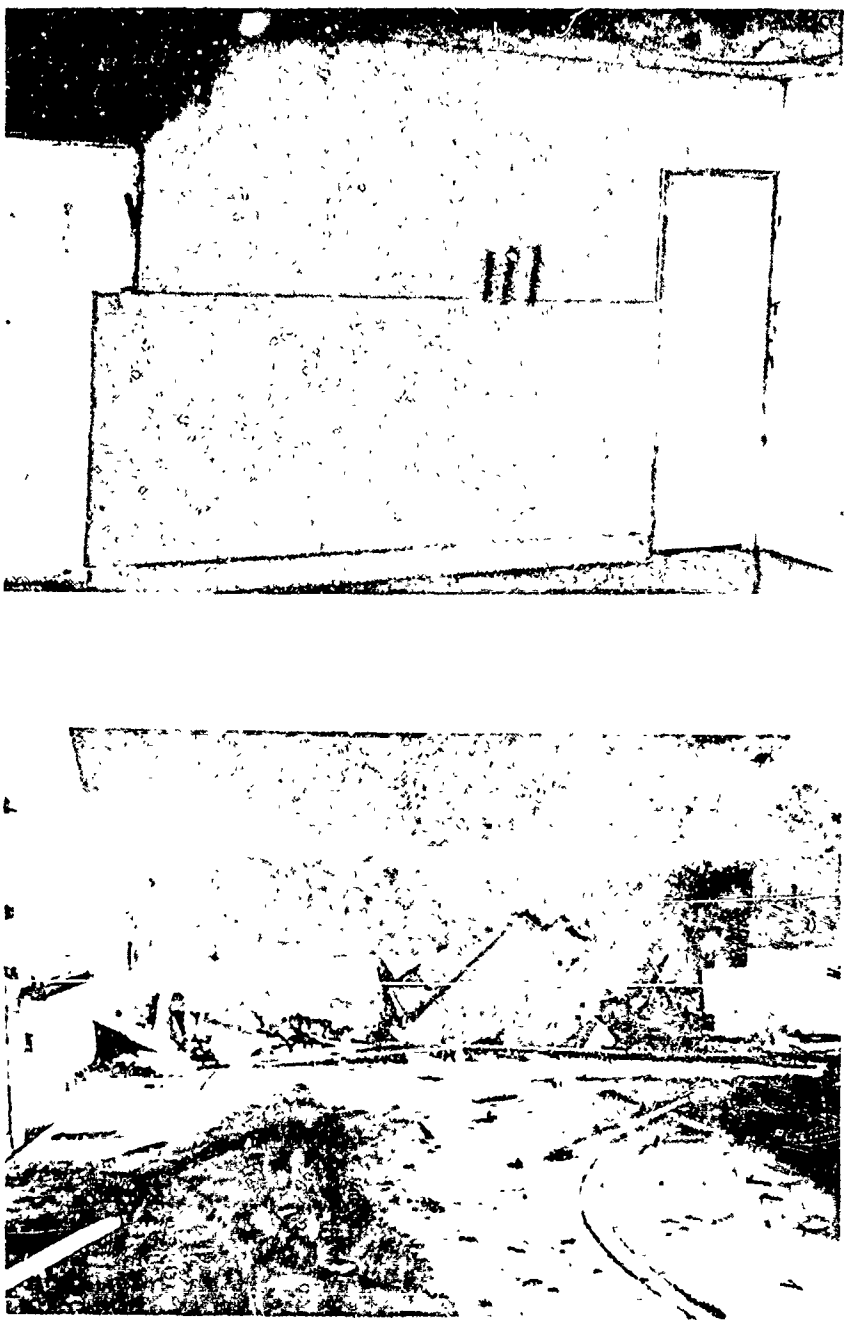

Fig. 111-1. Pre and Posttest Photographs, Wall Number 111.

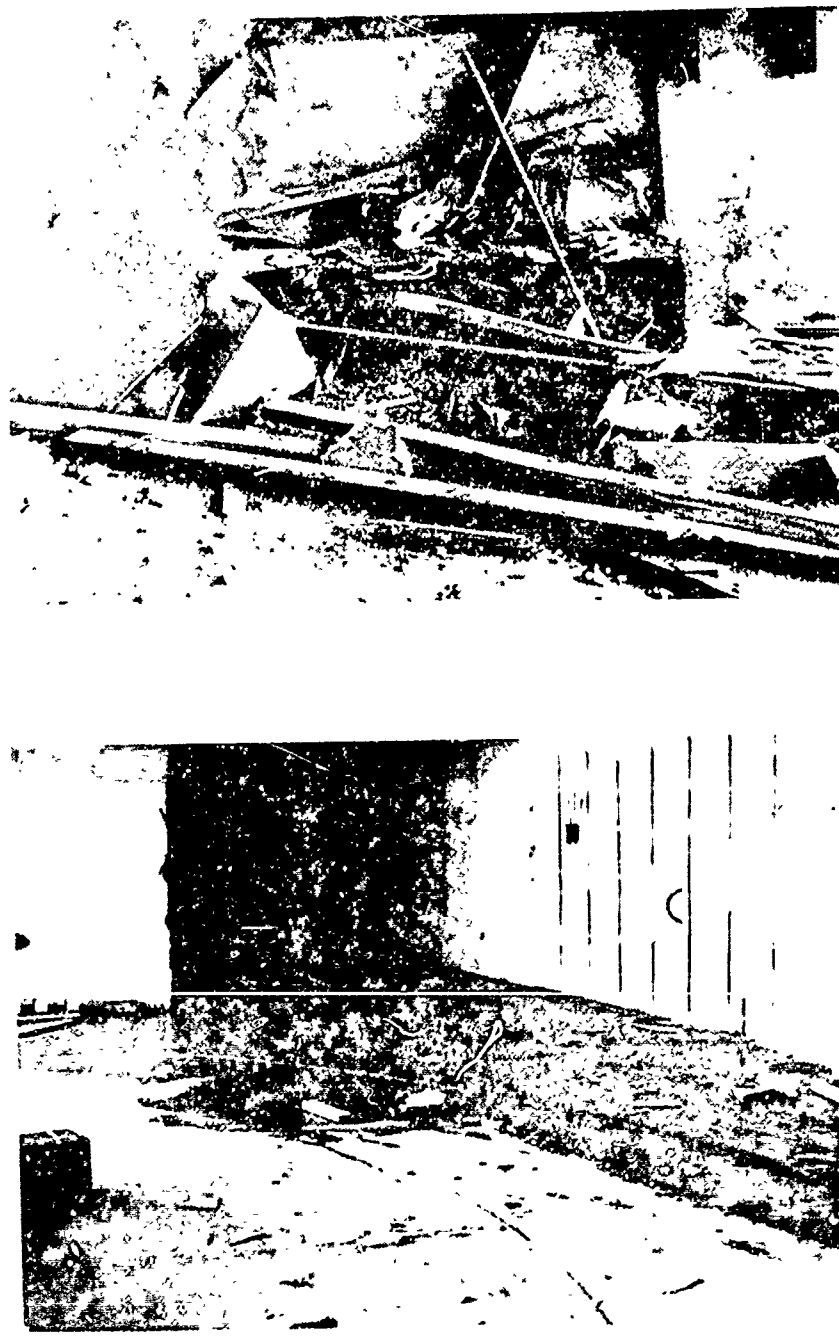

Fig. 111-2 Posttest Photographs, Wall Number 111.

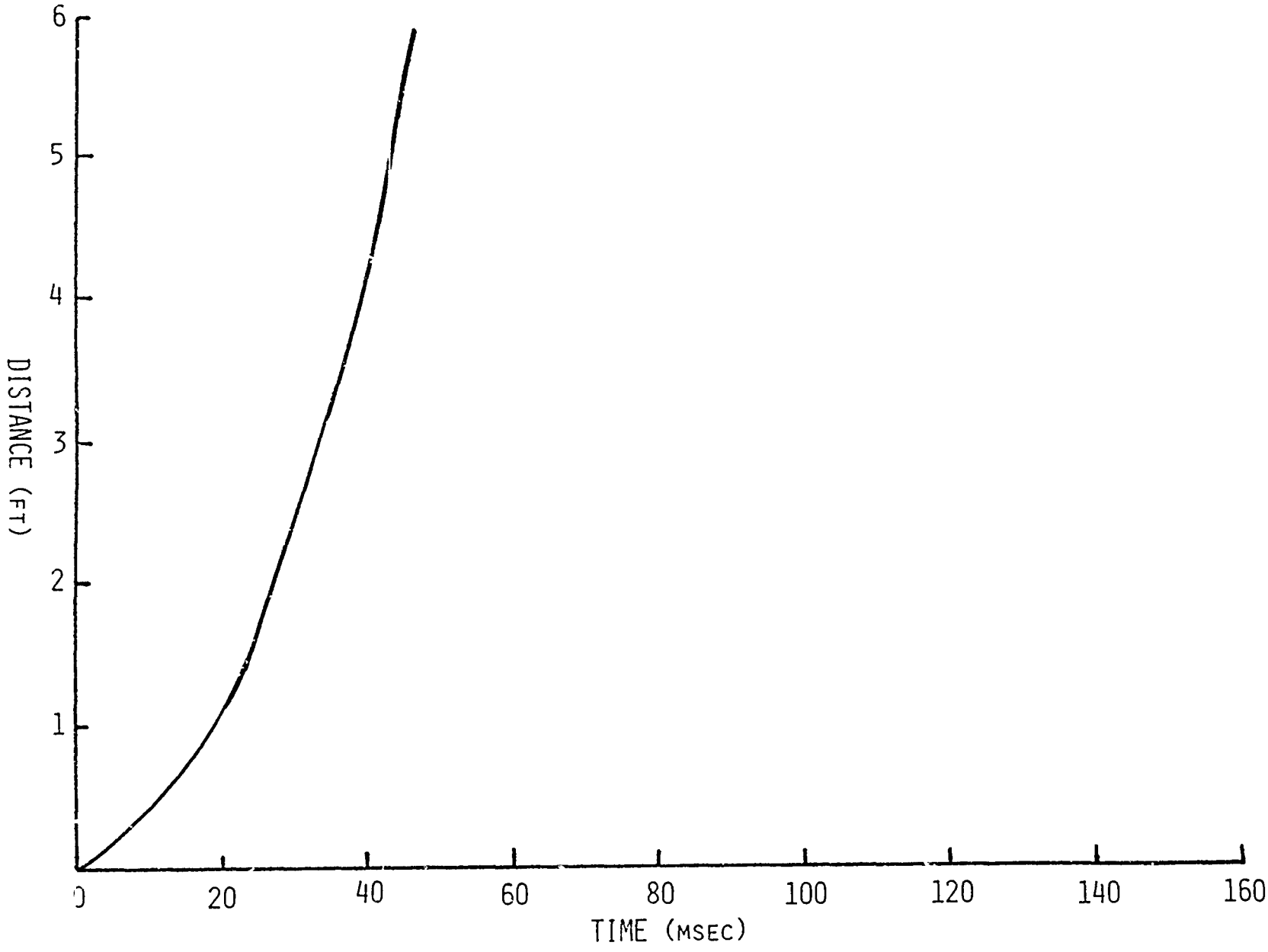

Fig. 111-3. Displacement as a Function of Time, Wall Number 111.

Test Report Wall No. 112

Type: 4-in. Sheetrock; timber stud; interior; with door (door open fot this test).

Support Conditions: Simple plate.

All four edges of the wall were attached to the tunnel.

Special Conditions: Tested 37.5 ft behind a nonfailing wall with a 27% window opening.

Test Results

This wall was exposed to the air blast from five 60-ft strands of Primacord (average peak incident overpressure 3.8 psi). The wall started breaking up as soon as it left the supporting frame. The sheetrock was detached from the studs and remained in fairly large pieces until impact with the far wall. Pre- and posttest photographs of this test are presented in Figs. 112-1 and 112-2. Note in Fig. 112-1 that the door which was left open, did not travel with the wall but stayed at its original location, and apparently just fell down. A plot of displacement as a function of time is presented in Fig. 112-3.

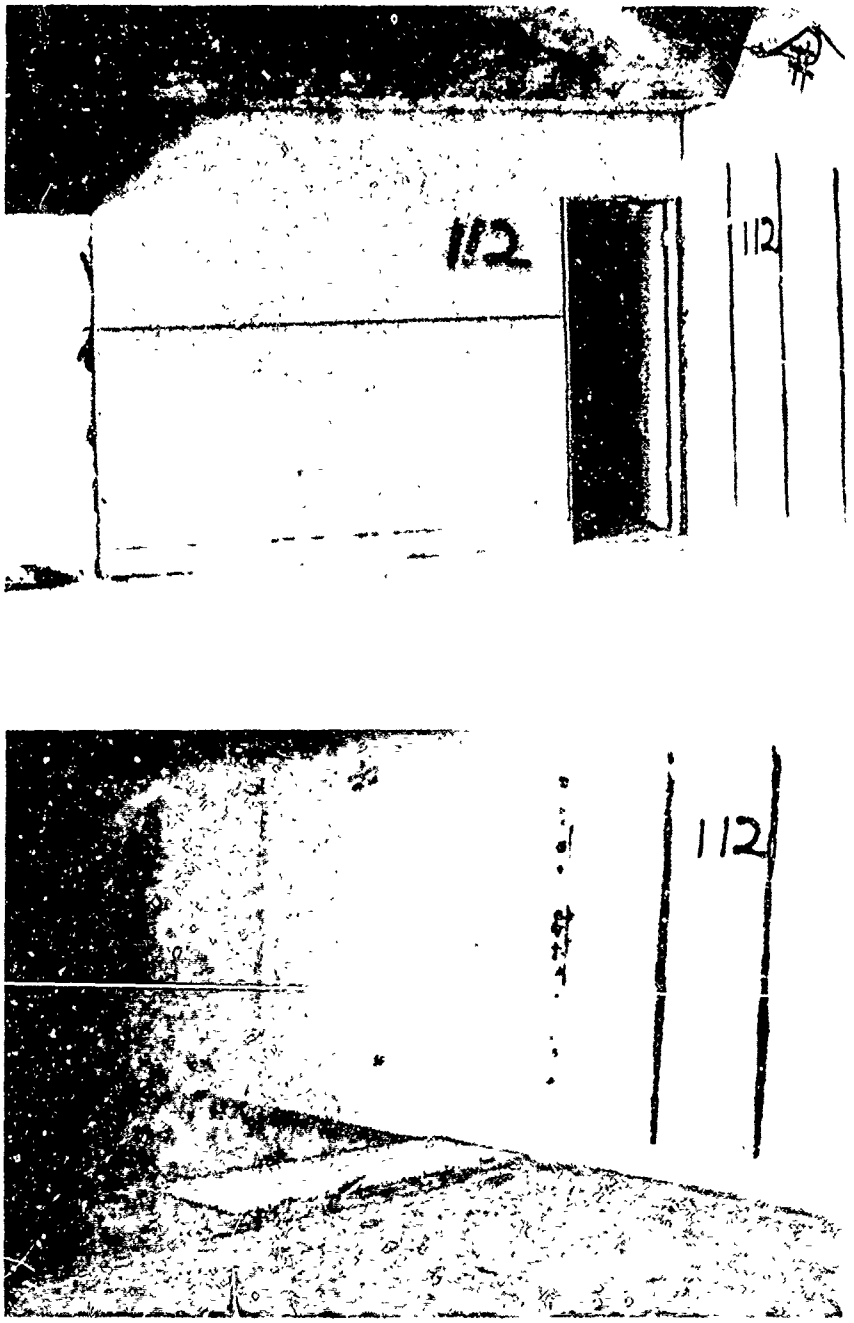

Fig. 112-1. Pre and Posttest Photographs, Wall Number 112.

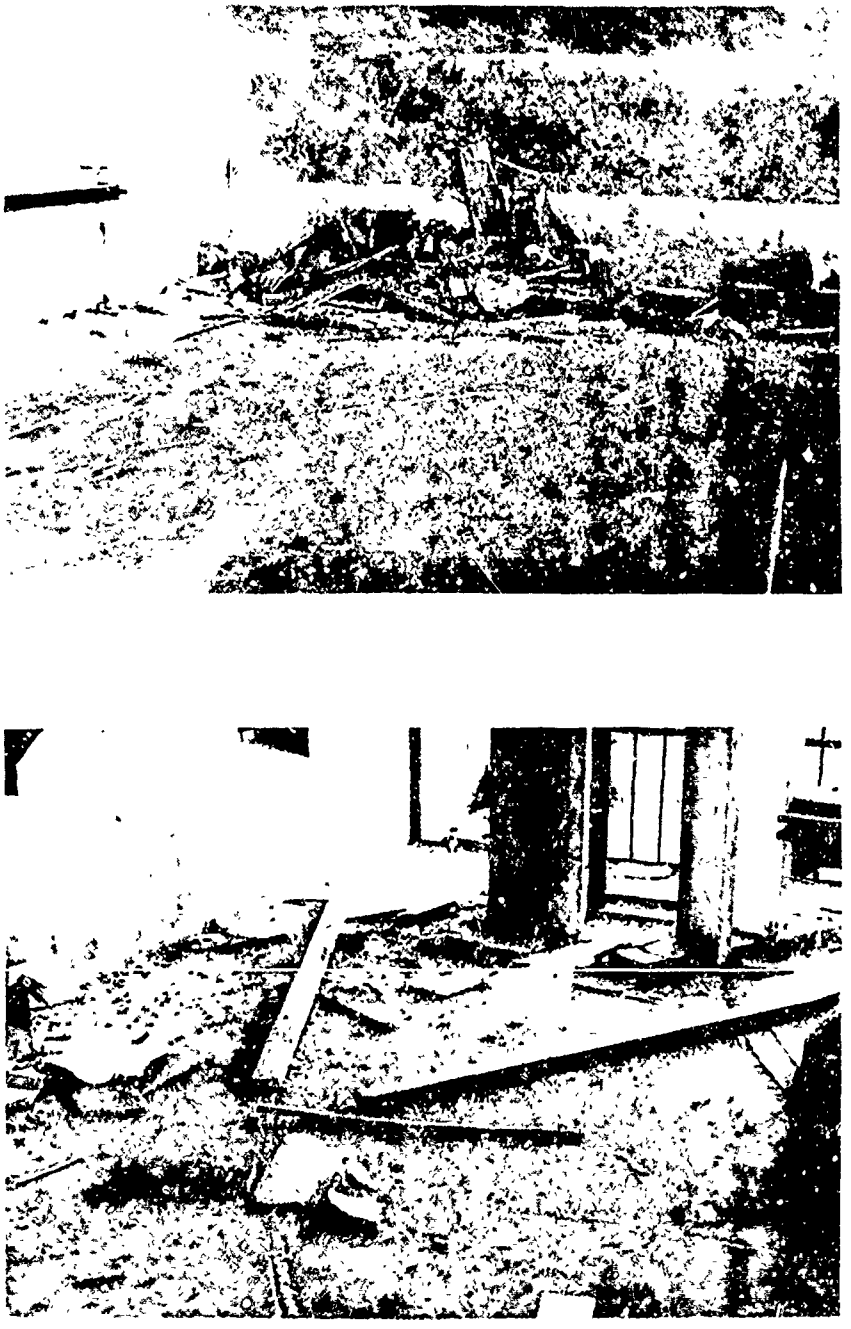

Fig. 112-2. Posttest Photographs, Wall Number 112.

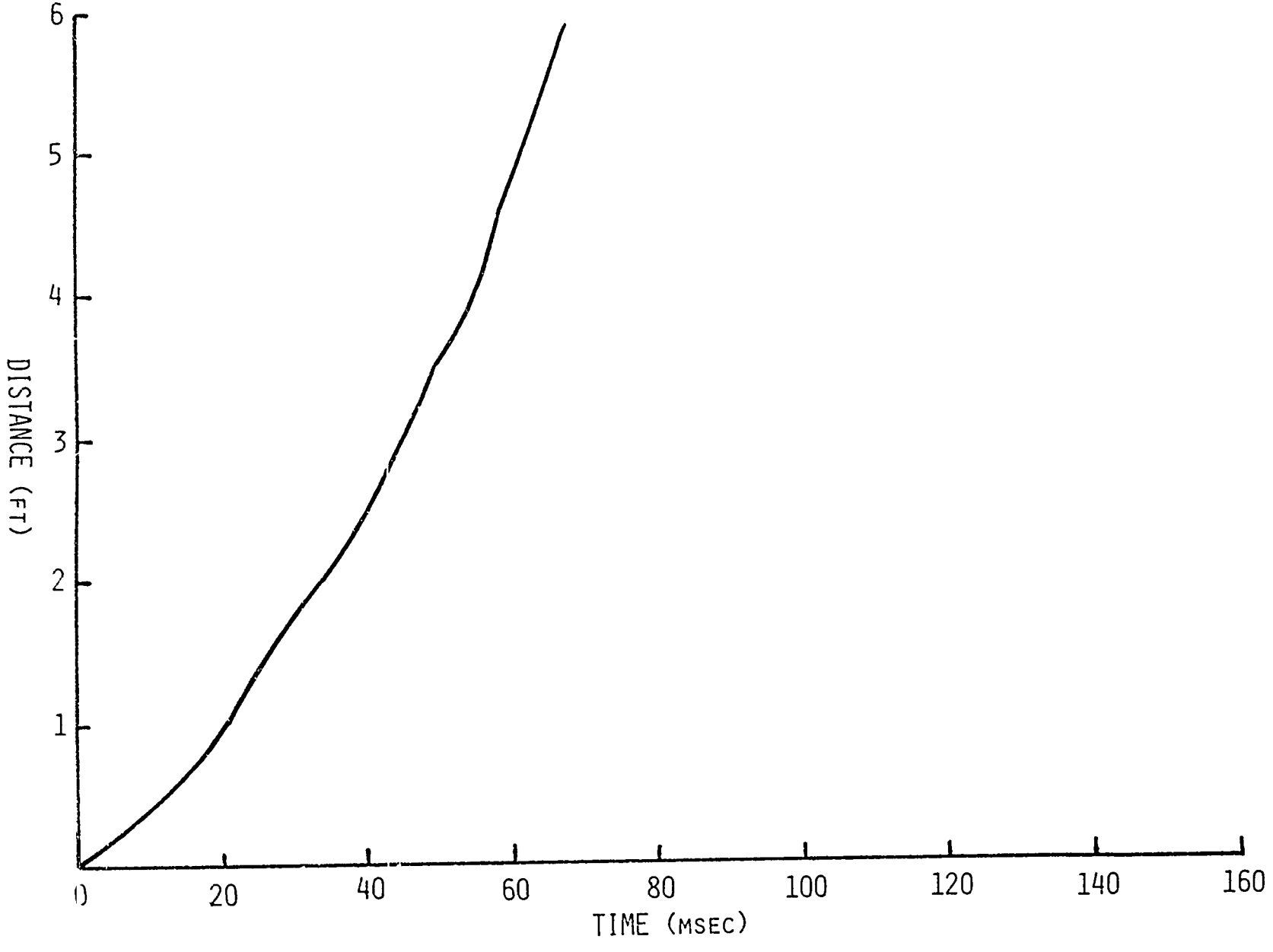

Fig. 112-3. Displacement as a Function of Time, Wall Number 112.

Test Report Wall No. 113

Type: 4-in. Sheetrock; metal stud; interior; with door (door closed for test).

Support Conditions: Simple plate.

All four edges were attached to the tunnel.

Special Conditions: Tested 37.5 ft behind a nonfailing wall with a 27% window opening.

Test Results

This wall was tested once using two 60-ft strands of Primacord (average peak incident overpressure 1.7 psi). The door failed first and traveled ahead of the wall. With the exception of the header over the door and a metal stud at one edge, the wall remained intact until impact at the far wall. See pre- and posttest photographs, Fig. 113-1 and 113-2. A plot of displacement as a function of time is presented in Fig. 113-3.

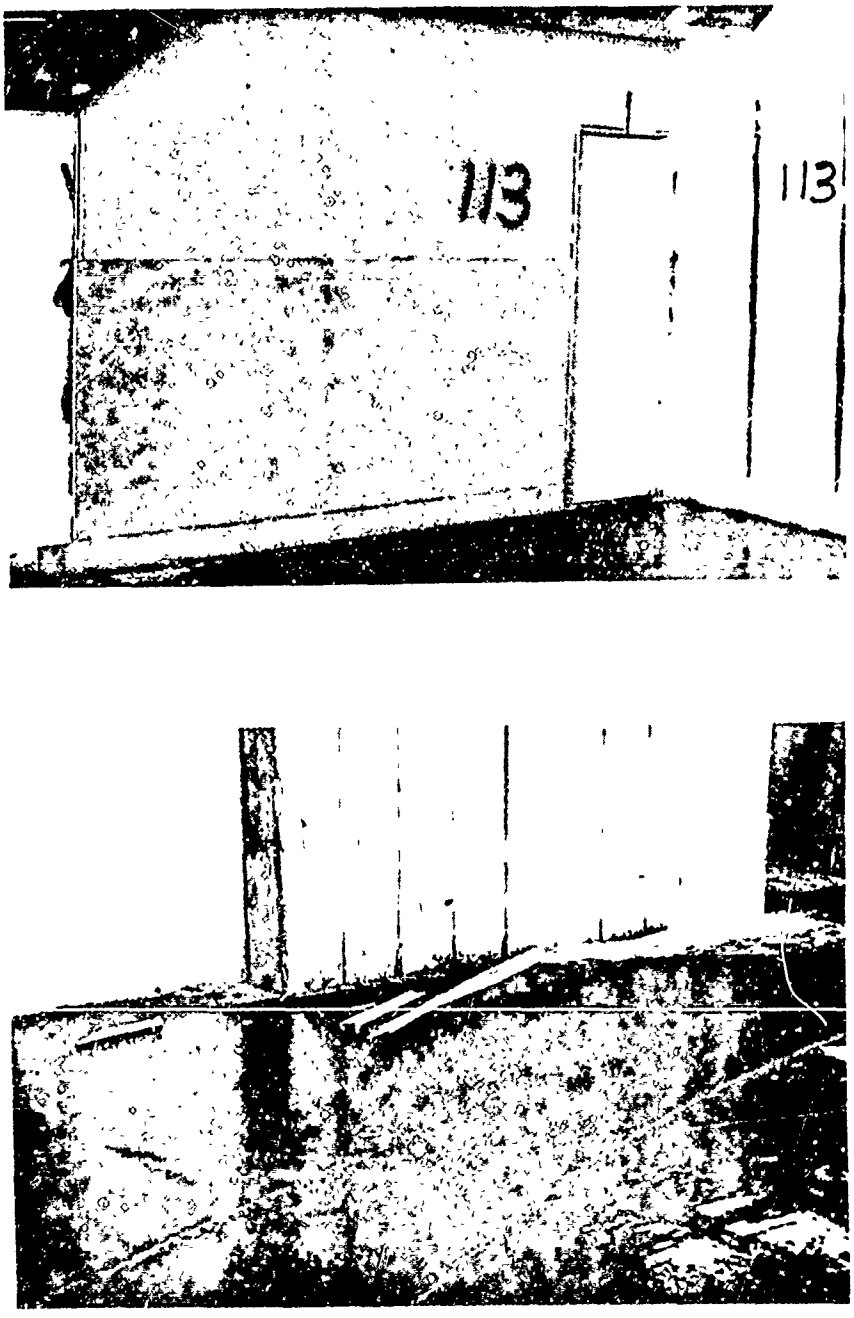

Fig. 113-1. Pre and Posttest Photographs, Wall Number 113.

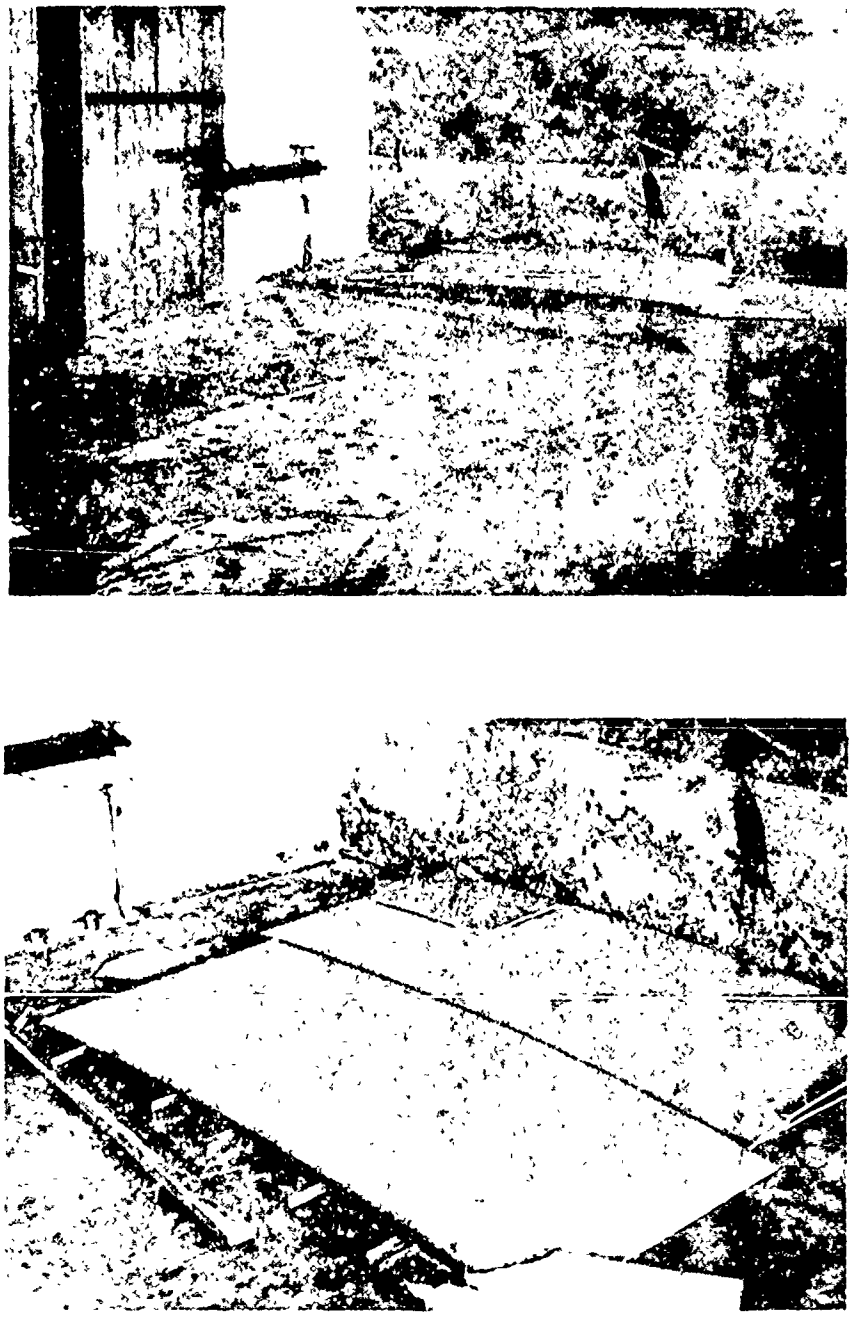

Fig. 113-2. Posttest Photographs, Wall Number 113.

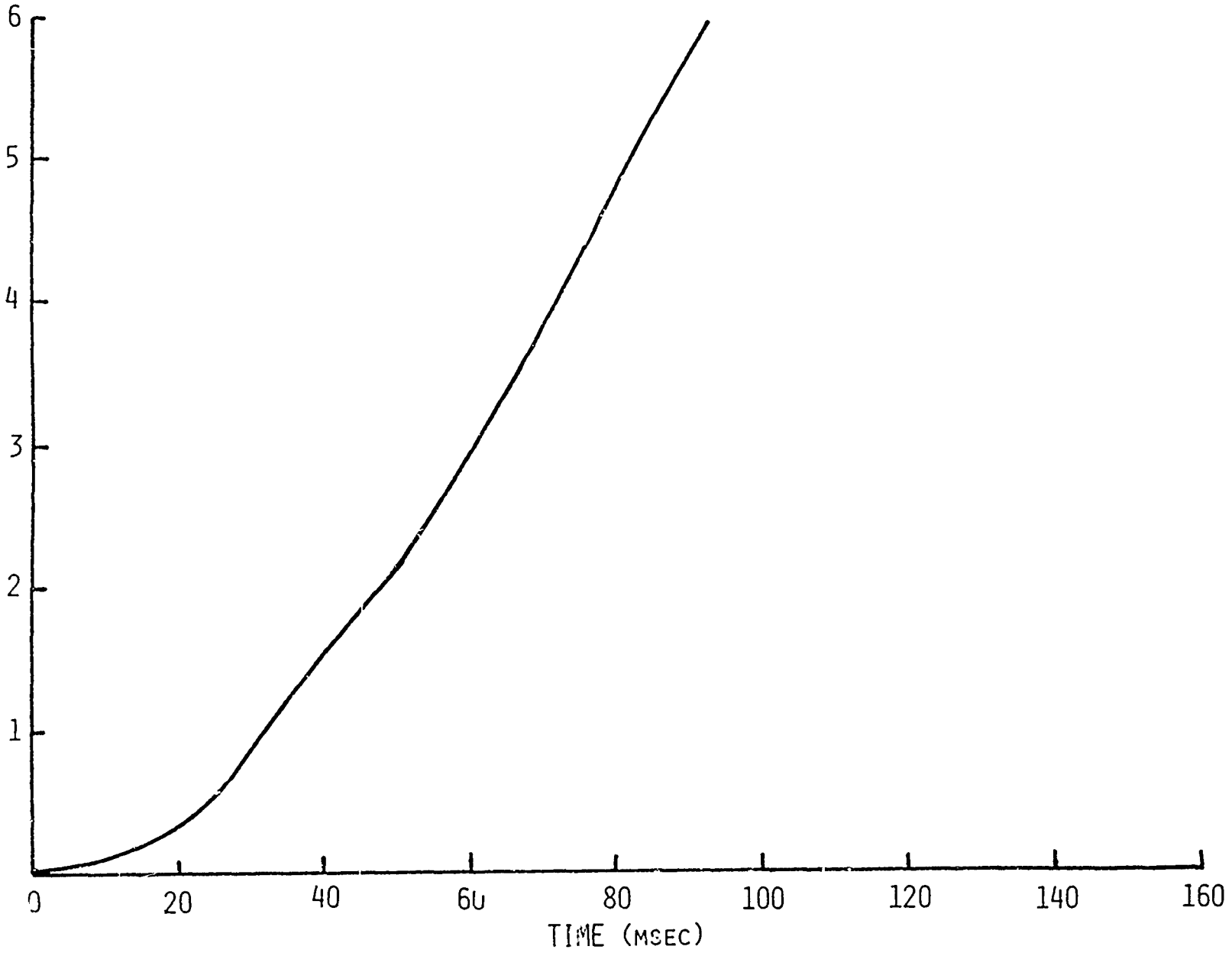

Fig. 113-3. Displacement as a Function of Time, Wall Number 113.

Test Report Wall No. 114

Type: 4-in. Sheetrock; metal stud; interior; with door (door closed for test).

Support Conditions: Simple plate.

All four edges were attached to the tunnel.

Special Conditions: Tested 37.5 ft behind a nonfailing wall with a 27% window opening.

Test Results

This wall was tested using five 60-ft strands of Primacord (average peak incident overpressure 3.8 psi). The door frame failed first and the door traveled ahead of the rest of the wall. A crack at the center sheetrock joint appeared soon after the wall parted from the support and widened as the wall traveled across the casemate. It appeared that the front sheetrock face was partially torn loose from the metal studs before impact with the far wall. Pre- and posttest photographs of this wall are presented in Figs. 114-1 and 114-2. A plot of displacement as a function of time is presented in Fig. 114-3.

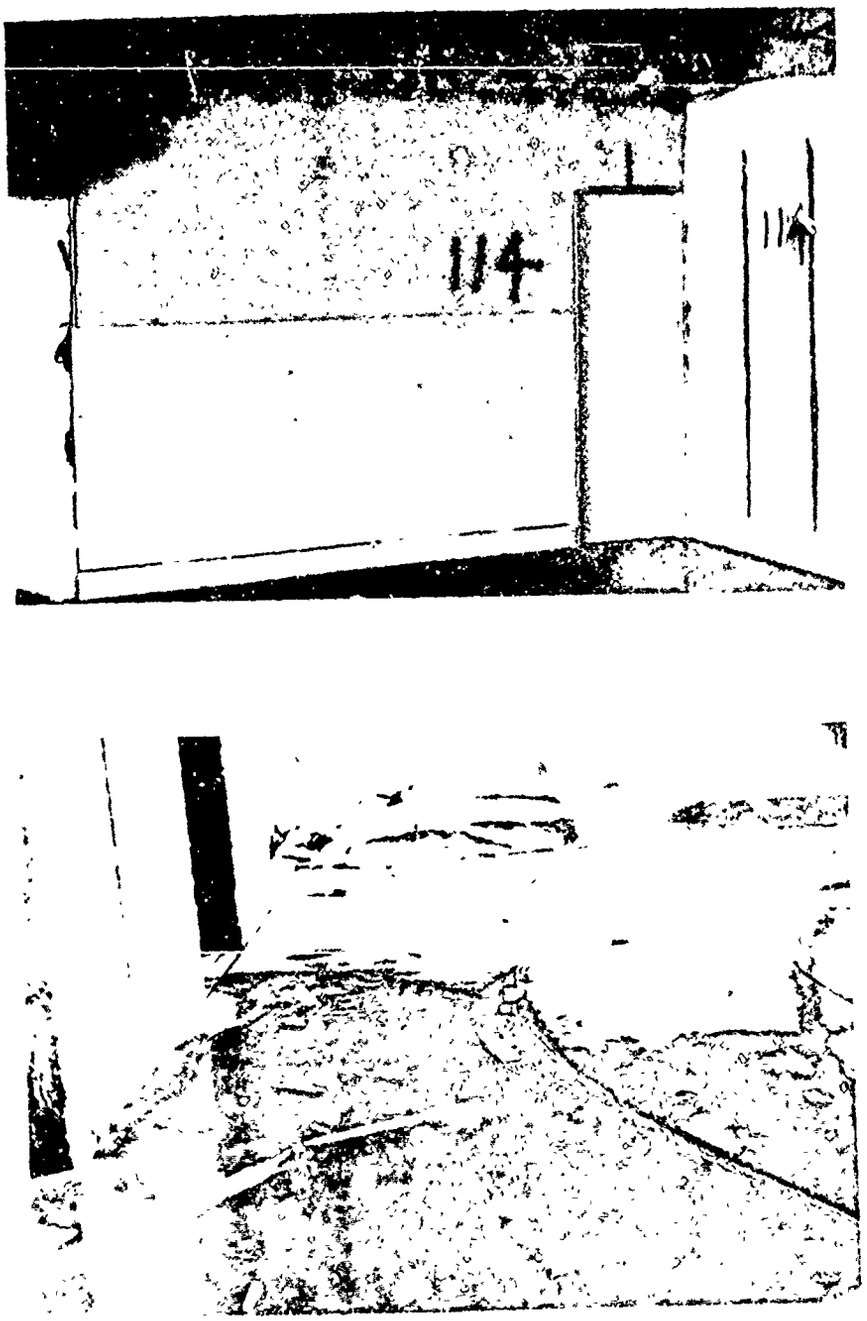

Fig. 114-1. Pre and Posttest Photographs, Wall Number 114.

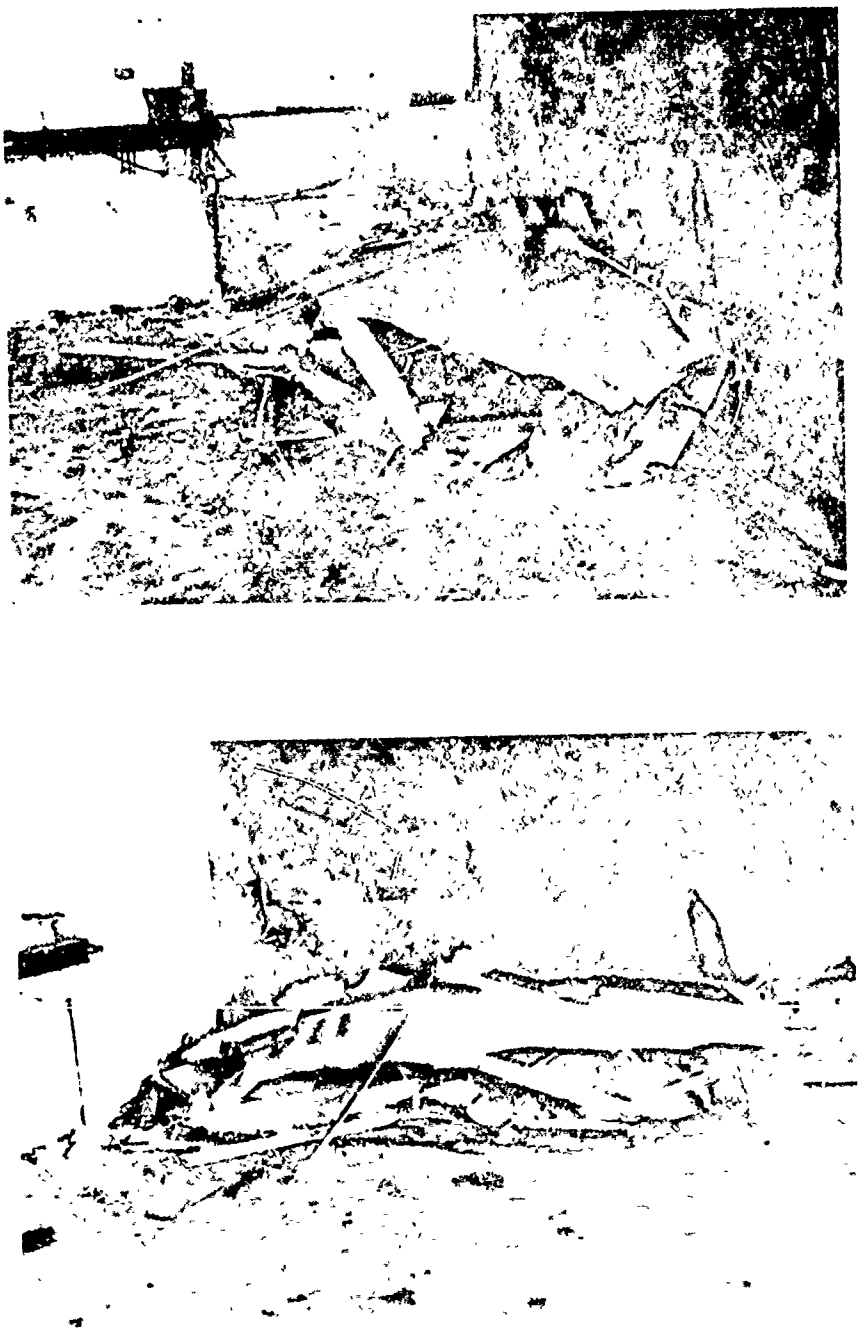

Fig. 114-2. Posttest Photographs, Wall Number [illegible]

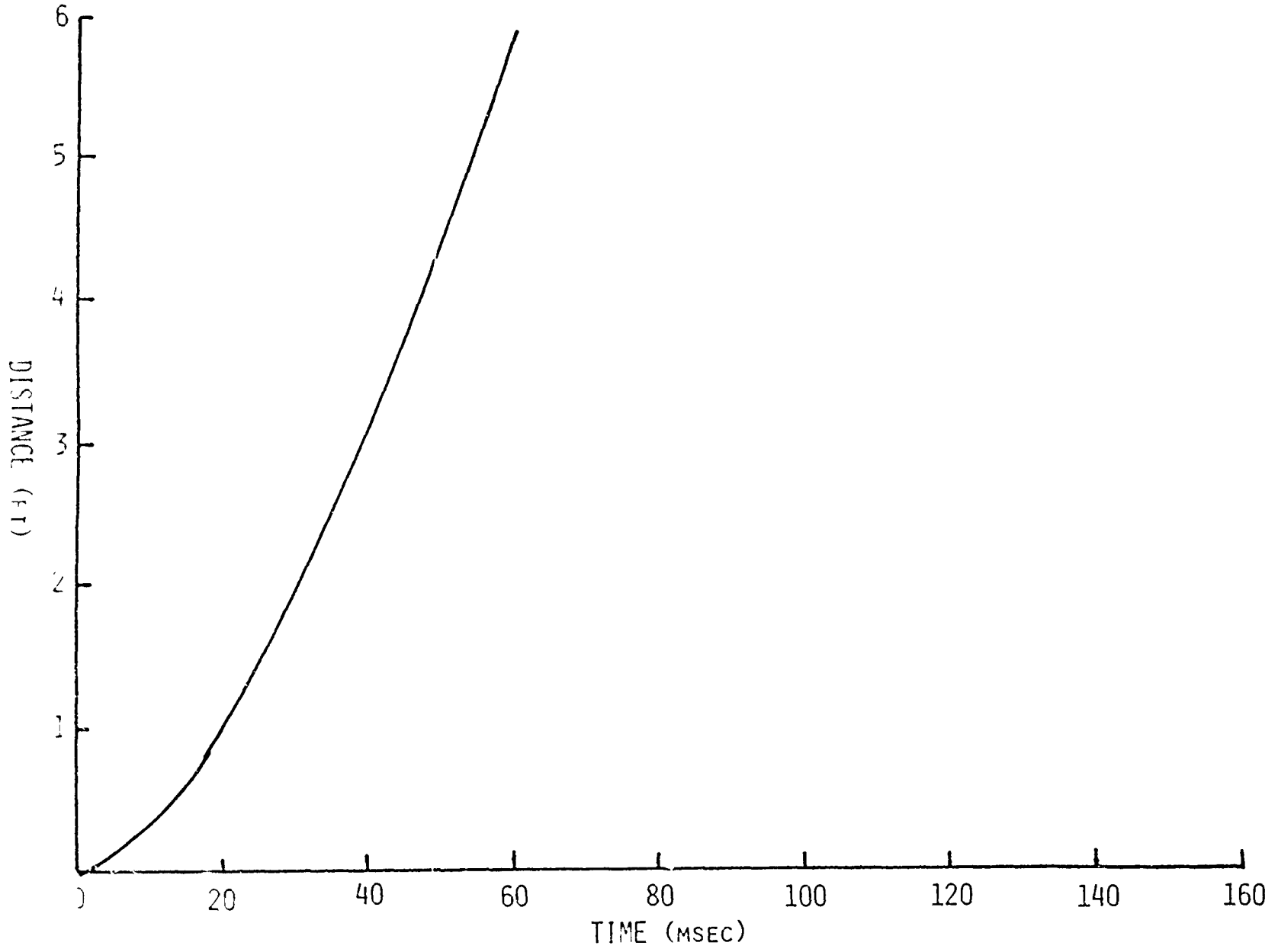

Fig. 114-3 Displacement as a Function of Time, Wall Number 114.

Test Report Wall No. 115

Type: 8-in. Concrete block; interior; solid (with no openings).

Support Conditions: Gapped arched, one-way.

A gap of less than 1/8 in. was left between the wall and the tunnel roof. Gaps at the sides of the wall permitted free movement.

Special Conditions: Tested 14.5 ft behind a nonfailing wall with a 27% window opening.

Test Results

This wall was tested once using five 60-ft strands of Primacord (average peak incident overpressure 4.1 psi). The initial crack was horizontal and appeared between the fifth and sixth rows (the wall contained 11 rows). Secondary cracks appeared horizontally at the mortar joints two rows above and below the initial crack. Several large pieces, containing 8-10 blocks each, traveled 40 to 50 ft before hitting the ground. A posttest photograph of this test is presented in Fig. 115-1. A plot of displacement as a function of time is presented in Fig. 115-2.

Fig. 115-1. Posttest Photograph, Wall Number 115.

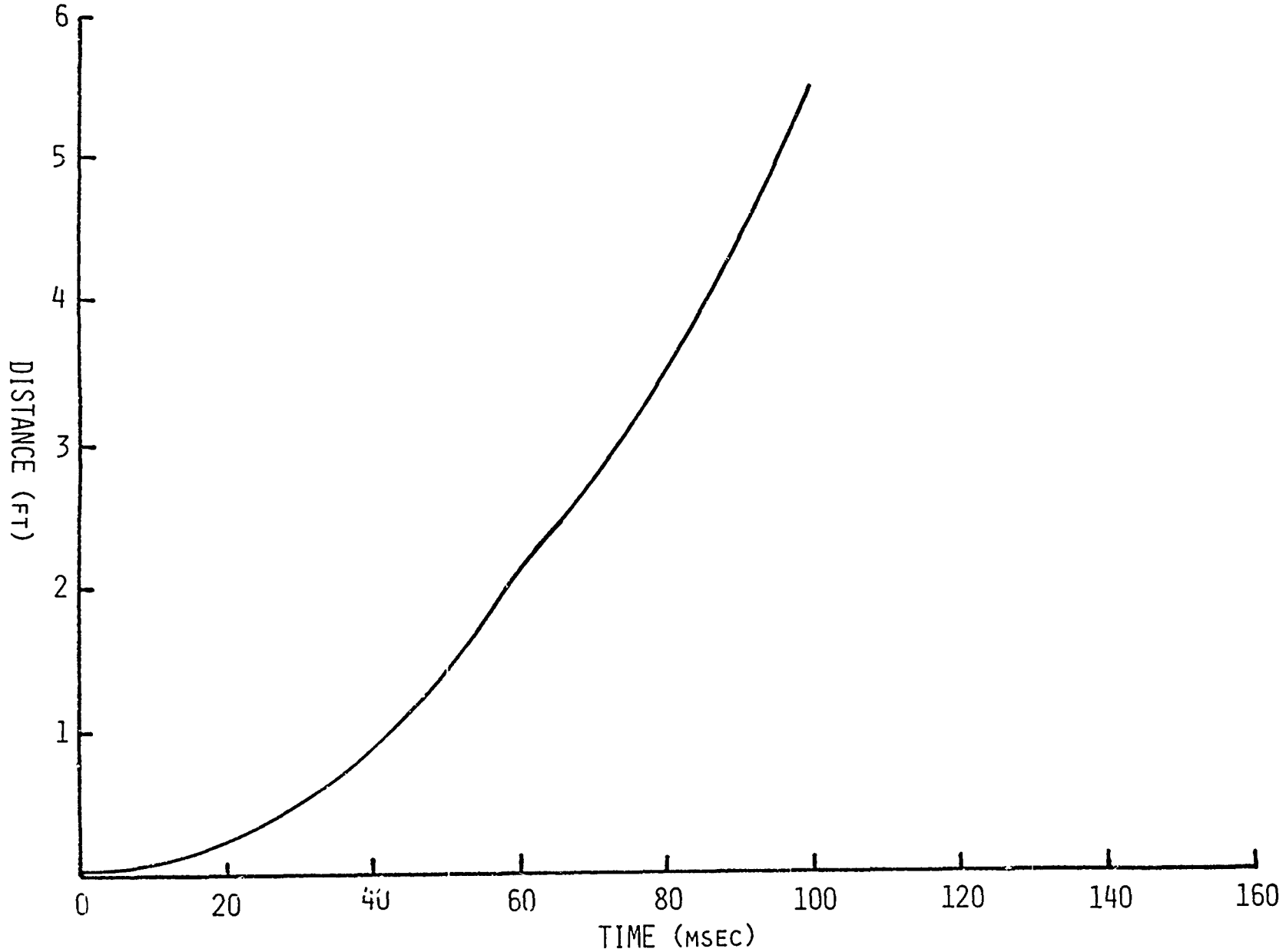

Fig. 115- 2. Displacement as a Function of Time, Wall Number 115.

Test Report Wall No. 116

Type: 8-in. Concrete block; interior; solid (with no openings).

Support Conditions: Gapped arched, one-way.

A gap of less than 1/8 in. was left between the wall and the tunnel roof. Gaps at the sides of the wall permitted free movement.

Special Conditions: Tested 14.5 ft behind a nonfailing wall with a 27% window opening.

Test Results

This wall was tested once using two 60-ft strands of Primacord (average peak incident overpressure 1.7 psi). The initial crack appeared between the seventh and eighth rows of block with numerous secondary cracks quickly appearing between the third and seventh rows and a diagonal crack appeared in the upper right hand corner. The wall completely disintegrated and hit the tunnel floor within the first 20 to 25 feet. Debris was scattered to approximately 40 ft with about 90% of it remaining within the first 25 ft. Posttest photographs of this wall are presented in Figs. 116-1 and 116-2. A plot of displacement as a function of time is presented in Fig. 116-3.

Test Report Wall No. 116

Type: 8-in. Concrete block; interior; solid (with no openings).

Support Conditions: Gapped arched, one-way.

A gap of less than 1/8 in. was left between the wall and the tunnel roof. Gaps at the sides of the wall permitted free movement.

Special Conditions: Tested 14.5 ft behind a nonfailing wall with a 27% window opening.

Test Results

This wall was tested once using two 60-ft strands of Primacord (average peak incident overpressure 1.7 psi). The initial crack appeared between the seventh and eighth rows of block with numerous secondary cracks quickly appearing between the third and seventh rows and a diagonal crack appeared in the upper right hand corner. The wall completely disintegrated and hit the tunnel floor within the first 20 to 25 feet. Debris was scattered to approximately 40 ft with about 90% of it remaining within the first 25 ft. Posttest photographs of this wall are presented in Figs. 116-1 and 116-2. A plot of displacement as a function of time is presented in Fig. 116-3.

Fig. 116-1. Posttest Photographs, Wall Number 116.

Fig. 116-2. Posttest Photographs, Wall Number 116.

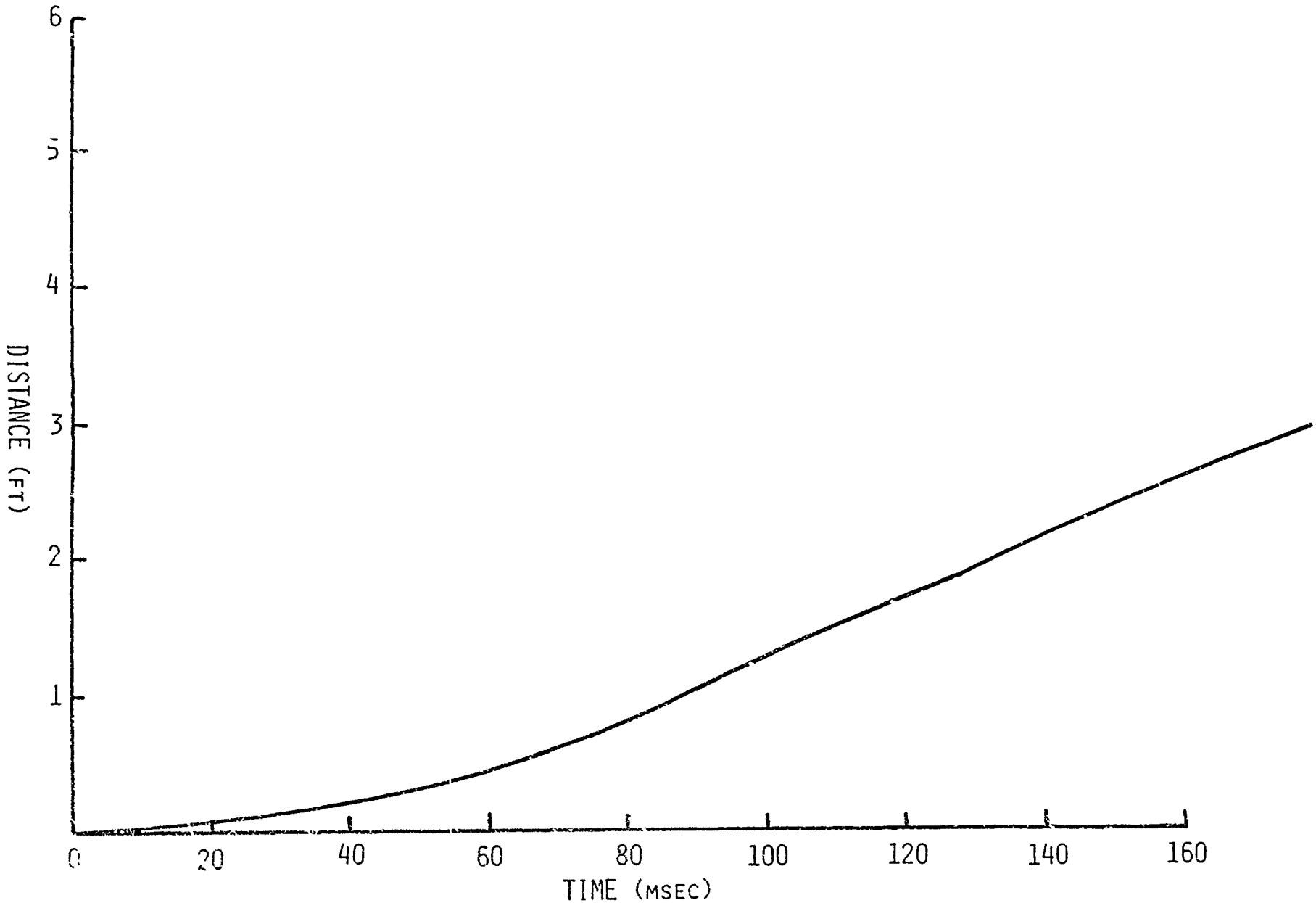

Fig. 116-3. Displacement as a Function of Time, Wall Number 116.

Test Report Wall No. 117

Type: 8- in. Concrete block; solid (with no openings).

Support Conditions: Cantilever beam fixed at the bottom,and enclosed in a light-weight steel "picture frame for construction and handling purposes. A four-in. gap was left at the top and a two-in. gap was left at each side.

Special Conditions: Tested 37.5 ft behind a nonfailing wall with a 27% window opening.

Test Results

This wall was tested using five 60-ft strands of Primacord (average peak incident overpressure 3.8 psi). The first crack appeared at the joint between the fifth and sixth rows of block. Secondary cracks rapidly appeared breaking the wall into sections two to three blocks high and about four to six blocks long. The bottom third impinged the floor within the first 15 ft. The top two thirds hit at distances of from 25 to 35 feet. Pre- and post-test photographs of this wall are shown in Figs. 117-1 and 117-2. A plot of displacement as a function of time is presented in Fig. 117-3.

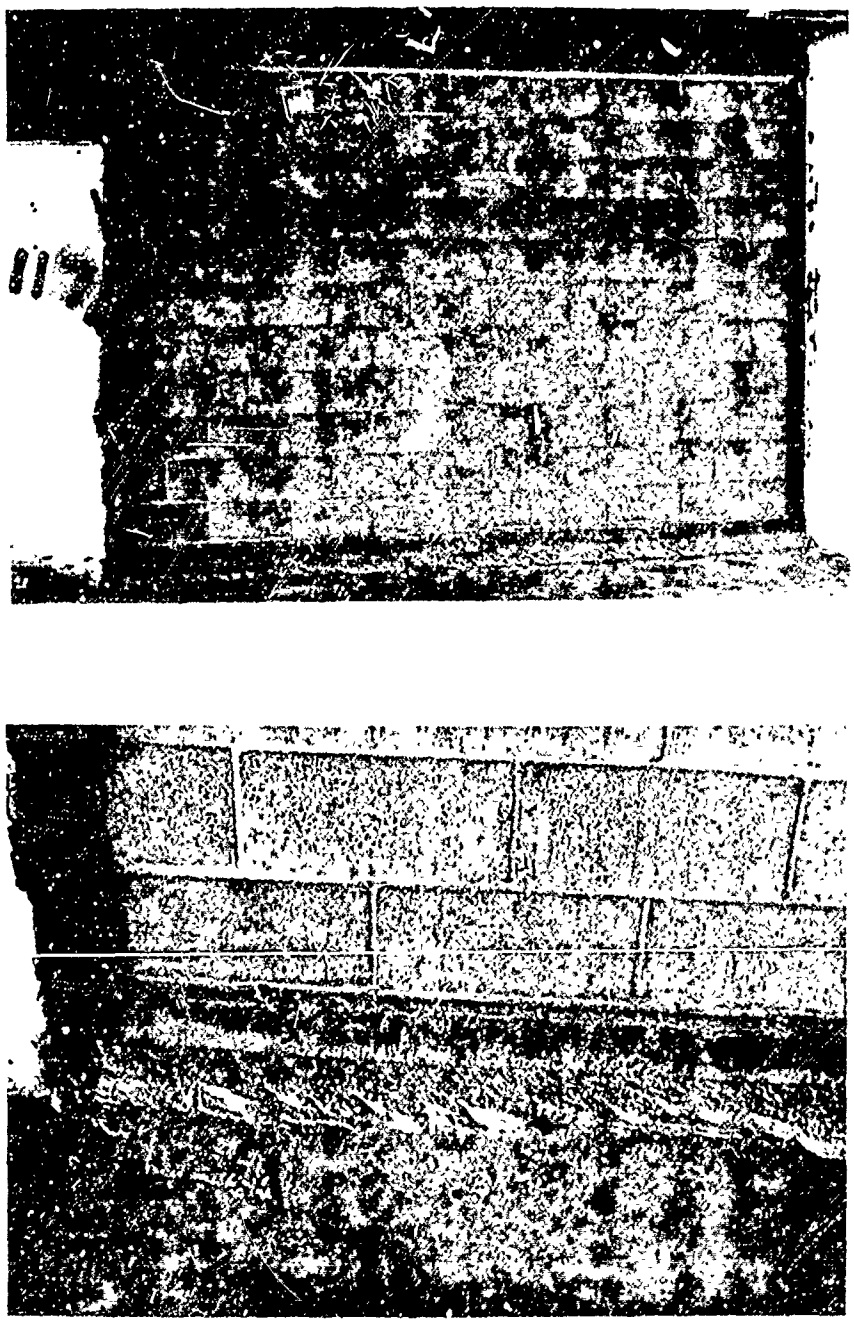

Fig. 117-1. Pretest Photographs, Wall Number 117.

Fig. 117-2. Posttest Photographs, Wall Number 117.

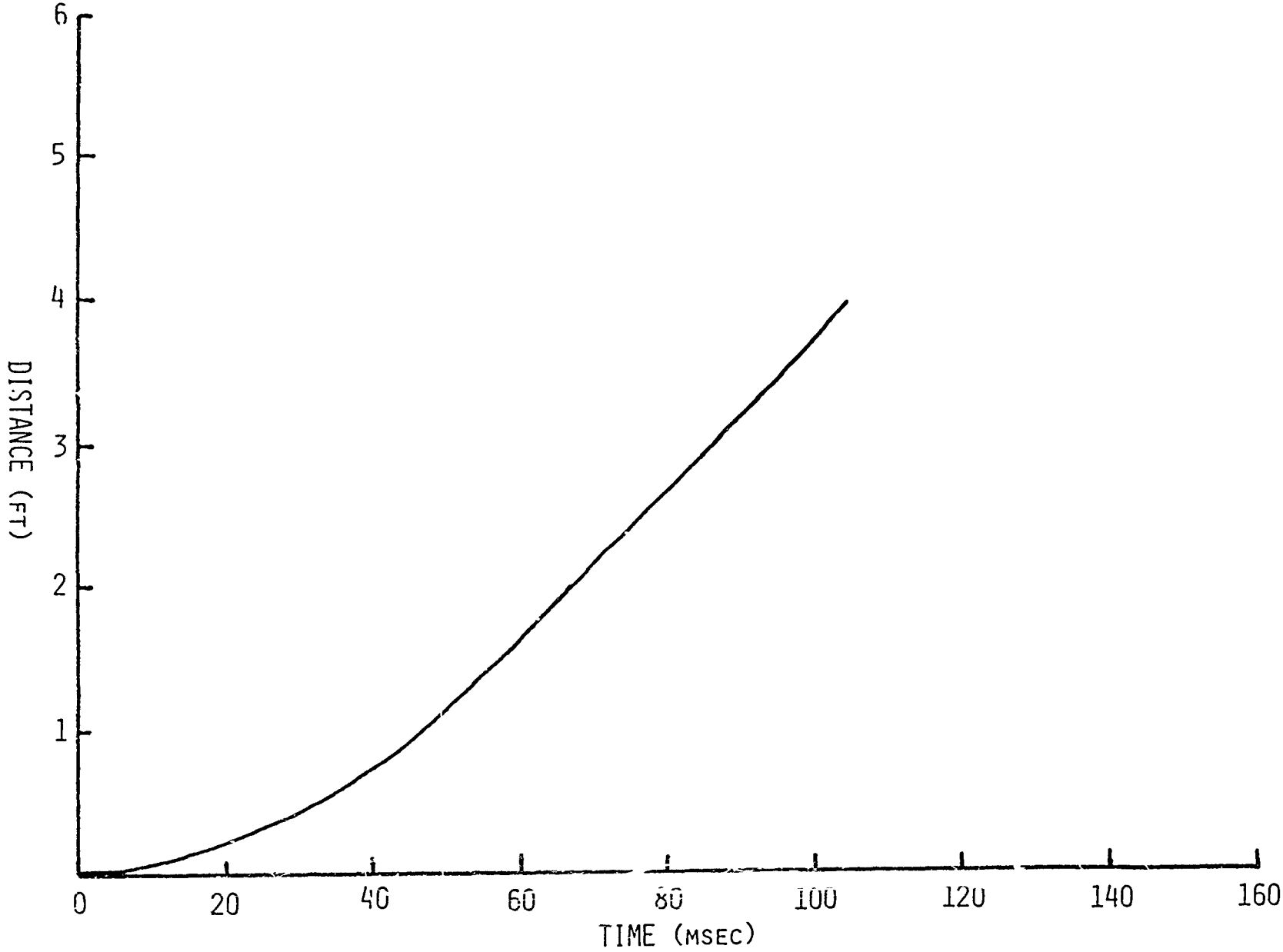

Fig. 117-3. Displacement as a Function of Time, Wall Number 117.

Test Report Wall No. 118

Type: 8-in. Concrete block; interior; with doorway opening.

Support Conditions: Cantilever beam fixed at the bottom with an approximate six-in. gap at the top, a four-in. gap on the left side and a 27-in. doorway opening on the right side.

Special Conditions: Tested 37.5 ft behind a nonfailing wall with a 27% window opening.

Test Results

This wall was tested using five 60-ft strands of Primacord (average peak incident overpressure 3.6 psi). Two initial cracks were noted between the third and fourth rows and one between the fourth and fifth rows. The film record was badly obscured by dirt and smoke flowing through the doorway opening but as nearly as could be determined the bottom third of the wall broke into small sections and fell over and hit the floor. The top two thirds remained intact and hit the floor at a distance of 25 to 30 ft. Photographs of this wall are presented in Figs. 118-1 through 118-3. A plot of displacement as a function of time is presented in Fig. 118-4.

Fig. 118-1. Pre and Posttest Photographs, Wall Number 118.

Fig. 118-2. Posttest Photographs, Wall Number 118.

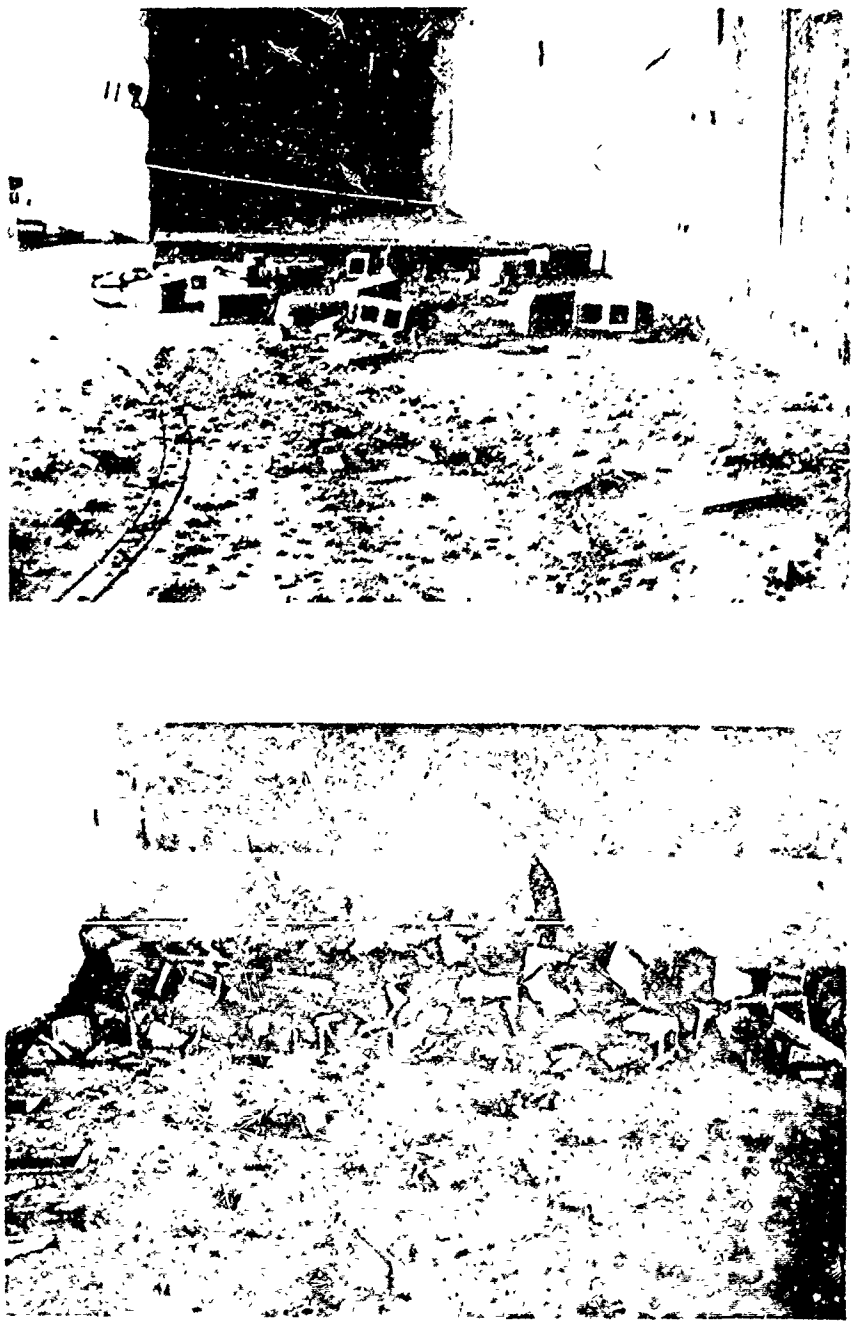

Fig. 113-3. Posttest Photographs, Wall Number 118.

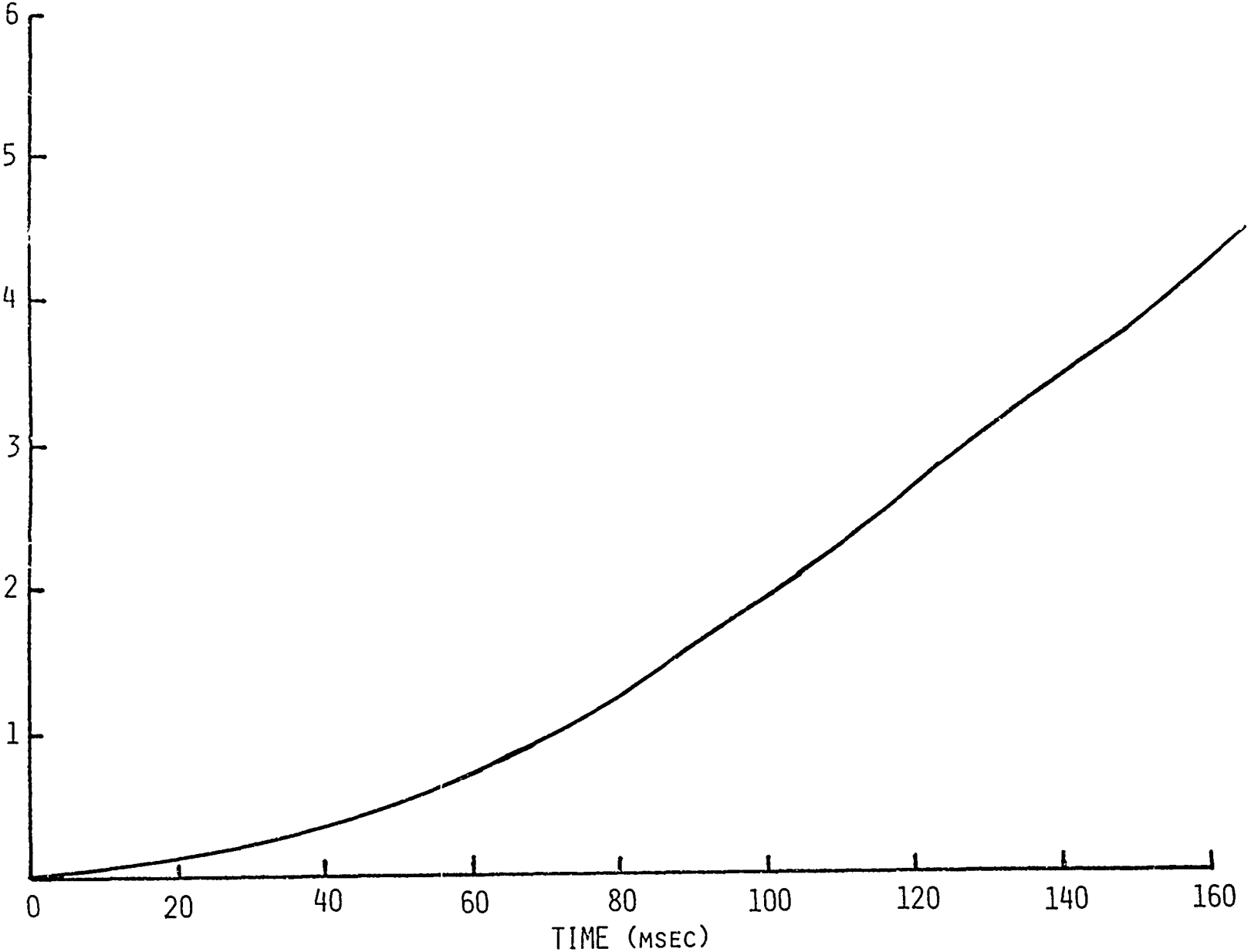

Fig. 118-4. Displacement as a Function of Time, Wall Number 118.

Test Report Wall No. 119

Type: 6-in. Clay tile; interior; solid (with no openings).

Support Conditions: Cantilever beam fixed at the bottom with a four-in. gap left at the top, and a two-in. gap left at each side.

Special Conditions: Tested 37.5 ft behind a nonfailing wall with a 27% window opening.

Test Results

This wall was tested using two 60-ft strands of Primacord (average peak incident overpressure 1.6 psi). The first and only crack appeared between the fifth and sixth rows of clay tile (there were 16 rows in the wall). The bottom piece fell over, and slid along the floor, and the top piece traveled approximately 16 ft before striking the floor and starting to break up. Photographs of the wall are presented in Figs. 119-1 through 119-3. A plot of displacement as a function of time is presented in Fig. 119-4.

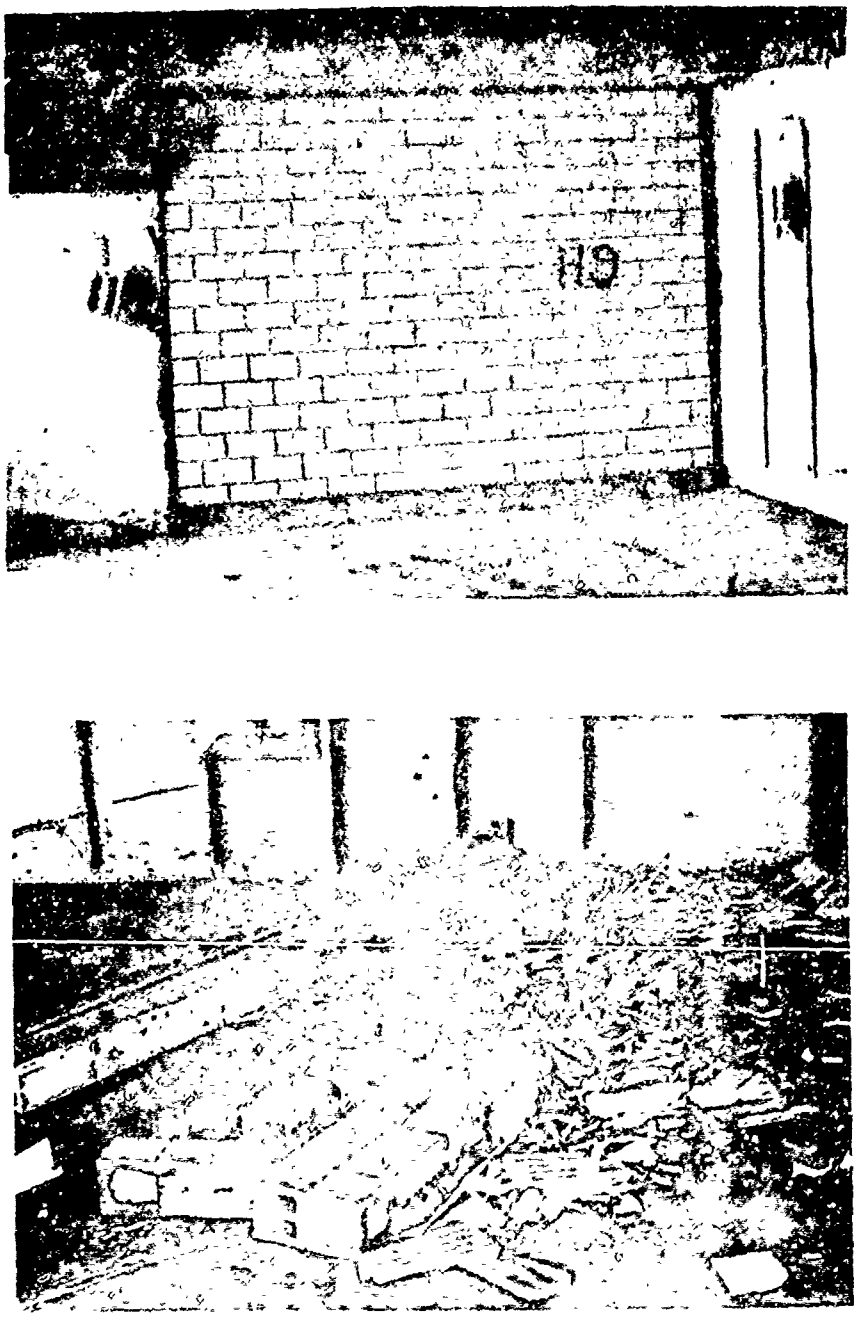

Fig. 119-1. Pre and Posttest Photographs, Wall Number 119.

Fig. 119-2. Posttest Photographs, Wall Number 119.

Fig. 119-3. Posttest Photographs, Wall Number 119.

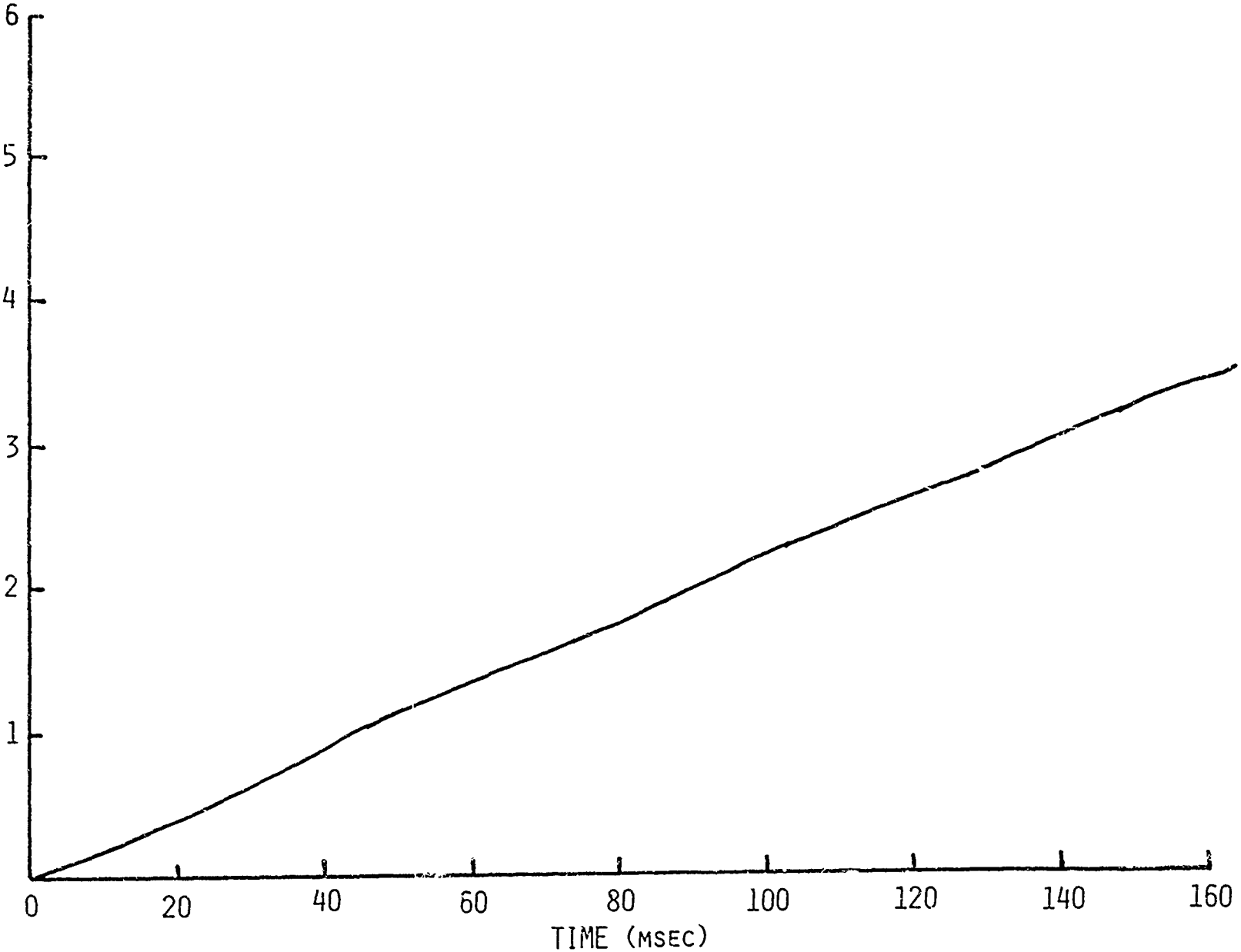

Fig. 119-4. Displacement as a Function of time, Wall Number 119.

Test Report Wall No. 120

Type: 6- in. Clay tile; interior; solid (with no opening).

Support Conditions: Cantilever beam fixed at the bottom with a four-in. gap left at the top and a two-in. gap left at each side.

Special Conditions: Tested 37.5 ft behind a nonfailing wall with a 27% window opening.

Test Results

This wall was tested using five 60-ft strands of Primacord (average peak incident overpressure 3.9 psi). The initial crack appeared between the fourth and fifth row of blocks. The lower portion fell to the floor. The upper portion moved out and up striking the top of the tunnel. The impact broke the corner block on the one side and caused a diagonal crack as shown in Fig. 120-1, a sketch of the crack pattern. The upper portion remained airborne most of the way across the casemate. The photographs of the wall are presented in Figs. 120-1 and 120-3. A plot of displacement as a function of time is presented in Fig. 120-4.

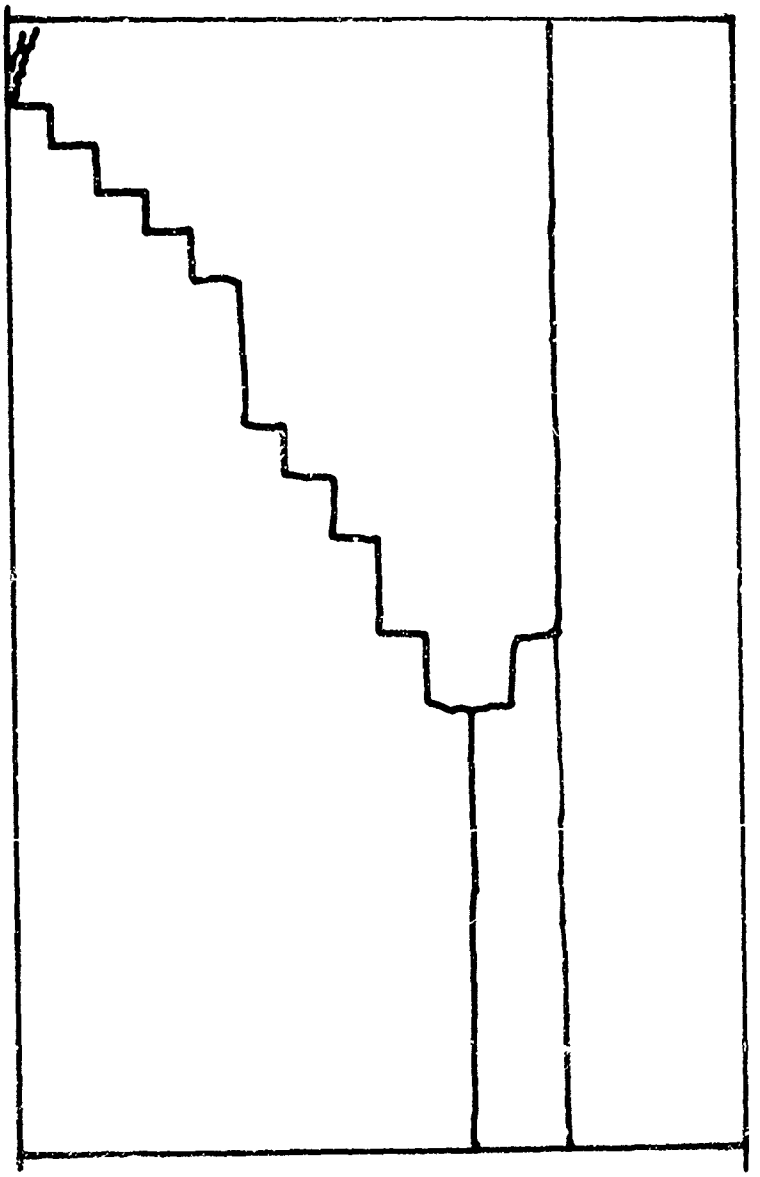

Fig. 120-1. Crack Pattern, Wall Number 120.

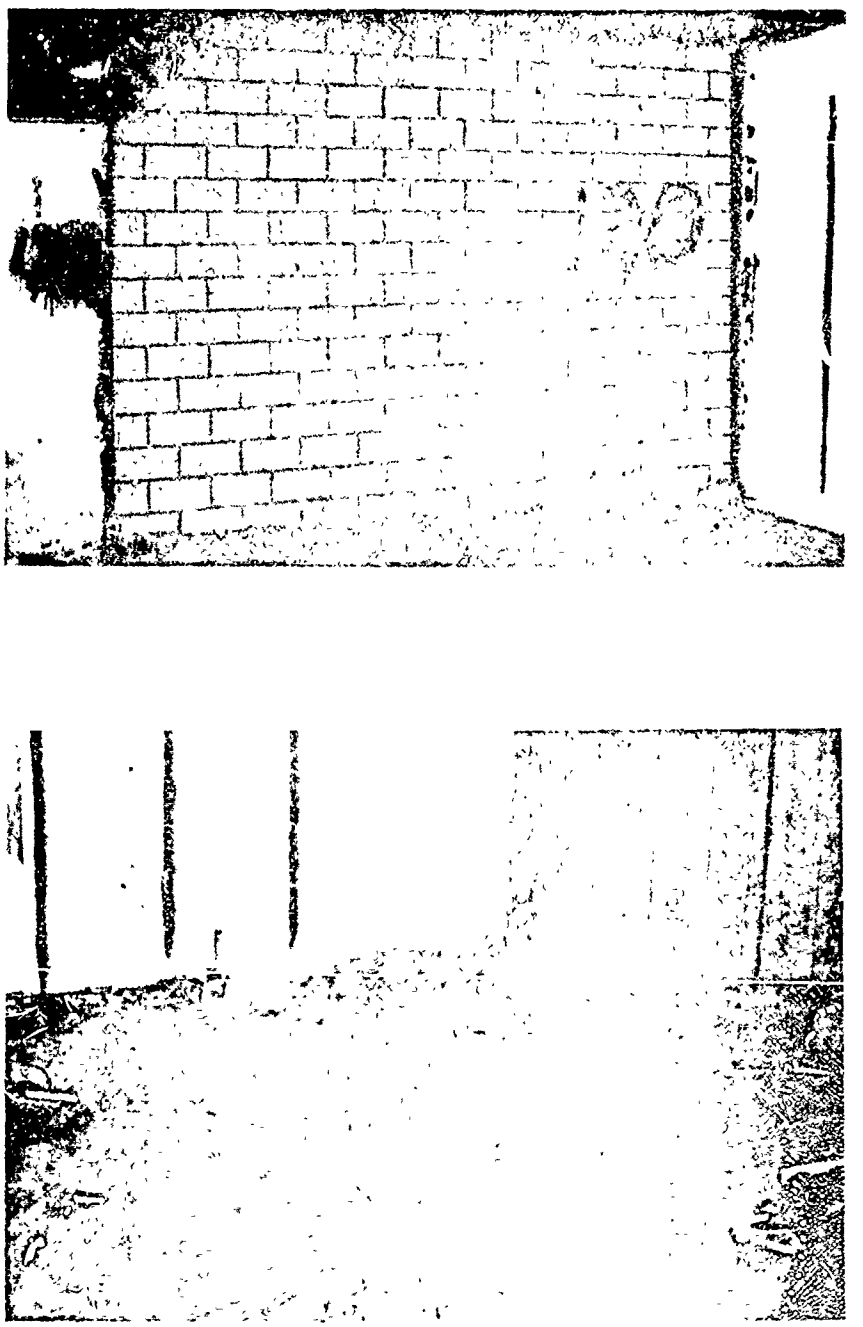

Fig. 120-2. Pre and Post

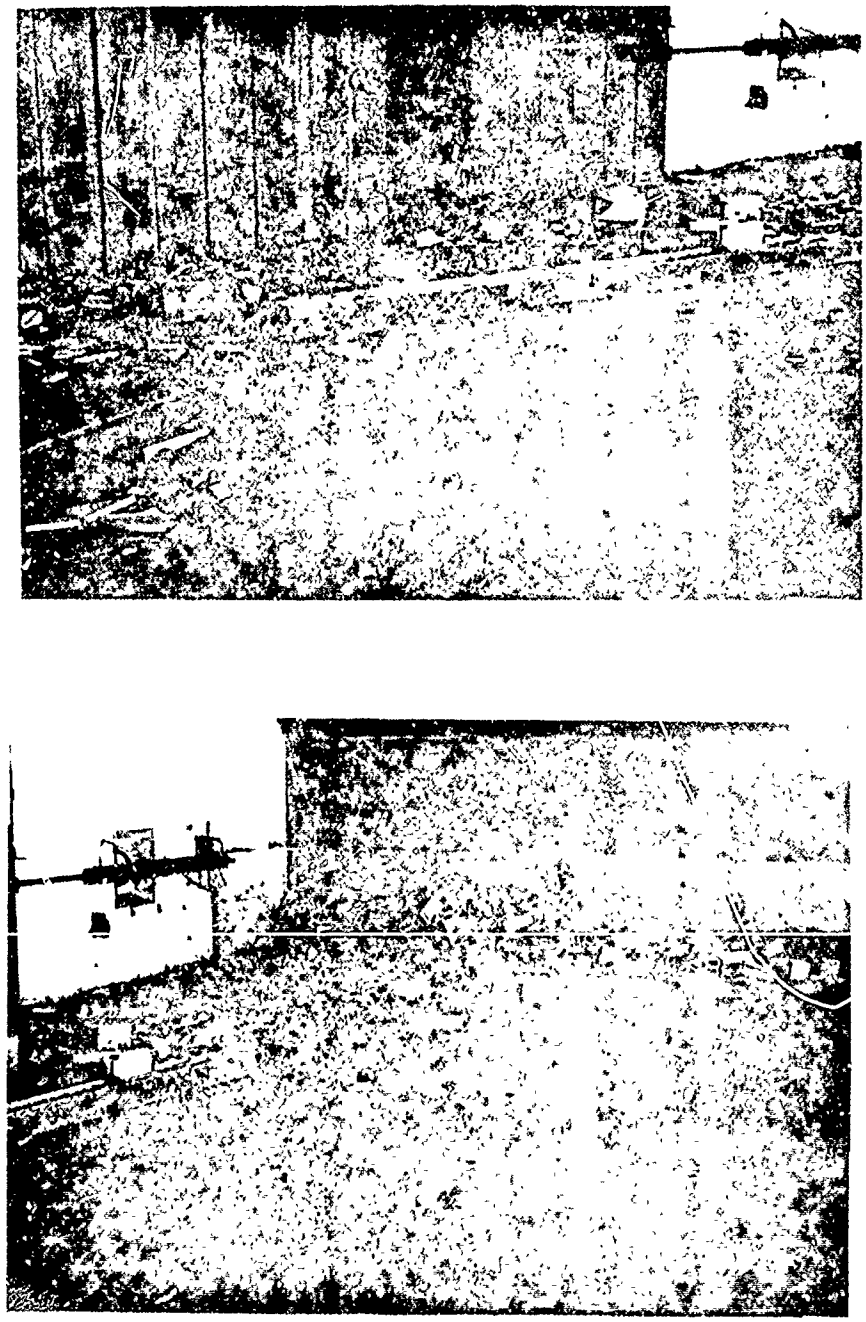

Fig. 120-3. Posttest Photographs, Wall Number 120.

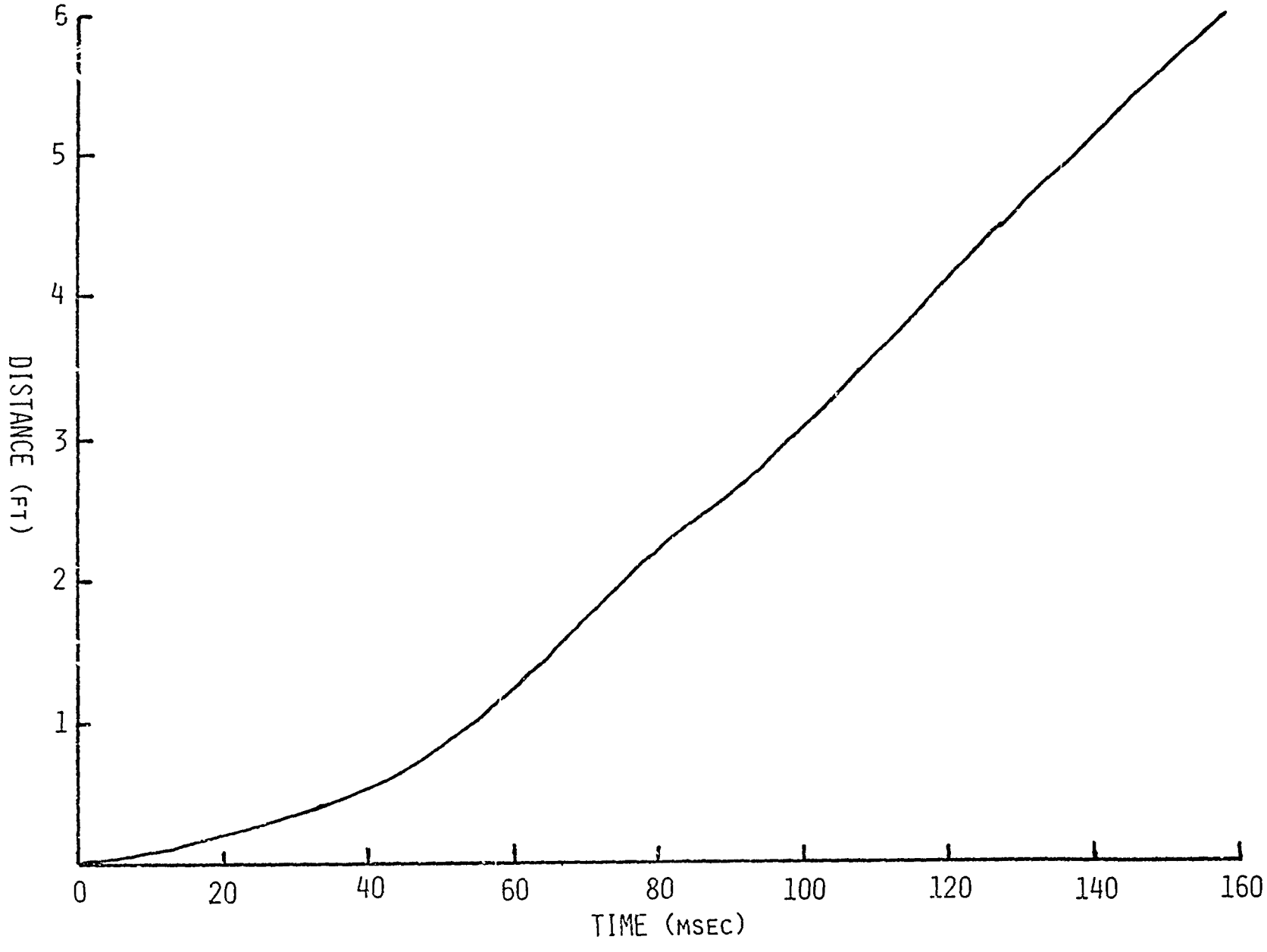

Fig. 120-4. Displacement as a Function of Time, Wall Number 120.

Appendix B

STATIC TEST PROGRAM

Appendix B

STATIC TEST PROGRAM

Introduction

In conjunction with the Shock Tunnel dynamic tests, a static test program was conducted to determine the quality of construction of the test items fabricated, to obtain estimates of the strength of specimen walls prior to the dynamic tests, and to gather sufficient data to make a statistical comparison between laboratory specimens and real world masonry.

Specimens for the static test program are constructed at the same time and of the same materials as the test walls. Typical specimens for the brick and concrete block walls follow:

Brick Test Specimens

1. Brick-mortar beams for flexural strength testing.
2. Brick-mortar blocks for compressive and shear strength tests.
3. Brick-mortar couplets for tensile bond strength tests.
4. Mortar cylinders for compressive and tensile strength tests.
5. Bricks for modulus of rupture and compressive strength tests.

Concrete Block Specimens

1. Concrete block-mortar beams for flexural strength tests.
2. Mortar cylinders for compressive and tensile strength tests.
3. Concrete blocks for compressive strength tests.

Composite walls of brick-concrete block construction are accompanied by similar specimens, except that the beams and masonry assemblies are also of composite construction.

Beams

Most beams were tested for flexural strength in the concrete tester equipped with the transverse beam apparatus, following the standard method for a simple concrete beam with third-point loading, ASTM designation C78-64. A diagram of a brick beam in place for this test is shown in Fig. B-1. Sketches of the various brick and concrete block beams investigated are shown in Fig. B-2. For the concrete block beams, which were both higher and longer than the other beams, and therefore did not fit the tester when the complete transverse beam apparatus was used, a method similar to ASTM C293-64, the standard method of test for flexural strength of simple concrete beams with center point loading was used. For these beams, the load was applied at the center of the supported section through a 2 in. diameter steel roller. Listed under beam properties in Tables B-1 and B-2 are the results of the brick and concrete block beam tests conducted to date.

Static tests were also conducted on brick and concrete beams which were built horizontally into a 4 ft wide heavy-walled passageway and mortared into the passageway so they arched under load. Photographs of these beams in place are shown in Fig. B-3 and Fig. B-4 diagrams the methods of loading these beams and lists the loads necessary to break them. Figure B-5A and B-5B show typical failure crack patterns in the brick beams, and Figs. B-6A

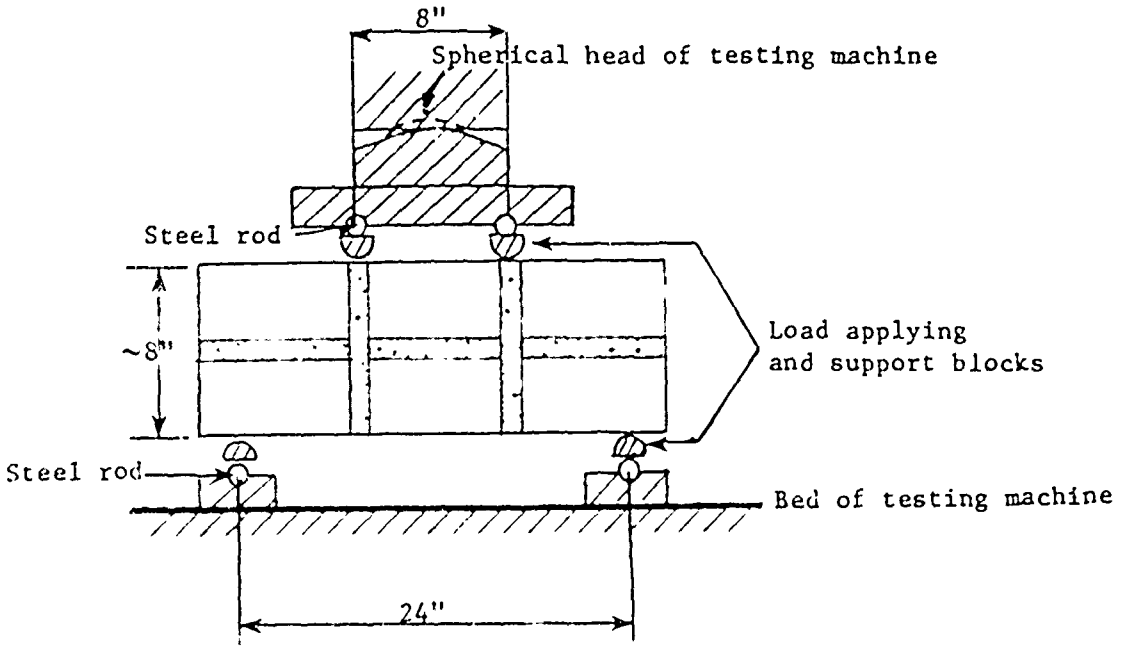

Fig. B-1. Brick Beam Flexural Test, Third-point Loading.

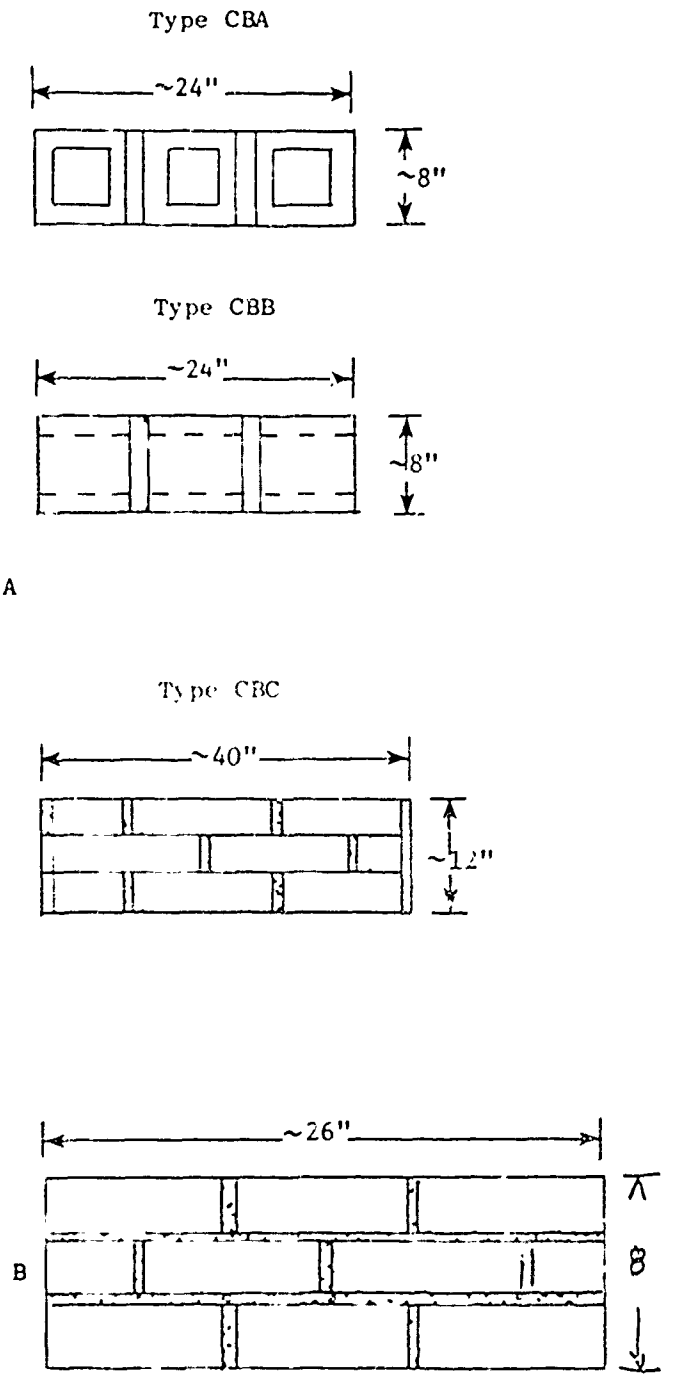

Fig. B-2. Brick and Concrete Beam Patterns.

TABLE B-1

Summary of Static Test Data

Brick

Designation			Beam Properties		Mortar Properties (average)		Bond Properties (average)		Composite Compression Strength (psi)
Batch No.	Date	Ident. No.	Brick Pattern	Flexural Strength (psi)	Compressive Strength (psi)	Tensile Strength (psi)	Tensile Strength (psi)	Shear Strength (psi)	
11	6/71	64			1566				
		65			2046				
		66			2109				
		67							
		68-1	B	208					
		68-2	B	253					
		69	B	125					
12	2/72	71-1	E	172	1754	410	61	61	2203
		71-2		191					
13	4/72	74	B	273	2531	459	102	81	2133
		75		150					
		76		159					
14	6/72	80	B	208	1814	165	-	73	2237
		81		160					
		82		179					
15	12/72	83	B	181	2127	245	101	-	2638
		84		152					
		85		117					
		86		195					
		87-1		153					
		87-2		171					
		88-1		155					
		88-2		119					
16	6/73	92	B	173	1819	518	-	-	2526
		94		220					
		95		167					
8	1969	96	B	164	3162	647	87	-	2526

TABLE B-2

Summary of Static Test Data

Concrete Block

Designation			Beam Properties		Mortar Properties (average)		Block Properties (average)
Batch No.	Date	Ident. No.	Block Pattern	Flexural Strength (psi)	Compressive Strength (psi)	Tensile Strength (psi)	Compressive Strength (psi)
2CB	2/72	72-1	CBA	73	2531	459	3484
		72-2	CBB	184			
		72-3	CBB	122			
		73-1	CBA	62			
		73-2	CBA	50			
		73-3	CBB	147			
3CB	4/72	77	CBC(1)	180	2531	459	3580
		78-1	CBC	182			
		78-2	CBC	185			
4CB	4/73	89-1	CBC	84.2	2643	406	4038
		89-2	CBC	122			
		89-3	CBC	149			
5CB	5/73	90-1	CBB	178	1886	346	3941
		90-2	CBB	117			
		90-3	CBB	128			
		91-1	CBC	109			
		91-2	CBC	167			
6CB	6/73	93-1	CBC	110	2197	518	4000

(1) Note on concrete block beams CBC center point loading was used because of limit of height on loader.

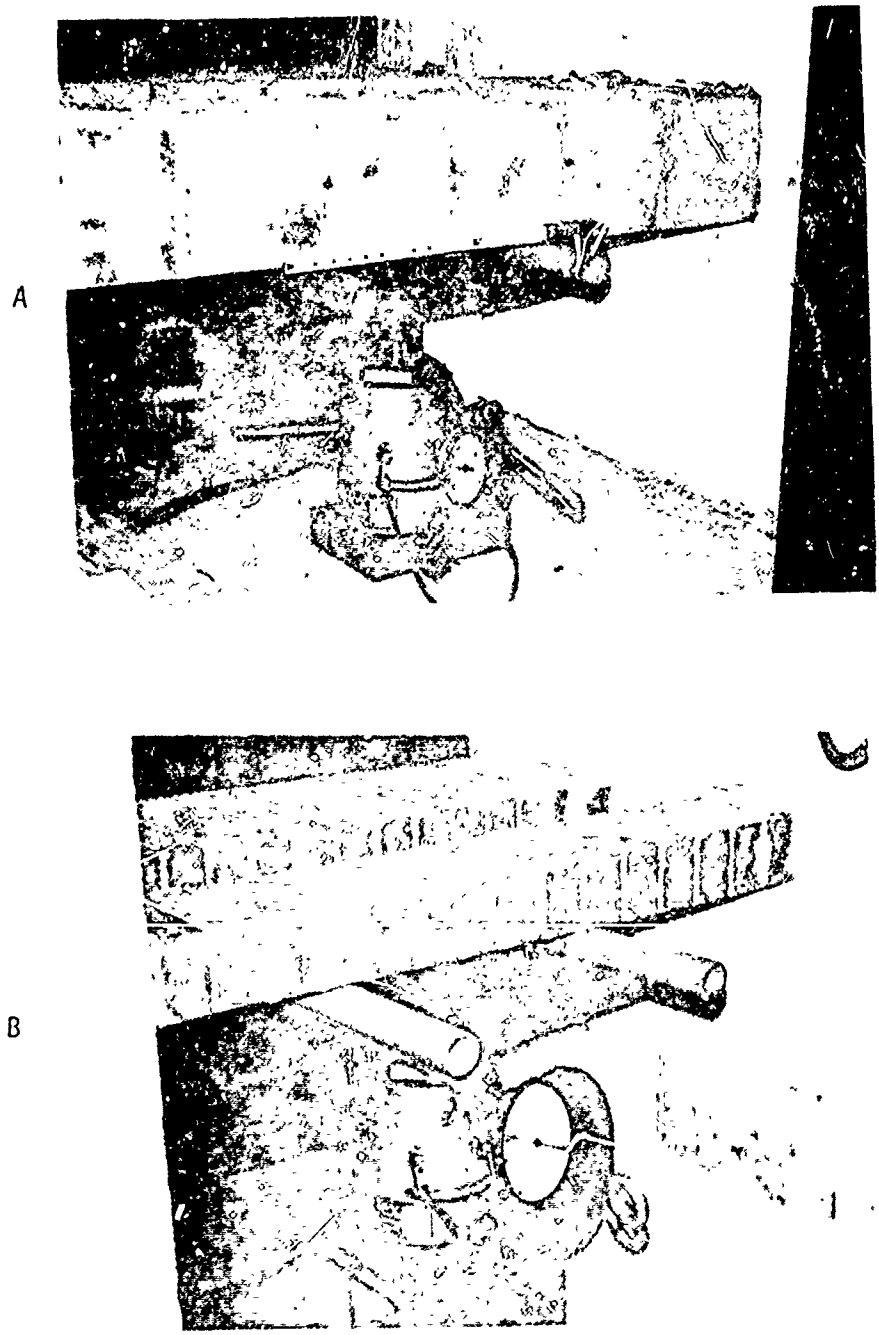

Fig. B-3. Test Method for Brick and Concrete Block Arched Beams.

Results of Tests on Brick Beams

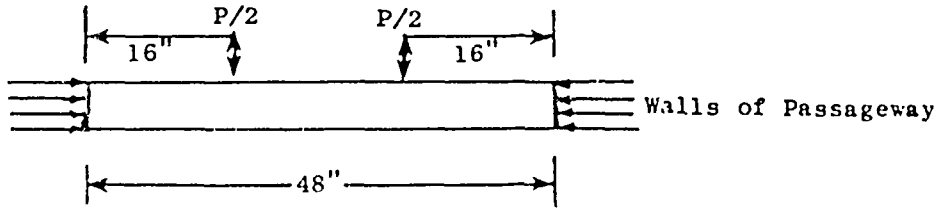

Test #1	P = 12100
2	P = 10500
3	P = 8836
avg.	P = 10479

Results of Tests on Concrete Block Beams

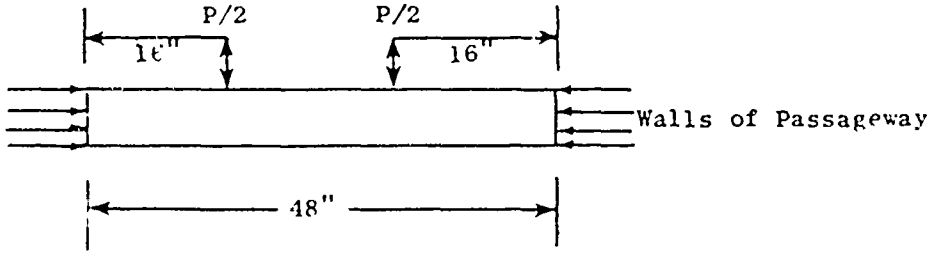

Test #1	P = 12700 lbs
2	P = 10500 lbs
avg.	P = 11600 lbs

Fig. B-4. Method of Loading and Test Results for Brick and Concrete Block Arched Beams.

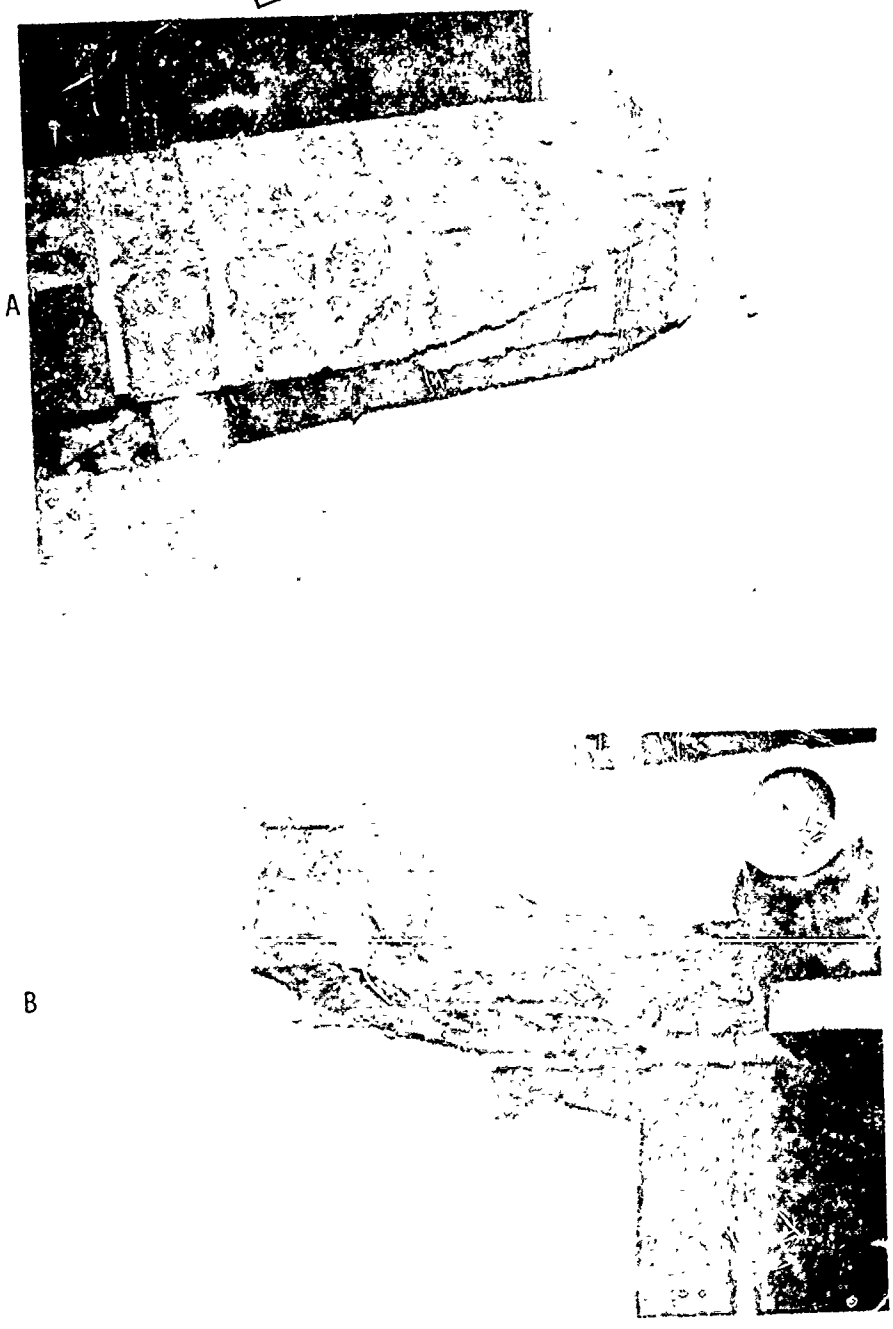

Fig. B-5. Typical Failure Crack Patterns in Reinforced Brick Beams

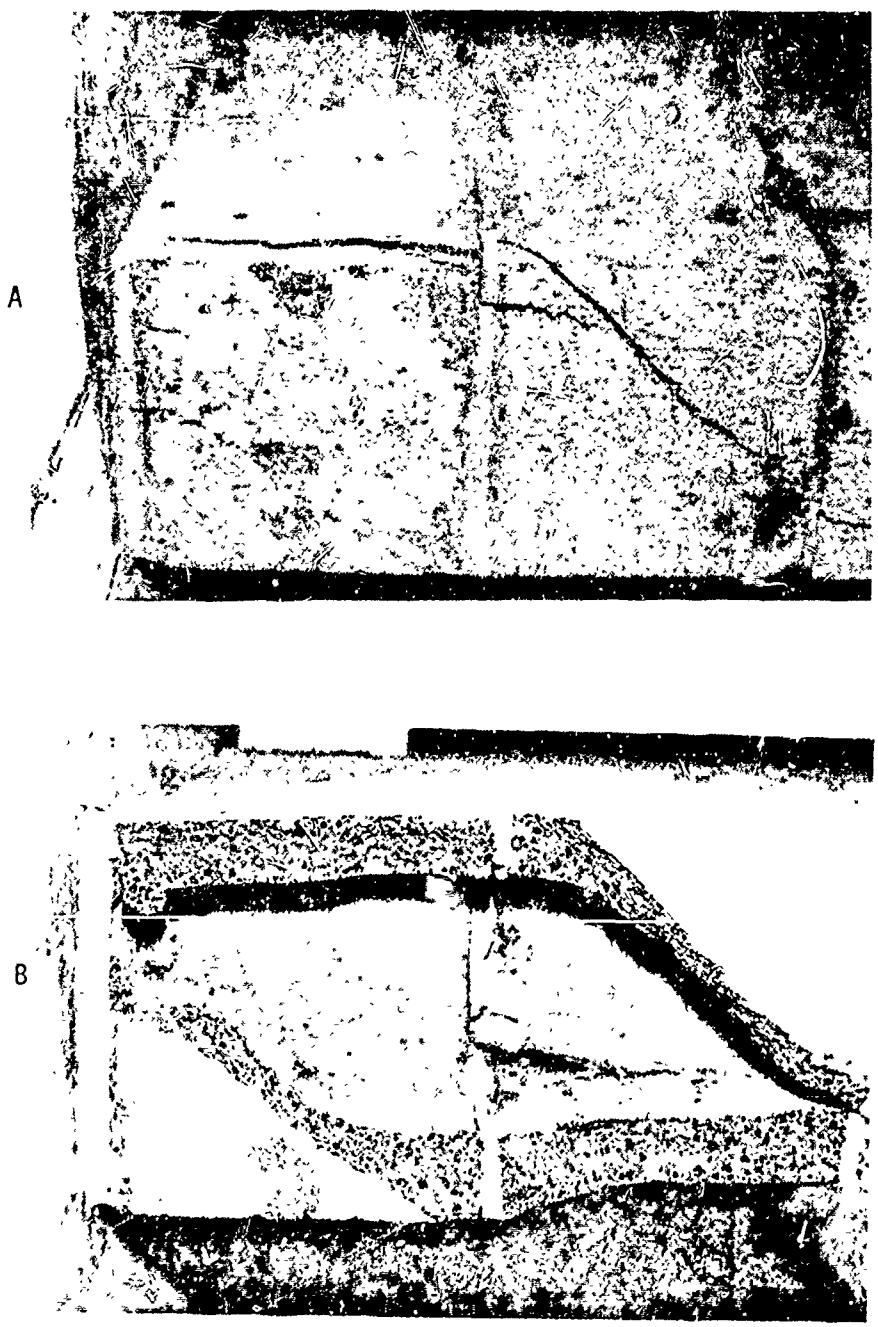

Fig. B-6. Typical Failure Concrete Arched Beam.

and B-6B show a concrete block beam after failure and at a later time when further deflection of the beam caused pieces to fall out. A sketch of the loading method and results of tests on concrete block-brick composite beams is shown in Fig. B-7. Also included in these tables are data for tests of brick and mortar couplets and mortar cylinders.

Additional data for compressive tests of brick assemblies and line load tests (see Section 2) of brick, concrete block, and assemblies of brick and concrete block are given in Tables B-3 through B-11. Similar tables were presented in Ref. 1, but errors in them were discovered. These errors have been corrected in this report and additional data has been added.

In the tables with data from standard compression tests (B-3,B-4, and B-10): P = the actual load; f_c' = failure stress = P/A, where A is the area of the loaded face; and E = the modulus of elasticity (Young's modulus) = $f_c'/(\delta/\ell)$, where δ/ℓ = sample strain, with δ = sample deformation, and ℓ = the original sample length in the direction of loading.

In the tables with data from line loading tests (B-5 through B-9,and B-11): P = the actual load; f_ℓ = the line load failure "stress" = P/w where w is the length of the line being loaded; and E* = the line load "modulus of elasticity" = $f_\ell/(\delta/\ell)$ where (δ/ℓ) = sample strain, with δ = sample deformation and ℓ = the original sample length in the direction of loading.

Results of Tests on Brick - Concrete Block Beams

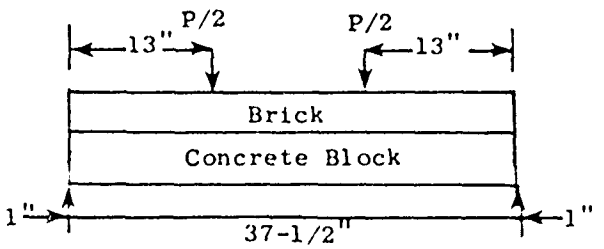

Test #1	P = 9388 lbs
2	P = 7731 lbs
3	P = 7180 lbs
avg.	P = 8100 lbs

Fig. B-7. Method of Loading and Results From Composite Brick and Concrete Block Beam Tests.

TABLE B-3

Static Test Data for 8-1/2" x 3-7/8" x 8-1/2"
Brick Assemblies in Compression - Standard Test

Group	Specimen Number	P (lbs)	f_c' (psi)	E
1	1	60,000	1,800	355,000
	2	67,000	2,000	410,000
	3	71,000	2,200	435,000
	average	66,000	2,000	400,000
2	1	97,000	2,900	486,000
	2	63,000	1,900	257,000
	3	87,000	2,600	465,000
	4	99,000	3,100	597,000
	5	89,000	2,700	333,000
	6	47,000	1,400	240,000
	average	80,000	2,400	396,000
3	1	87,000	2,600	781,000
	2	93,000	2,900	548,000
	3	89,000	2,800	264,000
	4	58,000	1,800	188,000
	5	88,000	2,800	489,000
	6	73,000	2,300	304,000
	average	81,000	2,500	429,000
Grand Average		78,000	2,400	410,000

TABLE B-4

Static Test Data for 8-1/2" x 8-1/2" x 8-1/2"
Brick Assemblies in Compression

Group	Specimen Number	P (lbs)	f_c' (psi)	E
1	1	200,000	> 2,800	784,000
	2	140,000	1,900	370,000
	3	196,000	2,700	342,000
	average	179,000	> 2,500	499,000
2	1	190,000	2,600	635,000
	2	200,000	> 2,900	1,013,000
	3	200,000	> 2,900	777,000
	4	200,000	> 2,900	724,000
	5	200,000	> 2,900	608,000
	6	200,000	> 2,900	555,000
	average	198,000	> 2,800	719,000
3	1	167,000	2,300	442,000
Grand Average		189,000	> 2,700	625,000

TABLE B-5

Static Test Data for 8-1/2" x 3-7/8" x 8-1/2"
Brick Assemblies in "Line Loading"

Group	Specimen Number	P (lbs)	f_ℓ (p.in.)	E*
1	1	34,500	4,000	307,000
	2	33,700	4,200	385,000
	average	34,000	4,100	352,000
2	1	18,000	2,100	250,000
	2	28,000	3,300	337,000
	3	23,000	2,700	228,000
	4	32,000	3,700	276,000
	5	33,500	3,900	263,000
	6	35,000	4,200	302,000
	average	28,300	3,300	276,000
3	1	28,000	3,300	248,000
	2	22,500	2,700	261,000
	3	2[illegible]500	[illegible],500	248,000
	average	23,700	2,800	252,000
Grand Average		28,100	3,300	282,000

TABLE B-6

Static Test Data for 8-1/2" x 8-1/2" x 8-1/2"
Brick Assemblies in "Line Loading"

Group	Specimen Number	P (lbs)	f_t (lb/in.)	E*
1	1	51,000	6,000	560,000
	2	46,000	5,400	532,000
	3	52,000	6,000	446,000
	average	49,700	5,800	513,000
2	1	37,500	4,400	303,000
	2	39,500	4,600	534,000
	3	45,000	5,300	196,000
	4	35,000	4,100	357,000
	5	47,500	5,600	559,000
	average	40,900	4,800	390,000
3	1	48,000	5,600	159,000
	2	36,000	4,200	355,000
	3	36,500	4,300	221,000
	average	40,200	4,700	245,000
Grand Average		43,100	5,100	384,000

TABLE B-7

Test Data for Vertical "Line Loading" of Brick/Mortar Specimens

Δ_t	P	f_c'	f_ℓ
1/4"	10,900	171	680
	13,465	211	840
	13,990	217	825
	15,200	237	950
1/2"	13,980	260	875
	33,000	515	2,070
	34,000	540	2,160
	19,000	297	1,191

TABLE B-8

Static Test Data for Brick Concrete Block Composite
"Line Load" on Brick

Specimen Number	P (lbs)	f_ℓ (lb/in.)	E*
1	44,000	5,200	620,000
2	32,000	3,800	413,000
3	40,000	4,700	417,000
Average	39,000	4,600	483,000

TABLE B-9

Static Test Data for Brick Concrete Block Composite
"Line Load" on Block

Specimen Number	P (lbs)	f_ℓ (lb/in.)	E*
1	23,000	3,000	261,000
2	21,000	2,800	327,000
3	25,500	3,300	199,000
4	23,000	3,000	174,000
Average	23,200	3,000	240,000

TABLE B-10

Static Test Data for Concrete Blocks in Compression

Specimen Number	P (lbs)	f_m' (psi)	E
1	116,500	3,610	635,000
2	84,300	2,610	520,000
3	63,600	1,970	592,000
4	66,200	2,050	259,000
Average	82,600	2,560	501,000

TABLE B-11

Static Test Data for Concrete Blocks in "Line Loading"

Specimen Number	P (lbs)	f_ℓ (lb/in.)	E^*
1	31,400	4,100	302,000
2	27,000	3,500	192,000
3	26,500	3,500	250,000
4	36,000	4,700	429,000
Average	30,200	4,000	293,000

Appendix C

LOW LEVEL FATIGUE

Appendix C

LOW LEVEL FATIGUE

Studies of fatigue generally deal with the effects of repetitive or cyclic loading on objects, and the term "low level fatigue" refers to the effects of a relatively small number (less than 100) of such loading cycles. In this report, the "objects" are arching masonry walls, and the cyclic loadings are from blast waves.

The most commonly recognized cause of cyclic or multiple loadings on building elements such as walls, are earthquakes. A very important question, both in the design of new buildings to withstand eathquakes, and in the analysis of the ability of existing buildings to resist earthquakes, is the effects of such multiple loadings on the strengths of exterior walls. By accident rather than design, the experimental portion of this study of the effects of blast loadings on walls (which was carried out in a large shock tunnel) has developed important information on just that question. While the topic is not an integral part of the basic study effort, we believe it highly desirable that the information be made available to the earthquake engineering design and analysis community as quickly as possible; thus this appendix.

To understand how the multiple loading information was obtained it is necessary to consider the geometry of the shock tunnel and how it operates. The geometry of the tunnel is shown in a cutaway view in Fig. C-1.

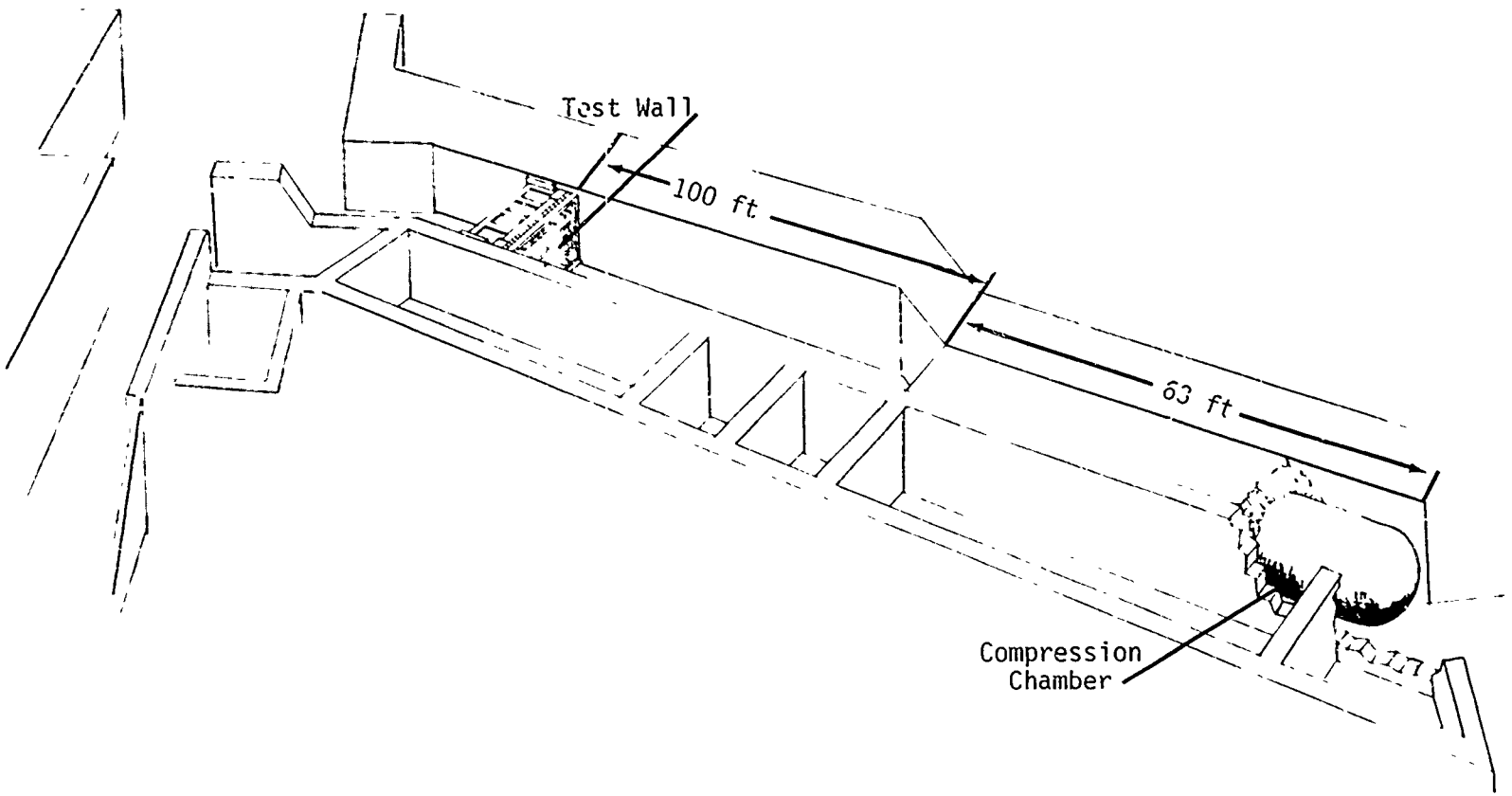

Fig. C-1. Cutaway View of Shock Tunnel Showing Wall in Place.

On the right is the 8-ft diameter, 63-ft long steel cylinder, called the compression chamber which is closed at one end; on the left, 100 ft from the open end of the compression chamber, is a wall in place ready for test

To operate the tunnel one or more strands of Primacord (a line explosive also known as "detonating fuse") are strung the length of the compression chamber and exploded. The contents of the compression chamber are very rapidly converted to a mass of hot, high pressure gas that acts as a piston and generates a sharp fronted pressure pulse (a shock wave) that propagates toward the test wall. The peak overpressure of the shock wave depends on the number of strands of Primacord used. (Very roughly, peak overpressure in psi equals 1.2 times the number of strands.)

The shock wave generated by this process is generally characterized by a portion with constant pressure about 50 msec long, followed by a portion, also about 50 msec long, in which the pressure decreases to a value slightly below ambient pressure. The length of the wave is about 100 ft, that is, when its head is at the test wall, its tail is approximately at the open end of the compression chamber.

After striking a test wall that does not immediately fail, the shock wave will be completely reflected, and will be redirected toward the closed end of the compression chamber. Upon striking the end, it will again be reflected toward the wall, and the process will continue until the shock wave

dissipates. (Shock wave energy and impulse is lost upon each reflection.) Since the shock wave exerts pressure on the wall while it is undergoing reflection, the wall experiences more than a single loading cycle.

The type of loading pulse experienced by the wall is shown in Fig. C-2, a trace from a pressure gauge mounted in an instrument wall made of steel and wood, and specially designed not to fail under blast loading. Note that the maximum of each loading cycle is approximately 2/3 the maximum of the preceding cycle.

Pressure gauges were not mounted on the masonry test walls because of the possibility that the walls would fail and destroy the gauges, but gauges were mounted in the tunnel sidewall near the test walls, and loadings on the walls themselves could be derived from these gauge readings. Unfortunately for this duscussion, records longer than about 100 msec were rarely kept. (The test program was designed to give information on wall failures from initial loadings.) However, later loadings on those walls that did not fail can be inferred from the 100 msec records by assuming that -- as with the pulse shown in Fig. C-2 -- the dissipative processes in the shock tunnel are such that each cycle following the first will have peak overpressure 2/3 of that of the cycle immediately preceding it.

Four 8-in. thick, brick, arching walls did not fail on initial loading; four others failed. Each of the walls that did not fail on initial loading was left in the tunnel and was re-tested at least once. The wall numbers,

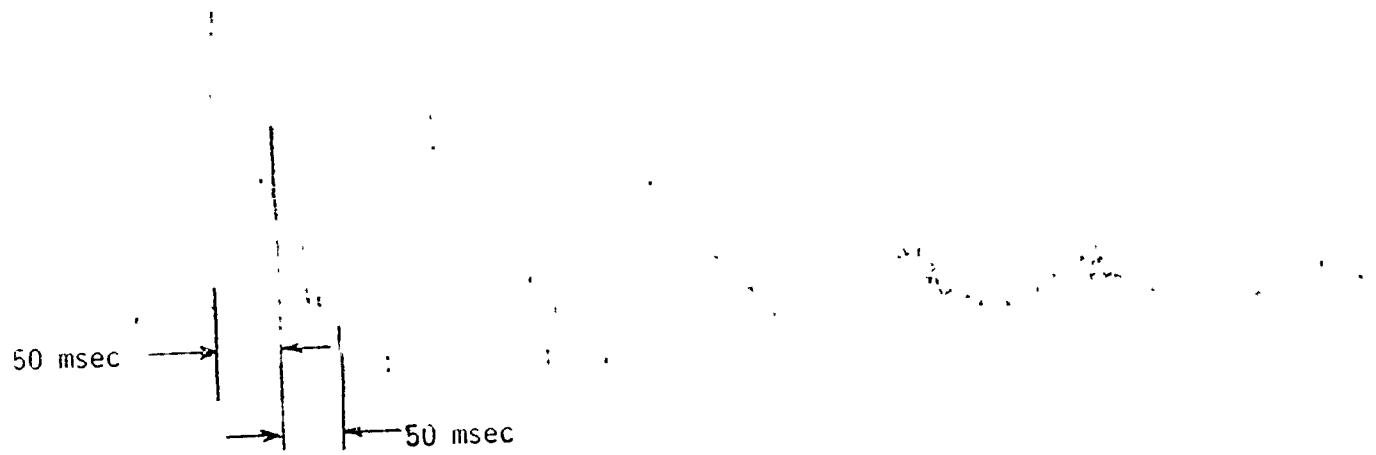

Fig. C-2. Shock Tunnel Pressure Gauge Traces. Gauges Mounted in Nonfailing Wall (Peak reflected overpressure, first peak 5 psi.)

peak initial loading (reflected) pressure, and a description of what happened to these eight failing and non-failing walls are shown in Table C-1.

But for the walls that did not fail, the table only shows part of the loading picture because of the multiple reflections that occurred. A more complete loading description for these walls would be that given in Table C-2. In that table, the underlined pressures are the measured pressures from Table C-1, that is, the maximum pressure experienced by each wall at the beginning of every test. Each other pressure value is 2/3 of the value immediately preceding it. No overpressures smaller than one psi are listed.*

A dramatically different loading picture emerges. Wall number 71, for example, is seen to have experienced 10 loading cycles (from three separate tests) with peaks greater than 1 psi before it failed. After four loading cycles, (during the first of which the wall cracked) it clearly had significant resistance to pressure forces, because it next experienced a loading cycle with a peak over 50 larger than that of the initial loading cycle, (5.8 psi vs. 3.8 psi), and this was followed by a cycle with a peak of the same order as that of the first cycle (4 psi).

A similar, but more impressive pattern occurred with wall 87 which experienced 14 loading cycles prior to failure, and after the sixth cycle

* Note that for an 8-in. thick brick wall, a pressure on the wall of 1 psi is equivalent to a 1.8 g inertial force, a very high earthquake loading.

TABLE C-1

Summary of Tests on 8-in. Thick, Brick, Arched Walls

Wall Number	Reflected Pressure (psi)	Comments
71	3.8	Wall cracked
	5.8	Crack enlarged
	8.6	Wall failed
74	3.8	Wall cracked
	11.0	Wall failed
75	11.9	Wall failed
76	11.1	Wall failed
87	10.3	Wall cracked
	12.7	Cracks enlarged
	16.3	Wall failed
88	15.7	Wall cracked
	7.2	Cracks enlarged
94	15.5	Wall failed
96	13.4	Wall failed

TABLE C-2

Loadings on Walls Experiencing Low Level Fatigue

Wall Number	Peak of Loading Pressure Cycles
71	$\underset{\text{x}}{3.8}$, 2.5, 1.7, 1.1, $\underset{\text{x}}{5.8}$, 4.0, 2.6. 1.8, 1.2, $\underset{\text{x}}{8.6}$ wall cracked — cracks enlarged — wall failed
74	$\underset{\text{x}}{3.8}$, 2.5, 1.7, 1.1, $\underset{\text{x}}{11.0}$ wall cracked — wall failed
87	$\underset{\text{x}}{10.3}$, 6.9, 4.6, 3.1, 2.1, 1.4, $\underset{\text{x}}{12.7}$, 8.5, 5.7, 3.8, 2.6, 1.7, 1.1, $\underset{\text{x}}{16.3}$ wall cracked — cracks enlarged — wall failed
88	$\underset{\text{x}}{15.7}$, 10.5, 7.0, 4.7, 3.2, 2.1, 1.4, $\underset{\text{x}}{7.2}$, 4.8, 3.2, 2.1, 1.4 wall cracked — cracks enlarged

experienced a cycle with a peak pressure (12.7 psi) greater than that of the first cycle (10.3 psi).

Comparison of the results of tests 94 (Table C-1) and 88 (Table C-2) sharply underlines the fact that arching walls that crack but do not fail retain significant strength after several cycles of loading. The two walls were loaded at essentially the same initial overpressure (about 15.5 psi); one failed, one did not.* However, the wall that did not fail subsequently experienced some 11 loading cycles with peak pressures greater than 1 psi, (one of which was over 7 psi) and at the end of this sequence was still standing. (The wall was pulled down for convenience.)

The phenomenon of low level fatigue was not restricted to the brick walls. An 8-in. thick concrete block wall (for which a 1 psi pressure loading is equivalent to a 2.6g inertial loading) withstood two separate tests with peak loading pressures of 8.2 and 4.3 psi (plus, of course, the many multiple loadings) before a third test at 8.5 psi caused failure. A 10-in. thick composite brick and concrete block wall (1 psi equivalent to 1.6 g) was hit three times with peak loading pressures of 7.8, 7.8, and 11.4 psi and was still standing after the third shot.

* Such apparently contradictory results from tests on seemingly identical walls are not unexpected. Static tests on sample brick-mortar test elements constructed at the same times as the walls, showed a very wide variation in mechanical properties. For example, flexural tests on 19 beams, 26 in. long and with 8- in. x 8-in., cross section, fabricated at seven different times over a four year period, gave flexural strengths (using standard ASTM methods) that ranged from 117 psi to 273 psi. The range from 8 beams all fabricated at the same time was from 117 psi to 195 psi. Other investigators have noted similar wide variations in properties of masonry elements.

These results provide some important insights into what can happen to walls subjected to earthquake forces, even though the spectral characteristics of multiple loadings caused by blast are far different from those that can occur in an earthquake. All of the walls that did not fail on initial loading, cracked during the first loading cycle.* They were subsequently subjected to a number of cycles of loading (that were very high relative to design earthquake loads) -- some of which were even greater than the load that initially cracked the wall -- and still displayed very high resistance to the out-of-plane loads. Clearly, the fact that a wall has cracked as the result of an applied load, need not mean that it has lost its ability to withstand subsequent loadings of the same or even greater magnitude. Extending this point, a wall that has cracked for any reason(e.g., thermal stresses, prior earthquakes) could well resist significant out-of-plane earthquake loadings.

* The walls actually cracked at their flexural strength which was attained at a loading pressure of less than 1 psi.